Asymmetric Induction Using Heterocyclic Precursors

Thesis

A THESIS

entitled

ASYMMETRIC INDUCTION

USING

HETEROCYCLIC PRECURSORS

presented by

JANET LARGE

in partial fulfilment of the requirements for the degree of

DOCTOR OF PHILOSOPHY

in

THE DEPARTMENT OF CHEMISTRY

FACULTY OF SCIENCE

THE OPEN UNIVERSITY

October 2002

Submission date: 7 February 1997

Award date: 2 May 2003

To David with love.

On graduating in 1990 with an honours degree in science from The Open University, the author undertook research under the supervision of Dr. J. M. F. Gagan and Dr. R. T. Brown in the Department of Chemistry, Victoria University of Manchester, the results of which are embodied in this thesis.

None of the work referred to in this thesis has been submitted in support of an application for another degree or qualification at this or any other university or institution of learning.

Acknowledgments

The author would like to sincerely thank Dr. J. M. F. Gagan for the opportunity to undertake this research and for his encouragement throughout and to Dr. R. T. Brown of Victoria University of Manchester, for his advice, help and enthusiasm whilst working in his laboratory.

I would also like to thank Professor J. Thomas for providing working space in the Department of Chemistry laboratories, at The University of Manchester. Professor M. Rubenstein, Dr. J. Cast and other members of staff for providing laboratory space, help and facilities at The School of Pharmacy and Chemistry, John Moores University, Liverpool, during the final stages of the work.

Grateful thanks are also given to the staff of the spectroscopy and chromatography laboratories at Manchester University for their invaluable assistance. Together with a special thank you to R. L. Beddoes of the Crystallographic Research Service Department also at Manchester University, for obtaining the X-ray structures given in the Appendix.

The author owes a considerable debt of gratitude to Professor D. H. G. Crout of The Department of Chemistry, University of Warwick, Coventry, for his invaluable support, advice, help and enthusiasm for the final production of her thesis.

Finally, I would like to acknowledge my debt to my colleagues at Manchester, especially Simon, Steve, Jian Li and Nani for providing an enjoyable environment in which to work, and to The Open University for financial support.

Abstract

A literature review suggested that certain rigid heterocyclic systems containing stereogenic centres of known absolute configuration, together with a prochiral reactive site, might offer a route to preparation of chiral molecules with a high degree of asymmetric induction by the stereogenic elements present in the heterocyclic ring.

In this project we investigated the heterocylic system 5,7-Dioxoperhydro-1,4-oxazepine **1,** formed from the reaction of dimethyl malonate with (+)-ephedrine as a chiral auxiliary. We have shown that replacement of the two hydrogens by alkyl groups at the C6 prochiral atom can be achieved with a high degree of stereoselectivity (>90%), brought about by the steric control exercised by the stereo features of the ephedrine moiety and the twist-boat conformation of the oxazepine ring.

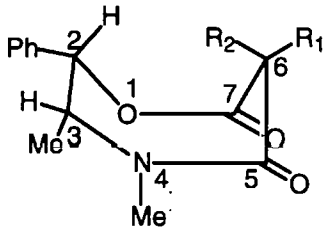

1 where R_1 and R_2 are hydrogen

Stereoselective monoalkylation of the pseudo-equatorial hydrogen (R_1) gave the exo monosubstituted products **14-17**. A second alkyl substituent was then introduced selectively at C6 to afford the disubstituted oxazepines **18-22**. The absolute configurations shown were established by spectroscopic methods, notably by nOe, ^1H NMR methodology, together with X-ray crystallography in certain cases. Release of the newly created stereogenic centre from the chiral auxiliary was achieved by ring opening processes at the heteroatom sites in the oxazepine ring.

As one example of the use of our method of asymmetric induction, we showed that α-substiuted α-amino acids are attainable by preparing 2-methyl-3-phenylalanine methyl ester by functional group interconversion of **19** after ring cleavage.

An oxazepine based upon *S*-prolinol (**34**) as chiral auxiliary was also successfully prepared for further study of its asymmetric inducing properties.

Finally preliminary steps in the synthesis of oxazecines and oxazenines were examined to lead to an understanding of ring size in our procedure.

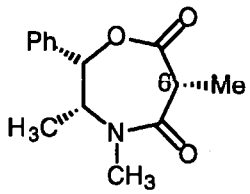

14

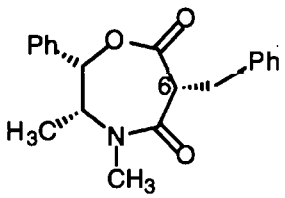

15

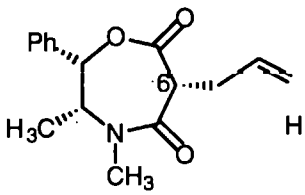

16

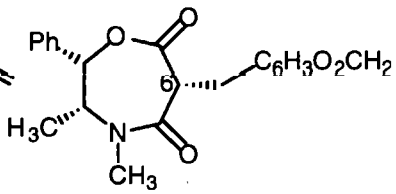

17

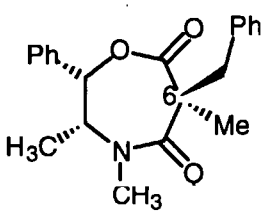

18

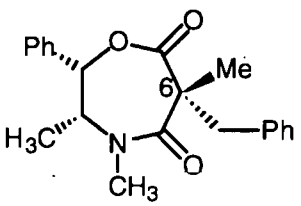

19

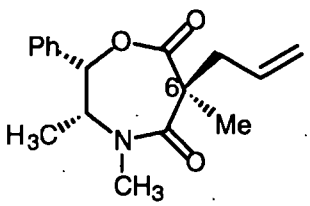

20

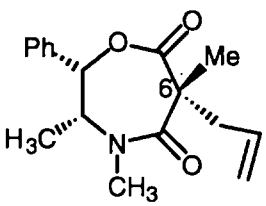

21

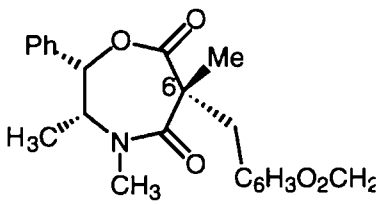

22

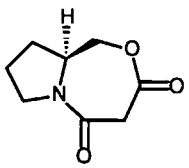

34

Abbreviations

AllylCl	Allyl chloride
AllylOAP (AllylMeOAP)	Allylated oxazepine (Allylated methyloxazepine)
R-Alpine-borane	β-Isopinocampheyl-9-borabicyclo [3,3,1] nonane
9-BBN	9-borabicyclo [3,3,1] nonane
BnBr (Cl)	Benzyl bromide (chloride)
BnOAP (BnMeOAP)	Benzylated oxazepine (Benzylated methyloxazepine)
°C	Degrees Centigrade
COSY	*C*orrelated *s*pectroscop*y*
DBU	1,8-Diazabicyclo [5,4,0] undec-7-ene
DCM	Dichloromethane
de	Diastereomeric excess
dr	Diastereomeric ratio
DIPA	Diisopropylamine
DMAD	Dimethyl acetylenedicarboxylate
D_2O	Deuterium oxide
Elem. Anal.	Elemental analaysis
Et	Ethyl
Et(R'O)AlCN	Ethyl-(alkoxy)aluminium cyanide
Et_2O	Diethyl ether
EtOAc	Ethyl acetate (ethyl ethanoate)
I_2	Iodine vapour
Ipc_2BH	Diisopinocampheylborane

IR	Infrared
LDA	Lithium diisopropylamide
Me (I)	Methyl (iodide)
MeAllylOAP	Methylated allyloxazepine
MeBnOAP	Methylated benzyloxazepine
MeCN	Acetonitrile
MePipOAP	Methylated piperonyloxazepine
MeOAP	Methylated oxazepine
MeOH	Methanol
NMR	Nuclear magnetic resonance
nOe	Nuclear Overhauser effect
Pet.	Light petroleum
Ph	Phenyl
Pip	Piperonyl
PipCl	Piperonyl chloride
PipOAP	Piperonylated oxazepine
ppm	Parts per million
Red-Al	Sodium bis (2-methoxyethoxy) aluminium hydride
TBAB	Tetra-*n*-butylammonium bromide
TFA	Trifluoroacetic acid
THF	Tetrahydrofuran
TLC	Thin layer chromatograph
U.V.	Ultra Violet

The ring numbering system is based on the oxazepine ring.

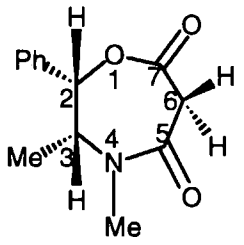

Oxazepine

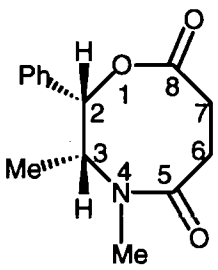

Oxazecine

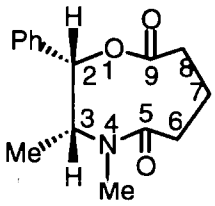

Oxazenine

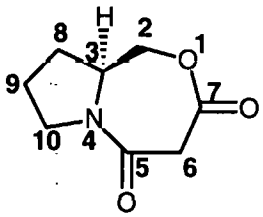

Pyrrolidinooxazepine

Contents

		page
1.	Introduction	1
2.	General methods of asymmetric synthesis.	4
	2.1 Methods relying on conformation	4
	Substrate controlled methods	4
	The advantage of cyclic systems	10
	2.2 Reagent controlled methods	23
	Asymmetric synthesis using boron reagents.	23
	Other reagents used for control.	33
	2.3 Catalyst controlled methods.	34
	Boron containing catalysts.	34
	Noble metal catalysts.	36
	2.4 Chiral auxiliary control	39
	Asymmetric synthesis using dihydropyrazines and their analogues.	39
	Asymmetric synthesis using imines as intermediates.	46
3.	Chiral induction with heterocycles.	53
4.	Chiral oxazepines in asymmetric induction.	59
	4.1. Initial work by Mukaiyama.	59
	4.2. Development work by Ford.	63

5. Summary. 69

6. Results and discussion 72

6.1. Synthesis of the oxazepine. 72

6.2. Conformation of the oxazepine ring. 81

6.3. Synthesis of the substituted oxazepines. 87

Monosubstitution. 89

Disubstitution. 98

6.4. Enantioselective synthesis of α-aminoacid derivatives. 113

Ring cleavage. 113

Conversion of the carboxylic acid into an amine. 121

Hydrolysis. 125

6.5. Synthesis of the proline derived oxazepine (pyrrolidinooxazepine ring). 131

6.6. Conformation of the pyrrolidinooxazepine ring. 139

6.7. Monosubstitution of the pyrrolidinooxazepine. 14

6.8. Alternative heterocyclic precursors. 142

Preparation of the homologues of the oxazepine. 144

Preparation of heterocycles using β-amino alcohols. 152

Preparation of the analogues of the oxazepine. 156

6.9. Formation of racemic α-methyl phenylalanine-discussion of an interesting by-product. 160

7.0. Conclusions and future work. 165

8.0. Experimental. 174

9.0. References. 224

10.0. Appendix. 233

10.1. Novel compounds synthesised during the course of this research project 234

10.2. An alternative reagent for the oxazepine synthesis. 237

10.3. X-ray crystallographic structures. 239

1. INTRODUCTION

Chirality plays a major role in living organisms. They are largely comprised of components that are chiral, and not surprisingly the bioactivity of drugs, insecticides, herbicides, flavours and fragrances at a molecular level is dominated by asymmetry. Models for the reaction of substrates with cell receptors and enzymes have developed from the 'lock-and-key' concept of Emil Fischer,[1] through the selective receptor theory of Langley[2] and Ehrlich's 'magic bullet' chemoreceptors,[3] to the present capability to map the three dimensional structure of enzymes and their active sites. As knowledge of the interaction of chiral drugs with human cell receptors advances, the necessity for the development of methodologies for the synthesis of enantiomerically pure isomers has assumed an increasing importance. The development of the drug captopril is an illustration of how the implication of chirality and its biological application was considered. Figure 1 shows that only one of the four possible isomers of captopril is stereochemically capable of binding effectively with the enzyme, and blocking the active site.[4]

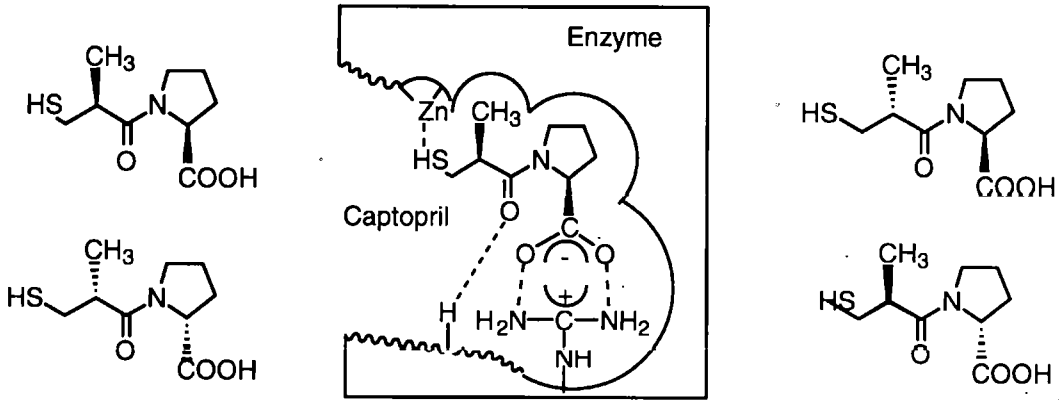

Figure 1

Individual isomers of many chiral compounds may show their own distinct biological activity in the human body. When the chiral compound is to be used medicinally, then enantiomeric purity may be essential, as for example in the use of the drug propranolol; the (*S*)-isomer acts as a β-blocker and the (*R*)-isomer as a contraceptive (Figure 2). The widely documented case of thalidomide, where one stereoisomer had tragic effects, has shown that there is a need for a great deal more investigation into the teratogenic effects of drug chirality on humans.[5] Separation of each isomer in its pure form, from the racemic mixture, can be an expensive exercise and if one isomer is biologically inert, it is wasteful in starting materials and resources. Furthermore the build-up of the unused isomer may be unsafe in the long term.[6]

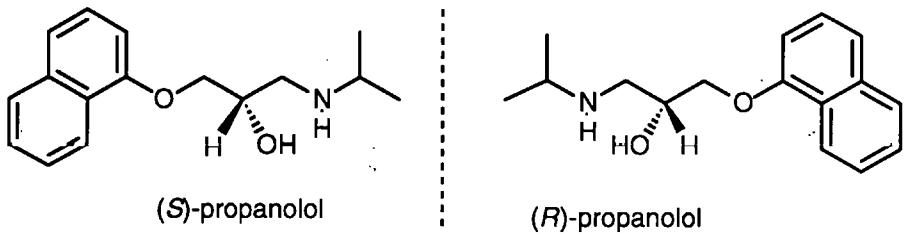

Figure 2

It is therefore essential that all the stereoisomers of a drug must have their biological activity investigated. The reaction of many pharmaceutical manufacturers to these problems and new regulations, has been to develop optically active drugs in their single stereoisomeric forms. However, any methodology for the production of only the one stereoisomer, (that has the biological activity required for use as the drug), must be proven before license to produce it is given by the Food and Drug Administration (FDA) of the U.S.A.

Over the last twenty to thirty years with the development of X-ray and electron diffraction, spectroscopic methods and chiroptical techniques, the ability to determine absolute configuration has improved. Also over this time period, there has been a great deal of investigation into the mechanisms of organic reactions, leading to a greater knowledge of the pathways that reactions may take. Stereoselective reactions are generally based on kinetic phenomena, and consideration of each of the rate constants for the different reactions leading to the isomeric products will indicate which product will predominate. Thus considerable progress in the methods of asymmetric synthesis has been made in recent years with these increased insights into the mechanisms and kinetics of reactions, together with the instrumental methods of product identification mentioned above.

Throughout the following chapters, reference is made to molecular modelling, as an aid to the interpretation of published work and of the experimental results that are the subject of this thesis. The molecular model mechanics programme used was PCMODEL, which uses an extensively modified version of the Allinger force field (MM2) called MMX.

2 General methods of asymmetric synthesis

2.1 Methods relying on conformation

Substrate controlled methods

Methods for inducing chirality have been developed over many years, although in some of the earliest research work into these methods, only partial asymmetric synthesis was achieved. These reactions are directed *intramolecularly*, usually by a stereogenic unit present in a chiral substrate. All the new chiral centres in the product are directly derived from the influence of the substrate. The stereogenic centre of the original substrate is not generally involved in the reaction steps, however care must be taken that racemisation does not occur at this centre. A new chiral centre is commonly formed at a diastereotopic (prochiral) site, by use of an achiral reagent, the direction of substitution being influenced by a nearby stereogenic centre in the original substrate. Most frequently, this centre exerts its influence because it includes a bulky substituent which interferes with the direction of approach of attacking reagents. This is illustrated in reactions using nucleophilic addition at carbonyl groups, where a stereogenic centre is used to induce stereo-differentiation.

In one of the earlier attempts to induce asymmetry, Prelog produced his well known empirical rule for Grignard addition reactions of α-keto-esters, which correlated the configuration of the predominant stereoisomer at the newly created asymmetric carbon atom, with the configuration at the carbinol carbon of the α-keto-ester. The carbonyl groups take-up the preferred anti-periplanar conformation and

the large group (L) is assumed to lie in the plane of the two carbonyl groups (Figure 3). Attack by the Grignard reagent at the prochiral carbonyl group is on its less hindered face: that containing the small group (S). However, stereodifferentiation was low.

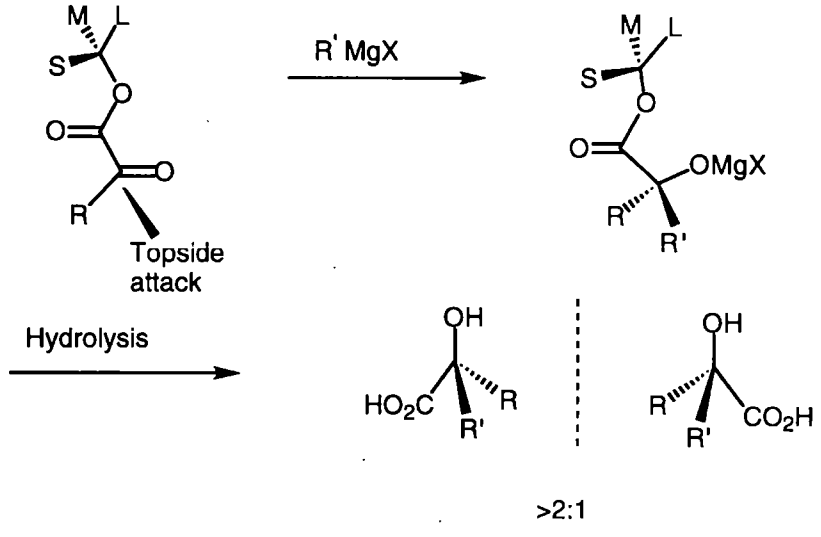

Figure 3

These early ideas were developed in investigations by Cram *et al.*, who postulated[7,8,9] a rule for the nucleophilic addition to compounds in which the carbonyl group was adjacent to the stereogenic centre. This combination helps to reduce the number of conformations through which the reaction takes place. The rule is that the oxygen of the carbonyl double bond orientates itself between the two least bulky groups, which thus places the largest group *trans* to the carbonyl group. The stereoisomer that would predominate on nucleophilic addition at the prochiral carbonyl group, then arises from the approach of the nucleophile from the side of the smallest substituent S (Figure 4a).

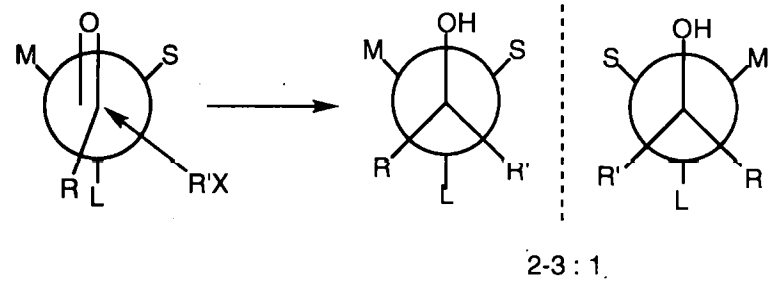

Figure 4a

An interpretation of this predominating diastereoselectivity as postulated by Cram's rule, has been suggested by the Felkin-Anh model[10, 11] (Figure 4b).

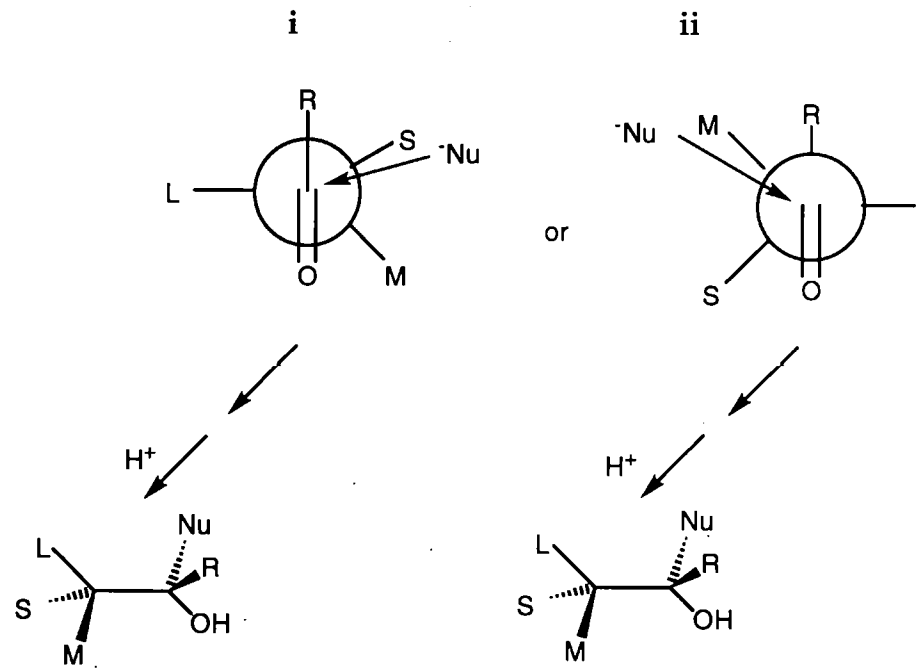

Figure 4b iii iv

This model makes the assumptions that in the reactive conformation as shown in **i** and **ii** (Figure 4b), the bonds to L, M and S are staggered relative to the carbonyl group, with the least sterically hindered site occupied by L. The nucleophile

will attack along the Bürgi-Dunitz trajectory (as shown in Figure 4b), which is at an angle of about 109° with respect to the plane of the carbonyl group. This trajectory was deduced from the study of nucleophiles and carbonyl groups of model compounds, using X-ray crystallography. More distant parts of the trajectory were based on calculations. The two conformations are assumed to be energetically similar (**i** and **ii**), and differentiation occurs because of non-bonded interactions between the nucleophile and either of the S and M substituents. The nucleophile is close to S in **i** but close to M in **ii**, thus the formation of the product **iii** is favoured over **iv**.

Examples of stereodirection by an already present α-stereogenic centre, can also be seen in the reduction of carbonyl groups in the presence of another functional group, and in the addition reactions of Grignard reagents (Figures 5a, b and c).

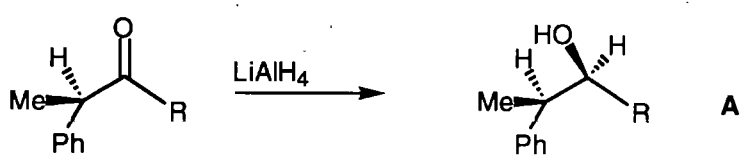

Figure 5a

When addition reactions are made to carbonyl groups of open chain compounds (**A** Figure 5a), there is too much conformational freedom for diastereoselectivity to be high. The bonds are free to rotate and stereoselectivity depends upon them spending most of their time in their preferred conformations. Stereoselectivity is negligible if there is little relative difference in size between the groups at the stereogenic centre. In general, to achieve good diastereoselectivity, there must be a significant difference in steric bulk between the groups at the stereogenic centre, so that one side of the carbonyl group will be relatively more hindered than the other in the preferred conformation.

Diastereoface differentiation to give **A** (in Figure 5a)[12] can also be enhanced if the bulk of the R group is increased, resulting in increased steric hindrance between the R and the Me groups. Thus, in the lithium aluminium hydride reduction of a chiral ketone the selectivity for the product increases from 46% ee if R is methyl to 96% ee if R is *tert* -butyl (Figure 5a).[12] However, modelling (PCMODEL) shows that the situation is more complicated and cannot be interpreted solely in terms of increased steric bulk, and that with either R= Me or *tert*-Bu there are two stable conformations. The two pairs of conformers for each compound are shown in Figure 5b.

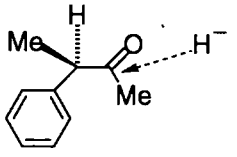

8.6 kcal mol^{-1}

v

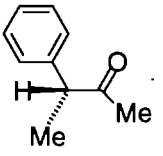

11.4 kcal mol^{-1}

vi

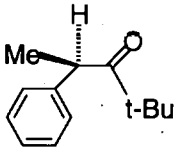

16.4 kcal mol^{-1}

vii

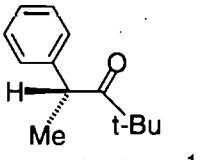

19.7 kcal mol^{-1}

viii

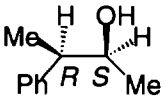

A 1

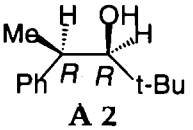

A 2

Figure 5b

In the lowest energy conformers (**v** and **vii**), one face of the carbonyl group is blocked by the methyl group. The same face is blocked whether R=Me or *tert*-Bu. Conformers **v** and **vii** with the lowest energy are the most stable, and attack by H^-

on the *si* or *re* face (for **v** and **vii** respectively), would be predicted to give the corresponding products **A1** and **A2** as observed.[12]

Not all asymmetric induction in open chain compounds relies on the influence of a bulky substituent. Instead a strategically placed functional group may become the agent which determines the configuration of a new chiral centre. This is illustrated in the intramolecular 1,3-diastereoselection shown during the synthesis of HR780 (Figure 5c) by Wess *et al.* [13] HR780 is an inhibitor of the enzyme HMGCoA reductase and may be used in the treatment of atherosclerosis. The ketone function of reactant **A1** is reduced stereospecifically because the borohydride appears to coordinate to the neighbouring hydroxyl group.

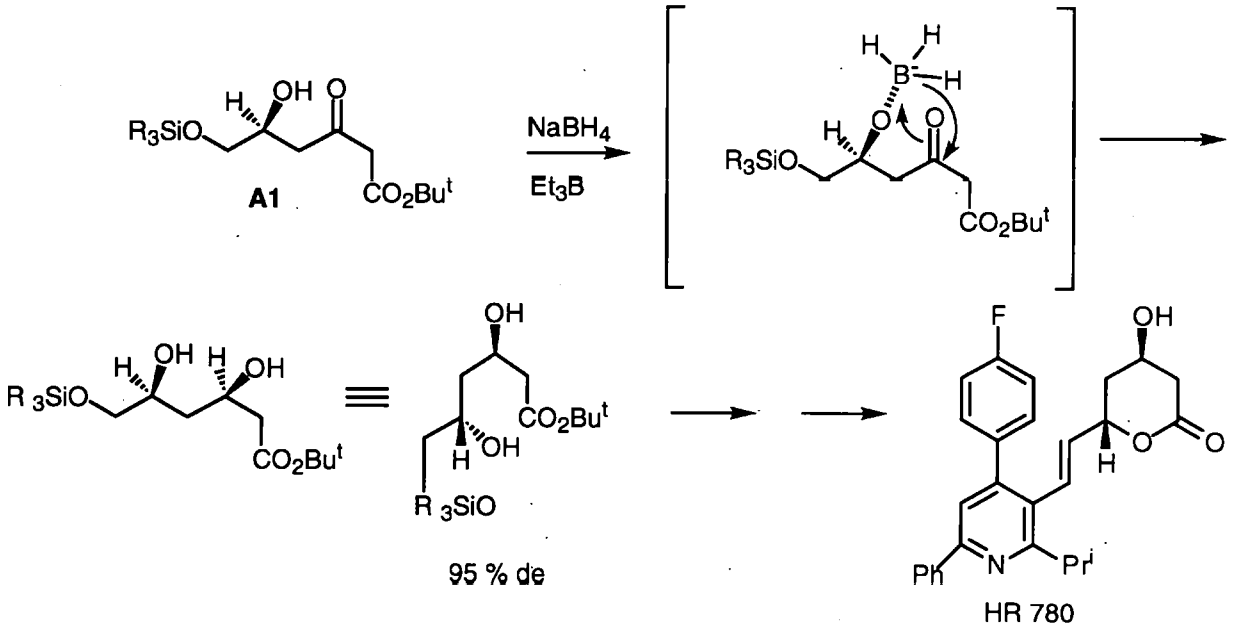

Figure 5c

The advantage of cyclic systems

Progress in diastereselectivity can be achieved when using cyclic systems with their lesser ability for rotational freedom, as in the formation of **B** in figure 5d.[6]

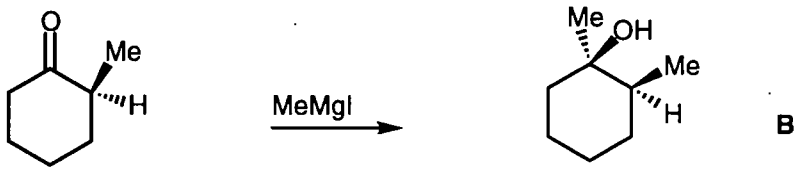

Figure 5d

This can also be seen in the reduction of 4-*tert*-butylcyclohexanone (Figure 6), for it is the equatorial alcohol isomer that predominates.[14] Delivery of the hydride ion would be from the upper face of the cyclohexanone ring, to give the more stable equatorial alcohol.

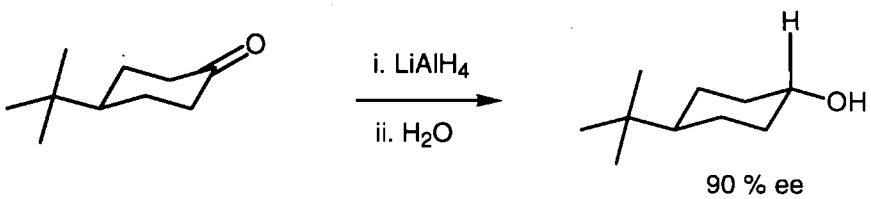

Figure 6

An ingenious way of using a substrate-controlled method was developed by Seebach[15] in the synthesis of α-methylproline (Figure 7). This can also be described as a self-reproduction of chirality.

Condensation of (*S*)-proline with pivaldehyde gives the oxazolidinone (**C**). This compound is highly sensitive to hydrolysis and on contact with moist air spontaneously formed proline with unchanged optical activity in comparison to the starting material, proving that racemisation does not occur during the pivaldehyde or hydrolysis reactions.

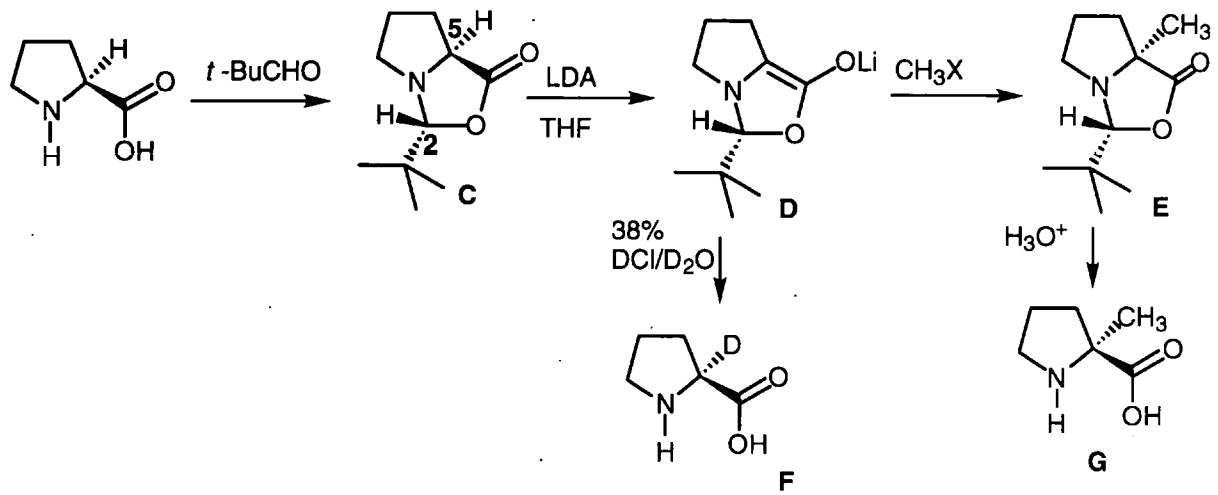

Figure 7

The oxazolidinone could be crystallised from pentane at -40 °C for use in subsequent reactions. The bulky *tert*-butyl group in **C** is placed *exo* with respect to the bicyclo ring system, creating a new stereogenic centre in high stereoselectivity. The enolate of the lactone was formed using lithium diisopropylamide in tetrahydrofuran at -78 °C (**D**). Deuterolysis of **D** gave α-deuterioproline (**F**) again of the same optical activity as the starting proline. Trapping of the enolate with an electrophile (iodomethane), gave a single bicyclic diastereomer (**E**) which was more stable than the original condensation product (**C**). Acid hydrolysis of **E** led to the

(*S*)-α-methylproline (**G**). From these results, it appears that after the original stereogenic centre is destroyed on conversion into an sp^2 centre (by enolisation), the alkylation is directed solely to the *exo*-face of the bicyclic system.

Some general conclusions are possible from the assignment of configuration to the product **G** obtained from the enolate **D**.

(i) The electrophilic substitution occurs with overall retention of configuration.

(ii) In the bicyclic derivative **C**, the *tert*-butyl group is placed *exo* with respect to the bicyclo ring system and is *cis* to the C-5 hydrogen, at the bridgehead. Compound **C** is therefore the (*2R,5S*) enantiomer.

(iii) The enolate (**D**) has the *R* configuration.

(iv) Electrophilic attack on the nucleophilic centre of **D** is from the *re* face, thus placing the new substituent and the *tert*-butyl group *cis* to each other on the *exo*-face

Alkylation with reactive electrophiles gave products in excellent yields and with high diastereoselectivity (Table 1).

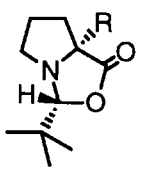

R	% Yield	% de
CH_3	93	>99
$CH_2CH_2{=}CH_2$	87	>99
$CH_2C_6H_5$	91	>99

Table 1

Less reactive electrophiles (e.g. *tert*-butyl and *sec*-butyl iodides) gave no product. Such electrophiles approaching the enolate from the *exo*-face of the bicyclic molecule, would encounter increased steric hindrance from the already present (*cis*)*tert*-butyl moiety .

The Seebach group[16,17] have shown that other simple amino acids such as (*S*)-alanine, (*S*)-valine, (*R*)-phenylglycine, (*S*)-phenylalanine and (*S*)-methionine can be converted into imidazolidinones, which can be deprotonated to give chiral enolates. Diastereoselective alkylation of these enolates and hydrolysis gave α-alkyl-α-amino acids. Using (*S*)-alanine they prepared the aromatic acid **AA** without racemization (Figure 8).

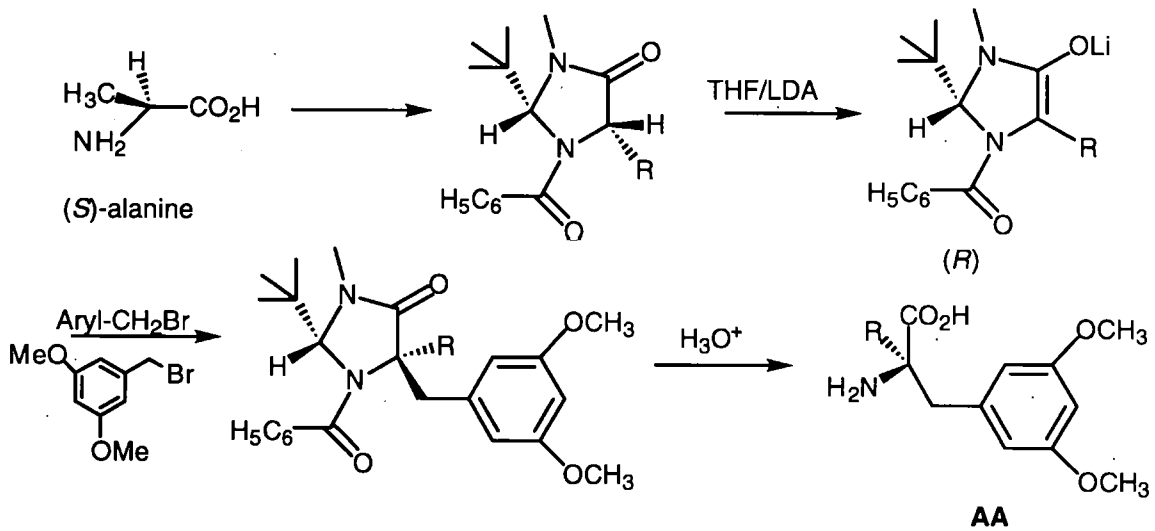

Figure 8

The Seebach "self - reproduction of chirality",[18] which uses strongly basic anhydrous conditions at -78 °C, has been developed by O'Donnell *et al.*[19,20] by the use of phase-transfer catalysis or KOtBu at room temperature for ethylations of protected oxazolidinones, where R is t-Bu (Figure 9).

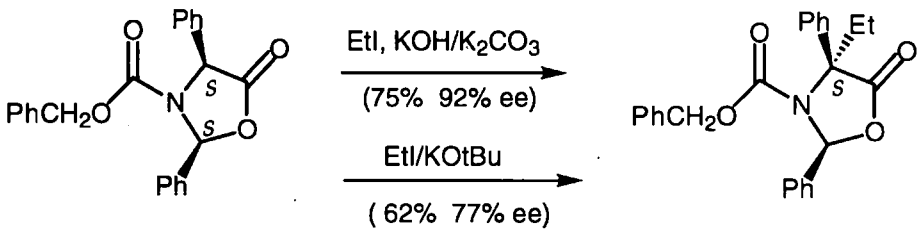

Figure 9

This work was extended by the Seebach group[21] to the α–alkylation of optically active carboxylic acids without racemization, using "self-reproduction of chirality". The acetal derivatives of α-hydroxycarboxylic acids were alkylated *via* the lithium enolate to give products, with retained configuration (Figure 10).

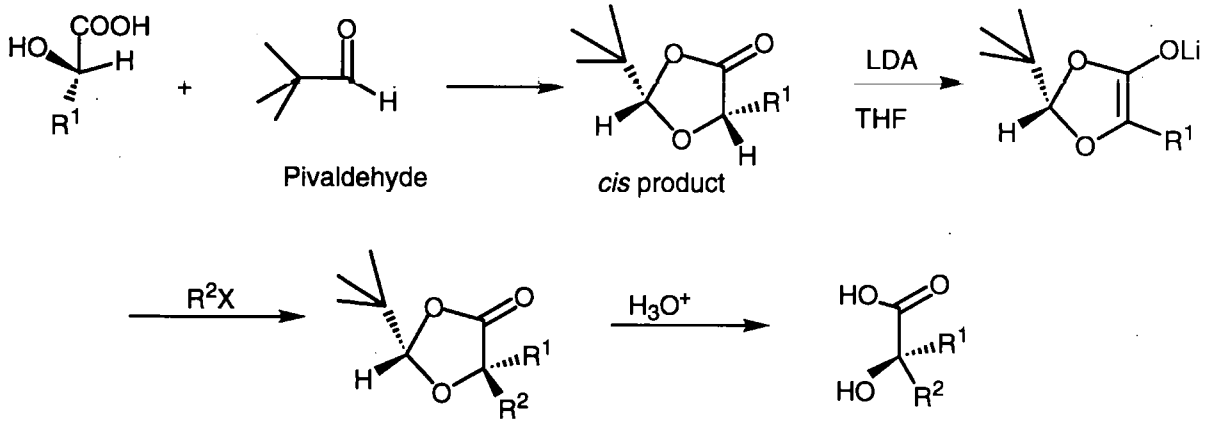

Figure 10

Use of a number of different alkyl halides gave α–substituted hydroxy acids with excellent diastereoselectivities (Table 2).

R^1	R^2X	% Yield	% de
CH_3	C_2H_5I	82	97
CH_3	C_3H_7I	72	97
CH_3	C_4H_9I	68	97
CH_3	$C_7H_{15}I$	84	96
CH_3	$CH_2CH{=}CH_2Br$	77	98
CH_3	$CH_2C_6H_5Br$	81	96
C_6H_5	C_3H_7I	84	95
$CH_2C_6H_5$	CH_3I	30	>95
$CH_2C_6H_5$	C_2H_5I	45	>95
$CH_2C_6H_5$	C_3H_7I	40	>95
$CH_2C_6H_5$	$CH_2CH{=}CH_2Br$	40	>95

Table 2

Using a similar approach in the synthesis of α-disubstituted α-amino acids from suitable oxazines (Figure 11a). Williams *et al.* [22] were able to produce these compounds in high yields with very good to excellent enantioselectivities (Table 3).

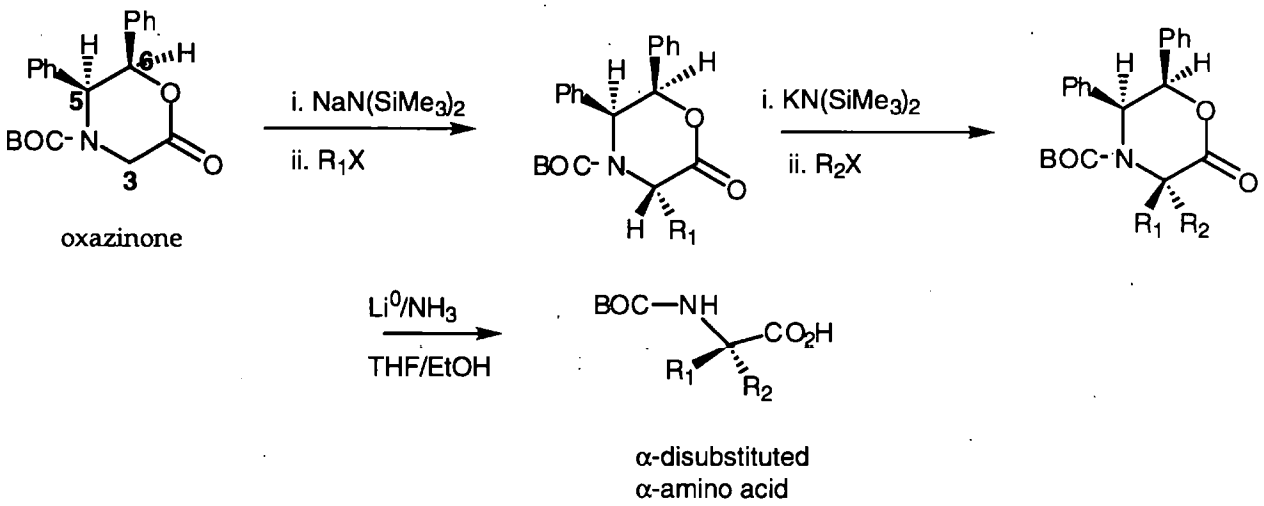

Figure 11a

		Amino Acid	
R	R_2	% Yield	% ee
CH_2=CHCH_2-	-	50-70	98
CH_3-	-	54	97
PhCH_2-	-	76	98
PhCH_2-	-	93	>99
CH_3-	CH_2=CHCH_2-	70	100
CH_3-	PhCH_2-	93	100
n-C_3H_7	CH_2=CHCH_2-	60	100
CH_3-	PhCH=CHCH_2-	95	100

Table 3

Figure 11b illustrates the expected twist-boat conformation for the intermediate enolate (cf. House *et al.* [23]), which positions the phenyl group at C-5 of the oxazinone in a pseudoaxial orientation. This creates an environment at C-3, sterically shielded from electrophilic attack and the incoming alkyl group approaches the less shielded face, to favour in both cases, the product formed by *si* face attack. The major advantage of this method is the ability to generate the Boc derivatives of these α-disubstituted α-amino acids directly.

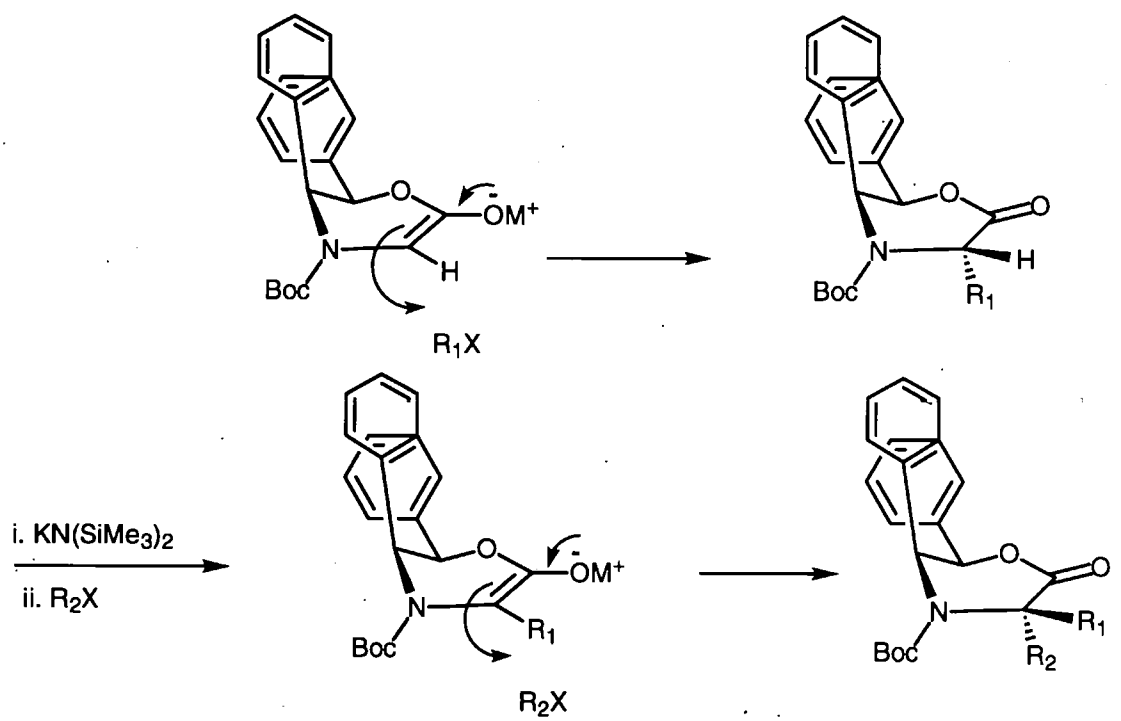

Figure 11b

Another example is seen in the asymmetric synthesis of the unusual amino acid statine by Williams *et al.*[24] The key step involves substrate control during the coupling of the starting hemiacetal with ketene silylacetal **a** in Figure 12a.

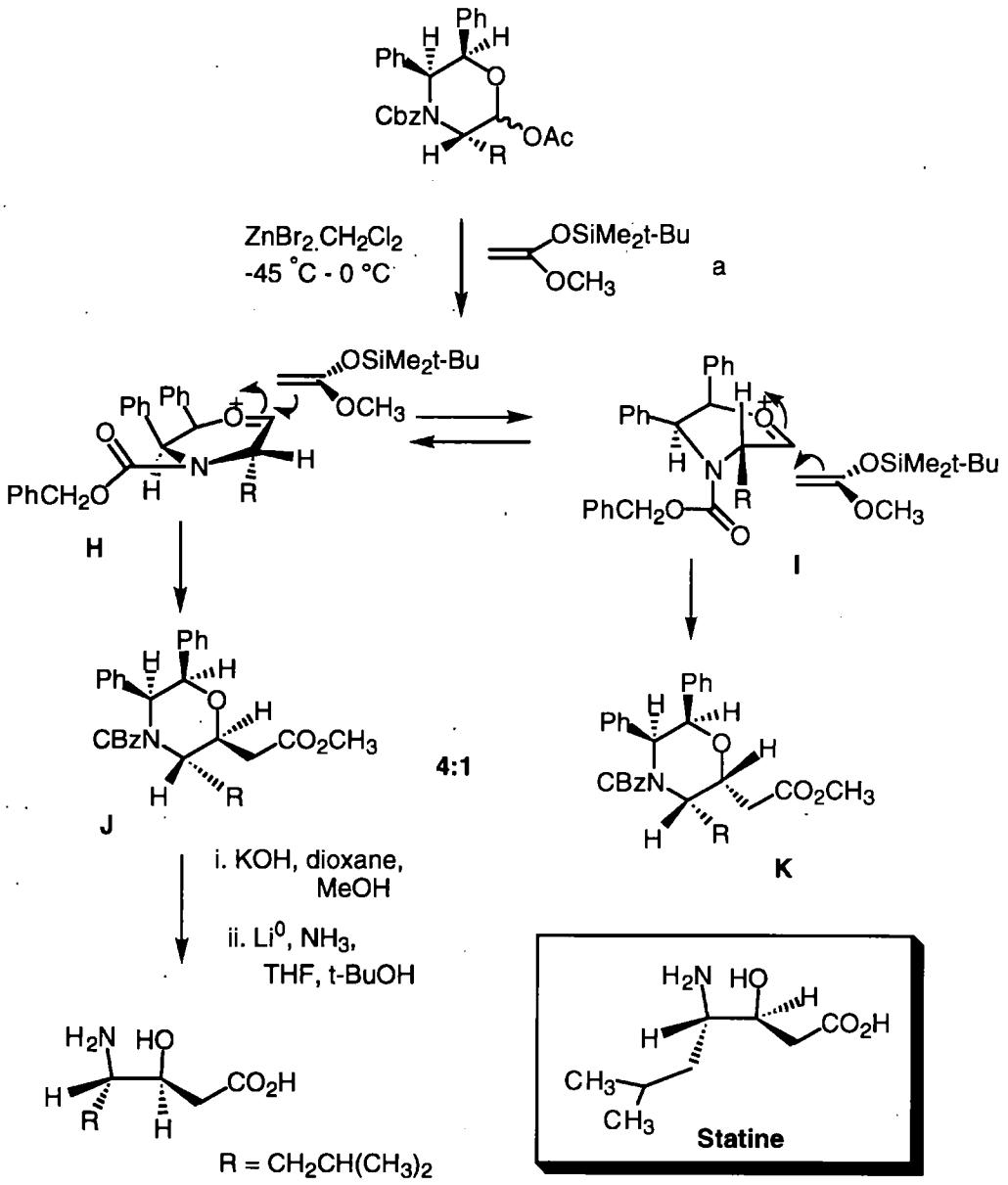

Figure 12a

Here it is presumed that the conformation of the oxonium ion that has been generated, influences the diastereoselectivity of the reaction. The diastereoselectivity of **4:1** for compounds **J** and **K** was observed when the R group was either *iso*- butyl or methylcyclohexyl. However when the methyl derivative was prepared the selectivity was 3:**2** in favour of diastereoisomer **K**. It was presumed[24] that the conformation of

the two relevant oxonium ions generated was as shown in Figure 12a (**H** and **I**). Conformer **H** was thought to be favoured in the *iso*- butyl and methylcyclohexyl systems, when the steric bulk of these two groups is better accommodated when they are placed in the *pseudo* -axial position. This conformation was considered to minimise strain and diaxial compression between the R group, the carbobenzyloxy group and the methine ring proton respectively. Attack by the ketene silylacetal would presumably now proceed at the *si* face. In the methyl system the equilibrium between the conformers (**H** and **I**) was assumed to shift in favour of conformer **I**, where the less bulky methyl group is able to adopt a *pseudo* -equatorial position, which places the phenyl ring, adjacent to the oxonium ion, into an axial orientation, thus shielding the *si* face from nucleophilic attack. Indirect evidence for the involvement of the planar oxonium ion as the reactive species, was provided by separating the diastereomeric (roughly equimolar) acetates and reacting each isomer separately with the ketene silylacetal. The resulting diastereomers were obtained in the same ratio (4:1) as that obtained when the diastereomers were used as a mixture.

However molecular modelling using PCMODEL suggests a different interpretation of these results. Thus the two major comformers with the *iso*-butyl substituent (***a*** and ***b***, Figure 12b) differ in energy by 5.1 kcal mol^{-1}. The corresponding isomers of the conformer with the methyl substituent (***c*** and ***d***, Figure 12b) differ in energy by the even larger amount 5.4 kcal mol^{-1}. (These calculations are carried out at the MMX level.)

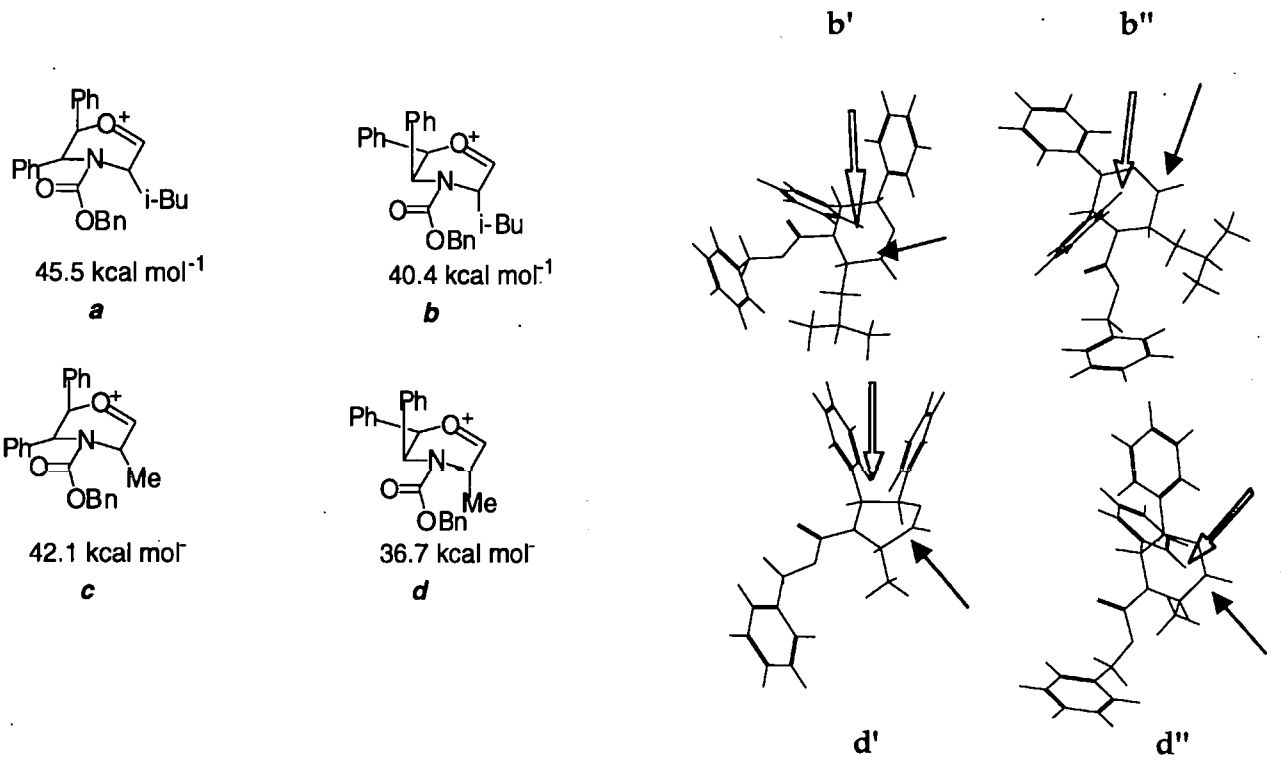

Figure 12b

The most stable conformer of each pair (***b*** and ***d***, respectively) has the conformation of conformer **H** in Figure 12a. There is no shift in equilibrium towards conformer ***c*** as suggested by Williams *et al.*[24] Indeed, the equilibrium between ***c*** and ***d*** (Figure 12b) lies even more towards conformer ***d*** than with the *iso*-butyl substituted compound (***a*** and ***b***). These results are explicable if approach of the nucleophile from above and behind the oxonium carbon atom is assumed (the Bürgi-Dunitz trajectory):

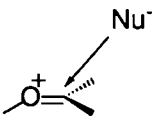

In both conformers ***a*** and ***b*** (Figure 12b) the lower (*re*) face of the oxonium system is obstructed by the *iso* butyl group. This is illustrated in the energy minimised structures ***b'*** and ***b*** ''(figure 12b). The top (*si*) face is relatively unhindered except that a hydrogen atom (open arrows in structures ***b'*** and ***b''***, which are two views of the energy minimised conformer ***b***), is situated above the *si* face and at a distance of 2.7Å from the oxonium carbon atom (arrowed). The same is true for the methyl substituted analogue ***d', d''***. This overhanging feature may offer some obstruction to the nucleophile appoaching the *si* face along the Bürgi-Dunitz trajectory.

In the methyl substituted analogue ***d***, the *re* face is much less obstructed (see stucture ***d''*** in Figure 12b). In this case, the obstruction by the phenyl ring hydrogen atom is apparently greater than that offered by the methyl group and attack is relatively more rapid on the lower, *re* face, but only by a small amount as indicated by the 3:2 product ratio in favour of the **K** isomer (Figure 12a).

The induction discussed so far has depended upon the bulk of attached groups or strategically placed functional groups, to direct the asymmetry of the new stereogenic centre. Agami *et al*,[25-28] have used a morpholine derivative **L** (Figure 13), as a chiral template to synthesise α-*N*-methylamino esters. Here again, the key step in this synthesis is substrate controlled, but the configuration of the starting compound is now the directing influence. Diastereoselective C-C bond formation (retention of configuration) is observed on the substitution of the thiophenyl moiety, when alkylzinc halides were used.

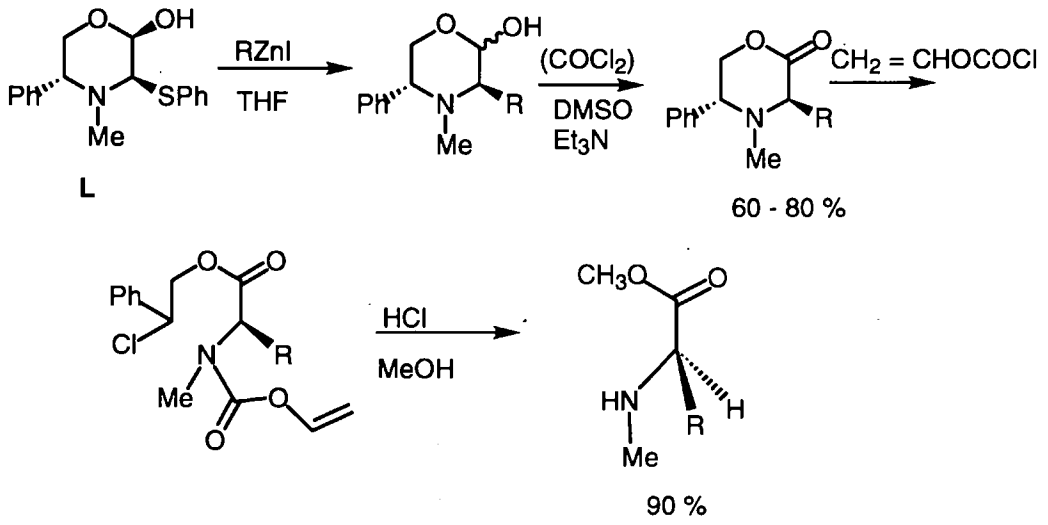

Figure 13

Figure 14 shows a possible mechanism for the reaction, which accounts for the necessity for two equivalents of the organozinc halide and the *syn* attack of the double bond with respect to the hydroxyl group. The first forms a zinc alkoxide with the hemiacetal and the second is needed for the alkylation. The formation of an immonium ion intermediate and the subsequent stereodirecting effect from the metaloxy group also formed, account for the overall stereo-retention.

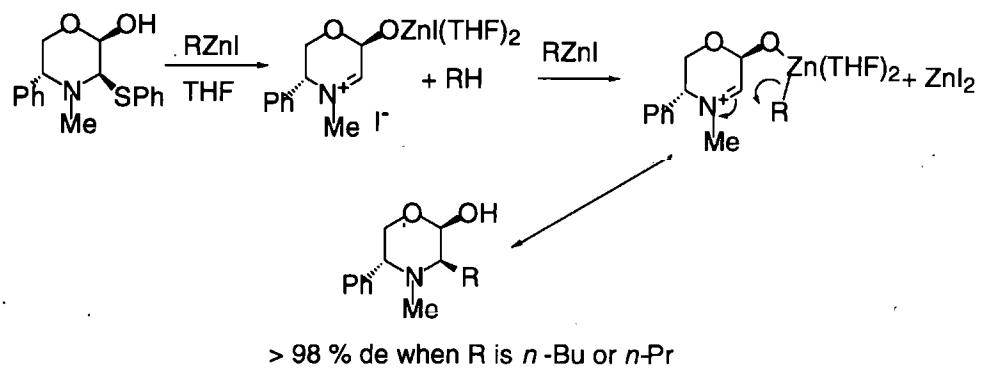

Figure 14

Stereochemically, the zinc alkoxide intermediate that is formed is in a position to direct an axial attack, thus leading to overall retention of configuration. The combination of conformational control in the cyclic system and the intervention of the ring heteroatom in the reaction is a potent force for inducing stereochemistry.

2.2 Reagent controlled methods

As this brief survey has shown, asymmetric syntheses involving only substrate control-led methods rely on enantiomerically pure starting materials. The chiral product is not formed from an achiral starting material, but additional stereogenic centres are formed in the enantiomerically pure substrate. In reagent-controlled asymmetric synthesis, a chiral reagent directly converts an achiral substrate into the chiral product. Here the control is *intermolecular*. For these control methods, there is a much wider choice of starting material than in the substrate-controlled procedures, as there is no need for an enantiomerically pure substrate.

Asymmetric synthesis using boron reagents

Reduction using boron hydrides bearing chiral groups illustrates this asymmetric control method.[29] Figure 15 shows that in reactions involving *R*-Alpine-borane, a rigid six-membered heterocyclic transition state incorporating the carbonyl group may be passed through. This cyclic transition state adopts a boat-like conformation, in which the larger group (R_L) is placed in the *pseudo*-equatorial position. The hydride is then transferred preferentially from the carbon atom adjacent to the carbon atom bonded to the boron to the upper face (*re* face) of the carbonyl group.

The enantioselectivity of the reaction is reasonable and is particularly effective with acetylenic ketones up to 86 % ee. The α-pinene is regenerated and can be reconverted into Alpine-borane.

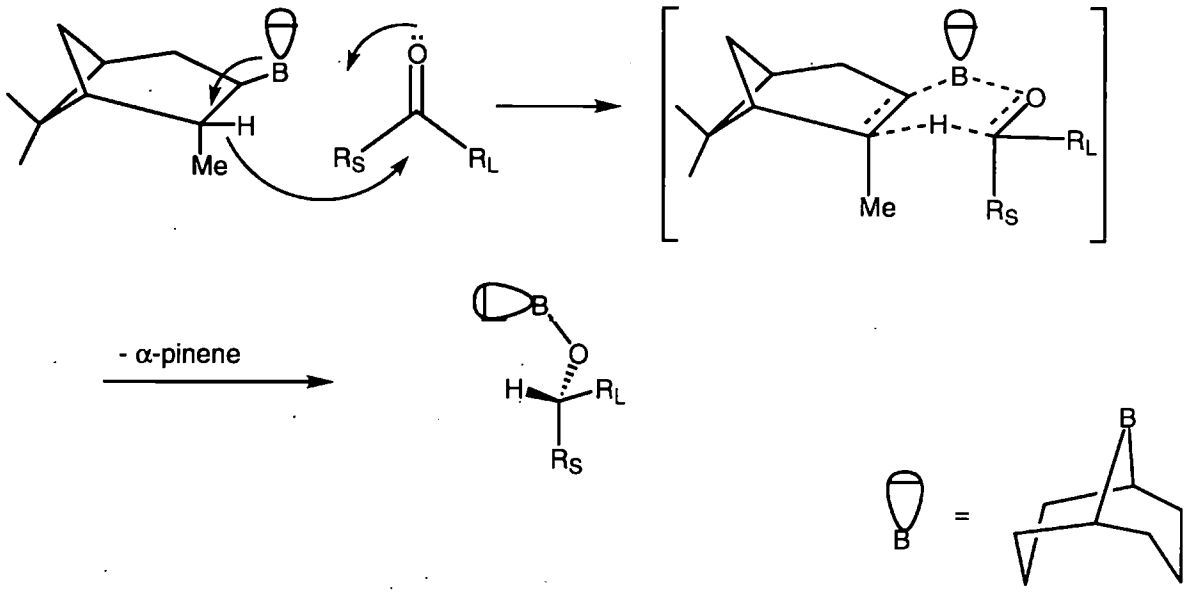

Figure 15

Earlier work by Corey and co-workers[30,31] has established probably the most general method of asymmetric ketone reduction. A variety of achiral ketones were reduced using chiral oxazaborolidines as catalyst (**M** Figure 16) and catecholborane as reductant (Figure 16). This method is thought to involve a transition state assembly as shown in Figure 16. The secondary alcohols are produced with good enantioselectivity (80-97 % ee) and the chiral reagent is again regenerated.

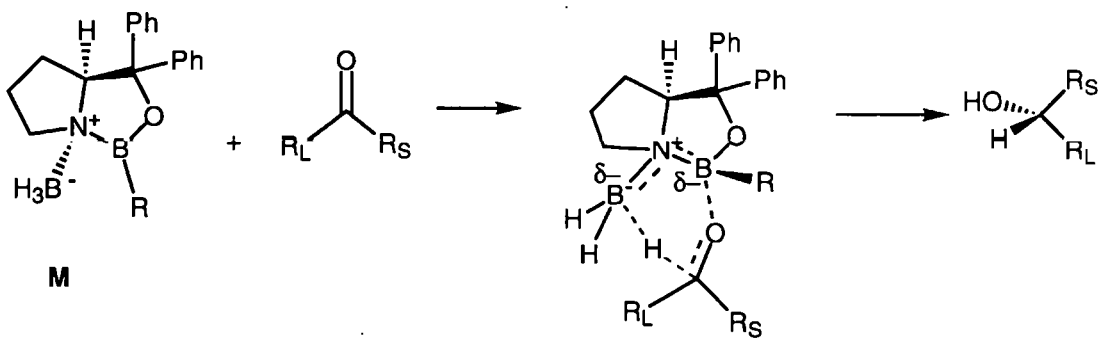

Figure 16

In the asymmetric hydroboration of alkenes[32,33] the chiral reagent Ipc_2BH (diisopinocampheylborane) is widely used. It is commercially available in both enantiomeric forms (Figure 17a). This reagent works well with both acyclic and cyclic alkenes and is a key reagent in the synthesis of loganin (**N** Figure 17b), the precursor of secologanin and the terpenoid indole alkaloids.

Figure 17a

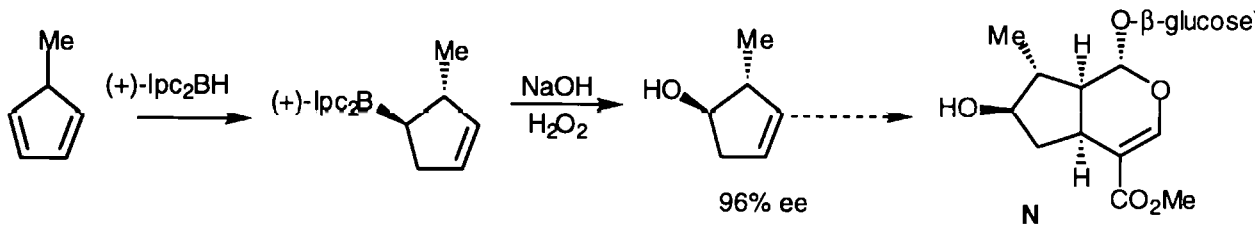

Figure 17b

Work by Hua *et al.* [34] on asymmetric hydroboration of sulphinimines using stereoselective reduction with 9-borabicyclo[3,3,1]nonane (9-BBN), resulted in the efficient synthesis of optically pure α-amino acids (Figure 18). A six-membered-ring transition state is proposed where the boron chelates with the oxygen of the sulphinamide and the approach of the hydride reagent therefore occurs from the *si*- face of the sulphinimine. The use of this reducing agent gave the *R*-diastereoisomer exclusively, as illustrated in Figure 18. The reported optical purity was >95%.

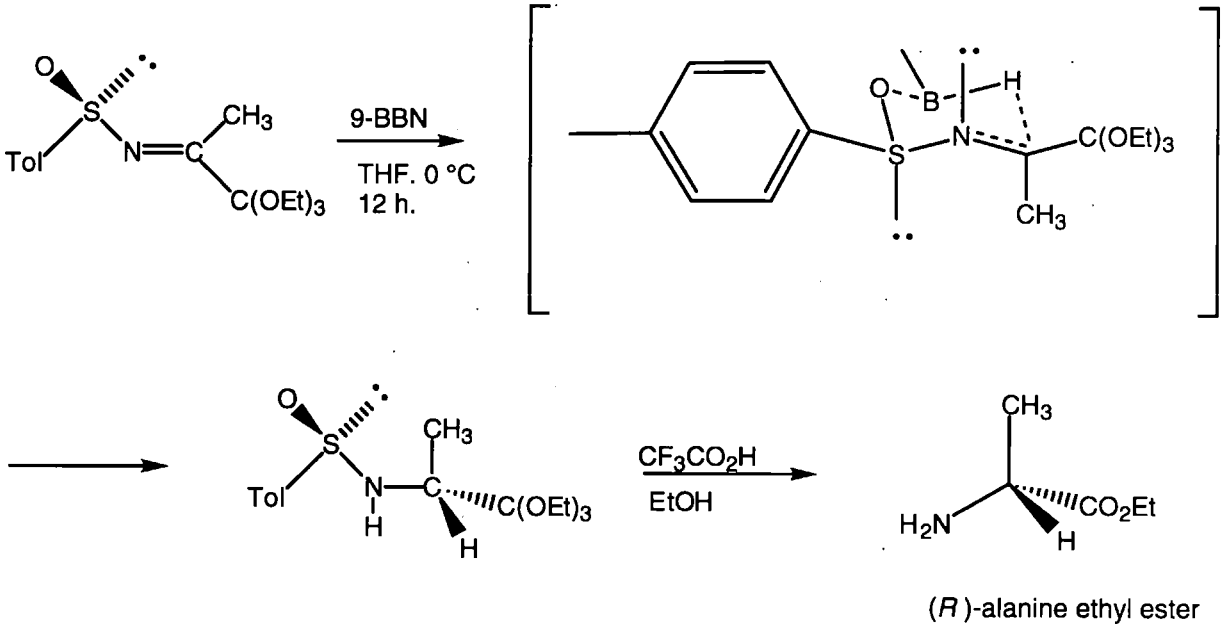

Figure 18

In another novel synthesis of optically active α-amino acids, Demir[35] used a chiral boron reagent derived from (-)-norephedrine and a BH_3.THF complex, to reduce *E* or *Z* oxime ethers enantioselectively (Figure 19a).

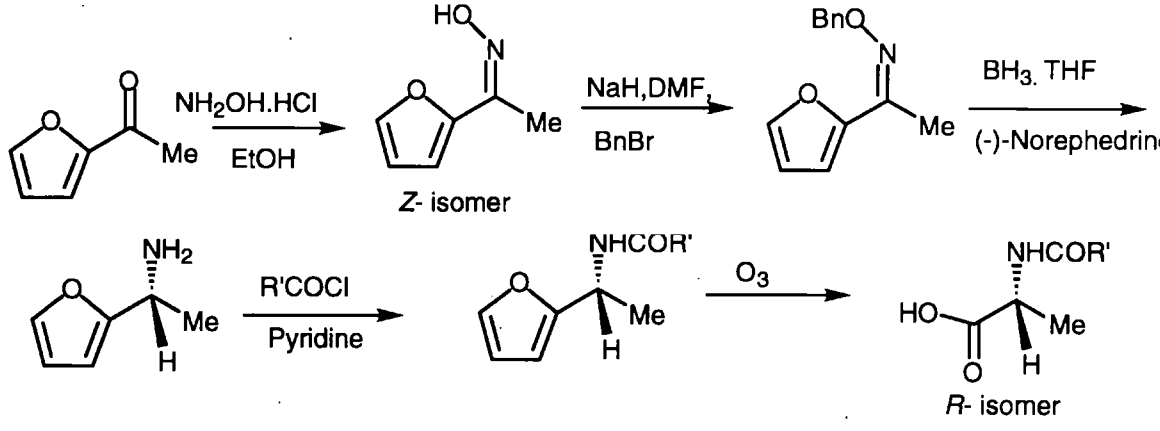

Figure 19a

Analysis of the Demir chemistry was investigated using PCMODEL. The Demir reaction is postulated to proceed *via* the intermediate complex **A** (Figure 19b). This intermediate contains three configurational/conformational variables:

1. The configuration at B-1 can be either *R* or *S*.
2. The configuration at N-2 can be either *R* or *S*.
3. The five-membered heterocyclic ring can adopt one of two envelope conformations in which C-4 is either above or below the plane defined by B-1, N-2, C-3 and C-5.

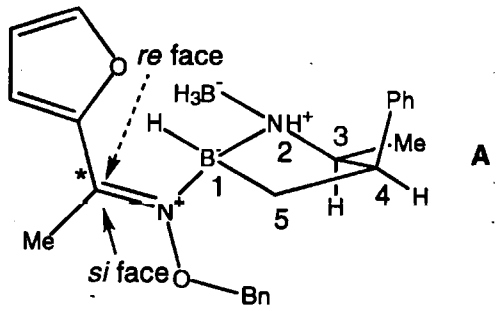

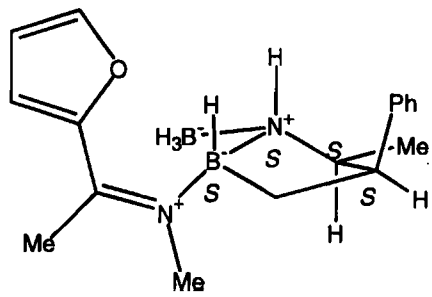

1a

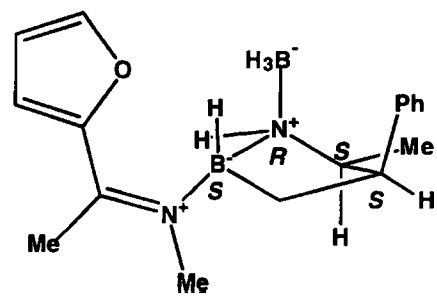

1b

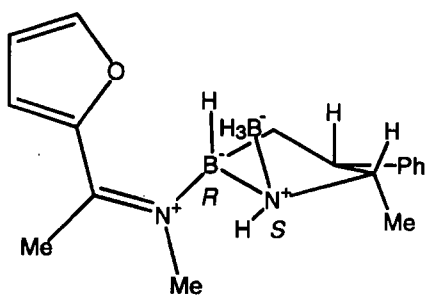

2a

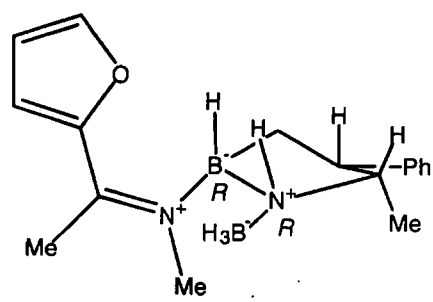

2b

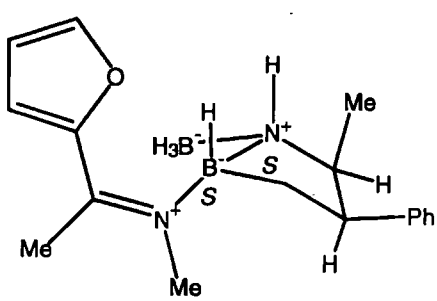

3a

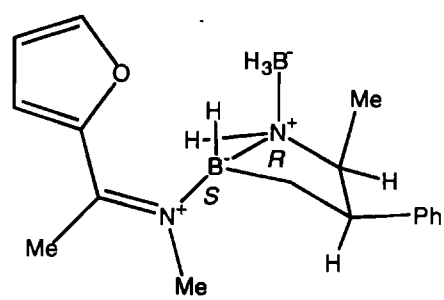

3b

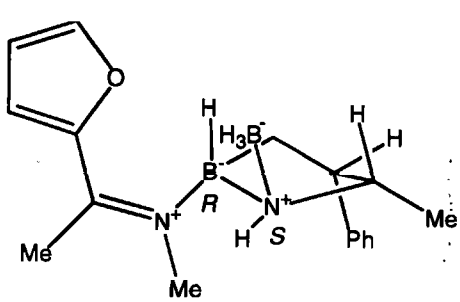

4a

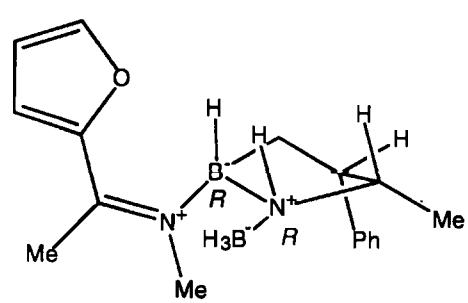

4b

Figure 19b. (In **A** dashed arrow indicates behind and full arrow indicates in front).

According to the proposed mechanism, a hydride ion is delivered by the BH_3 group to the asterisked carbon atom in structure **A**. This can deliver a hydride ion either to the *si* face (from the front in structure **A**) or to the *re* face (from behind in structure **A**). In the first case, the *R*-amine is formed, in the second the *S*-amine is formed.

PCMODEL cannot handle an oxygen atom attached to a quaternary nitrogen (parameters missing). Accordingly the benzyloxy group in **A** is replaced by a methyl group in the modeling studies. Parameters for the B-O bond are also not available and so the ring oxygen similarly has been replaced by a methylene group.

The two alternatives in each of the variables 1-3 (p.27) lead to eight different combinations of configuration/conformation. These are shown as **1a, b** to **4a, b** in the Figure. When these structures are energy-minimised, the data given in the Table can be extracted from the minimised structures.

Structure	Config. B-1	Config. N-2	Ph subst.	MMX energy/ kcal mol^{-1}	H.....C distance Å	Face attacked
1a	*S*	*S*	axial	0.87	3.0	*re*
1b	*S*	*R*	axial	5.30	4.0	*re*
2a	*R*	*S*	equatorial	1.68	3.8	*si*
2b	*R*	*R*	equatorial	3.83	3.4	*si*
3a	*S*	*S*	equatorial	-0.54	2.9	*re*
3b	*S*	*R*	equatorial	1.71	3.9	*re*
4a	*R*	*S*	axial	4.96	4.1	*si*
4b	*R*	*R*	axial	10.40	3.5	*si*

Table 4

It can be seen that whether attack takes place on the *re* or *si* face of the carbon-nitrogen double bond depends on whether the configuration at B-1 is respectively *S* or *R*. In column six is given the distance between the hydrogen atom of the BH_3 group in the minimised structure that is closest to the electrophilic carbon atom, and the carbon atom itself. The two lowest energy structures, **1a** and **3a** have correspondingly the lowest values for this distance. In other words, in these lowest energy structures, the hydride ion to be delivered is already closest to the target carbon atom. Both of these structures deliver the hydride ion to the *re* face of the double bond leading ultimately to the *S*-amine, as observed experimentally. Changing the configuration of the double bond from *E* to *Z* would reverse the stereochemical course of the reaction and *R*-amine would be produced.

Because the formation of the borane complex is reversible, it would appear likely that the active complex reacts mainly through the lowest energy conformation. (The complexes would have a Boltzmann distribution.) The relative energies of these complexes are determined by the interaction between the substituent on the ring boron and the substituent at N-2, and the methyl and phenyl groups at C-3 and C-4 respectively. Thus the chirality of the *nor*-epehedrine controls the stereochemical outcome of the reaction. The group replacements made to make possible PCMODEL calculations will give relative energies different from the true compounds. However, because induction of asymmetry appears to arise from mainly steric effects, the overall conclusions are still valid.

The reducing component adopts a conformation in which it is *anti* to the bulky methyl and phenyl groups of the boron heterocyclic ring. This forces hydride delivery to the *re*-face of the *E*-isomer and to the *si*-face of the *Z*-isomer.

The final enantiomer of the amino acid is therefore fully dependent on whether the *E* or *Z* isomer of the oxime ether is used.

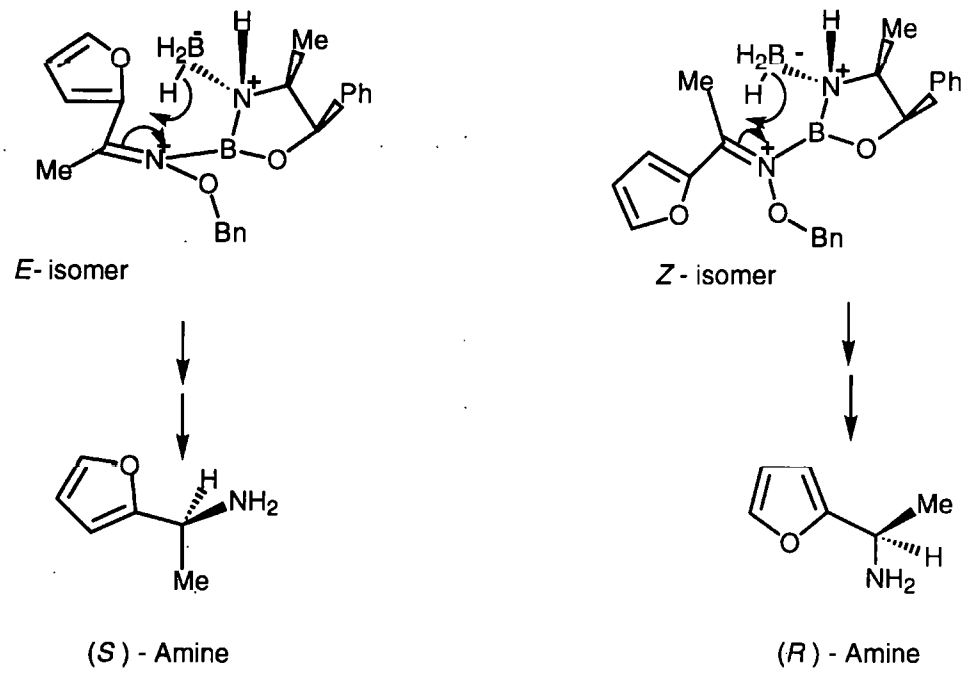

Figure 20

The (-)-norephedrine/BH_3.THF (Figure 20) complex gave the furylamines in good yield and 93-96 % ee (Table 5).

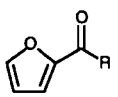

Furyl ketone R =	Oxime	Configuration	Furylamine % Yield	% ee
Methyl	*E*	(*S*)	77	96
	Z	(*R*)	72	94
Ethyl	*E*	(*S*)	81	96
	Z	(*R*)	78	93
i-Propyl	*E*	(*S*)	81	96
	Z	(*R*)	83	95

Table 5

The results of reactions where Demir and co-workers used different amino alcohols instead of (-)-norephedrine with the borane THF complex are shown in Table 6. These gave a lower degree of enantioselectivity (47-76% ee) for the furylamine, except for one of the compounds (**Q**), prepared from (*S*)-proline. All the amino alcohols were easily recovered for re-use.

Amino alcohol	Furylamine	
	% ee	configuration
(*S*)-3,4-Prolinol	61-73	*S*
(*S*)-3,5-Valinol	47-53	*S*
(1*R*, 2*S*)-Ephedrine	48-76	*S*
O (see below)	51-72	*S*
P (see below)	53-68	*S*
Q (see below)	78-95	*S*

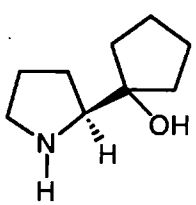

O

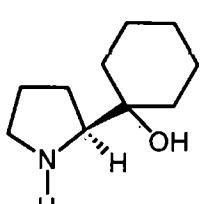

P

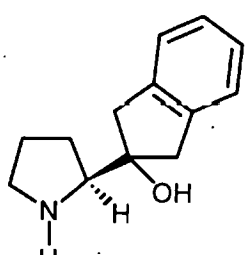

Q

Table 6

Other systems used for control

Further work on the use of sulphinimines in the asymmetric synthesis of enantiomerically pure α–amino acids, has been carried out by Davis *et al.* [36,37] Et(R'O)AlCN was used for the addition of cyanide to the sulphinimine. The configuration of the product was consistent with the complexation of the Et(R'O)AlCN and the sulphinyl oxygen as shown in Figure 22. The product diastereomeric ratios were in the range 82-96 %. Acid catalysed hydrolysis removed the sulphinyl auxiliary and hydrolysed the nitrile group to afford the enantiomerically pure amino acids (>95% ee).

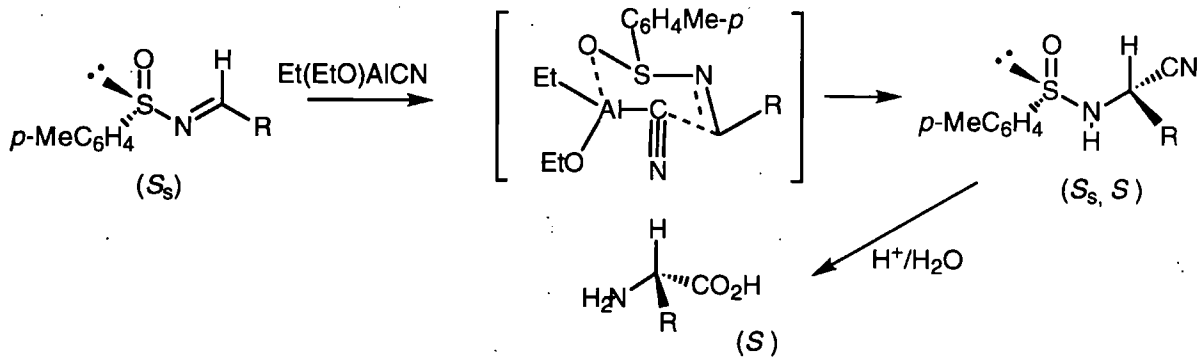

Figure 22

These examples of asymmetric synthesis illustrate that where there is a rigid transition state or a heterocyclic moiety present, greater enantio-selectivity or diastereoselectivity is achieved. These cyclic states hold the molecule in a fixed conformation, unlike the conformational freedom of even strongly *preferred* conformations of open chain compounds.

2.3. Catalyst controlled methods

In these methods the chiral information is brought into the transition state *via* a chiral catalyst, which directly converts an achiral substrate with an achiral reagent into the required chiral product. The overall control is again *intermolecular*. The great advantage of these methods is in the recovery of the unchanged catalyst, the latter generally being used in only catalytic amounts.

Boron containing catalysts

A general catalytic method for the enantioselective synthesis of amino acids was developed by Corey *et al.* [38] This group used catecholborane for the reduction of trichloroacetyl ketones in the presence of (*S*)-oxazaborolidine catalyst **S** (Figure 23), to the (*R*) secondary alcohols (**T**) with high enantioselectivity. The mechanism of this reaction was discussed above (see Figure 16).

The (*R*)-(trichloromethyl)carbinols (**T**) were treated with a basic solution of NaN_3 which gave a smooth conversion into the (*S*)-α-azido acids (**U**) and a clean inversion of configuration at the α-centre. The azido group was then converted into the amino group (**V**) by reduction with a hydrogen/palladium catalyst (Figure 23). It is thought that the reaction proceeds *via* the *gem*-dichlorooxirane intermediate shown in Figure 23.

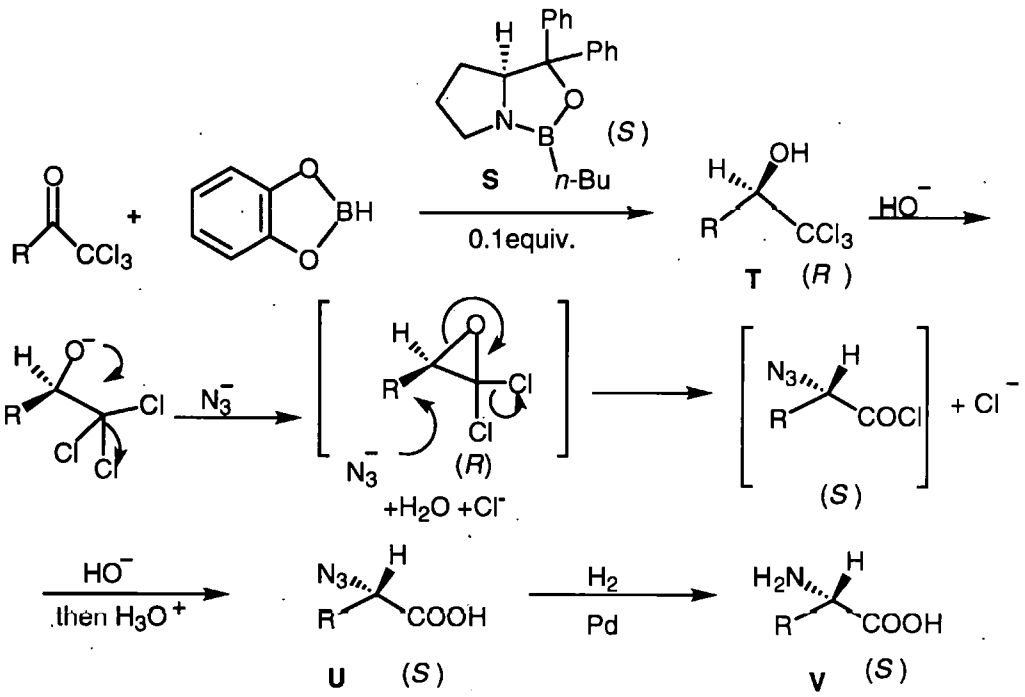

Figure 23

The high yields and mild conditions of this reaction (Table 6.), indicate a high degree of reactivity of the *gem*-dichlorooxirane intermediate, through an S_N2 displacement by the azide ion, with consequent ring opening to form the α-azide carbonyl moiety. This high reactivity accounts for the effectiveness of this synthesis of a range of alkyl glycines (Table 7).

R in $RCOCCl_3$	**T** (% ee)	% Yield of **U**	% Yield of **V**
n-C_5H_{11}	95	89	94
$C_6H_5(CH_2)_2$	95	92	92
4-$C_6H_5C_6H_4CH_2$	96	82	98
2-Naphthylmethyl	93	84	88
t-C_4H_9	98 (-20 °C)	80	94

Table 7

Noble metal catalysts

An important industrial application of catalyst control is in the synthesis of amino acids by catalytic asymmetric hydrogenation of amidoacrylates (**W** Figure 24). This catalytic reaction is the key step in the production of L-DOPA by the Monsanto process [39,40,41] (Figure 24), and relies on a diphosphine compound, DIPAMP, (Figure 25), which is chiral at phosphorus, and acts as a bidentate ligand in the formation of a soluble rhodium catalyst.

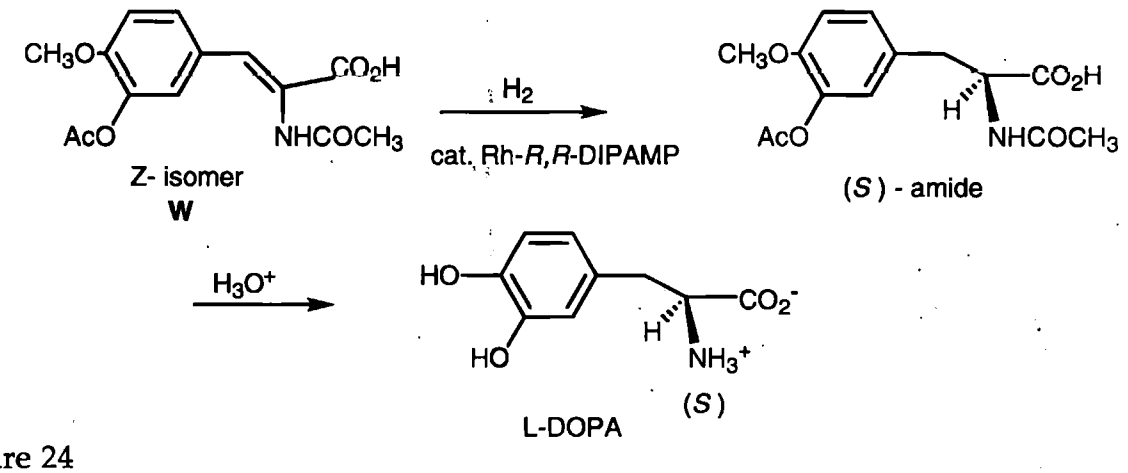

Figure 24

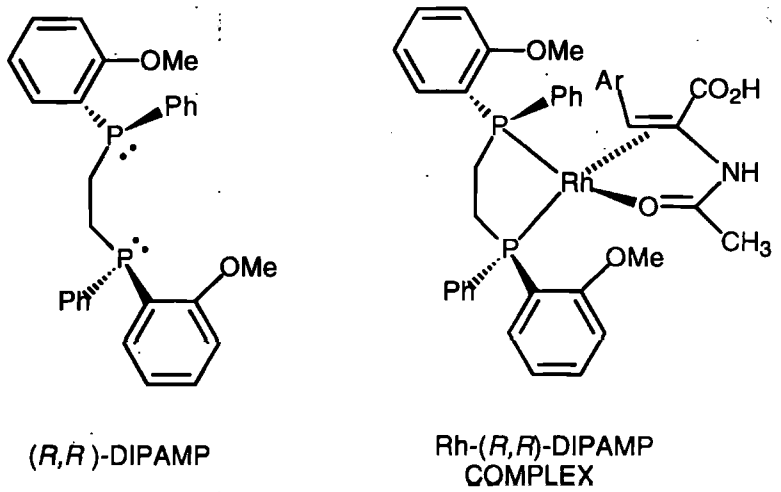

Figure 25

The complex formed (generally octahedral) between the transition metal and the biphosphine is a rigid, five-membered ring. The alkene and amide carbonyl groups are also coordinated to the rhodium. Rotation is prevented around the metal-phosphorus bond, which results in increased enantioselectivity in the reduction process of the amidoacrylate. L-DOPA is formed with an enantiomeric excess of 94%.

A number of other L-amino acids have been made by the same route with high enantioselectivity.[41]

Trost and Ariza [42,43] have developed a catalytic synthesis for α-alkylation of amino acids through their azlactones. An acyl enol ether is used as the alkylating agent. The overall alkylation reaction is shown Figure 26a. The minor product diastereisomer was removed by column chromatography.

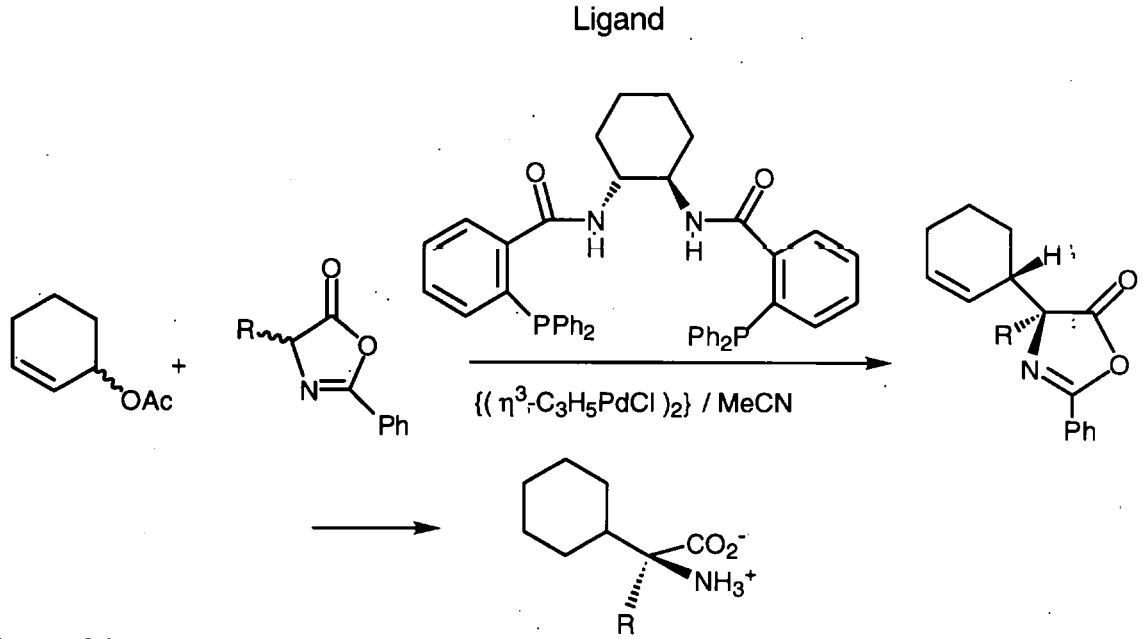

Figure 26a

Table 8 summarizes the results of the alkylation of a range of azlactones, and as was expected increasing the size of the R group (CH_3 in Figure 26a), increased the diastereomeric ratio (dr).

R	% Yield	Diastereomeric ratio	% ee
CH_3	90	8.7:1	99
CH_3Ph	74	12.4:1	99
$CH_2CH(CH_3)_2$	77(a)	13.3:1	99
$CH(CH_3)_2$	91	>19:1	95

Table 8 (a) Yield of pure major isomer only.

Their model for the catalyst is 'borrowed' from the basic principles of the active site of an enzyme, which it emulates. The molecular recognition of the active site (the fit of the reactant), defines the asymmetric induction of the alkylation. However detailed structural information is still not available, to explain why this family of catalysts, using the ligand shown in Figure 26a, should function so well. The authors depict a model of the "active site or chiral pocket", which does rationalise the result, in that the architecture of the "active site" forces the benzene ring to the outside (Figure 26b).

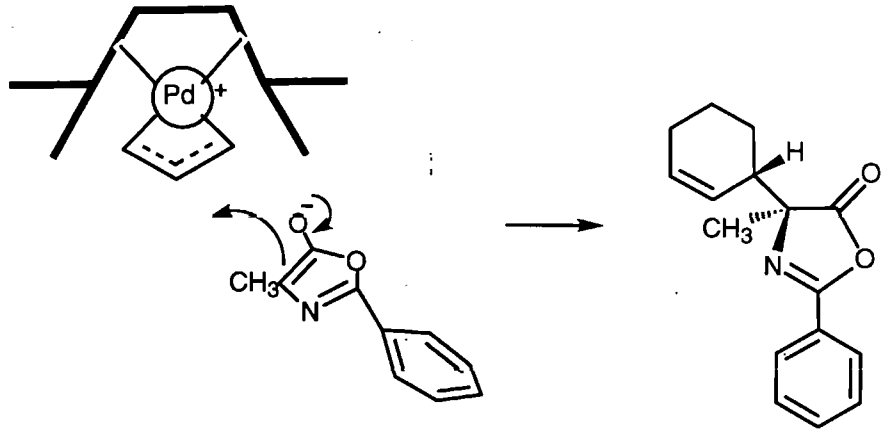

Figure 26b Major diastereoisomer

2.4 Chiral auxiliary control

Control in this group is *intramolecular* by a stereogenic centre in the substrate, as was described in section 2.1. However, the difference here is that the stereodirecting centre (chiral auxiliary) is introduced into an achiral substrate to direct the asymmetric reaction. Once the reaction is complete the chiral auxiliary may be removed unchanged without racemisation of the product, although it is not always possible to recover the chiral auxiliary intact. An additional advantage of this control is that if both possible products are formed, they will be diastereoisomers. Thus if diastereoselectivity is not great, the diastereomers may be separated by crystallisation or chromatography, giving a final product of very high ee.

Asymmetric synthesis using dihydropyrazines and their analogues

An example of this control method is illustrated by the conversion of glycine into mono- and di-substituted α-amino acids using heterocyclic templates based on dihydropyrazines. This technique has been developed over a long series of investigations by Schollkopf *et al.* [44-49] The starting compounds are bislactim ethers of diketopiperazines. They contain a chiral auxiliary, latent amino and carbonyl groups, and two sites which are readily cleaved by hydrolysis (Figure 27). X-ray structure analysis shows the ring to be planar.

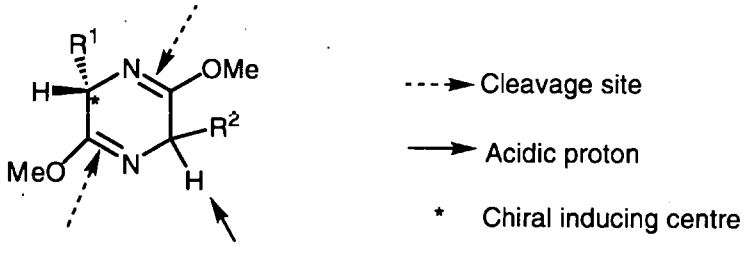

Figure 27

An illustration of this group's approach, is given in Figure 28. Here the regioselective reaction of the *cyclo*-(L-val-gly) bislactim ether with butyllithium, allowed a following diastereoselective reaction of the lithiated species with alkyl halides. Subsequent acid hydrolysis under mild conditions to minimise racemisation, liberated the (*R*)-amino acid methyl ester and the original chiral auxiliary as its ester, (methyl L-valinate).[44]

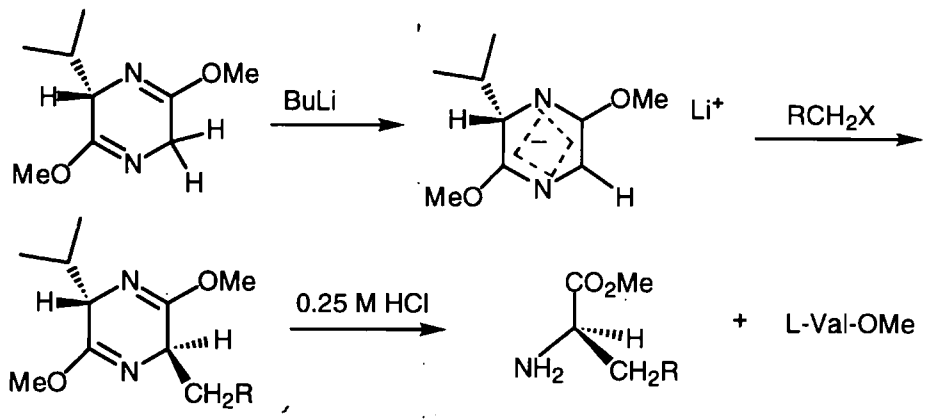

Figure 28

The authors postulated that the lithium compound generated a planar dihydropyrazine anion, strongly shielded on one face by the bulky *iso*-propyl group. The R group of the alkyl halide would then approach from above the heterocyclic ring close to the centre of induction, and on the opposite side of the ring to the *iso*-propyl group (Figure 29).

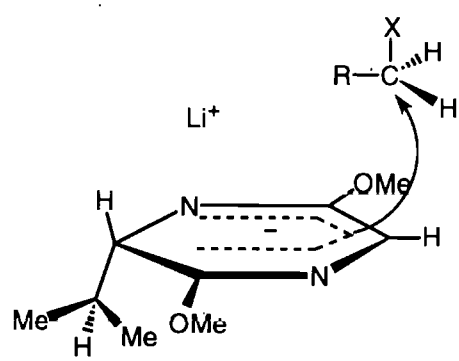

Figure 29 [R= Phenyl 91-95% ee]

This has proved to be a most versatile route to the enantioselective production of α-monosubstituted α-amino acids (Table 9).[44]

R (Figure 29)	% Yield	% ee.
$-CH_2-C_6H_5$	73	91-95
$-CH_2-CH=CH-C_6H_5$	86	>95
$-CH_2-COOC_4H_9-t$	82	>95

Table 9

The method has also been used with success to prepare α-substituted α-methyl amino acids,[47] but is only effective for the reactive alkyl halides, as shown inTable 10.

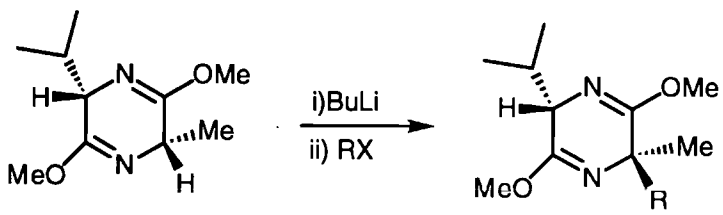

R	% de
$C_6H_5CH_2-$	>95
$CH_2=CH-CH_2-$	>95
$C_6H_5CH=CHCH_2-$	>95

Table 10

The lithiated derivative of the bislactim ether shown in Fig. 29 p.40 was also found to react with carbonyl compounds, which when dehydrated and cleaved hydrolytically yielded alkenyl substituted alanines (Figure 30).[46] If the lithium reagent

was exchanged for $Ti(NEt_2)_3$, vinyl aldehydes could be used similarly to yield the (2*R*,3*S*)-serine ester derivatives (Figure 30).[49] The use of this reagent generates only one configuration at C-1′, to give one diastereomer without the epimerisation seen in the route shown in Figure 31. The titanated bislactim ether gives almost exclusively the *syn*-addition products of the serine ester analogues.

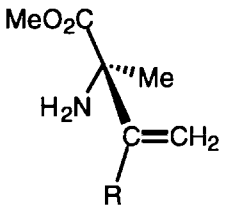

Akenyl substituted alanine

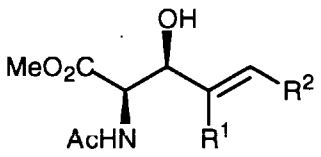

(2*R*), (3*S*)- serine ester

Figure 30

Following on from the work of Schollkopf,[49] Groth *et al*.[50] synthesised (2*S*,3*R*)-sphingosine (**X** Figure 31) from the corresponding α-amino acid ester in five steps *via* an asymmetric aldol addition of the lithiated bislactim ether shown in Figure 28 to (2*E*)-hexadecenal.

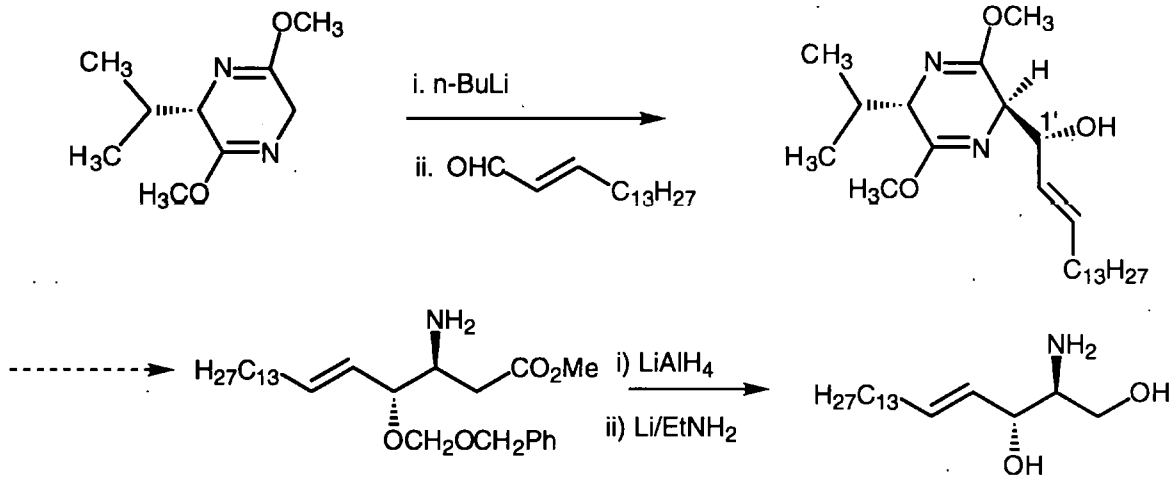

Figure 31

X

There was a 1:1 formation of diastereoisomers epimeric at C-1′ after the first step, but the diastereomeric products were easily separated by flash chromatography, and the chiral auxiliary (methyl L-valinate) was recovered after acid hydrolysis of the hydroxy protected initial product.

The most direct approach to the synthesis of α-methyl α-amino acids, is α-alkylation of chiral alanine anion equivalents. Use of cyclic derivatives such as Schollkopf's bislactim ether [44-50](Figure 28), have been investigated by Chinchilla *et al.* [51,52] They focused their attention on 2,3-dihydro-6*H*-1,4-oxazin-2-ones (Figure 32), as iminic alanine derivatives (cf. Schollkopf's syntheses). In these compounds the phenyl group should favour formation of the more stabilised enolate; the 6-position has the same stereogenic centre for transfer of its chirality to the 3-position as in the Schollkopf's bislactim ether; and the imino-lactone ring can be easily hydrolysed. X-ray structures and nOe studies were used to determine their relative configurations, and corroboration by molecular mechanics calculations showed that the preferred conformation was a quasi-boat structure, with the *iso*-propyl group in an axial

position. This was also the predicted conformation for the enolate anion and would favour *anti*-attack at the 3-position by approaching electrophiles (Figure 32).

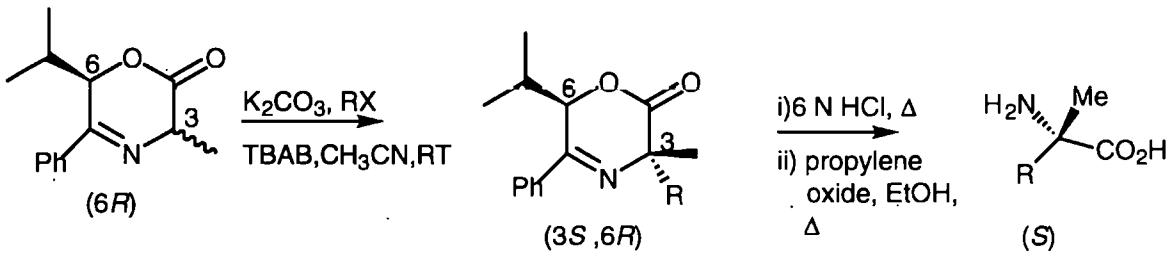

Figure 32

Bull *et al.* [53-55] also looked at the possibility of using masked glycine enolates for alkylation. They wished to create a new chiral auxiliary that did not have the disadvantages of Schollkopf's bislactim ether, which is a volatile oil, shows poor diastereoselectivity with linear or β-branched electrophiles and is susceptible to acid catalysed hydrolysis. They decided to prepare a robust, highly crystalline *N,N*-dialkylpiperazine-2,5-dione which on deprotonation would give an enolate as shown in Figure 33. The conformation of the enolate was deduced from molecular modelling studies and shows that the ring system is essentially planar, with the *iso*-propyl group fixing the position of the *N*-4 benzyl group *anti* and the *N*-1 benzyl group *syn* to itself. This arrangement blocks the *si* face against alkylation. They also predicted that the proximity of the *N*-1 benzyl group to C-6 would increase the diastereoselectivity of alkylation for this auxiliary, above that which was achieved by Schollkopf's bislactim ethers. This system is employing a chiral relay network from the chiral *iso*-propyl group through the non-stereogenic *N*-benzyl protecting groups.

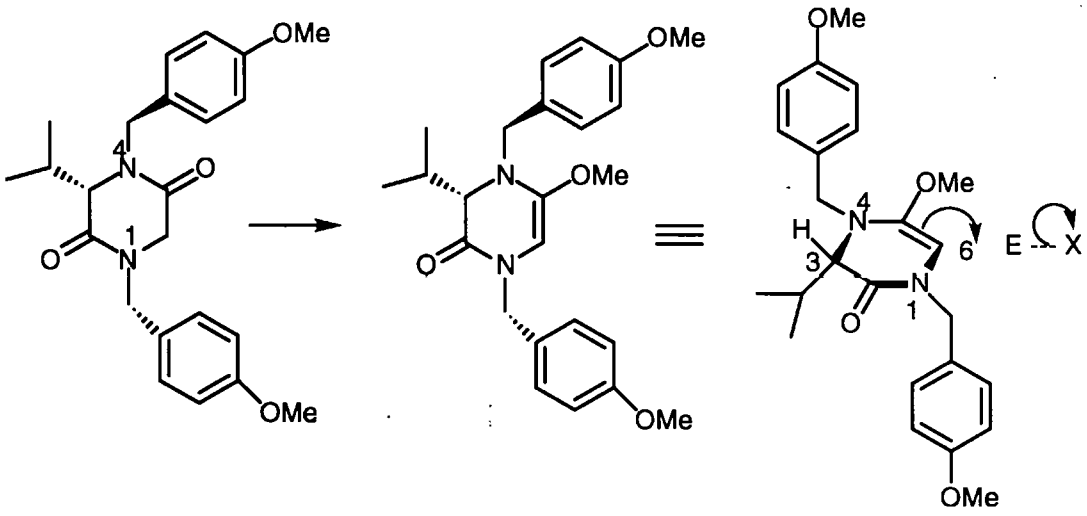

Figure 33

Table 11 gives the results[53] of a number of different alkylations using the enolate prepared by Bull *et al* group and the *N*-*N*-dimethylated piperazine-2,5-dione, in which the methyl groups do not have the capacity to enhance the stereoselectivity in the relay method as do the benzyl groups.

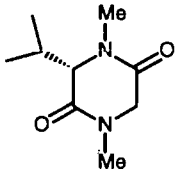

B1

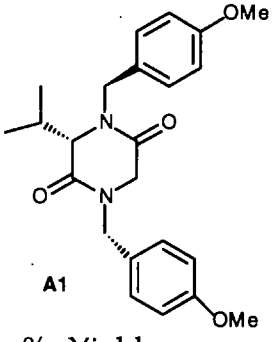

A1

Electrophile	% de		% Yield	
	B1	**A1**	**B1**	**A1**
Methyl iodide	50	93	54	72
Benzyl bromide	91	98	81	88
Allyl bromide	74	94	83	63
Ethyl iodide	*	90	-	78
Iso-propyl iodide	*	96	-	90

Table 11 (* only starting material B1 was recovered)

Asymmetric syntheses using imines as intermediates

A method for diastereoselective Strecker synthesis of optically pure α-amino acids from achiral aldehydes has been developed by Chakraborty *et al.* [56] using α-phenylglycinol as a chiral auxiliary. The (*R*)-phenylglycinol enantiomer is used to form the L-amino acids and the (*S*)-enantiomer to form the D-amino acids (Figure 34).

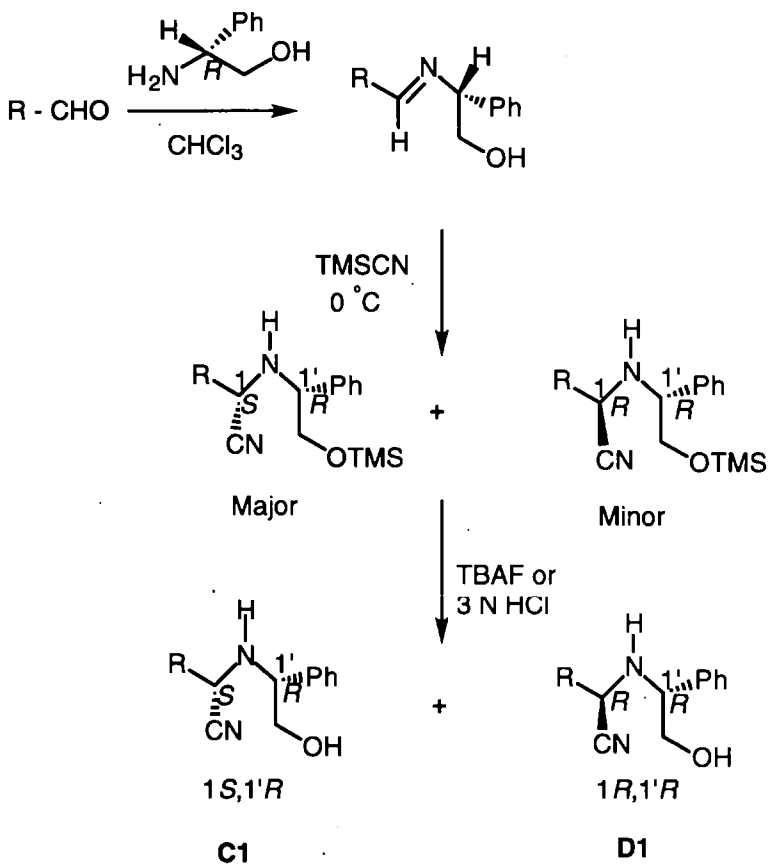

Figure 34

The reaction of various aldehydes with a single enantiomer of α-phenylglycinol resulted exclusively in *E*-isomers. Treatment with trimethylsilyl cyanide in chloroform, followed by hydrolysis, gave good yields of the α-aminonitriles (**C1** and **D1**). The high diastereoselectivity favours the 1*S*, 1'*R*- diastereoisomeric ratio (d.r.) in > 80:20 ratio (Table12).

R-CHO	C1:D1(dr)	% Combined yield
Benzaldehyde	82:18	92
p-Tolualdehyde	85:15	90
p- Methoxybenzaldehyde	90:10	95

Table 12

The diastereoselectivity is explained by the favourable conformation of the imine **E1** shown in Figure 35a, which gives rise to the major isomer (1*S*,1'*R*). In this state the hydroxymethyl group is furthest away from the imine moiety, reducing steric interference and there is extra stabilisation from intramolecular hydrogen bonding (Figure 35a).

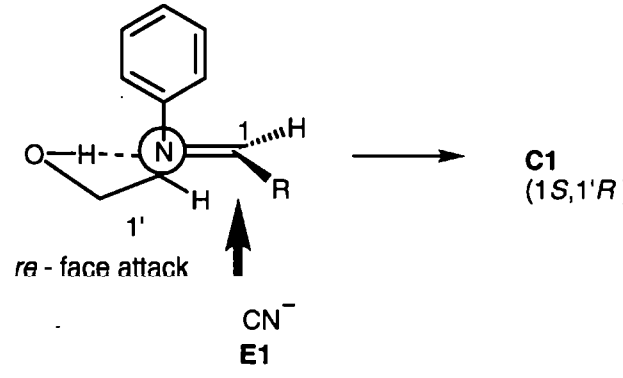

Figure 35a

Diastereoselectivity was reduced with THF as solvent or when α-methylbenzylamine was used as chiral auxiliary.

Using PCMODEL it can be shown that three major conformations of the imine (Figure 34, R=Ph) exist, differing in the angle of rotation of the hydroxymethyl group about the bond joining it to the benzylic carbon atom. These conformations and the calculated MMX energies are shown in Figure 35b. In conformation **A**, hydrogen bond formation is observed as suggested by Chakroborty.[56] However, the MMX energy of this conformer is only slightly lower than the energies of the other two conformers, which do not exhibit hydrogen bonding. The MMX calculation indicates that hydrogen bonding in conformer **A** stabilises the structure by 2.2 kcal mol^{-1} relative to the other two conformers. However, this stabilisation is partly offset by increased torsional strain of 1.2-1.6 kcal mol^{-1} relative to the other two conformers. Nevertheless, in all three conformers of the *R*-isomer shown, the phenyl group hinders approach of the nucleophilic cyanide to the *si*-face. Attack consequently would be predicted to occur on the *re*-face as was observed experimentally. Although the PCMODEL calculations do not indicate significant extra stabilisation in the ground state, the hydrogen bonding interaction would become more significant in lowering the transition state energy as charge accumulates on the nitrogen atom during attack of the cyanide ion on the imine carbon atom.

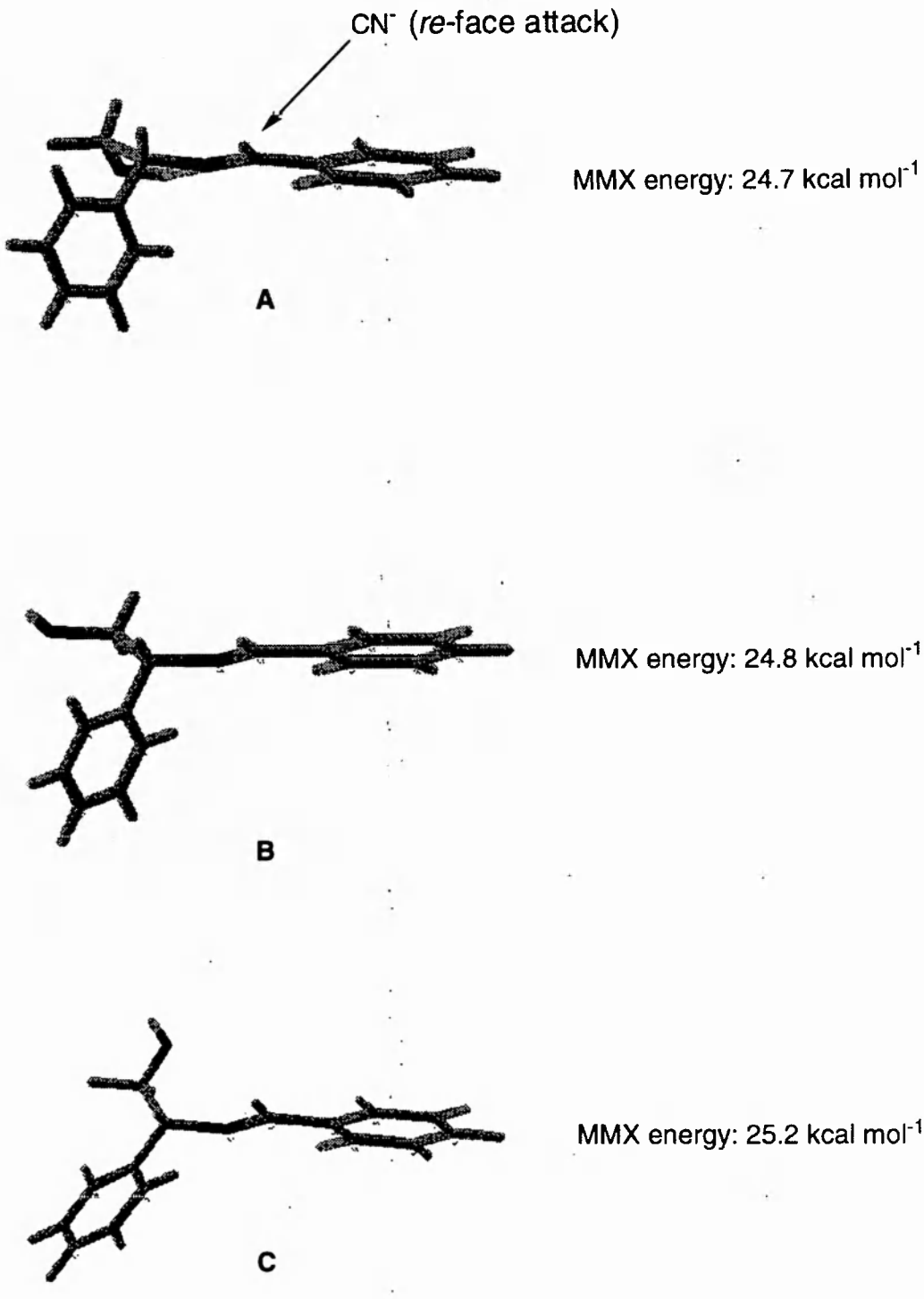
CN⁻ (re-face attack)
MMX energy: 24.7 kcal mol⁻¹
A
MMX energy: 24.8 kcal mol⁻¹
B
MMX energy: 25.2 kcal mol⁻¹
C

Figure 35b

The configuration of the diastereomeric α-aminonitriles was determined by NMR and nOe studies (**C1** and **D1** Figure36).

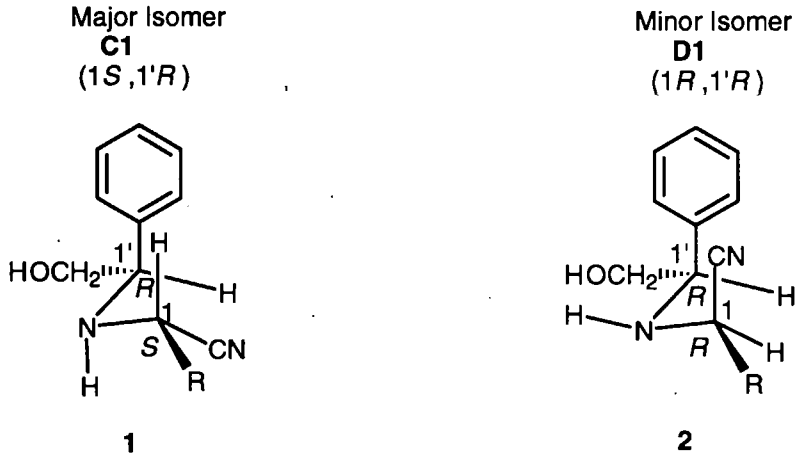

1 **2**

Figure 36

In the most stable conformation (**1** Figure 36) of the major isomer **C1**, the methine proton α to the cyano group is shielded by the phenyl group. In the most stable conformer (**2**) of the minor isomer **D1**, the bulk of the aromatic group keeps this proton away from this shielded position. As would be expected from these observations, the NMR spectra of these two compounds showed different chemical shifts for this methine proton. The signal due to the methine proton in the major isomers, consistently appeared at higher field of approx. δ 0.2. The nOe evidence gained from the acid mediated cyclised product of **C1** (Figure 37) indicates the *cis*-relationship of the two protons at C-1 and C-1′.

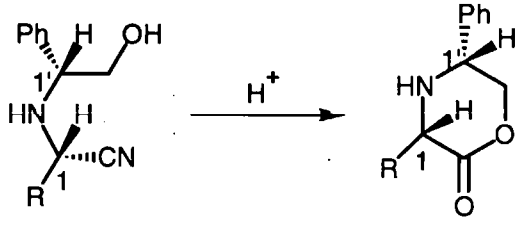

Figure 37 **C1**

Finally reaction of the α-aminonitriles (**C1** and **D1**) with saturated methanolic HCl for 5 h at room temperature, converted the nitrile group into the methyl ester. Subsequent reaction with lead tetraacetate and dilute HCl gave the amino acid as its methyl ester (Figure 38). However it was not possible to regenerate the chiral auxiliary.

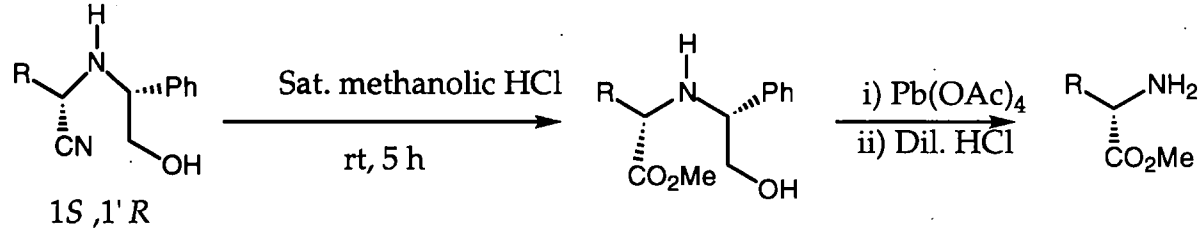

Figure 38

Imines formed from glycine derivatives are also useful for the synthesis of α-amino acids as illustrated by the work of Yeh *et al.* [57] Following on from the work of McIntosh and co-workers,[58] they investigated enolate alkylation of the Schiff base formed from glycine *tert*-butyl ester and a camphor sulfonamide as the chiral auxiliary (**F** Figure 39).

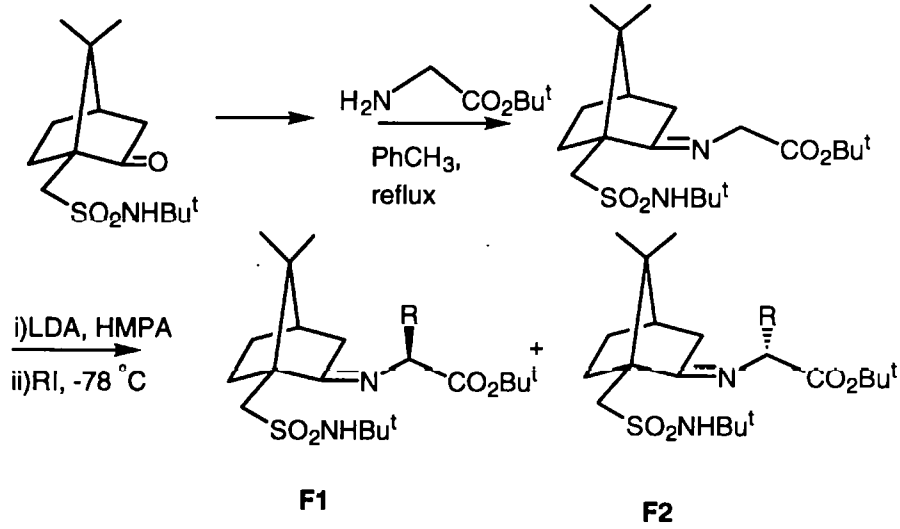

Figure 39

The diastereoselectivity was good for methylation, but ethylation, allylation and benzylation initially gave diastereoisomer ratios of only 3:1 to 1:3. However after a single recrystallisation from acetone-hexane the ratios improved to >100:1 (Table 13).

RX	F1:F2	(ratio after recrystallisation)
CH_3I	>20:1	(>98:2)
C_2H_5I	3:1	(>98:2)
$CH_2=CHCH_2Br$	2.4:1	(>98:2)
$PhCH_2Br$	1:3	(>98:2)

Table 13

The use of iminoglycine derivatives as starting chiral templates for the asymmetric synthesis of α-amino acids, has also been investigated by Guillena *et al.* [59] They prepared the iminoglycine compound shown in Figure 40, which after alkylation and hydrolysis, was easily separated from the recovered chiral auxiliary. Diastereoselectivity in formation of the alkylated glycine derivative, using KOBu^t/LiCl was >90:10, with yields of 77% for allylation and 54% for benzylation.

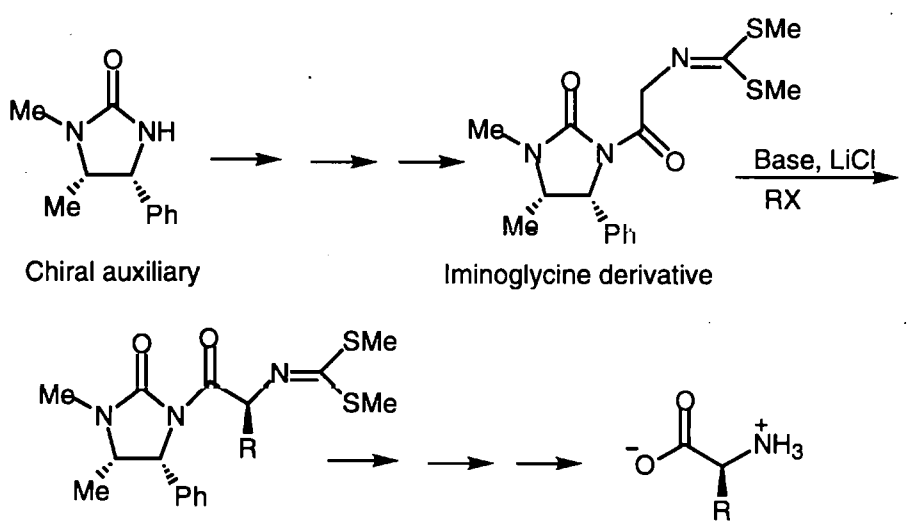

Figure 40

3. Chiral induction with heterocycles

In the manufacture of enantiomerically pure drugs there are many examples of syntheses which may be placed in the categories discussed above. Some may fit specifically into one category and others may exhibit a combination of two or more of these asymmetric synthesis control methods. Our interest lay in the use of chiral auxiliaries to control asymmetric synthesis. Our previous survey has shown that in the control of asymmetric induction where a chiral auxiliary is used, the highest stereoselectivity will be achieved in cases where the chiral auxiliary is incorporated into a cyclic structure, thereby introducing rigidity. A fully bonded structure clearly has advantages as a rigid template over a transient reactive species. Since heterocyclic compounds also have functionality built into their ring systems, they seem to have obvious potential for directing stereoselectivity, or as rigid chiral templates to induce asymmetry. It is therefore not surprising that we have seen several workers in the field of asymmetric synthesis choosing to work with heterocyclic systems, and that their efforts have proved to be highly successful.

A further advantage offered by heterocyclic systems is exemplified by the reaction shown in Figure 41.[60] Heteroatom centres frequently allow for easy subsequent cleavage of the 'template', to generate the required product. The possibility of regenerating an expensive or hard-won starting material by bond cleavage at a heteroatom is an extra bonus!

In the preparation of 1-arylpropylamines, Takahashi *et al.* [60] used chiral heterocyclic compounds to induce asymmetry with a high level of diastereoselectivity (Figure 41). The prolinol urea reacted with aldehydes to give a heterocycle which was open to highly stereoselective nucleophilic attack at the 6-position by diethylzinc. Alkylation was accompanied by ring cleavage.

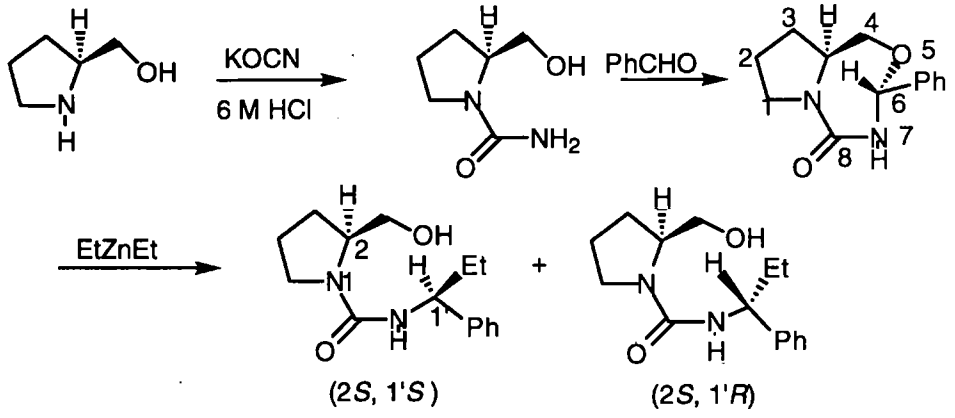

Figure 41 **93 : 7**

Reduction of the alkylated product, (*N*-1'-phenylpropyl-2-hydroxymethyl-1-pyrrolidinecarboxamide), with Red-Al [sodium bis(2-methoxyethoxy)aluminium hydride] gave the (*S*)-1-phenyl-*N*-methylpropylamine and regenerated the chiral auxiliary, (*S*)-prolinol (Figure 42).

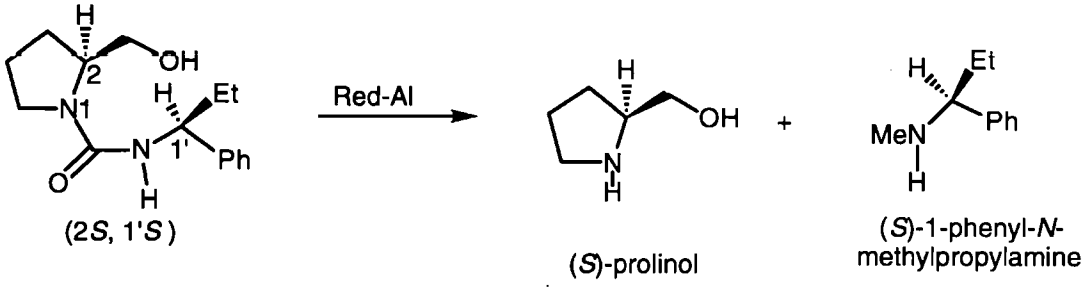

Figure 42

This reaction scheme illustrates a further advantage arising from the use of heterocyclic compounds as precursors. This is the exploitation of conformational, or even better, configurational restrictions in building the ring system. Shown here is the key step of the scheme shown in Figure 41, where ring closure follows condensation of

the aldehyde with the primary amine group of the intermediate urea. The formation of the 5-oxa-7, 8-diazaperhydroazulen-8-ones proceeds with high stereoselectivity to the configurationally controlled *re*-face attack on the imine by the hydroxyl group (Figure 43).

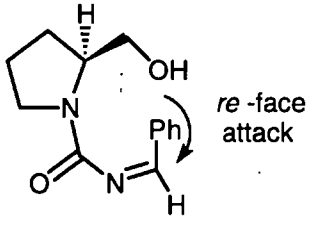

Figure 43

In another approach, Meyers *et al.* [61] developed chiral bicyclic systems for enantioselective synthesis. Fusing on a second ring further restricts conformational flexibility. The chiral system used to synthesise α-disubstituted carboxylic acids is a bicyclic lactam (Figure 44), prepared from *S*-valinol and 3-benzoylpropanoic acid.

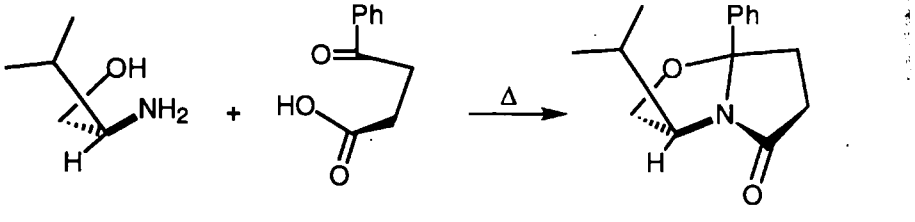

Figure 44

Monoalkylation of the bicyclic lactam gave the *endo* isomer as the predominant product (in ratios *endo:exo* from 9:1 to 30:1), as determined by X-ray crystallography (Figure 45). The diastereomers were again alkylated and gave the dialkyl derivatives, with good to excellent stereoselectivity. The use of diastereoisomeric mixtures is acceptable in this second step, as the stereochemistry at

the α-carbon is lost when the planar enolate is formed during alkylation.The stereoselectivity is restored because the electrophile enters from the *endo* face.

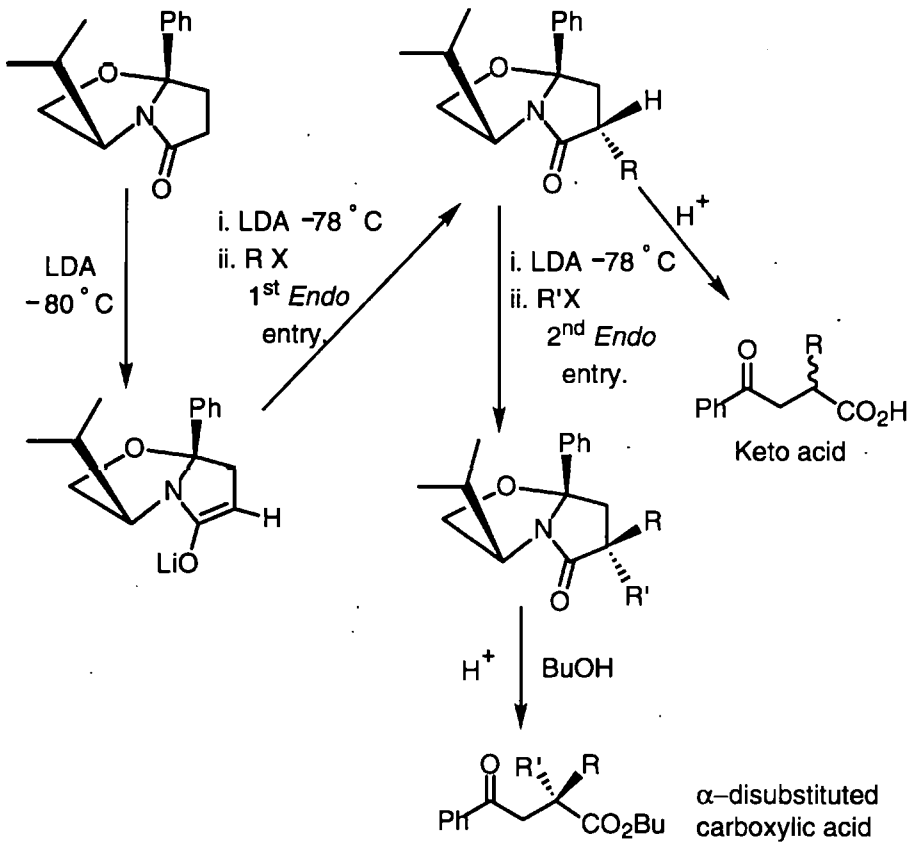

Figure 45

Hydrolysis of the monosubstituted lactams to give the α-alkyl acids, resulted in a substantial amount of racemisation, even though the isolated keto acids were not significantly racemised under the same reaction conditions. Of course racemisation is not a problem with the disubstituted lactams.

By alteration of the order of substitution it was found to be possible to produce either isomer of the α–disubstituted carboxylic acid (Table 14), as the final product as shown in Figure 45. From Table 14 it can be seen that to maximise diastereoselectivity, it was better to introduce the bulkier group in the second step, (for example the benzyl

group). Presumably this is owing to the greater difficulty of moving a bulky benzyl group into the *exo*-face, to allow *endo*-entry of the second substituent. However, the *iso*-propyl group seems to encounter sufficient steric hindrance to have to adopt the *endo*-position predominantly, irrespective of whether it is introduced in the first or second step.

R	R'X	R'entry (endo/exo)
Me	$PhCH_2Br$	42 : 1
$PhCH_2$	MeI	12 : 1
Me	EtI	7.5 : 1
Et	MeI	10 : 1
Me	*p*-$MeOPhCH_2Br$	30 : 1
p-$MeOPhCH_2$	MeI	13 : 1
Me	*i*-PrI[a]	3 : 1
i-Pr	MeI	1 : 10

Table 14

[a] Alkylation occurred only at 0 °C in the presence of HMPA

A number of variations on this synthesis have been reported. Replacing 3-benzoylpropanoic acid with levulinic acid,[62] puts a methyl group at the bridgehead, leading to a series of methyl ketones. Meyers *et al.* have extended this work to the synthesis of *Aspidosperma* alkaloid precursors.[63]

More recent developments[64,65] have shown that nitrogen containing heterocycles can also be generated from these bicyclic lactams. It has been possible to synthesise optically pure pyrrolidines and piperidines (Figure 46).

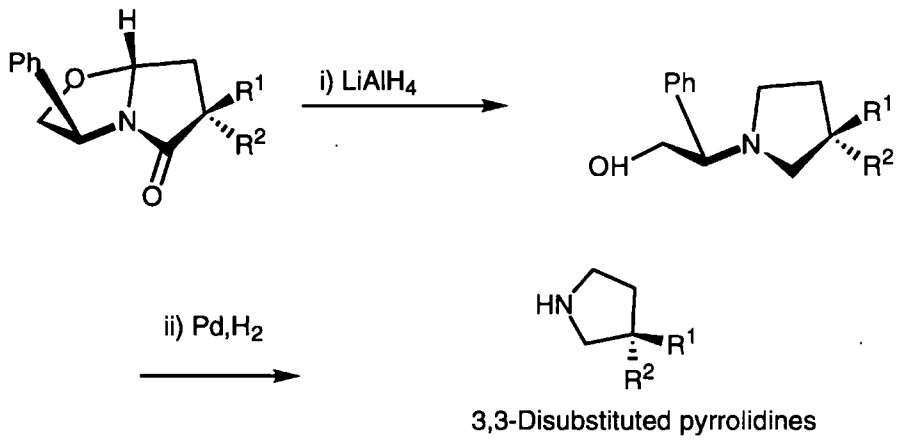

Figure 46a

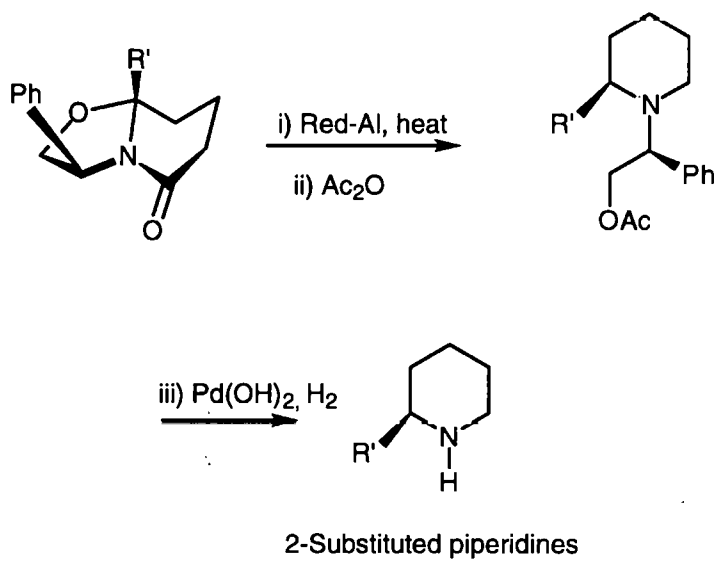

Figure 46b

4. Chiral oxazepines in asymmetric induction

4.1 *Initial work by Mukaiyama*

A heterocycle that attracted our attention and which formed the basis of this and other research projects, was the interesting chiral malonate equivalent, oxazepine **1** [(2*R*, 3*S*)-3,4-dimethyl-2-phenylperhydro-1,4-oxazepine-5,7-dione] (Figure 47), which had been developed by Mukaiyama *et al.*[66]

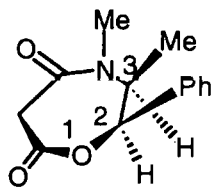

1

Figure 47

This was prepared in three steps from methyl hydrogen malonate and 2*R*, 3*S*-ephedrine hydrochloride with 2-chloro-1-methylpyridinium tosylate (Mukaiyama's reagent) as the coupling reagent (Figure 48). The configuration of this compound will obviously depend upon which enantiomer of ephedrine is used initially.

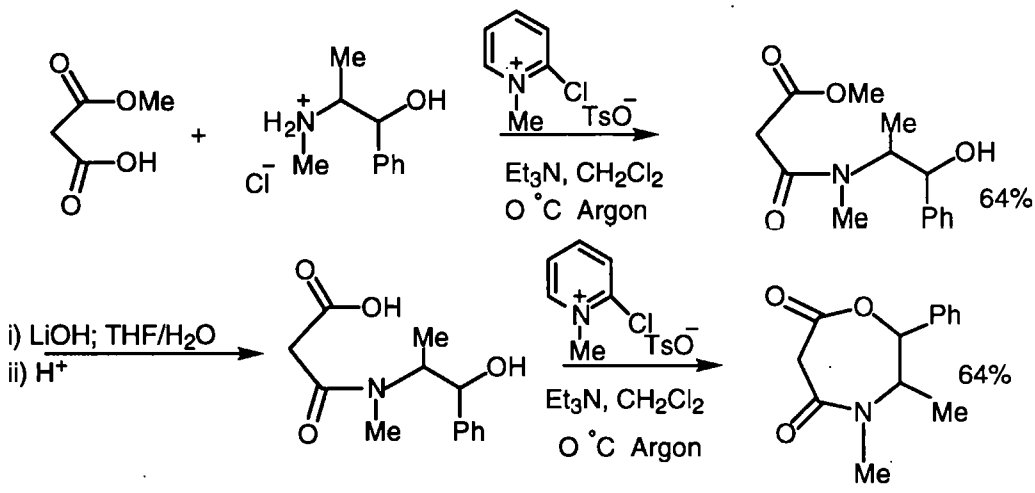

Figure 48

Mukaiyama was able to synthesise highly optically pure δ-oxocarboxylic acids by Michael addition of the oxazepine to αβ-unsaturated ketones (Figure 49).[67]

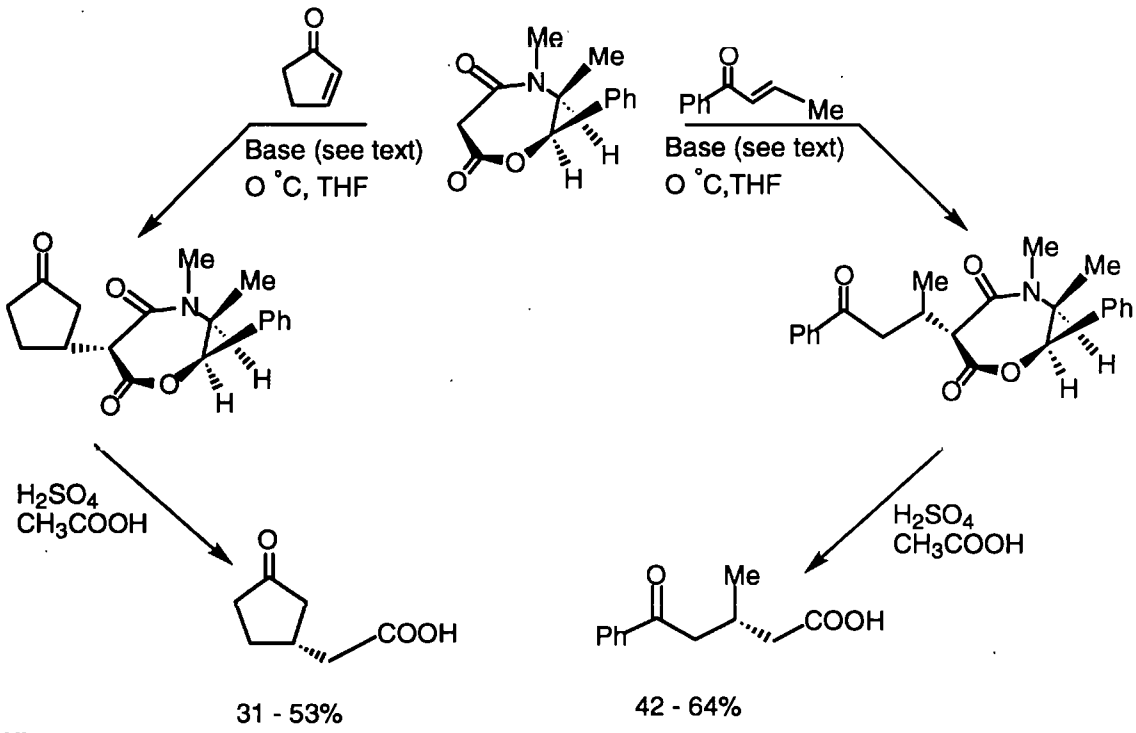

Figure 49

Several different bases were used (*tert*-BuOK, Ph_3CLi, DBU), which gave the spread of yields shown. The best results were obtained with DBU, when optical purities (ees) of up to 96% were obtained.

Mukaiyama's group also used the condensation of aldehydes and ketones with oxazepine **1** to synthesise highly optically active β-substituted alkanoic acids **2** (Figure 50a).[66] Condensation of aldehydes at position 6 in the oxazepine ring generated alkylidene derivatives with the *E*-configuration **3**. An example is given for this reaction with benzaldehyde (Figure 50b). The conjugate addition of Grignard reagents then resulted in the highly stereoselective formation of a chiral centre on the exocyclic carbon atom of the product **4**. Optical purities (ees) of 99% were obtained using THF as solvent in the presence of a catalytic amount of nickel^{II} chloride at low temperature. Hydrolysis in acid solution with decarboxylation gave β-substituted acids. For example, with *n* -butyl magnesium bromide and the benzaldehyde condensation product **3**, (*S*)-(+)-3-phenylheptanoic acid (**5**) was obtained (Figure 50b). Ethanal, propanal, butanal and *iso*-butanal were also used to give similar results.[67]

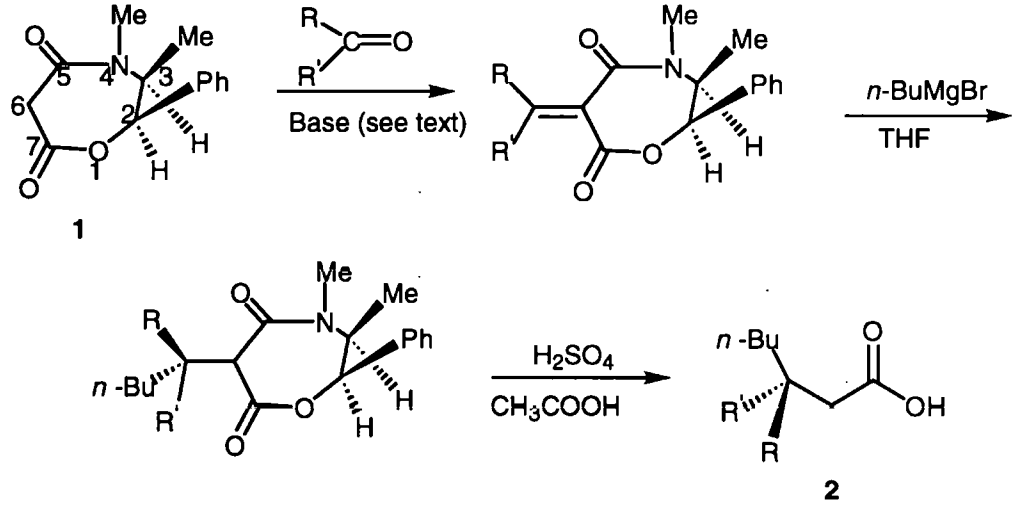

Figure 50a

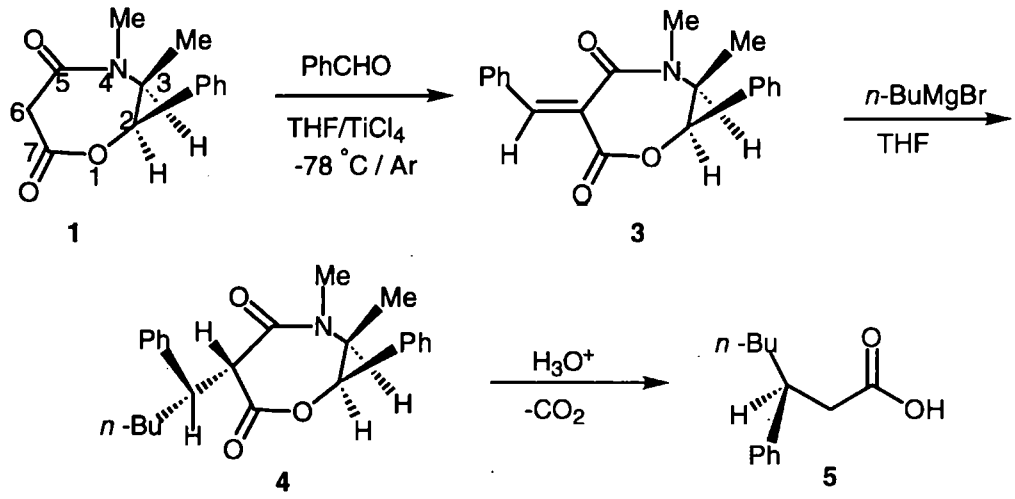

Figure 50b

The absolute configuration of the product **5**, indicates that attack by the Grignard reagent is from the opposite face of the oxazepine ring to that occupied by the methyl and phenyl groups, as might be expected on steric grounds (Figure 51).

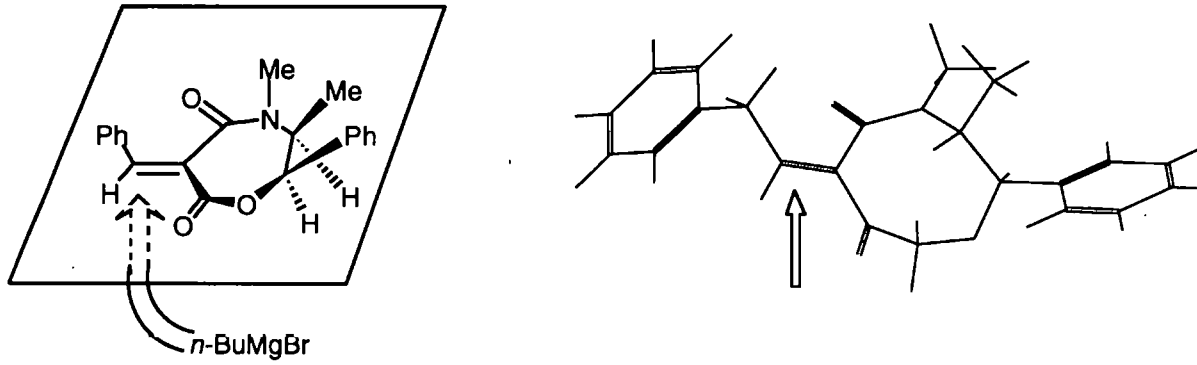

Figure 51 (*E* isomer)

4.2 *Development work by Ford*

M.J.Ford in this laboratory also synthesised Mukaiyama's chiral oxazepine precursor **1**, shown below.

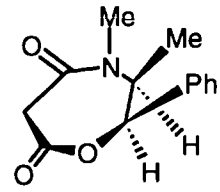

1

Using Mukaiyama's procedure, repeated efforts at preparation of this compound gave very low yields (<10%), and a detailed investigation was led by Ford into finding an improved method of synthesis of **1**[68,69] (Figure 52). Amide formation was achieved simply in one step in almost quantitative yield, by extended reflux in methanol of ephedrine and dimethyl malonate. The most difficult step in the synthesis is the cyclisation of the hydroxy acid, for which Mukaiyama used his preferred (and expensive) reagent, 2-chloro-1-methylpyridinium iodide. Ford discovered that a much improved yield (55%) could be achieved by a method using the cheaper reagents cyanuric chloride and pyridine, rather than the longer, lower yielding and more expensive process used by Mukaiyama. The number of steps required in the synthesis was reduced and also the number of chromatographic separations.

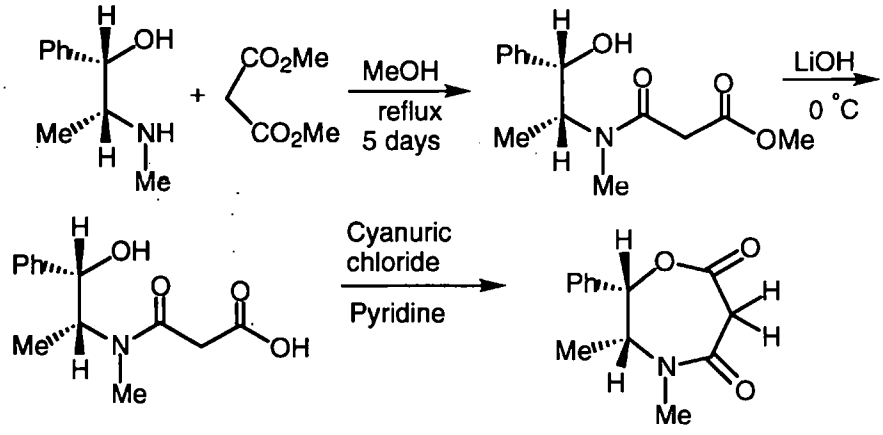

Figure 52 >95% 55%

It is surmised that the role of the cyanuric chloride condensing agent is as shown in Figure 53, with the formation of the triazinone being the driving force for the reaction. Ford suggested, with some corroborating evidence, that the pyridine was not acting solely as a base, but possibly activating the reagent in some manner,[71] analogous to the action of acyl chlorides and pyridine.

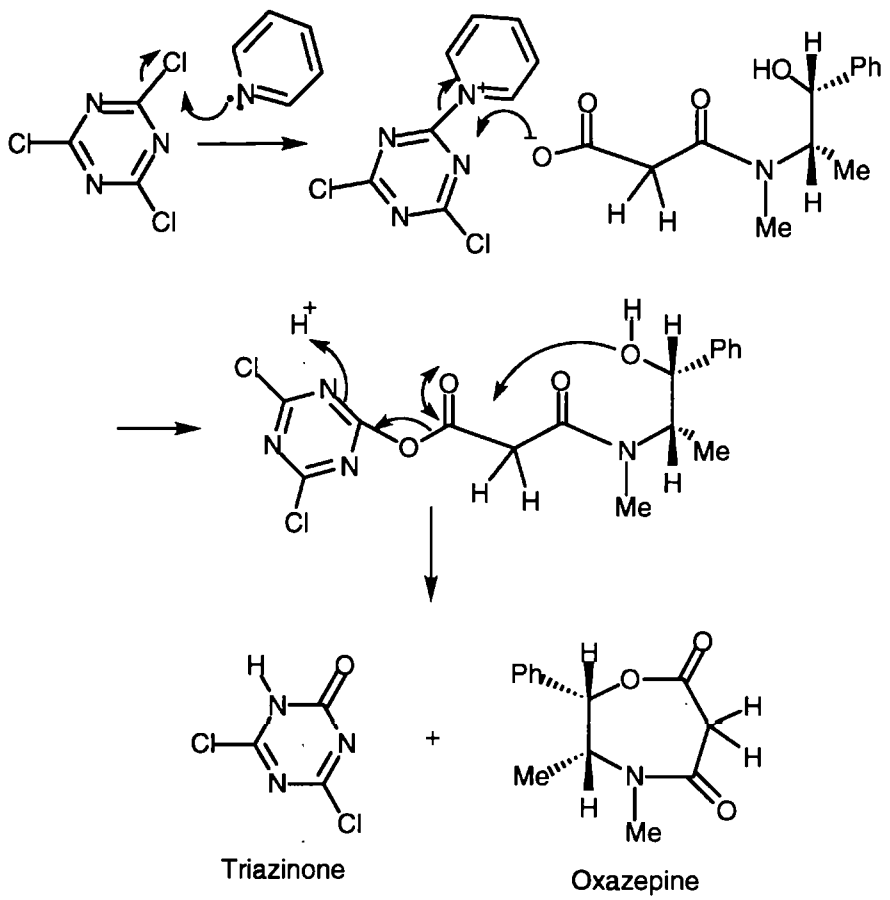

Figure 53 Suggested mechanism for coupling using cyanuric chloride.

It was known that the cyclopentene-1, 2-dione dimer **6** (Figure 54) reacts with dimethyl malonate,[70] in the presence of triethylamine to give the racemic form of the cyclic pentenolone **8**, *via* the achiral monomer **7**.

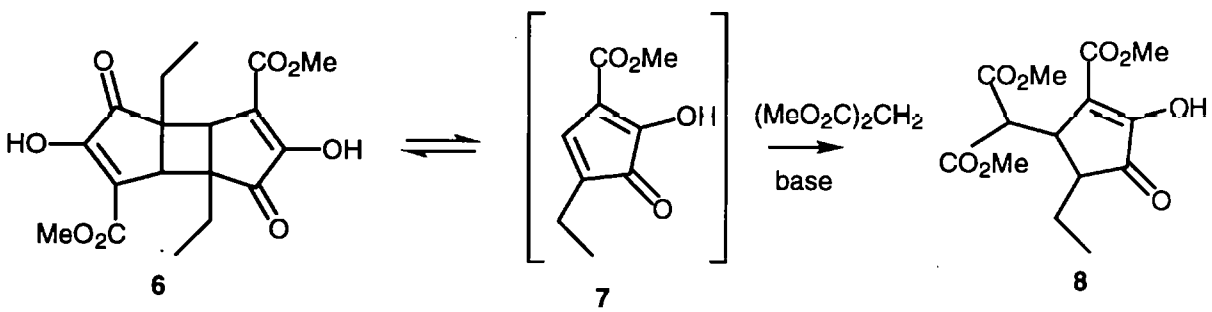

6 **7** **8**

Figure 54

Reaction between the chiral oxazepine, which can be considered as a chiral malonate, and the dimer (in the presence of base), led to the synthesis of a diastereomerically pure cyclopentenolone adduct **9** (Figure 55). The deprotonated oxazepine adds stereoselectively to the achiral intermediate, in a thermodynamically-controlled Michael addition.

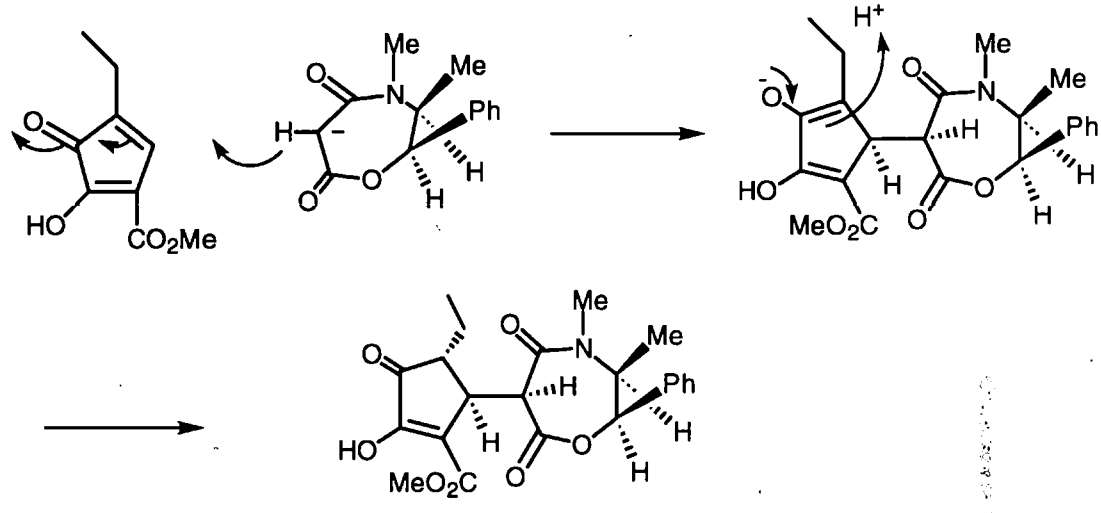

Figure 55

Opening the oxazepine ring in the methylated derivative of the adduct with sodium methoxide followed by treatment with acetic anhydride/pyridine yielded the open chain compound **10** shown in Figure 56.

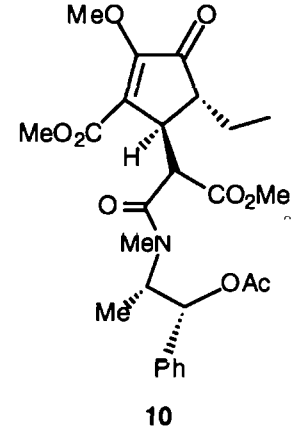

Figure 56

A further series of reactions, of which the most important was a retro-Michael exchange reaction with dimethyl malonate, generated the polysubstituted cyclopentene **11** (Figure 57).

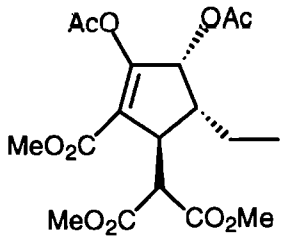

Figure 57 **11**

Compound (**11**) proved to be a valuable intermediate in the synthesis of secologanin derivatives and through them to indole and related alkaloids.[71,72] NOe studies[71] on both the unsubstituted oxazepine and the Michael adduct **9** Figure 55, showed that the preferred conformation of the 7-membered ring is the twist-boat **1A** (Figure 58).

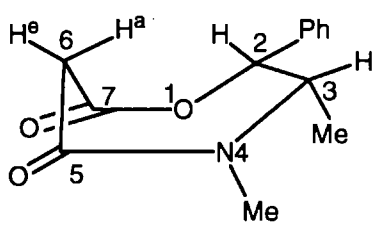

Figure 58 **1A**

In the adduct **1A** it is the pseudoequatorial hydrogen atom at C-6 which is replaced by the carbocyclic ring. Subsequently a single crystal X-ray structure determination, on the methyl ether of the adduct, confirmed both the shape of the oxazepine ring and the induced configuration in the cyclopentenone ring (Figure 59).

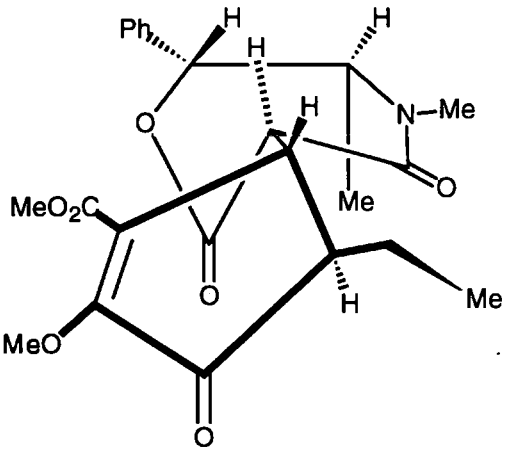

Figure 59 Viewed along the bond joining the two rings.

5. SUMMARY

These examples of asymmetric induction, drawn from investigations by a number of reseach groups, have confirmed the potential of heterocyclic systems as effective (enhanced) precursors for the synthesis of diastereomerically and enantiomerically pure isomers. The essential features that need to be incorporated into a suitable heterocyclic system are:

i) a readily available and inexpensive chiral auxiliary, from which a heterocyclic ring can be constructed.

ii) sufficiently bulky substituent groups in the auxiliary to create significant hindrance to one of the alternative steric pathways of reagent approach.

iii) an active centre at which a stereoselective reaction can take place.

iv) functionality within the ring that allows selective cleavage of bonds to generate the chiral product, preferably in more than one step. If the original chiral auxiliary can be recovered after the ring opening steps, this would be an added advantage.

In respect of the asymmetric synthesis of α-amino acids, Schollkopf[48] stated the strategy perfectly: " Our approach is based on heterocyclic chemistry and on the following concept: A heterocycle is built up that contains-besides a chiral inducing centre-a latent amino group and a latent carboxyl group, both incorporated in such a way that the heterocyclic anion is an equivalent of an amino acid carbanion, to which an electrophile can be added diastereoselectively. Moreover, the heterocycle must have two sites susceptible to hydrolysis, so that it can be cleaved, finally liberating the optically active target amino acid and the chiral auxiliary."

It is against the background of this strategy that we report investigation of the use of 1,4-oxazepine-5, 7-diones and their analogues as heterocyclic precursors for selective synthesis of chiral compounds. In order to exemplify this approach our initial target has been α-amino acids. However this is purely illustrative as the method can be employed in the synthesis of other chiral molecules, as indicated in the following chapter.

The proposed project was to build heterocyclic systems, which incorporated chiral centres of known absolute configuration with a reactive centre, where substitution at that centre was sterically controlled by the asymmetric elements present.

The oxazepine (compound **1** p. 63) contained these prerequisites, and with a wide range of chiral β-amino alcohols available it was hoped to build a number of analogous heterocyclic systems by a similar method, and larger heterocyclic systems homologous with compound **1**, using maleic, succinic and glutaric anhydrides with ephedrine.

The next stage was to bring about substitution at the reactive prochiral centres, and to show that substitution had been sterically controlled, then to cleave the ring, release the new chiral compound and possibly recover the oxazepine intact.

The use of PCMODEL in the preceeding chapter has been helpful in the interpretation and analysis of a number of the syntheses and reaction schemes that were discussed. The investigation of some of the reaction schemes illustrated the conformations of reactant molecules that can exist, and the energies of each of these conformers (Figure 5b p. 8), leading to a better understanding of possible pathways to the product. The demonstration of possible steric hindrances to the approach of a

nucleophile have also been shown (Figure 12b p. 20), enabling an explanation to be offered for the ratio of products formed.

Although PCMODEL is not definitive, it can be usefully indicative. It will be used in the Results and Discussion chapter to show the lowest calculated energy conformations of the stuctures formed, and the possible direction of attack by nucleophiles.

6. RESULTS AND DISCUSSION

6.1 Synthesis of the oxazepine

The work of both Mukaiyama and Ford had demonstrated that the

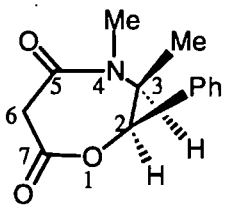

1

ephedrine derived oxazepine **1** induced a high level of asymmetric induction (Chapter 4 p59-66). Thus the potential of this compound as a chiral precursor for asymmetric synthesis was apparent. Favourable results in condensation and Michael addition reactions suggested that stereo-controlled substitution reactions at C-6 should also be possible. It was therefore decided to prepare this oxazepine and to investigate alkylation reactions at its reactive methylene group.

The two forms of the chiral auxiliary, (*1R, 2S*)-(-)-ephedrine and (*1S, 2R*)-(+)-ephedrine (Figure 60), were used to synthesise the oxazepine, using the improved method of preparation devised by Ford.[69]

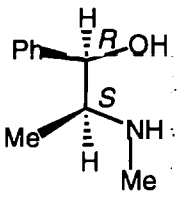

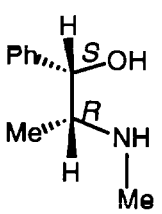

Figure 60 (-)-ephedrine (+)-ephedrine

Structures described throughout the thesis, were based on the oxazepine derived from (+)-ephedrine. However, the enantiomers of all the compounds described in the thesis can be obtained by starting from (-)-ephedrine

The methyl *N*-malonylephedrine compound **12** (Figure 61) was prepared in >95% yield. The IR spectrum showed peaks at 1730 cm^{-1} (ester carbonyl) and 1621cm^{-1} (amide carbonyl). The ^1H NMR spectrum revealed that the C-5 proton of the ephedrine moiety had shifted downfield from δ 2.60 in the ephedrine to δ 4.57 in the methyl *N*-malonylephedrine. After formation of the amide group, there was also a singlet at δ 3.60 (3H-OCH_3), and signals at δ 3.22 due to the malonyl methylene protons, which have moved downfield slightly from δ 3.10 in the dimethyl malonate.

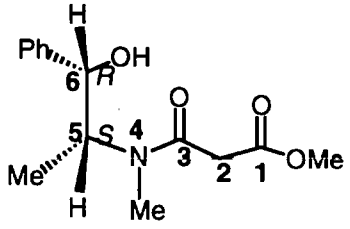

Figure 61 **12**

Base hydrolysis of these compounds (Figure 62a) went smoothly (again >95 % yield), but it was necessary to keep the temperature of the final acidification at below 5 °C, to limit decarboxylation (Figure 62b). Decomposition of the acid can take place by a cyclic mechanism, to give the enol, which then tautomerises to give the more stable ketone form.

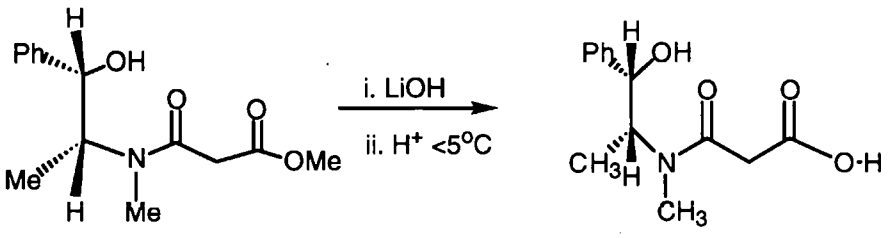

Figure 62a **13**

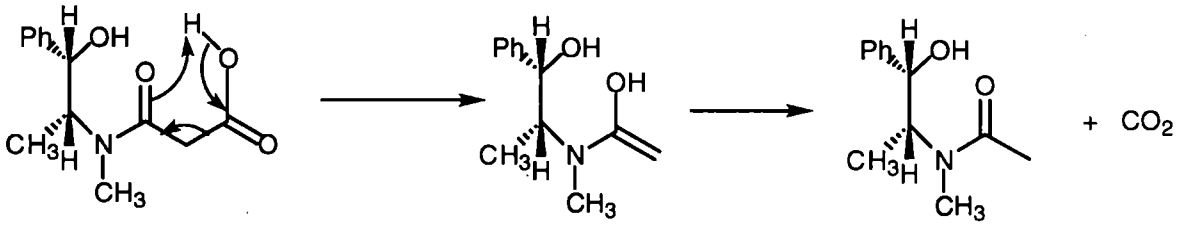

Figure 62b

The ^{1}H NMR spectrum of the hydrolysis product **13** (Figure 62a), showed that the 3H singlet at δ 3.60 (-OCH_3) for the methyl *N*-malonylephedrine had disappeared and there was a broad peak at δ 6.85 (1H-OH). The IR spectrum had the broad O-H stretching vibrations of the carboxylic acid plus the acid and amide carbonyl peaks, at 1731 and 1621 cm^{-1} respectively. The usual literature value for the IR frequency range of an amide carbonyl group is given as 1680-1630 cm^{-1}, but the lower than expected frequency of the amide carbonyl in both the compounds (Figure 61 and 62a), 1621 cm^{-1} is probably attributable to inter- or intramolecular hydrogen bonding. Although this is a tertiary amide, the presence of the hydroxyl group on the ephedrine moiety in both cases and the carboxylic acid in the hydrolysed compound, would give the opportunity for both forms of hydrogen bonding (Figure 62c).

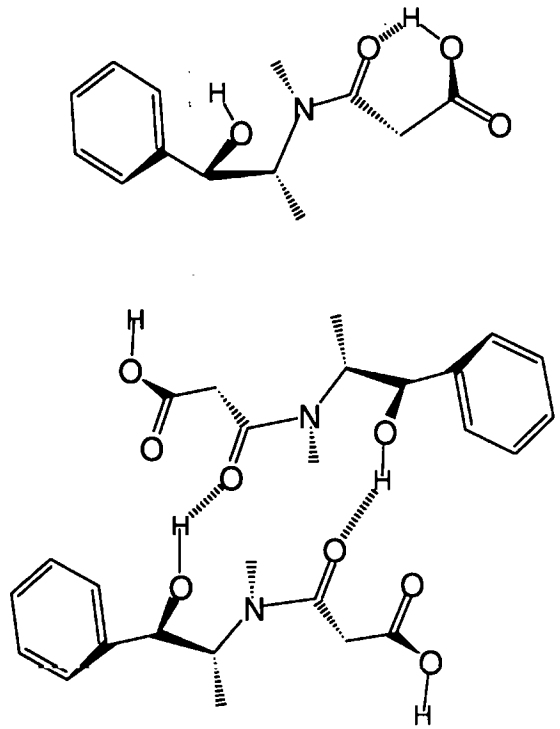

Figure 62c

The lactonisation stage was successful, proceeding to give the product **1** in yields of 45-55 % as shown in Scheme A below.

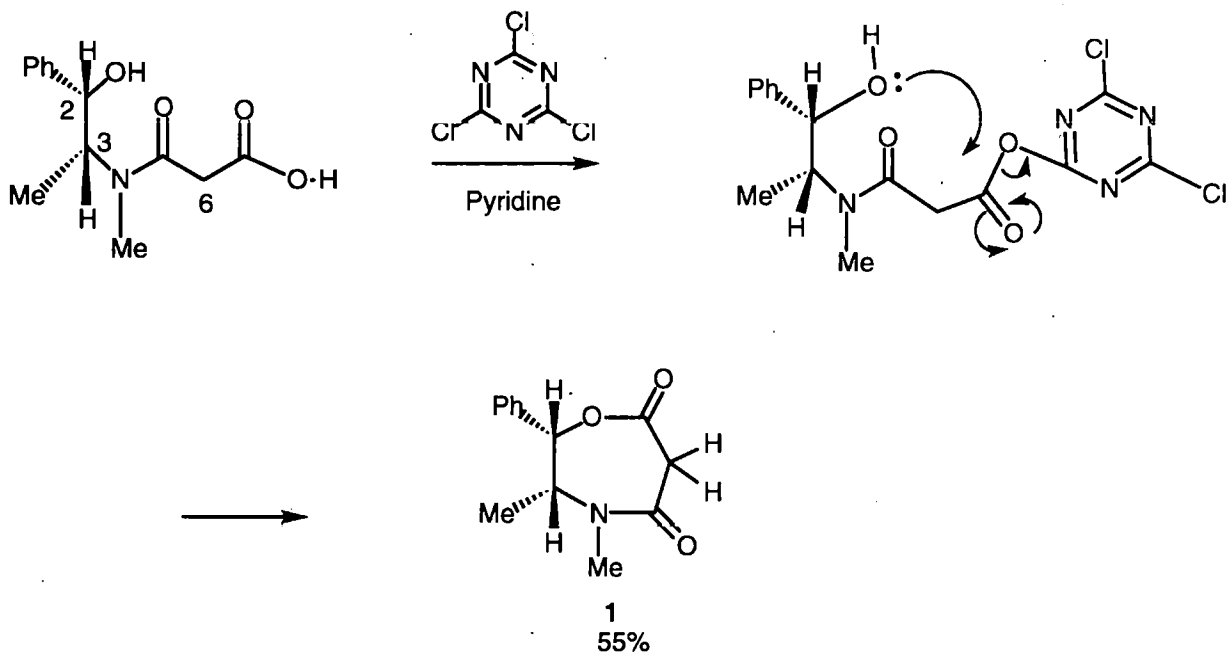

Scheme A

The authors postulated[69] that the pyridine was activating the cyanuric chloride perhaps as the reactive species shown in Scheme A above. A large quantity of highly coloured, presumably polymeric material was also produced at this stage. The broad O-H stretching peak had disappeared from the IR spectrum and the two carbonyl peaks had both shifted to higher frequencies (1745 and 1638 cm^{-1} from 1730 and 1621 cm^{-1} respectively), indicating formation of lactone and lactam functions. As the oxazepine has a seven-membered ring with little ring strain, the frequencies of the lactone and lactam would be expected to be within the range for saturated aliphatic ester and amide carbonyl groups (1750 - 1735 and 1680 - 1630 cm^{-1}), as was the case. However, this increased frequency of both carbonyl functions in the cyclic compound compared to the open chain compounds, might be thought to be too great just to involve the removal of the intramolecular hydrogen bonds. Studies with the β-diester diethyl malonate have shown that where there are two ester carbonyl groups there are two carbonyl frequencies, in this particular compound at 1745 and 1730 cm^{-1}. This is thought to be due to the presence of two conformers, with the higher frequency attributed to dipolar interaction.[70] Carbonyl absorptions may be raised by about 10 - 20 cm^{-1}, when a dipolar mechanism is thought to be involved, possibly due to the intramolecularly close approach of the two carbonyl oxygen atoms.[71] Two possible conformers for the β-diester diethyl malonate are depicted in Figure 63a. The distance between the two carbonyl oxygen atoms in the two conformers is 3.49 Å and 3.73 Å respectively.

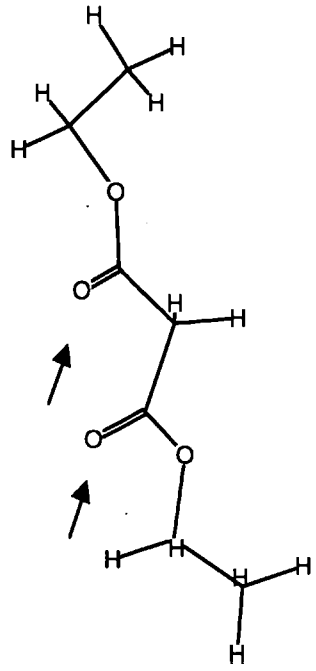

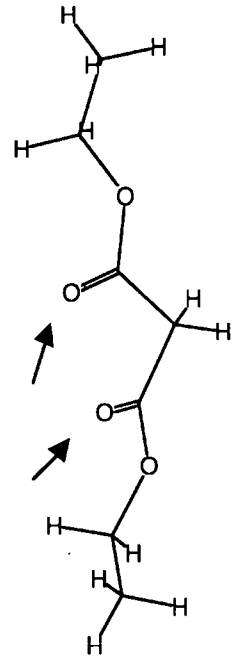

Distance between carbonyl oxygen atoms

3.49 Å 3.73 Å

Figure 63a (Distances calculated using PCMODEL)

As can be seen in **1A** (Figure 63b) the carbonyl oxygen atoms in the preferred conformation of the oxazepine ring, are in quite close proximity. The energy minimised structure of the preferred conformer of the oxazepine (PCMODEL) is also shown in Figure 63b and gave the distance between the carbonyl oxygen atoms as 4.2 Å.

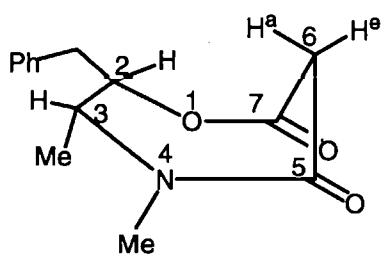

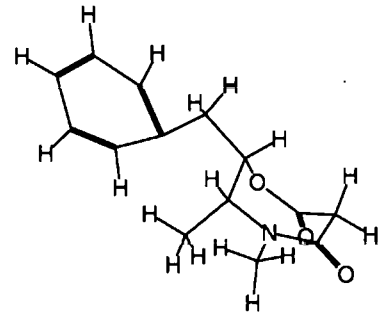

Figure 63b **1A**

The ^1H NMR spectrum showed that the signal for the H-2 proton had moved downfield from a doublet at δ 4.79 in the open chain compound to an apparent singlet at δ 6.00 in the oxazepine (Figure 65). This is a further confirmation of esterification and cyclisation because this proton has moved into a less shielded environment on formation of the lactone.

The Karplus equation

$$^3J_{ab} = J\ \cos^2\phi - 0.28$$

shows the correlation between the dihedral angle (ϕ), and the coupling constant (J) of vicinal hydrogens in rigid systems, and is represented graphically in Figure 64a.

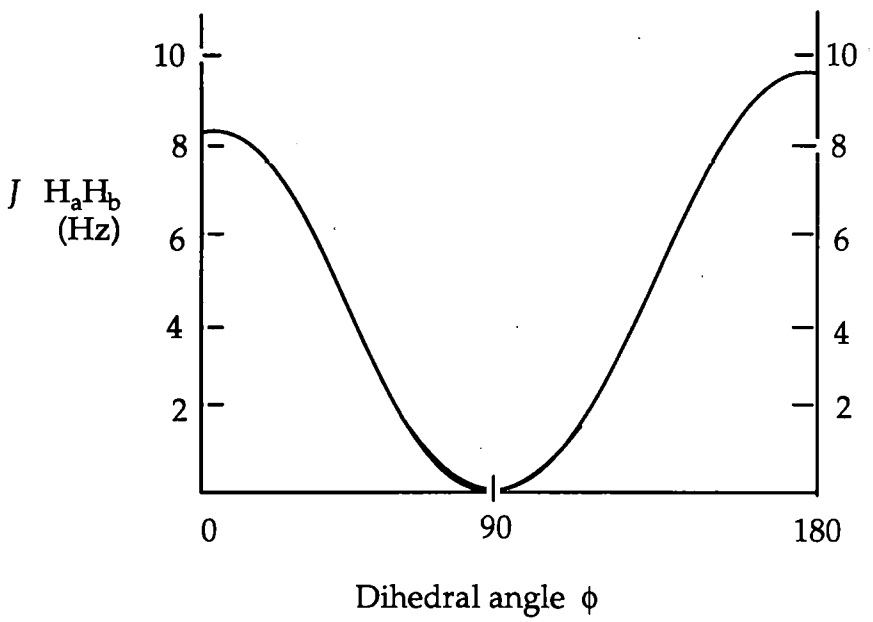

Figure 64a

In forming the oxazepine the dihedral angle between the H-2 proton and the H-3 proton (arrowed in Figure 64b) has become 90 °, thus explaining the presence of the signal as a singlet.

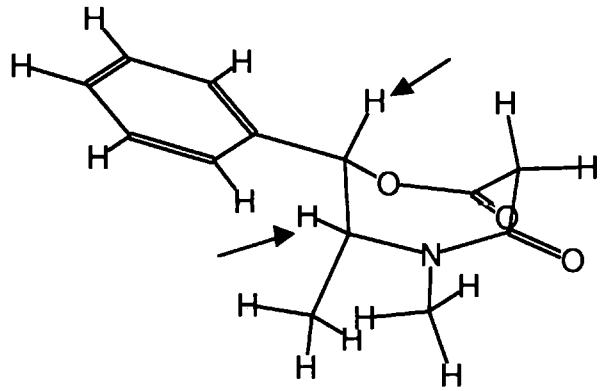

Figure 64b

The H-3 proton signal has moved upfield from δ 4.50 to δ 3.65, because the preferred conformation of the ring structure has put it into an environment in which it is more shielded (by the benzene ring). Also, as there is now zero coupling with the H-2 proton signal. The H-3 proton appears as a quartet. There is also the distinctive feature of the methylene protons at C-6, which show geminal coupling of J =17.5 Hz. These peaks are at δ 3.78 and 4.16. The open chain compound (**13** Figure 61 p.69) and the oxazepine (**1A** Figure 63 p.72), are shown in Figure 65, with a table of comparative δ values from their respective ^{1}H NMR spectra.

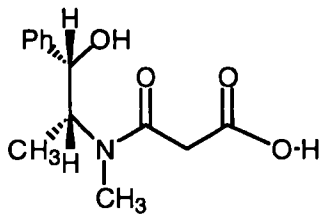

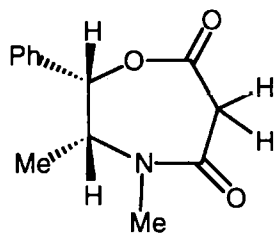

Open Chain Compound **13** (Figure 62a p.70)

	δ ppm
C-C*H*$_3$	1.109
N-C*H*$_3$	2.73
C-C*H*$_2$	3.15
C-C*H*	4.50
Ph-C*H*	1 4.79
-Ph	7.25 - 7.30

Oxazepine **1A** (Figure 63 p.72)

	δ ppm
C(3)-C*H*$_3$	1.19
N(4)-C*H*$_3$	3.00
C6-*H*(x2)	3.78 and 4.16
C(3)-C*H*	3.65
Ph-C*H*	6.00
-Ph	7.28 - 7.48

Figure 65

6.2 Conformation of the oxazepine ring

Ford had already established, through X-ray crystallographic and nOe studies, that the major conformer of this oxazepine was the twist boat structure[70,71] **1A** (Figure 63b).

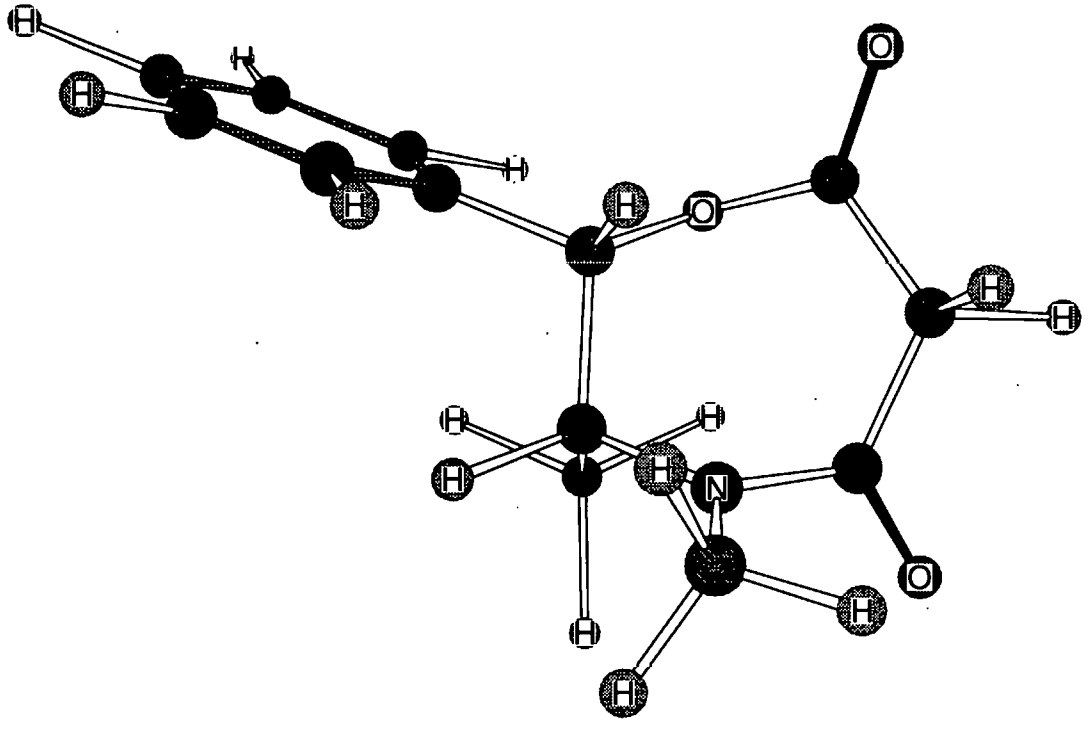

Figure 66

The energy minimised[70,76] three dimensional representation of the oxazepine is depicted in Figure 66, and shows the proximity of the proton at C-2 and the pseudoaxial proton at C-6 (distance = 2.0 Å). This is also supported by the nOe enhancement studies.[70] This conformational analysis also shows the relatively unhindered position of the pseudoequatorial proton at C-6, which would suggest that it should be the easier proton to remove by base. The acidity of the C6

protons will be influenced by the stability of the carbanion formed, and the stereochemistry of the carbanion will determine the stereochemistry of the product. Modelling of the basic oxazepine ring (*ie.* without the phenyl and methyl groups at the stereogenic centres) shows the minimum energy conformation. The enantiomeric forms of this conformation are shown in Figure 67a. Introduction of the phenyl and methyl groups into each of these conformations to give chiral centres of the same configuration, gives chiral products that are diastereoisomers (Figure 67b). Calculating the energy of the two systems shows that the most favourable conformation is Basic ring 1 with an energy of 22.6 kcal $mole^{-1}$ (Figure 67b). This analysis agrees with the structure shown above in Figure 66.

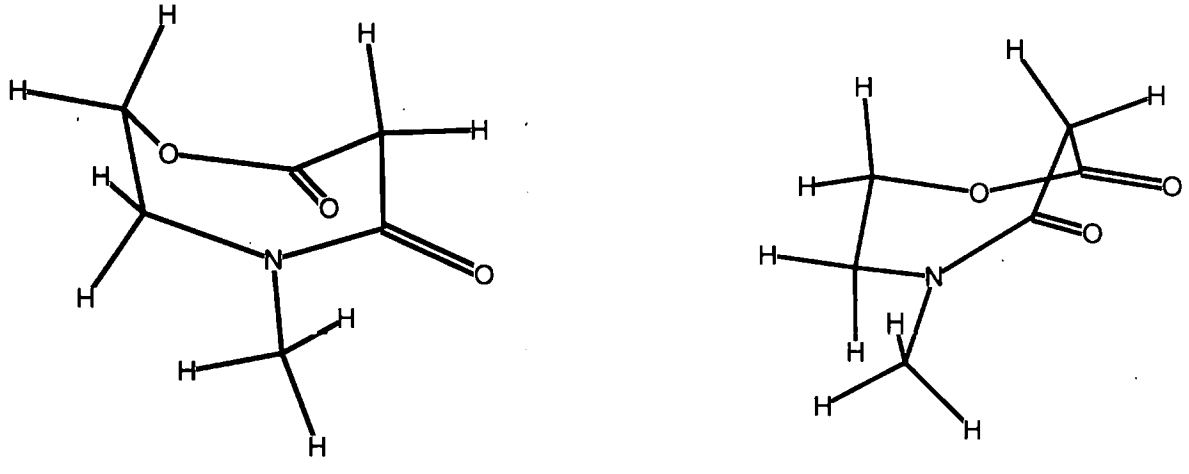

Enantiomer conformations (PCMODEL structures)

Figure 67a

The calculated difference in energy (3.4 kcal mol^{-1}) would suggest that in the equilibrium mixture at room temperature, less than 1% of the less stable isomer would be present.

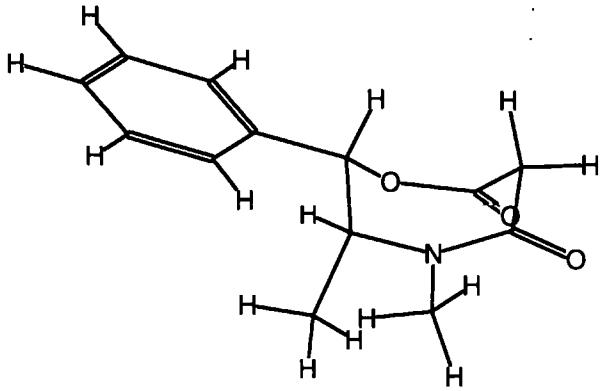

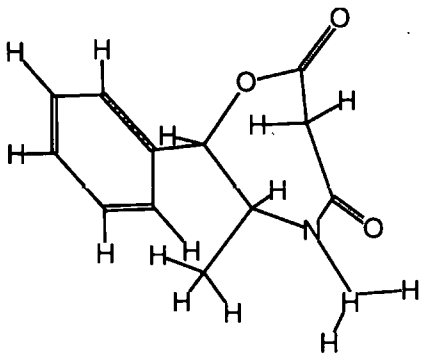

Chiral diastereomeric conformations

Basic ring 1 22.6 kcal mol^{-1} Basic ring 2 26.0 kcal mol^{-1}

Figure 67b

Assuming that Basic ring 1 is the preferred conformation, the unhindered position of the pseudoequatorial proton does appear to allow it to be the most easily removed. Nevertheless it is the pseudoaxial proton that is the most acidic, because when it is removed the lone pair of electrons that are left behind, will lie in an orbital nearly orthogonal to the carbonyl groups and therefore nearly in the plane of their respective Π-systems. (The angles for this are 123 ° and 106 ° respectively, whereas for the pseudoequatorial proton they are 10.6 ° and 5.9 ° respectively).

However, regardless of which proton is removed, the carbanion formed will assume the lowest energy and most stable conformation. Using the Basic ring structures 1 and 2 from Figure 67b, it is possible to calculate (PCMODEL) the

minimum energies of the corresponding carbanions (Figure 68). Basic ring structure 1 provides the lower energy conformation (30.1 kcal mole^{-1}) for the carbanion (Carbanion 1 Figure 68).

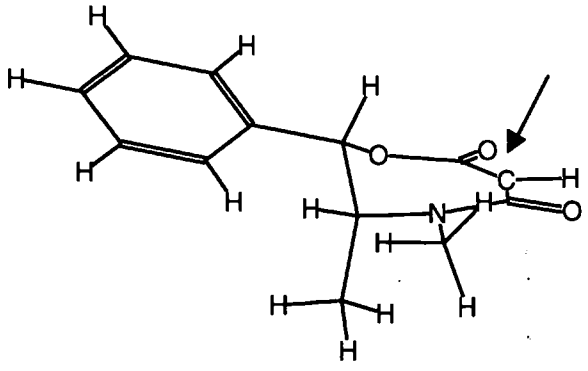

Carbanion 1 30.1 kcal mol^{-1}

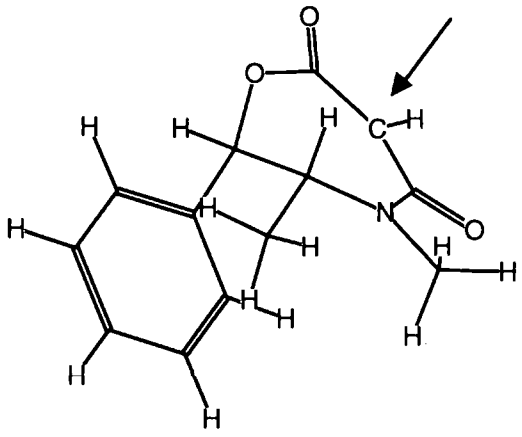

Carbanion 2 36.3 kcal mol^{-1}

Figure 68

The predicted attack on either of these carbanion systems would take place from the upper (*si*) face, because in Carbanion 1 the methyl group shields the lower (*re*) face and in Carbanion 2 the phenyl group shields this face. Figure 69, shows Carbanion 1 in which the preferred direction of approach is from the face opposite to that of the methyl group. (PCMODEL treats the carbanion as a delocalised system.) However, epimerisation is possible with the remaining hydrogen and in the observed product substitution is *cis* to the methyl and phenyl groups, and the most stable and lowest energy configuration will be formed (as shown in Figure 70).

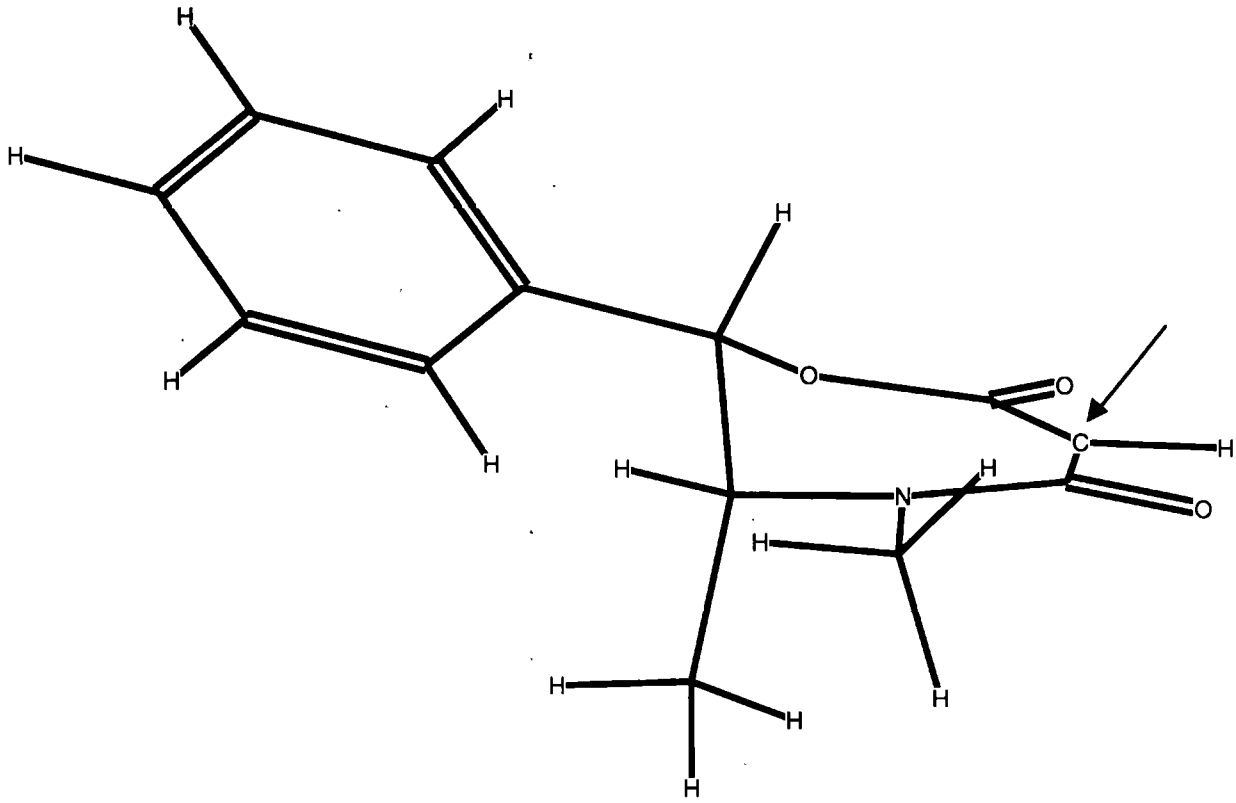

Figure 69

Figure 70 shows the expected energy minimised conformation[74,75] of the derived oxazepine substituted by a benzyl group.

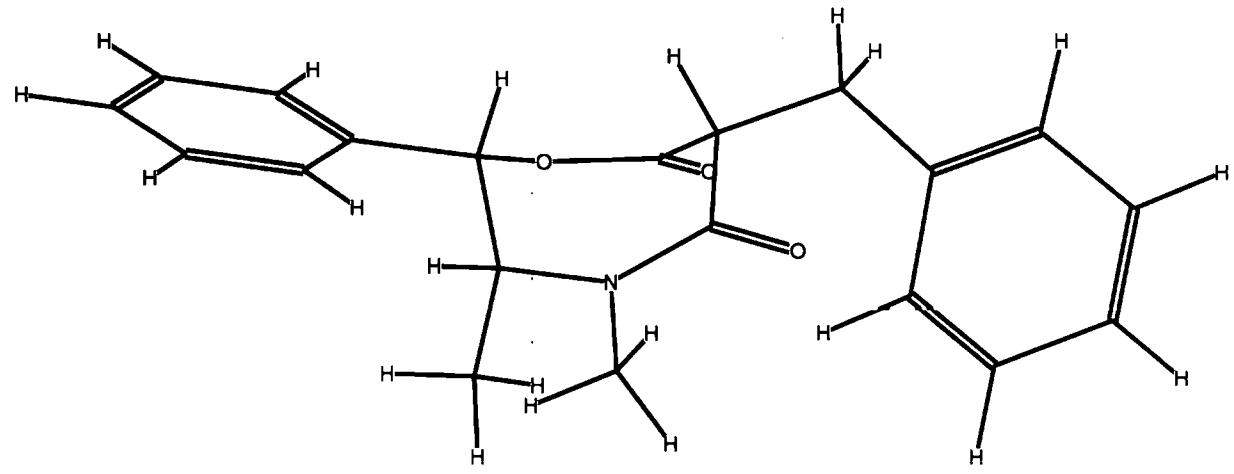

Figure 70

Formation of a further substitution product will again depend upon the stereochemistry of the carbanion formed. Figure 71 shows the plan and side view of the most stable conformation of the anion. A second substituent, would then be expected to add to this anion from the less hindered side of the ring, the top (*si*) face as drawn, to afford the absolute configuration of the disubstituted oxazepine shown in energy minimised conformation in Figure 72.

Plan view

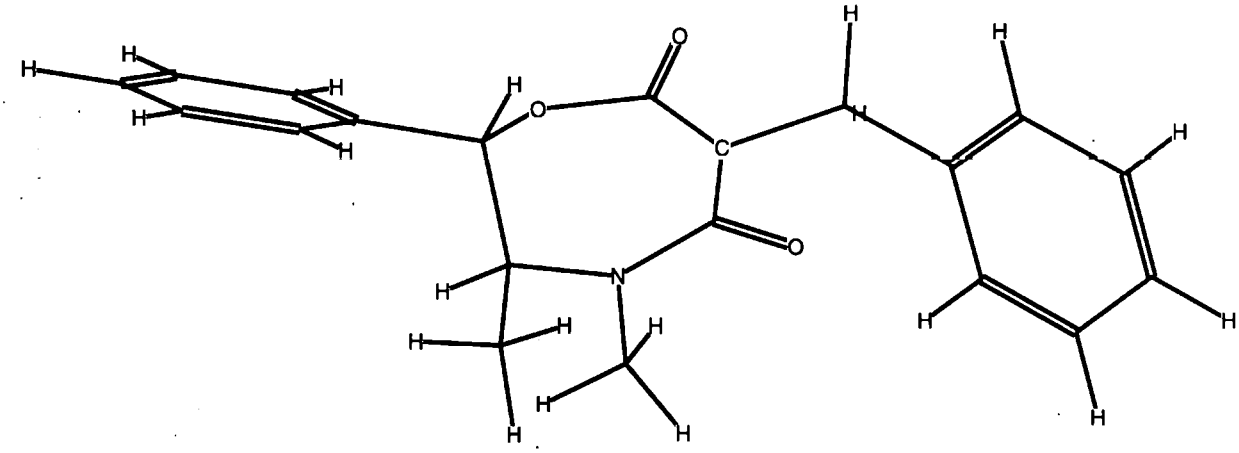

Side view

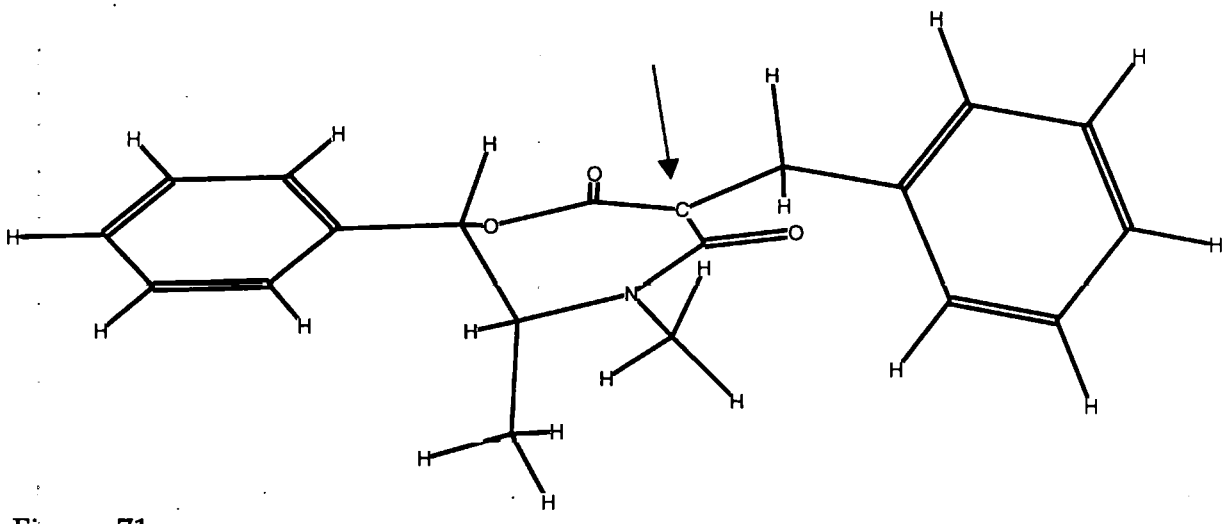

Figure 71

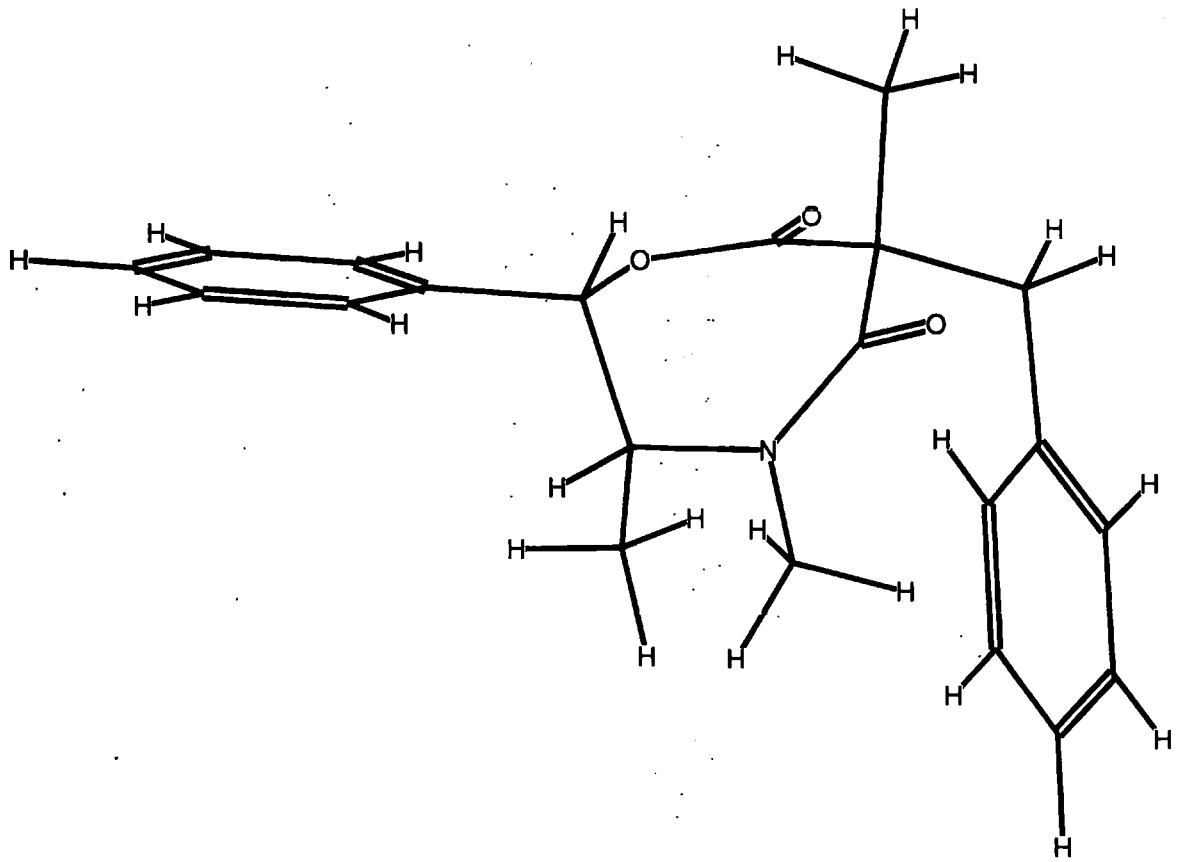

Figure 72

6.3 Synthesis of the substituted oxazepines

The analysis above suggests that the pseudo axial proton should be easily removed by base, but this was far from the case. Its removal proved extremely difficult. As the aim was to convert the oxazepine into its anion for alkylation, only non-nucleophilic, or weakly nucleophilic bases were tried, since if powerful bases were used there was concern that the ring would be ruptured, by cleavage of the lactone or lactam functions. This fear seems to have been realised, as after several of the reactions, no recognisable product could be isolated. On the other hand use of potassium carbonate or sodium hydride led to almost complete

recovery of the starting oxazepine. Only with potassium *tert*-butoxide was successful formation of the enolate anion and alkylation achieved. A complete list of results for these 'alkylation trials' is given in Table 15, showing the different bases tried and the reaction conditions used.

It is difficult to understand why the various bases used gave such distinctly different results. As can be seen from the table, the only successful base was potassium *tert*- butoxide.

Base	Solvent	Temp.	Haloalkane	Result
Et_3N	DCM(dry)	Reflux	BnCl	Possible ring opening
K_2CO_3	DCM(dry)	Room	BnCl	Oxazepine recovered
LDA	THF(dry)	-78 °C	EtI	Possible ring opening
DBU	THF(dry)	-78 °C	EtI	Possible ring opening
NaH	THF(dry)	-30 °C	EtI	Oxazepine recovered
$(CH_3)_3CO^-K^+$	THF(dry)	Room	MeI	Methylated oxazepine

Table 15

Monosubstitution of the oxazepine

Once a satisfactory base, potassium *tert*-butoxide, had been discovered for effecting deprotonation at C6 of the oxazepine substitution, a series of substitution reactions was undertaken. The reaction is shown in Scheme B and the subsequent results are listed in Table 16 below.

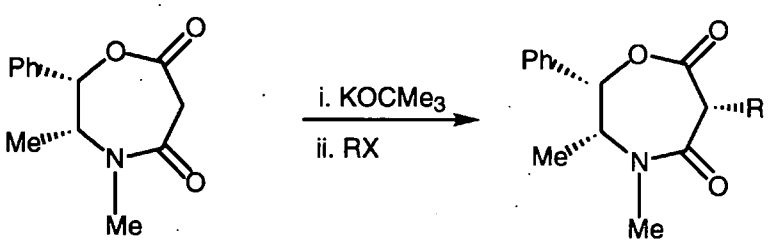

Scheme B

	R	X	% Yield	% de
14	Me	I	95	>98
15	Bn	Cl	95	>98
16		Cl	95	>98
17	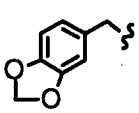	Cl	95	>98

Table 16

Products **14, 15, 16 and 17** are illustrated below:-

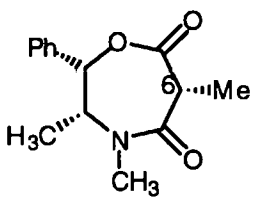

14

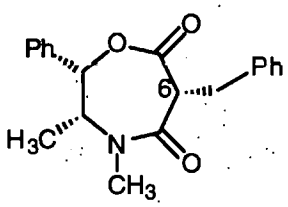

15

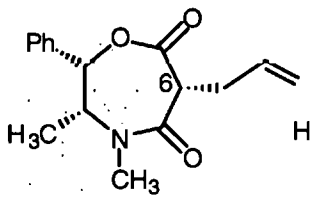

16

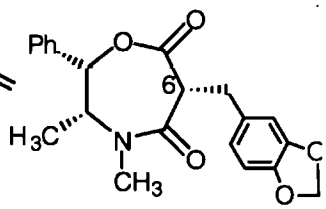

17

Monosubstitution using methyl iodide at room temperature to give product **14**, was effected almost quantitatively (95% yield). Initial evidence that substitution had taken place was seen in the ^{1}H NMR spectrum. The signals for the methylene protons (at δ 3.78 and δ 4.16) and their distinctive coupling (J =17.5 Hz) was absent. Instead there was an observed doublet attributable to the introduced methyl group at δ 1.58 coupled with the H-6 pseudoaxial proton (J =5.0 Hz). The signal for the H-6 proton now appeared as a quartet (J=5.0 Hz) at δ 4.07 (Figure 73).

Further supporting evidence that these compounds had been synthesised was gained from mass spectrometry and accurate mass determinations (Table 16). For compound **14** the CI mass spectrum showed a peak at 265 (M^++NH_3, 100%) and a peak at 248 (M+H^+, 63%), with no other peak above 20% abundance relative to the major peak (100% relative abundance).

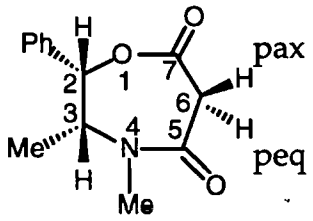

Oxazepine

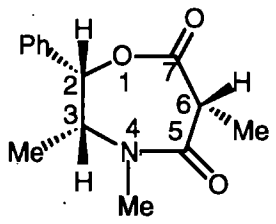

Methylated oxazepine

Figure 73 (peq - pseudoequatorial pax - pseudoaxial)

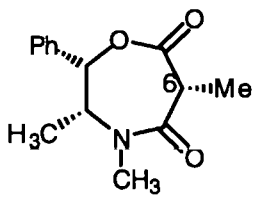

14

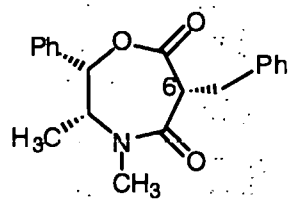

15

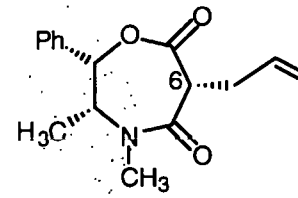

16

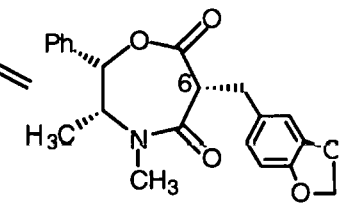

17

	$(M + H)^+$	Mass	
		Calculated	Found
14	248	248.1287	248.1288
15	341	341.1865	341.1858
16	274	274.1443	274.1446
17	368	368.1498	368.1502

Table 17

Compound **14** can be modelled using the Basic ring structures 1 and 2 from Figure 67b (p. 83). Two configurations (**a** and **b** Figure 74) are possible for each structure, depending upon which hydrogen atom is substituted at C6. The MMX energies span a range of 25.8-31.8 kcal mol^{-1}, thus all are possible. However, the H-2/H-6 distance of 2.0Å, in the thermodynamically most stable structure **1b** (25.8 kcal mol^{-1}, Figure 74), only fits the following nOe enhancement calculations for the compound **14** (Figure 75).

Configurations for Monomethyl substituted **1A**

Using 'Basic' ring 1 conformations (Figure 67b p.83)

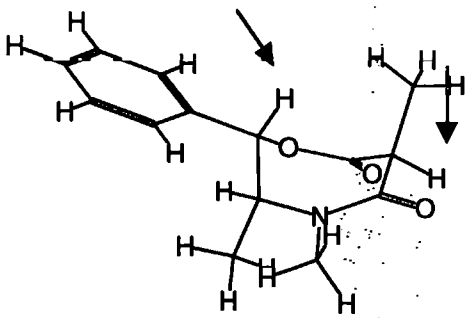

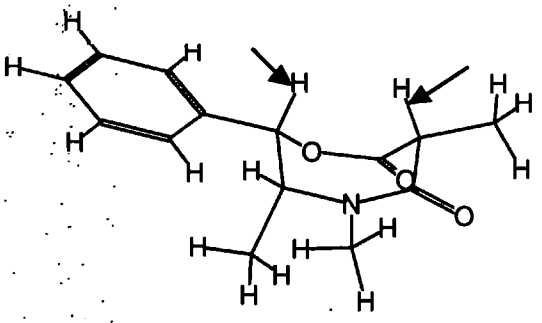

Distance between H2 and H6

3.78 Å

2.00 Å

Monomethyl **1a** 27.7 kcal mol^{-1}

Monomethyl **1b** 25.8 kcal mol^{-1}

Using 'Basic' ring 2 conformations (Figure 67 b p.83)

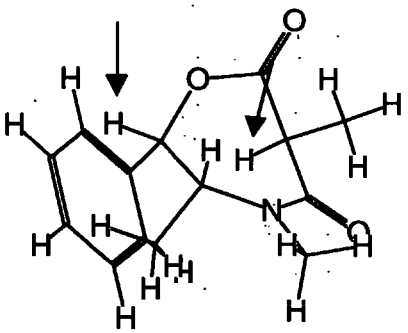

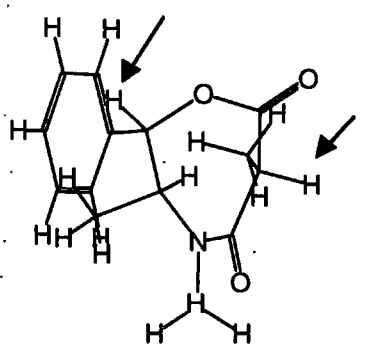

Distance between H2 and H6

3.73 Å

5.35 Å

Monomethyl **2a** 29.3 kcal mol^{-1}

Monomethyl **2b** 31.8 kcal mol^{-1}

Figure 74

Further evidence for the stereochemistry of compound **14** was gained from nOe studies. Figure 75 shows the portion of the nOe spectrum related to the H-2 proton labelled 'a' (δ 6.2) with the H-6 proton labelled 'b' (δ 4.2) and with the substituted methyl group labelled 'c' (δ 1.5).

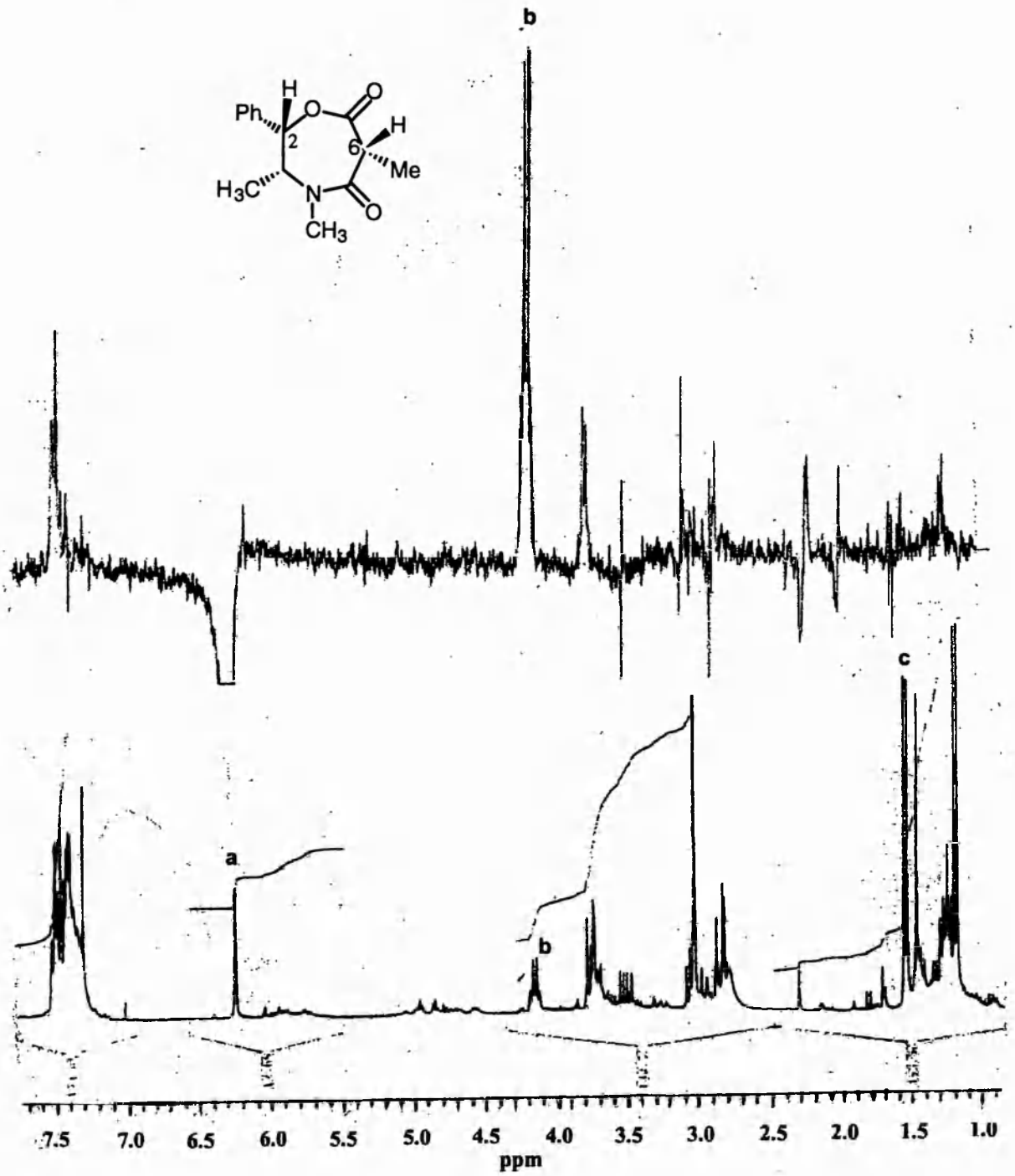

Figure 75

These enhancements are tabulated in Figure 76. It can be seen for compound **14,** that there is considerable enhancement between the H-6 proton and the H-2 proton with no observable effect between the H-2 proton and the substituted methyl group. If substitution had been effected in the axial position, then enhancement would have been expected between these two latter signals.

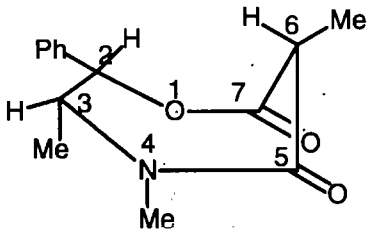

14

Group irrradiated	Group observed	% nOe
H-2	H-3	+1.1
H-2	H-6	+7.5
H-6	H-2	+2.0
C-6 Me	H-6	+7.5
H-6	C-6 Me	+0.7
H-2	C-6 Me	no observable effect

Figure 76

Monosubstitution using benzyl bromide, allyl bromide or piperonyl chloride with potassium *tert* butoxide as the base, gave excellent results with yields of around 95% in each case (Scheme B and Table 16 p.89). This was confirmed by repeat experiments, to yield further material for future use.

For the benzyl substituted oxazepine (**15**), the C-6 pseudoaxial proton showed a dd (J= 5.0 Hz) signal on the ^{1}H NMR at δ 4.22-4.29 which coupled with the C-6 benzylic protons at δ 3.25-3.35 and δ 3.60-3.73 (dd J 5.0 and 10.0 Hz). NOe enhancement values again showed evidence confirming the stereoselectivity of the substitution, with an even greater enhancement between the C-2 proton and the H-6 proton than in the methyl substituted oxazepine (Figure 77). This may be explained by the greater bulk of the benzyl group, needing to be positioned at a further distance from the two carbonyl groups. This leads to greater twisting of the boat conformation, with the result that the two protons are moved closer together.

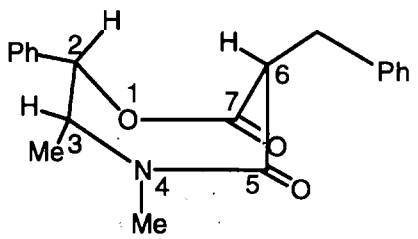

15

Group irrradiated	Group observed	% nOe
H-2	C-3 Me	+0.3
H-2	H-3	+5.8
H-2	H-6	+24.0
H-3	N-Me	+1.1
H-6	H-2	+8.0
H-6	C-6 CH_2	+3.9
H-2	C-6 CH_2	no observable effect

Figure 77

The allyl (**16**) and piperonyl (**17**) substitution products followed the same pattern, with the ^1H NMR again showing the disappearance of the distinctive coupling feature of the methylene C-6 protons in the oxazepine. In the case of the allyl substitution the H-6 proton showed coupling to the methylene protons (J=7.5Hz) of the allyl group, and for the piperonyl substitution it showed coupling with the methylene protons (J=7.5Hz) of the piperonyl group. Enhancement studies from nOe spectra also confirmed these structures (Figure 78). The H-2: H-6 interaction for the allyl and piperonyl substituted compounds, is similar to that of the benzyl substituted oxazepine, but all differ from the methyl substituted oxazepine. This seems to support the possibility that it is the bulk of the substituting group that is altering the conformation of the ring.

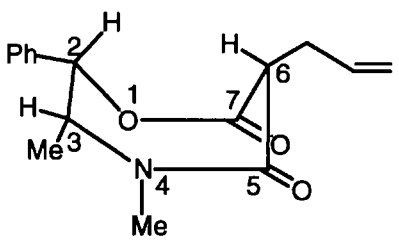

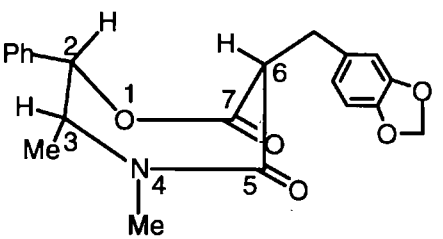

16

Group irradiated	Group observed	% nOe
H-2	H-3	+5.0
H-2	H-6	+22.0
H-6	H-2	+10.0
H-6	C-6 CH_2	+2.0
H-6	allyl CH	+2.0

17

Group irradiated	Group observed	% nOe
H-2	H-3	+5.1
H-2	H-6	+19.4
H-6	H-2	+6.3
H-6	C-6 CH_2	+1.4
H-2	C-6 CH_2	-1.1

Figure 78

The monosubstitution reactions were carried out at room temperature, and resulted in products with estimated diastereoisomeric ratio of >9:1. These diastereoisomeric ratios for the monosubstituted compounds, were estimated from ^{1}H NMR proton coupling patterns and confirmed by the nOe enhancement spectra.

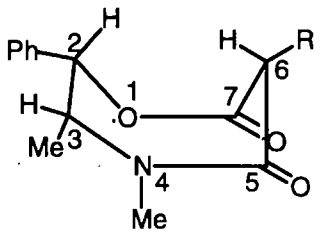

Coupling between the H-2 proton and the H-6 proton was seen for all the compounds **14, 15, 16 and 17**, with no evidence of any coupling between the H-2 proton and the substituted R group protons. The nOe enhancement spectra confirmed these findings, showing only enhancement between the H-2 and H-6 protons for all four compounds, with no observed enhancement between the H-2 proton and the substituted R group protons. Therefore, for each compound there was no observable evidence of a mixture of diastereoisomers from the ^{1}H NMR spectra or by nOe studies.

Disubstitution of the oxazepine

These reactions were again carried out using potassium *tert* -butoxide as the base. The first reaction attempted was the substitution of a benzyl group into the already methylated oxazepine (**14**), to give compound **18** (illustrated on p.100). The diastereoisomeric ratio (dr) achieved was only 2:1 for reaction at room temperature, but at -30 °C and at -78 °C the de increased to 4:1. It was decided that

to obtain the maximum dr in the disubstituted compounds, (with the second group in the pseudoaxial position), the second substitution should be carried out at -78 °C. The reaction is shown in Scheme C and the subsequent results are listed in Table 18 below.

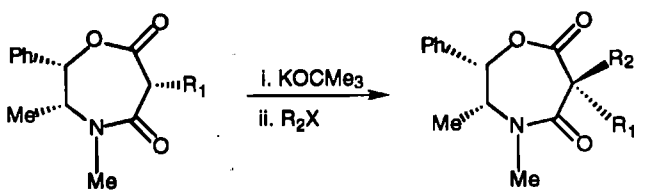

Scheme C

R_1	R_2	X	% Yield	% de	
Me	Bn	Br	70	60	18
Me		Br	80	>90	20
Bn	Me	I	80	>90	19
	Me	I	80	>90	21
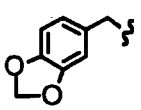	Me	I	80	>90	22

Table 18

Products **18 - 22** are illustrated below

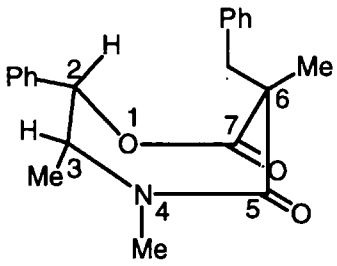

18

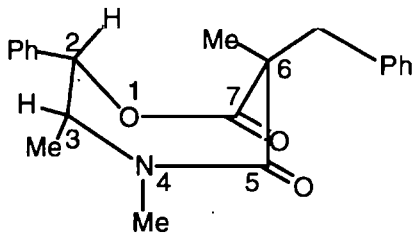

19

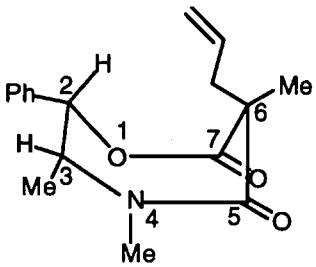

20

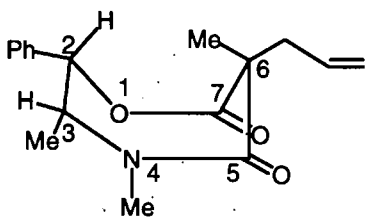

21

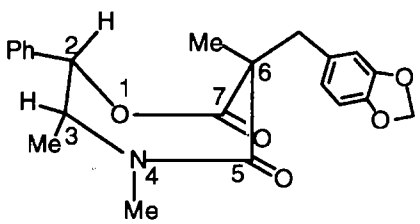

22

Table 18 shows that the second substitution proceeded successfully, with yields of 70-80% and diastereoisomeric excesses of >80% in most cases. Configurations were determined by nOe studies. The diastereoisomeric excesses in these cases were estimated by ^{1}H NMR.

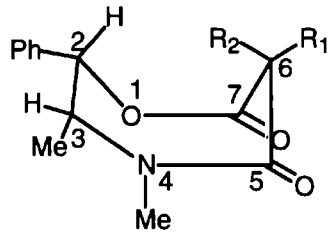

Coupling between the R_2 group protons and the R_1 group protons was seen for the disubstituted compounds **19, 20, 21** and **22**. The nOe enhancement spectra for these four compounds showed only enhancement between the H-2 and R_2 group protons, with no observed enhancement between the H-2 proton and the substituted R_1 group protons. Thus for these four compounds there was no observable evidence of the products being a mixture of diastereoisomers. However in the case of compound **18** a mixture of isomers was observed, the ^1H NMR signals of the C-2 protons of both isomers were present on the same spectrum for this compound, and could be readily identified because of their different chemical shifts. In compound **18** the value of δ for the C-2 H is 4.62 and for compound **19** the value is δ 5.60. It was therefore possible to calculate the de by comparison of the area of the signals for this proton (C2-H), from the spectrum.

During the first substitution under room temperature conditions, 1 mole of base per mole of oxazepine was used. The electrophile was added slowly and as there would have been alkylated enolate present, equilibration would give the thermodynamic product. Once all the electrophile had been added there would have been little or no base left.

However, during the second substitution there is no possibility of a second deprotonation, and hence the substitution is under kinetic control. Not only is there stereodirection by the chiral auxiliary, but the first group may also hinder the approach of the second reagent. In the relatively planar carbanion, if the second group is bulky it may compete for the pseudoequatorial position. This may indicate that for the second substitution it is not only the approach that is hindered, but that the positioning is also competitive. This can be seen in the case where a benzyl group was added to the already methylated oxazepine ring **18**, in which case the de was only 4:1, whereas for compound **19** in which the methyl group is the second substituent the dr was 9.1.

Modelling of the methyl/benzyl substituted compounds **18 and 19** (shown below), and using the Basic ring structures **1** and **2** from Figure 67b (p. 83), shows that two configurations at C6 (**a** and **b** Figure 79 p. 103) are possible for each structure. The MMX energies span a range of 40.6-49.9 kcal mol^{-1}. However, the distance between the H-2 and the C-6 Me protons of 2.26 A, in the thermodynamically most stable structure **1b** (40.6 kcal mol^{-1}, Figure 79), only fits the nOe enhancement determinations for the compound **19** (Figure 80 p.106). Thus supporting the assignment of the structure of the major isomer.

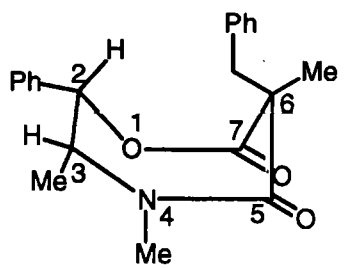

18

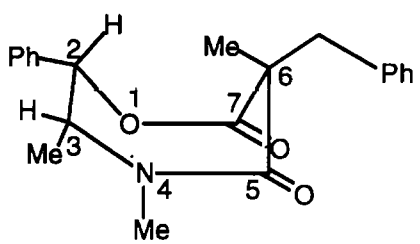

19

Basic ring 1 (Figure 67 b p.83)

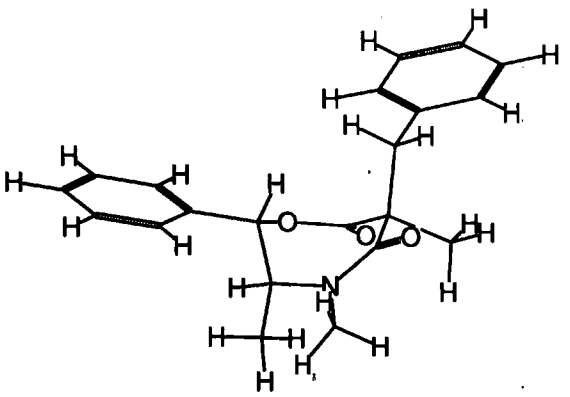

Benzylmethyl **1a** 42.6 kcal mol^{-1}

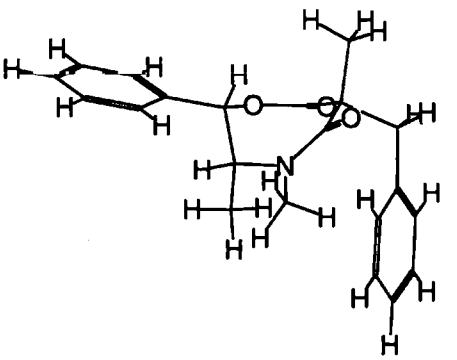

Methylbenzyl **1b** 40.6 kcal mol^{-1}

Basic ring 2 (Figure 67 b p.83)

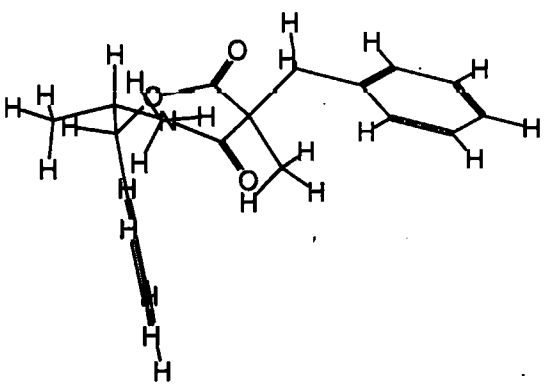

Benzylmethyl **2a** 49.9 kcal mol^{-1}

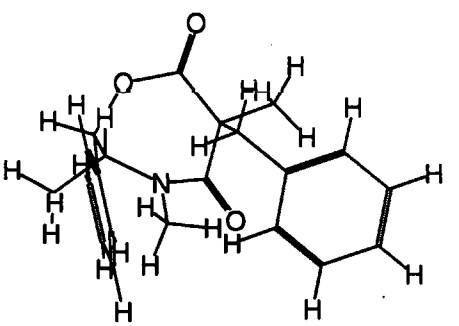

Methylbenzyl **2b** 47.8 kcal mol^{-1}

Figure 79

Again, as for the monosubstituted compounds, the initial evidence that substitution had occurred, came from the respective ^{1}H NMR spectra for each disubstituted oxazepine. The signal for the C-6 pseudoaxial proton had disappeared and an appropriate signal for the substituting group was present.

^{13}C NMR analysis for the mono- and di-substituted compounds gave spectra with the required equivalent carbon atoms for each compound, including the presence of two carbonyl carbon atoms in each case.

Methylation of the benzyloxazepine (**15**) gave a yield of 80% (crude product **19**) with a diastereoisomeric excess of 9:1. The ^{1}H NMR for this disubstituted product, showed the absence of the double-doublet (1H) signal at δ 4.22-4.29 (C-6 proton), and the presence of a singlet (3H, C-CH_3) signal at δ 1.88. The ^{1}H NMR spectra for compounds **15** (BnOAP) and **19** (MeBnOAP) are shown in Figure 80.

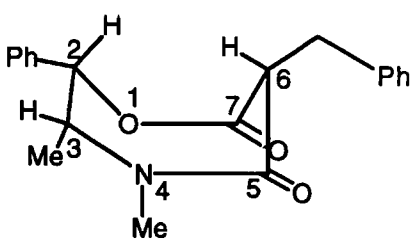

15

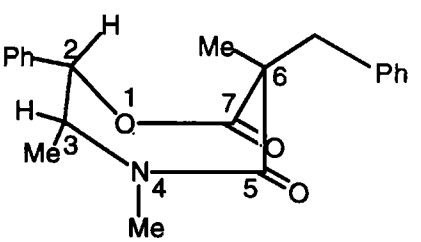

19

Benzyloxazepine **15**

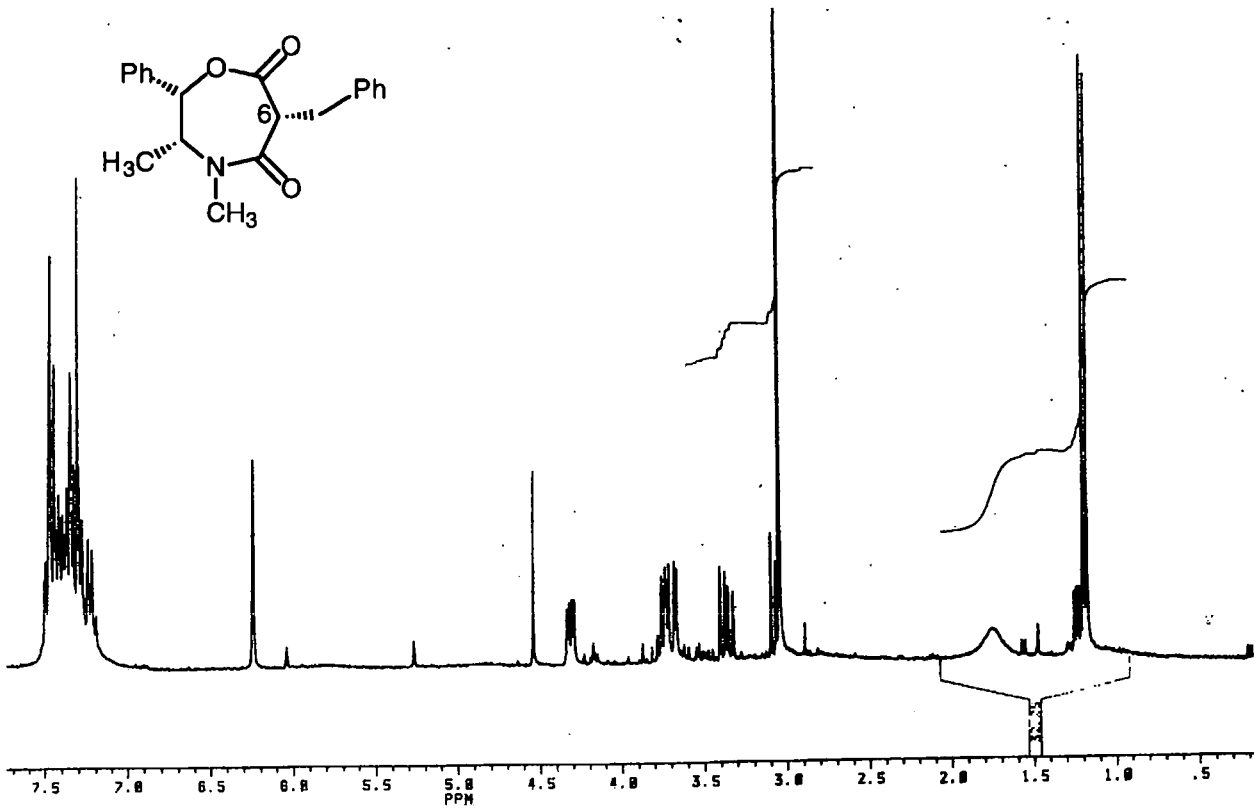

Methylated benzyloxazepine **19**

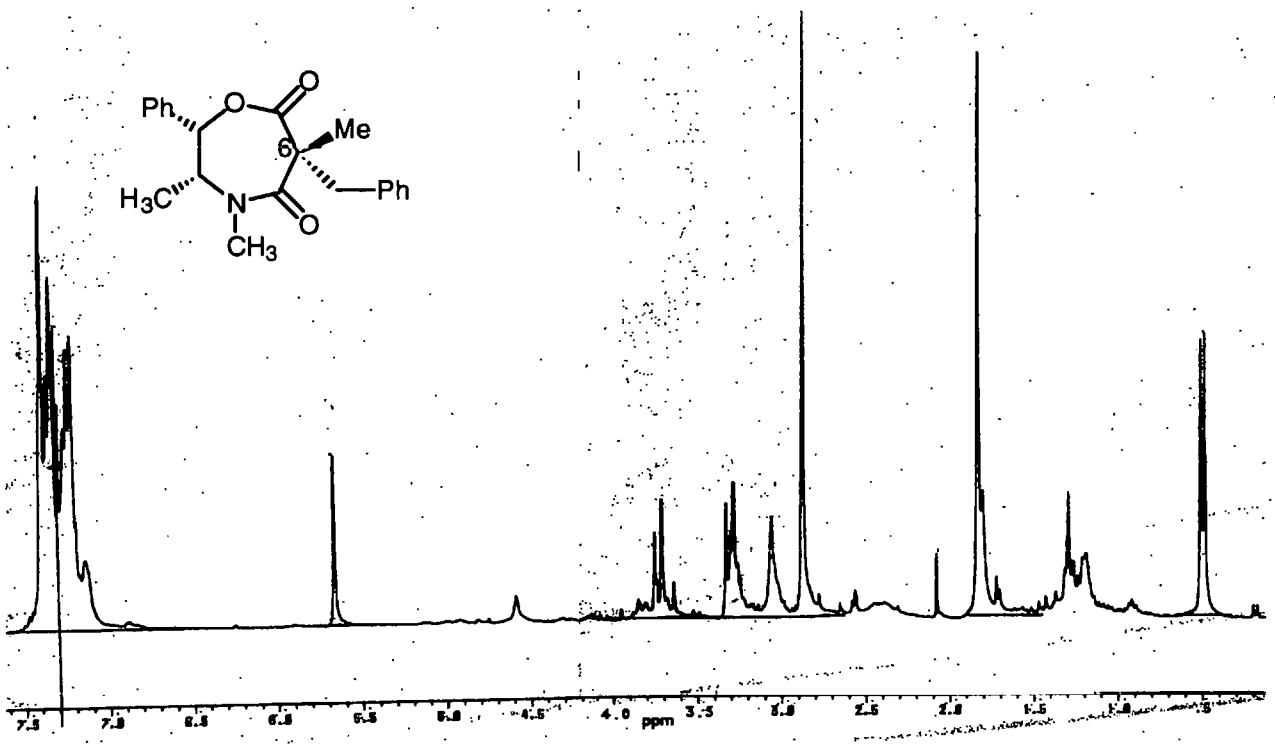

Figure 80

Calculations from nOe studies for **19** (Figure 80), showed enhancement between H-2 and the introduced methyl group at C-6. There was no observable effect between the H-2 and the C-6 benzyl group.

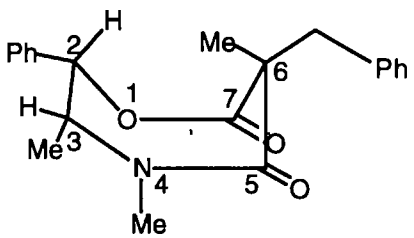

19

Group irradiated	Group observed	% nOe
H-2	H-3	+0.4
H-2	C6 Me	+1.5
C6 Me	H-2	+4.8
C6 CH_2	C3 Me	+3.2
C6 CH_2	N Me	+1.3
H-2	C6 CH_2	+2.0
H-2	C6 Ph	no observable effect

Figure 80

Evidence for the effective benzylation of the methyloxazepine **14** (Figure76 p.95) to give the disubstituted product **18** (figure 81) was also seen from the ^{1}H NMR spectra, with the appearance of a signal for one of the benzylic protons at δ 3.87 (doublet J=12.5). The signal for the other proton was partially masked by the

singlet for the N-CH_3 protons. The yield of crude product was 70%, and after column chromatography the recovered material gave a diastereoisomeric excess of 4:1. Fractional crystallisation increased the de to 9:1.

X-Ray crystallographic studies (see Appendix) confirmed the configuration and although the X-ray studies give the preferred conformation in the solid state, there is a similarity with the conformation deduced in solution, which was predicted by the ^1H NMR studies for this compound. The signal for the C-2 proton has moved up-field in this compound in comparison with the same proton in the spectrum of the compound resulting from methylation of the previously benzylated oxazepine. The converse is seen for the C-3 methyl protons, where the signal moves downfield as the conformation puts them in a more deshielded environment.

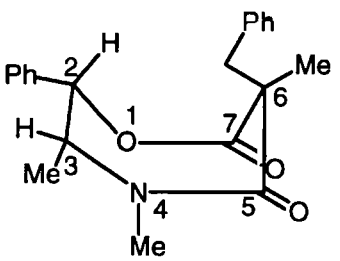

Figure 81 **18**

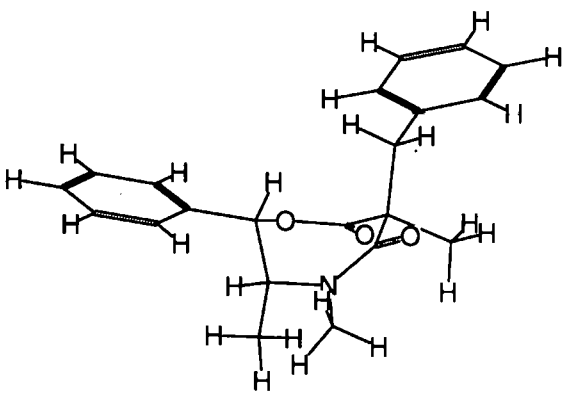

1a (from Figure 79 p.103)

The PCMODEL structure for Basic ring **1a** (Figure 79 p.103) and the X-ray structure **S311** are very similar, as the following Table 19 shows.

	Angle between		Distance between	
	H-2 and H-3	C-6 CH_2 and C-6 CH_3	H-2 and H-3	C-7=O and C-5=O
1a	78°	108°	2.6 Å	4.7Å
S311 (21)	79°	110°	2.4 Å	4.6 Å

Table 19

Preparation of the three disubstituted oxazepines shown in Figure 82, went smoothly with yields of 80% and des of ~80%, in each case.

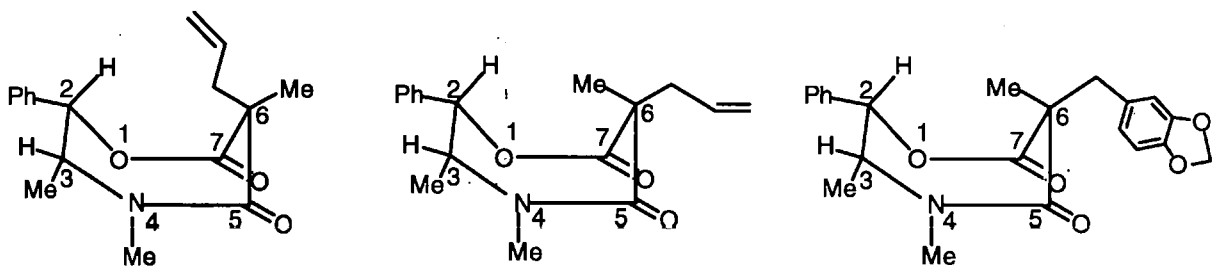

20 **21** **22**

Figure 82.

The initial structural evidence was again seen on the ^1H NMR spectra for these compounds, with the disappearance of the signal for the proton at C-6, and the appearance of the signals for the respective substituent groups. The allylated methyloxazepine **20** showed the signal for one of the methylene protons at δ 2.75 (dd). The other proton was masked by the signal for the N-CH_3 protons at δ 3.05.

The methyl group in the methylated allyloxazepine **21** gave a singlet peak at δ 1.66, and in the methylated piperonyloxazepine it also gave a singlet but in this case at δ 1.80.

NOe studies for the two compounds **20** and **21**, shown in Figure 83, gave further evidence for the configuration of the substitutions. Enhancement was observed between the C-2 proton and the second substituted group but there was no observable effect with the first substituted group.

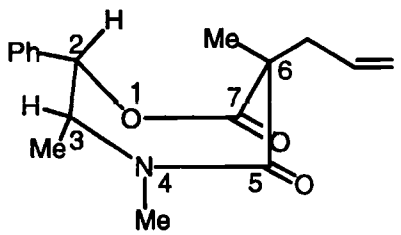

21

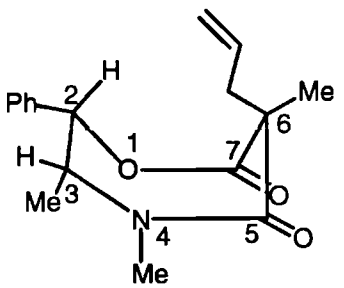

20

Group irradiated	Group observed	% nOe	Group irradiated	Group observed	% nOe
H-2	H-3	+4.6	H-2	H-3	+1.9
H-2	C-6 CH_3	+1.7	H-2	C-6 CH_2	+3.4
C-6 CH_3	H-2	+6.8	C-6 CH_2	H-2	+2.3
H-2	C-6 CH_2	no observable effect	H-2	C-6 CH_3	no observable effect

Figure 83

The IR frequencies for the lactone and lactam carbonyl functions in the disubstituted compounds were lower than in the monosubstituted oxazepines (see Table 20). This may be because the conformation of the ring in these compounds has altered sufficiently, so that the two carbonyl oxygens do not

approach as closely and the dipolar effect between them is decreased. Thus the frequency of the lactone and lactam functions is reduced.

Compound	Structure	C=O Frequencies cm^{-1}	
		Lactone	Lactam
1	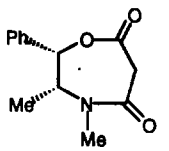	1745	1638
14	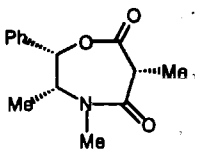	1749	1639
15	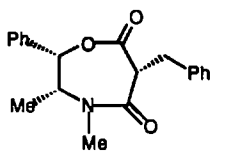	1750	1639
16	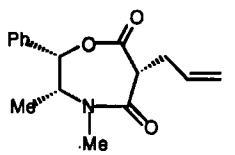	1747	1638
17	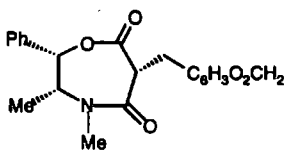	1745	1638
18	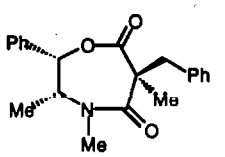	1727	1638

Compound	Structure	C=O Frequencies cm^{-1}	
		Lactone	Lactam
19	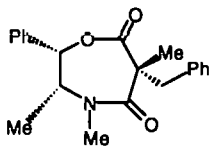	1733	1631
20	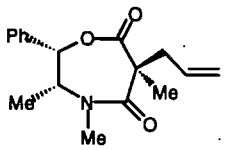	1732	1634
21	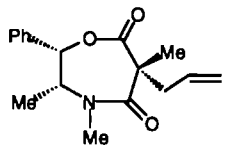	1736	1631
22	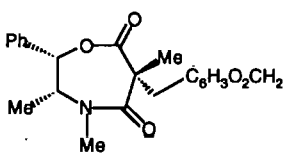	1730	1628

Table 20

X-Ray crystallographic studies (see Appendix) on the methylated allyloxazepine **21** confirmed its configuration, and indicated a similarity to the preferred conformation in solution which was inferred from the ^1H NMR and nOe studies on this compound.

The syntheses were further corroborated by mass spectroscopic analysis and accurate mass determinations (Table 21).

Compound	Structure	Accurate Mass		
		$(M + H)^+$	Calculated	Found
18	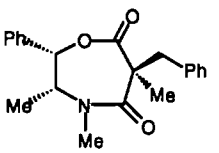	338	338.1756	338.1759
19	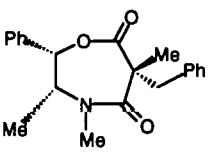	338	338.1756	338.1754
20	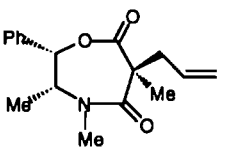	288	288.1600	288.1598
21	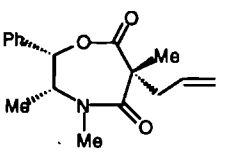	288	288.1600	288.1605

Table 21

6.4 Enantioselective synthesis of α-amino-acid derivatives

With the synthesis of the disubstituted oxazepines in hand, we were now in a position to move towards our major goal. It was envisaged that chemo- (and therefore regio-) selective ring cleavage followed by functional group transformations with retention of configuration, would lead to α-amino-acids **23** with predictable configuration.

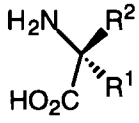

23

There are a large number of well known and standard methods which use achiral non-cyclic precursors to synthesise α-amino acids: the Hell-Volhard-Zelinski, the Strecker and amidomalonate syntheses for example. Many of these methods will yield a racemic mixture of *R* and *S* products which must of course then be resolved into the pure enantiomers. A comprehensive review and critical evaluation has been written by Robert M. Williams of the many newer methods of synthesis of α–amino acids.[72]

Ring cleavage

It was expected that hydrolytic ring cleavage would open the ring at the lactone, giving an hydroxyl group at C-2 and a carbonyl group at C-6 (Figure 84). This could be followed by a Schmidt reaction on the carboxylic acid to produce an amine without changing the configuration at C-6. The Schmidt rearrangement proceeds *via* an intermediate isocyanate. This would involve migration of the

chiral carbon atom C-6 to a nitrogen atom. The intermediate is formed with retention of configuration of the chiral migrating group (illustrated in more detail in Figure 91 p. 123). Finally hydrolysis, to cleave the amide at N-4 to an amine and a carboxylic acid, should give the α-amino acid, and in the most favourable case, lead to the release of the original chiral auxiliary (ephedrine).

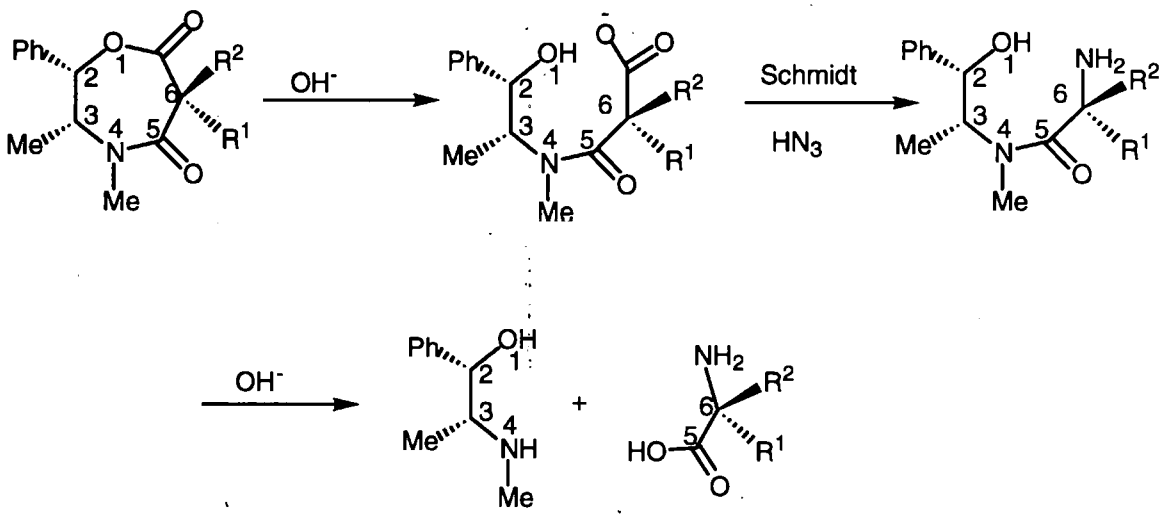

Figure 84

Hydrolysis of the unsubstituted oxazepine is readily achieved using potassium carbonate,[68] but cleavage of the substituted oxazepines proved much more difficult. Neither potassium carbonate in methanol, or lithium hydroxide or sodium methoxide gave any observed reaction and starting material was recovered in all cases (Figure 85). With potassium carbonate or lithium hydroxide, hydrolysis was attempted at both room temperature and above.

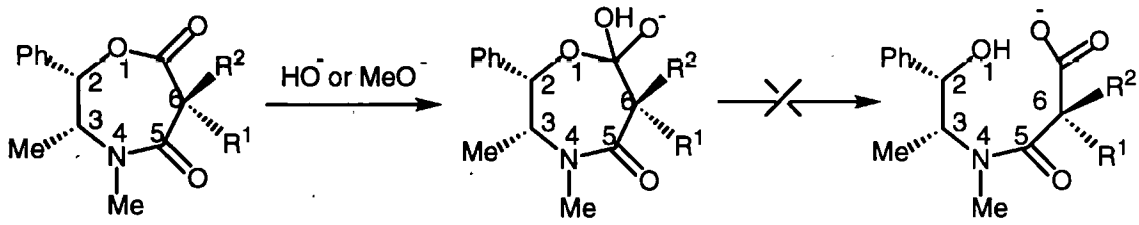

Figure 85

Hydrogenolysis was also attempted, in order to cleave the bond between the C-2 carbon and O-1 oxygen. The catalyst used was 5% Pd/charcoal. The reaction was carried out at a temperature of 25-30 °C and one atmosphere pressure (Figure 86). Again only starting material was recovered.

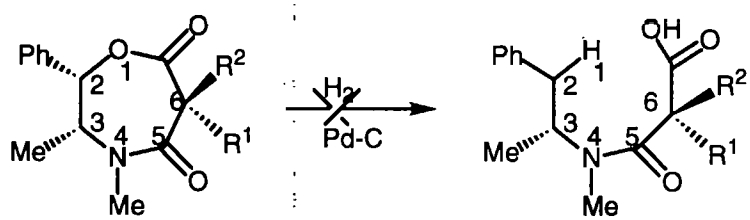

Figure 86

A summary of these cleavage reactions is given in Table 22 below. The starting material in all the following reactions was dimethylated oxazepine, also shown below.

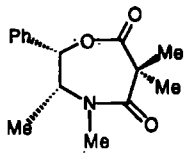

Starting Material

Reagent	Solvent	Temperature	Time	Result
K_2CO_3	MeOH (aq)	Ambient	36 h	No reaction
K_2CO_3	MeOH (aq)	Reflux	2 h	No reaction
LiOH	MeOH (aq)	Ambient	48 h	No reaction
LiOH	MeOH (aq)	~90 °C	4 h	No reaction
NaOMe	MeOH (dry)	Ambient	24 h	No reaction
H_2	MeOH (dry)	Ambient	48 h	No reaction

Table 22

As none of these cleavage attempts had been successful, it was possible that steric hindrance was a greater problem than had at first been thought. However it was feared that the use of a stronger hydrolysing agent would destroy the molecule completely. A possible solution considered was to use a reducing agent that was physically smaller. It was therefore decided to try sodium in liquid ammonia (Figure 87). The solvated electron acting as a nucleophile, attacks the

C-2 carbon to give a radical and cleavage occurs between the C-2 carbon and the O-1 oxygen. A second electron is added, followed by addition of two protons, to give the carboxylic acid. A disadvantage of this method is that it no longer regenerates the chiral auxiliary after the final cleavage step. The by-product is no longer ephedrine but *N*-methyl-1-benzylethylamine.

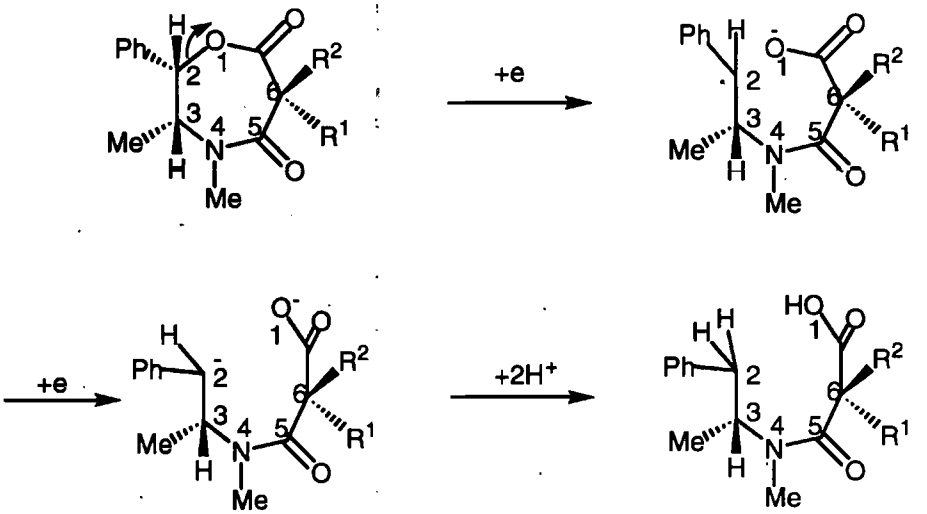

Figure 87 Reaction conditions: $Na/NH_{3(liq)}$ at -33 °C for 0.5 Hrs

Cleavage of three of the disubstituted oxazepines was attempted using this method (Figure 88).

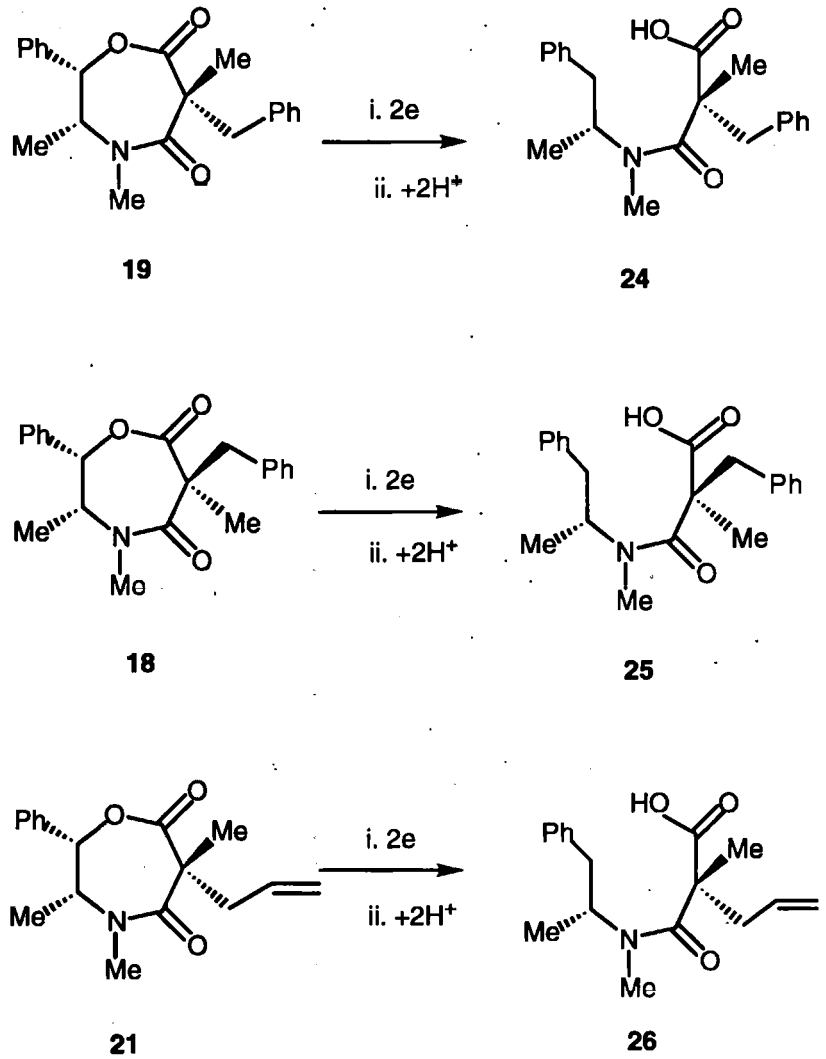

Figure 88

The IR spectra of the products gave the first indication that cleavage had occurred in each case. The spectra showed the appearance of the characteristic broad feature of the carboxylic acid O-H stretching frequency, plus the carbonyl stretching frequency of the carboxylic acid and amide groups (Table 23).

Compound	OH band cm^{-1}	Acid band cm^{-1}	Amide band cm^{-1}
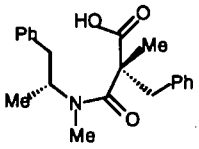 **24**	3200-2400	1724	1611
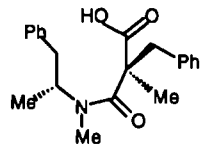 **25**	3600-2400	1728	1615
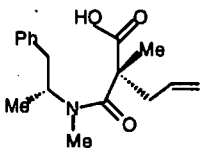 **26**	3400-2400	1725	1620

Table 23

The amide carbonyl frequency is lower than expected (1670-1630 cm^{-1}), as it was in the hydrolysed methyl-*N*-malonyl ephedrine (**13** Figure 62a, p.74). This is again probably due to inter or intra molecular hydrogen bonding.

For each of the cleaved disubstituted oxazepines illustrated in Figure 88, their ^1H NMR spectrum showed the disappearance of the distinctive signal for the proton at C-2 (δ ~5.60-5.90), where in the cyclic oxazepines it is adjacent to the lactone group. There was now a broad signal (δ ~2.50-3.00) on all three spectra, where the signal for the N-methyl is overlying the two methylene groups

(C-2 CH_2 and C-6 CH_2). The signal for the C-6 methyl protons was between δ 1.10 and 1.30 for all three compounds, with the two phenyl groups and the allyl group all showing their characteristic shifts (Table 24).

Substrate	Product	C-6 Ph	C-6 Allyl
		δ	δ
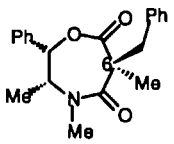	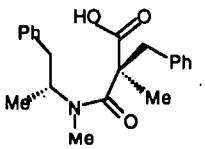		
18	**25**	~7.1	-
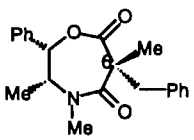	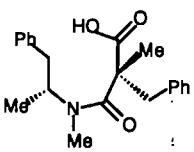		
19	**24**	~7.2	-
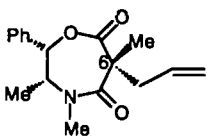	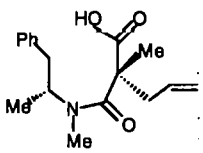		
21	**26**	-	5.00-5.20 (=CH_2)
		-	5.60-5.80 (-CH)

Table 24

Further confirmatory evidence came from the mass spectra and accurate mass calculations for all three compounds (Table 25).

Compound	$(M+H)^+$	Accurate Mass Calculated	Found
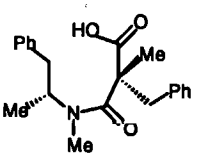 **24**	340	340.1913	340.1913
24 $(-CO_2)^*$	296	296.2014	296.2018
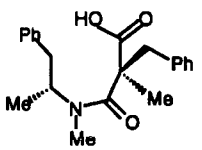 **25**	340	340.1913	340.1909
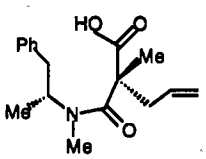 **26**	290	290.1756	290.1761

(* fragmentation as a result of the mass spectrum analysis)

Table 25

Conversion of the carboxylic acid into an amine

With the successful cleavage of the disubstituted oxazepine rings and isolation of the carboxylic acid products, conversion of the carboxylic acid group into the amine could now be attempted. For this transformation the Hofmann, Curtius (Figure 89) or Schmidt rearrangements are all effective, although the Schmidt reaction employs harsher reaction conditions. However the latter was

chosen for our case, since it is known that migration from carbon to nitrogen in the intermediate isocyanate proceeds in one reaction step with retention of configuration.

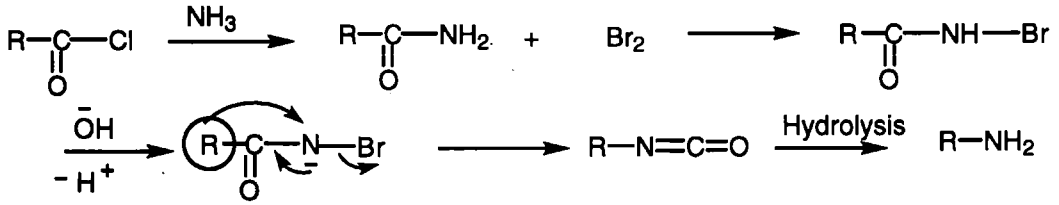

The Hofmann rearrangement

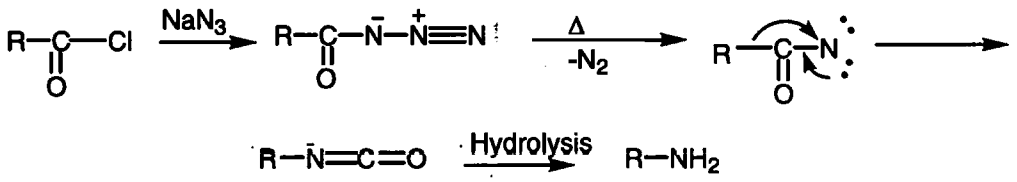

The Curtius rearangement

Figure 89

Applying the Schmidt reaction to compounds **24** and **25** would thus be expected to give compounds **27** and **28** respectively (Figure 90).

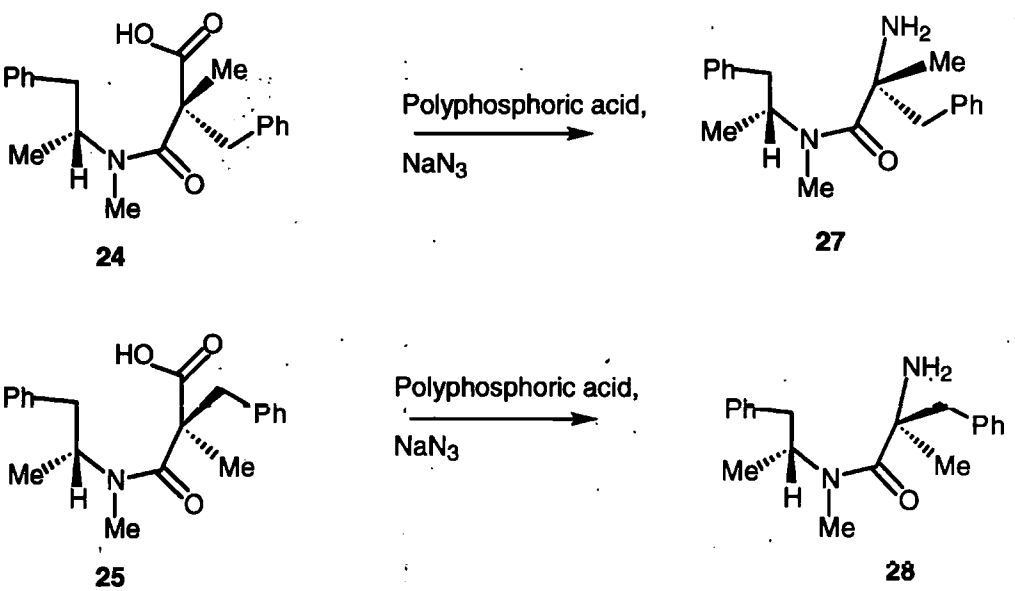

Figure 90

Mechanistically, this is illustrated for compound **24** in Figure 91.

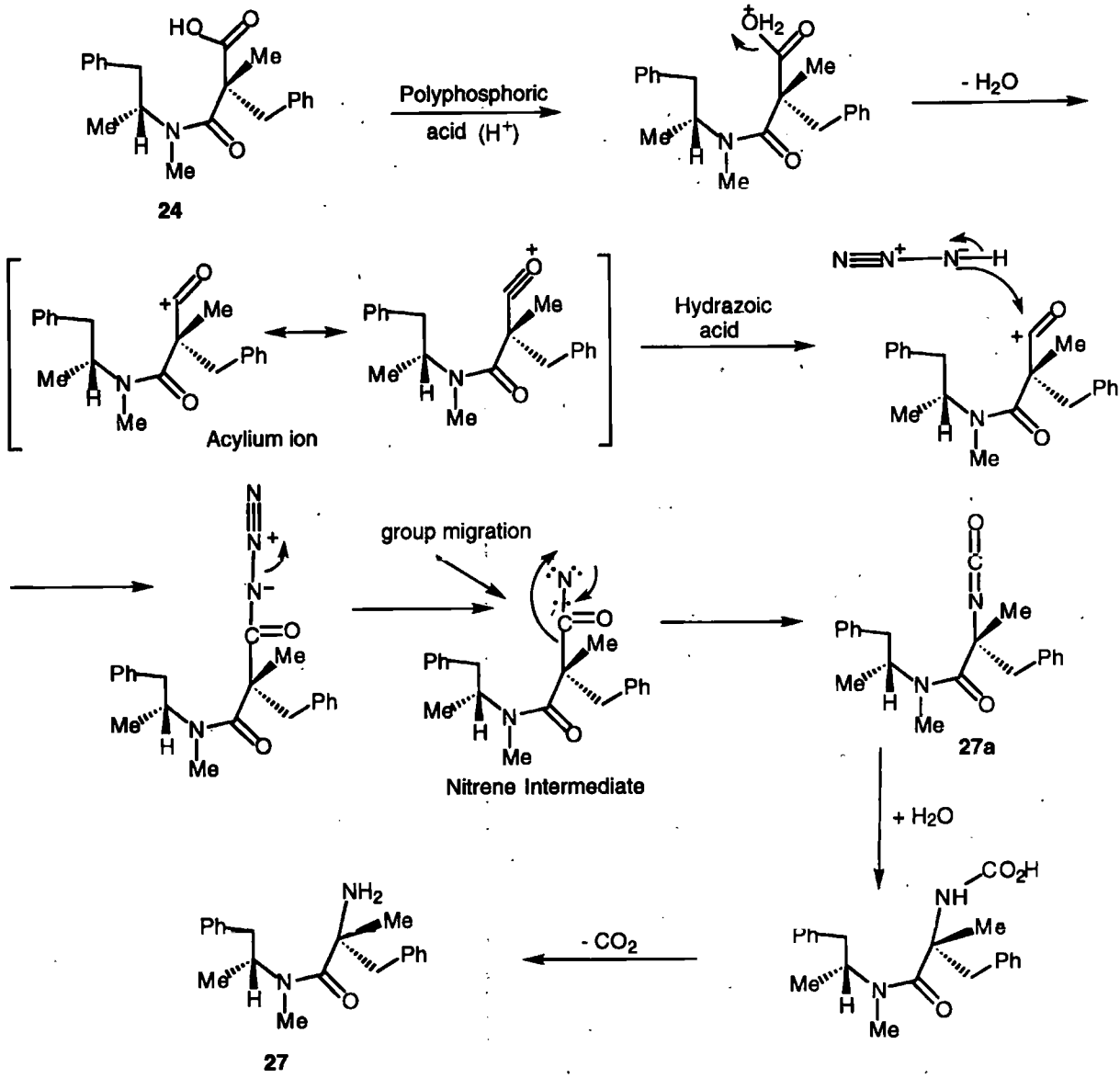

Figure 91 Proposed mechanism of the Schmidt reaction on **24**

The Schmidt reactions shown in Figure 90, were successfully carried out to give the compounds **27** and **28**, as confirmed by IR, ^{1}H NMR and mass spectral evidence.

The ^1H NMR spectrum for amine **27** showed a two proton signal at δ 8.47, assigned to NH_2, since it was removed after shaking the sample with D_2O. All the other proton signal features in both compounds were present; the two phenyl and two methyl groups, the *N*-methyl, and the characteristic coupling for the protons of the methylene group attached to the stereogenic centre (12.5 Hz). The mass spectra and accurate mass analysis gave further confirmation that the conversion to the amine had been successful (Table 26), with some isocyanate (**27a**) present in the amine **27**. Any isocyanate present at this stage would cause no problems, as it would be hydrolysed at the next stage.

		Accurate Mass	
	$(M+H)^+$	Calculated	Found
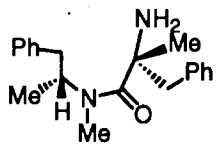 **27**	311	311.2123	311.2120
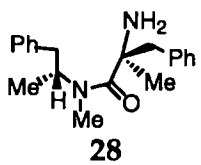 **28**	311	311.2123	311.2031
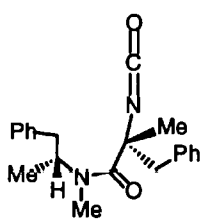 **27a**	337	337.1916	337.1916

Table 26

The IR spectra in both cases (**27** and **28**) showed one carbonyl stretching frequency at 1631 and 1634 cm^{-1} respectively (amide carbonyl), with the absence of a carboxylic acid carbonyl stretching frequency or any characteristic broad feature of the OH stretching band. There was also a broad NH band in each spectrum: at 3362 and 3363 cm^{-1} respectively, but this was not as well defined (not showing a clear double peak) as a normal primary N-H stretching signal. There was also evidence that some of the isocyanate (**27a**) was still present in the amine **27**, giving a sharp peak at 2138 cm^{-1} on the IR spectrum.

Hydrolysis

The final step in the syntheses was cleavage of the amides by hydrolysis, to give the α-amino acid and secondary amine (Figure 92).

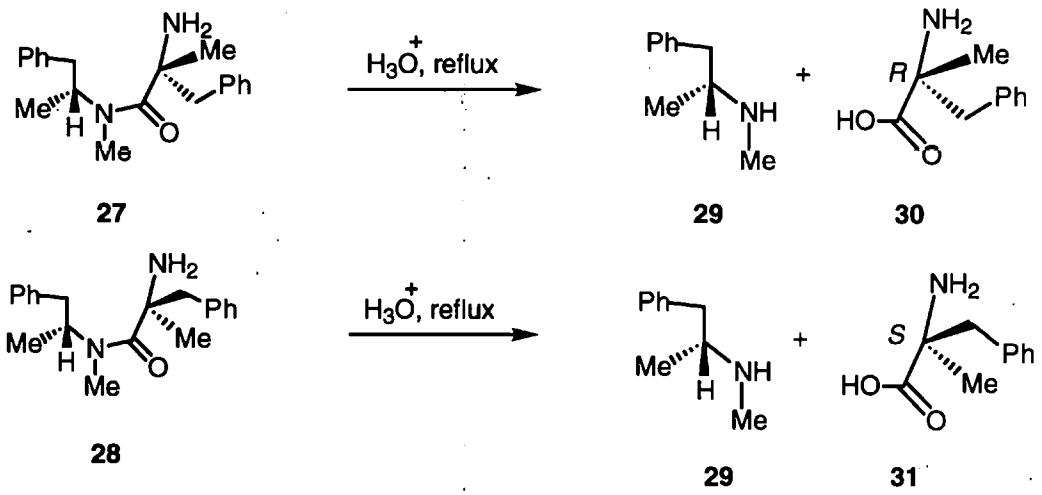

Figure 92

The amino amides **27** and **28** (Figure 91) were hydrolysed by reflux in 50% hydrochloric acid for two days, to give the free amino acids (**30** and **31**). Because of

the zwitterionic nature of these compounds they were isolated as their sodium salts.

IR spectra of the sodium salts of **30** and **31** (KBr disc) were determined, these showed two peaks at 3500 and 3400 cm^{-1} (NH_2) and the antisymmetric and symmetric stretching frequencies for the carbonyl group of the sodium salt at 1639 and 1403 cm^{-1}. The ^1H NMR spectra for both compounds (D_2O) gave peaks at δ 1.45 ($-CH_3$), 2.95 and 3.18 (d, J= 17.5 Hz ($-CH_2$)) and a multiplet at δ 7.19-7.42 ($-C_6H_5$).

For identification purposes it was decided to form the methyl ester of **30** by treatment with MeOH/HCl. Analysis of the methyl ester again showed the presence of the N-H stretching frequencies on the IR spectrum, but now with the ester carbonyl frequency at 1738 cm^{-1}, instead of the stretching frequencies of the carbonyl groups of the sodium salt of the acid. The ^1H NMR spectrum included peaks at δ 1.45 ($-CH_3$), δ 3.19 and 3.53 (d, J= 17.5 Hz ($-CH_2$)), δ 3.74 ($-OCH_3$) and δ 7.10-7.35 ($-C_6H_5$). The mass spectra and accurate mass analysis of the methyl ester of compound **30** gave further confirmation of product formation (Table 27).

		Accurate Mass	
	$(M+H)^+$	Calculated	Found
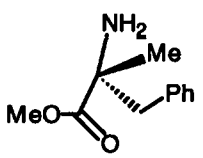			
methyl ester of **30**	194	194.1181	194.1186

Table 27

The stereochemical label of the prepared methyl ester of **30** can be inferred to be *R*- on the assumption that no epimerisation had occurred in any of the steps from compound **19**.

In an independant experiment racemic α-methylphenylalanine methyl ester was prepared according to Scheme D.

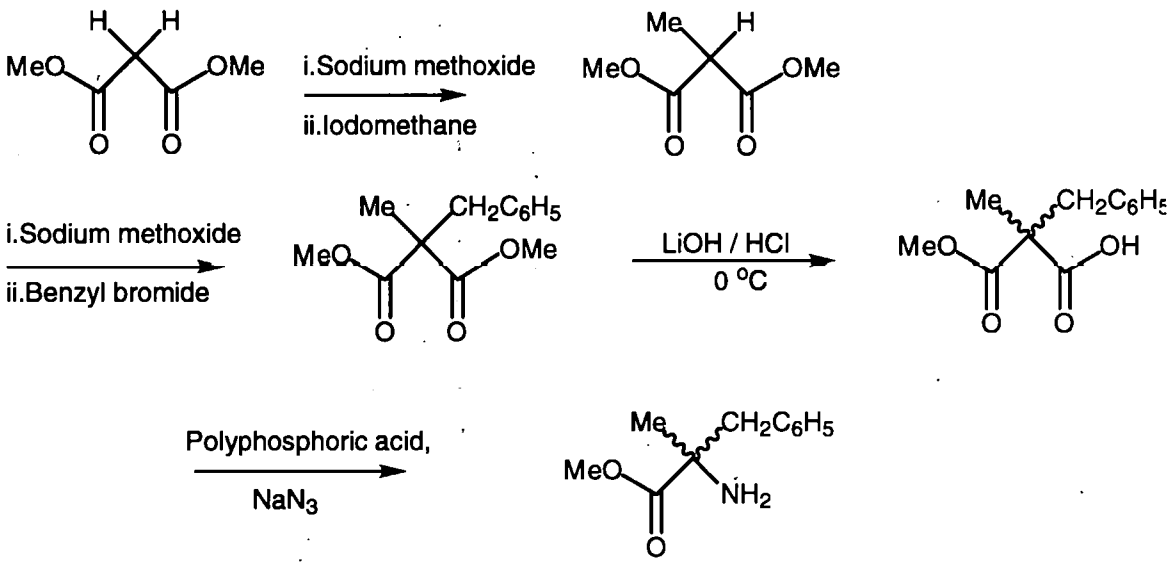

Scheme D.

The spectroscopic results for the methyl ester of compound **30** compared favourably with those for the methyl ester of racemic α-methylphenylalanine (Table 28).

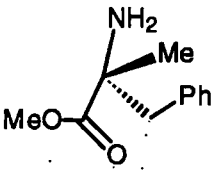

Methyl ester of compound **30**

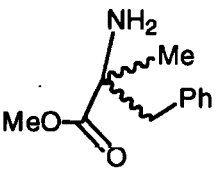

Racemate

IR	3340 cm^{-1}	3360 cm^{-1}
(evaporated	3200 cm^{-1}	3240 cm^{-1}
film)	1738 cm^{-1}	1736 cm^{-1}
^{1}HNMR (δ)	1.50	1.50
	3.20 (*J*= 12.5 Hz)	3.20 (*J*= 12.5 Hz)
	3.50 (*J*= 12.5 Hz)	3.50 (*J*= 12.5 Hz)
	3.75	3.75
	7.10-7.30	7.10-7.30
Mass ($M+H^+$)	194	194
Accurate mass	194.1181	194.1181
Calculated	194.1186	194.1181

Table 28

The IR spectrum for the by product amine fragment **29** (*N*-methyl-1-benzylethylamine), showed an N-H stretching band between 3500 and 3300 cm^{-1}, with no evidence for the presence of an hydroxyl or carbonyl group. Signals for the phenyl, N-methyl, C-methyl and the N-H protons, were all present on the ^{1}H NMR spectrum. The signals for the benzylic protons and single proton were seen as a multiplet from δ 2.70-3.10. These were similar to corresponding groups in the ^{1}H NMR spectrum of ephedrine (Table 29).

	δ Phenyl	δ N-methyl	δ C-methyl	δ N-H
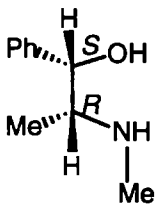				
Ephedrine	7.20	2.30	0.85	3.15
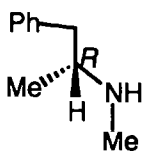				
Amine (**29**)	7.30	2.60	0.95	3.80

Mass Spectrum CI (NH_3) (**29**) $(M+H)^+$ 150

Accurate mass (**29**) Calculated 150.1283 Found 150.1283

Table 29

Figure 93 shows the whole scheme from oxazepine to the α-substituted phenylalanine. It illustrates the two routes to the **D** (*R*) and **L** (*S*) isomers.

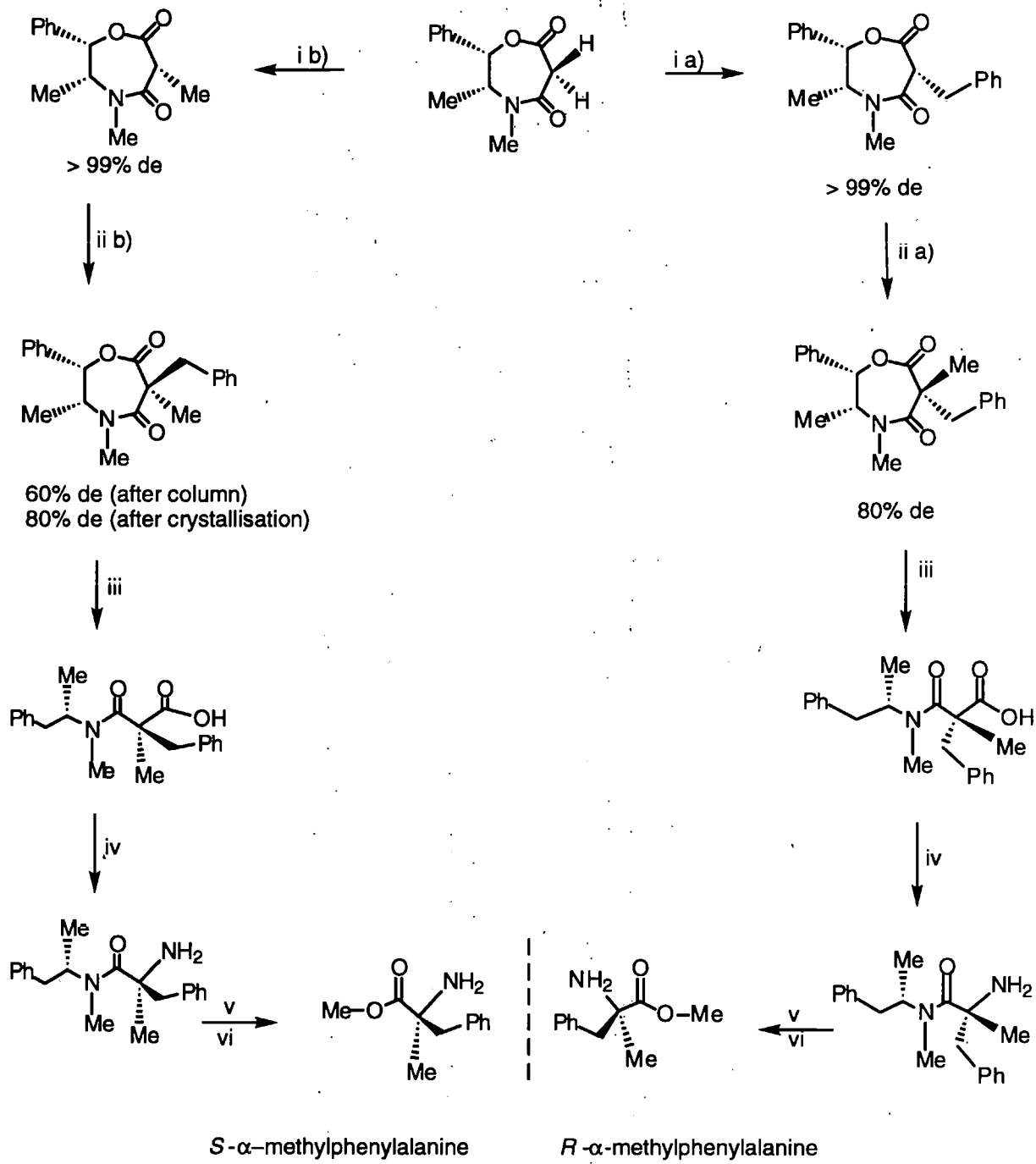

Figure 93 Reagents and conditions: i, $(CH_3)COK$, a) BnBr, b) MeI, room temperature; ii, $(CH_2)COK$, a) MeI, b) BnBr, -78 °C; iii, Na-liq.NH_3, -33 °C; iv, NaN_3-polyphosphoric acid, 35 °C, 48 hrs; v, 5 M HCl, reflux, 48 h; vi, MeOH (dry), $SOCl_2$.

6.5 Synthesis of the proline derived oxazepine

Another source of chiral auxiliaries is the wide range of β–amino alcohols, available by controlled reduction of naturally occurring L-amino acids. A number of the papers quoted previously have described the use of amino alcohols as either chiral reagents or chiral auxiliaries. Corey[29,30] used them as chiral reagent, in his synthesis of optically pure secondary alcohols (Figure 16 p.25). Chakraborty[55] uses a β-amino alcohol as a chiral auxiliary in the preparation of enantiomerically pure α-amino acids (Figure 34 p.46). Prolinol was used by Takahashi[59] as a chiral auxiliary in the synthesis of optically pure amines (Figure 41 p.54), and Meyers[60,61] used β-amino alcohols to produce his bicyclic lactams, well known for their wide synthetic usefulness (Figure 45 p.56).

These compounds should react with dimethyl malonate in a similar manner to ephedrine, to furnish the open chain precursors for subsequent cyclisation with cyanuric chloride/pyridine (Figure 94).

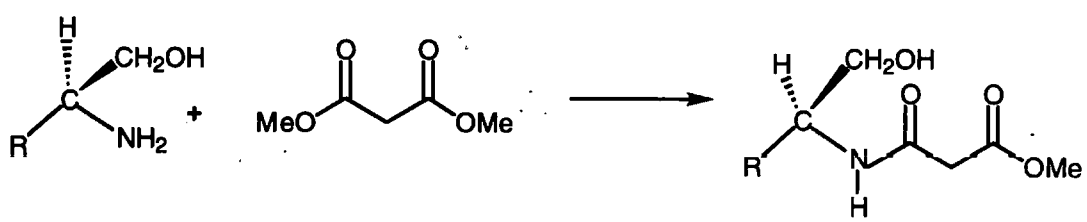

Figure 94

It was thought that the bicyclic compound formed from the reaction of prolinol and dimethyl malonate with subsequent lactonisation, would have a similar conformation to the ephedrine derived oxazepine (Figure 63b p.77) and therefore could show comparable asymmetric inducing properties.

Following the method developed by Ford,[68] the methyl-*N*-malonylprolinol compound was readily prepared in >90% yield (**32** Figure 95).

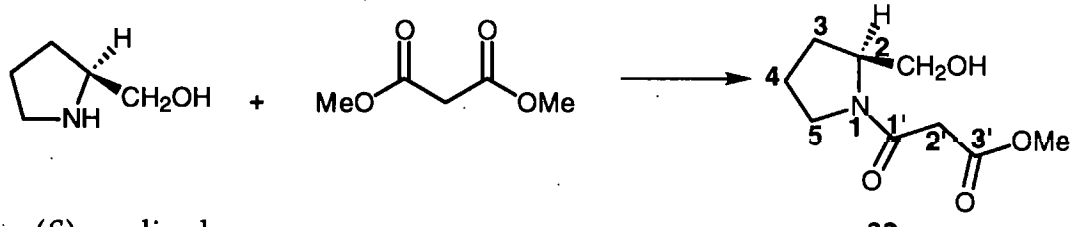

(*S*)-prolinol **32**

Figure 95

The IR spectrum of compound **32** showed peaks at 1736 cm^{-1} (ester carbonyl) and 1626 cm^{-1} (amide carbonyl). The ^1H NMR spectrum gave a multiplet signal at δ 1.82-2.10 (4H), corresponding to the C-3 and C-4 protons. Another multiplet at δ 3.55-3,82 (4H)) was assigned to the C-5 and the C*H*$_2$OH proton. The C-2 proton gave a broad signal at δ 3.55-3.82. The two proton singlet signal at δ 3.50 corresponded to the C-2' methylene protons and the second singlet peak at δ 3.82 was attributable to the C-3'-OMe protons.

Compound **32** was hydrolysed with LiOH, ensuring that the temperature during the reaction remained at 0 °C to minimise any decarboxylation (*cf.* Figure 62a p.74) to give compound **33** (Figure 96), in a good yield of >80%.

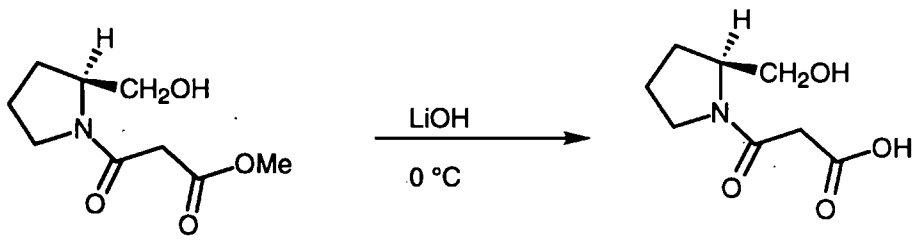

32 **33**

Figure 96

The ^{1}H NMR spectrum of **33** showed the absence of a singlet at δ 3.82. All of the other signals corresponded to those of compound **32**. Peaks in the IR spectrum were at 1727 cm^{-1} (acid carbonyl), 1614 cm^{-1} (amide carbonyl) and there were also the broad O-H stretching vibrations of the carboxylic acid. Table 30 compares the carbonyl frequencies for the ephedrine derived open chain compounds **12** and **13** with those of **32** and **33**.

	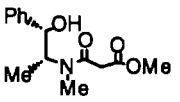 12	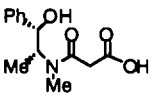 13	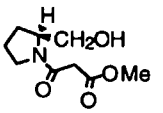 32	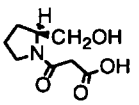 33
ester C=O (cm^{-1})	1730	-	1736	-
acid C=O (cm^{-1})	-	1731	-	1727
amide C=O (cm^{-1})	1621	1621	1626	1614

Table 30

The two prolinol open chain compounds show rather low frequencies for the amide carbonyl stretching frequency, as did the ephedrine derived compounds. This is again probably explained by hydrogen bonding (see p.74).

Using the cyanuric chloride/pyridine method of Ford,[68] cyclisation was achieved to give compound **34**, (Figure 97) with yields of 25% after chromatography. There was also a large quantity of highly coloured material formed, as was seen in the formation of the ephedrine derived oxazepine (p. 76).

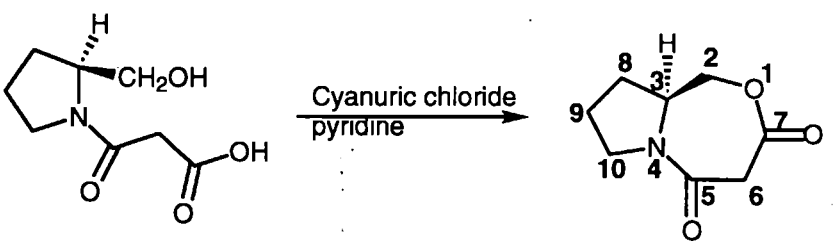

33 **34**

Figure 97

There were two carbonyl stretching frequencies shown on the IR spectrum for compound **34**, one at 1744 cm^{-1} and one at 1629 cm^{-1}, and the broad O-H stretching band of the carboxylic acid was absent. Compared to the open chain compounds, both the carbonyl groups have shifted to higher frequencies (1727 to 1744 cm^{-1} and 1614 to 1629 cm^{-1}). As this is a seven-membered ring these frequencies would be expected to be within the range of the normal saturated ester and amide carbonyl frequencies, (1750-1735 cm^{-1} and 1670-1630 cm^{-1}), which is as observed. The increased frequency for these carbonyl absorptions is comparable to those seen in the IR spectrum for the ephedrine derived oxazepine (Table 31). The explanation given previously (p.76), that the shifts result from dipolar interaction between the two carbonyl groups, is thought to be applicable to this compound also.

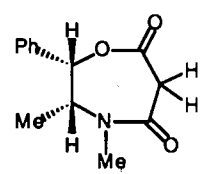

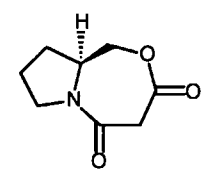

	1	**34**
Lactone C=O (cm^{-1})	1745	1744
Lactam C=O (cm^{-1})	1638	1629

Table 31

Further evidence corroborating the formation of compound **34** came from mass spectroscopic analysis and accurate mass determination of the $(M + H)^+$ ion (Table 32).

Mass Spectrum of **34**

	$(M+H)^+$	Calculated	Found
$C_8H_{11}NO_3$	169	169.0739	169.0738

Table 32

The ^1H NMR spectrum for **34** showed a downfield shift for the CH_2OH protons from δ 3.44-3.80 in **33** to δ 4.37-4.46 in **34**, indicating acylation on ring closure. On formation of the lactone these methylene protons are placed in a more deshielded environment than the original environment of an hydroxyl group. The methine proton at C-3 has shown an upfield shift from δ 4.14-4.29 in **33** to δ 3.78-3.90 in **34**, suggesting that the preferred comformation of the ring structure has placed it in a more shielded environment. The methylene protons at C-6 show the distinctive geminal coupling feature of J=9.50 Hz, at δ 3.62-3.67 and 3.90-4.00. The C-2 protons also show geminal coupling of J=12.00 Hz within the multiplet at δ 4.37-4.46. The C-8 and C-9 protons give a multiplet at δ 1.49-2.08, little changed from their position in the spectrum of monocyclic **32**, and because of their proximity to the deshielding effect of the nitrogen atom, the C-10 protons were again found downfield at δ 3.40-3.67.

Analysis of the 2D ^1H-^1H correlated spectrum (COSY) for compound **34** (Figure 98), confirms the assignments made above for the ^1H NMR spectrum. The COSY spectrum yields signals from protons that are directly coupled, enabling individual protons to be assigned *via* ^3J H,H coupling (H-C-C-H), as explained below.

The assignment of the C-2 methylene protons at δ 4.37 to 4.46, as the signal expected to be at the lowest field, enables the coupling of these two protons to the C-3 methine proton to be traced across and up to the diagonal at δ 3.78-3.90. The C-3 proton is then traced back to one of the C-8 protons (probably the proton under the ring) at δ ~2.10, then this C-8 proton can be traced across to its partner at δ ~1.60. Having identified the C-8 protons, the C-9 and C-10 protons are assigned in a similar manner. The C-9 protons coupled to the C-8 protons are found at δ ~1.65 and δ ~1.85, the C-10 protons coupled to the C-9 protons are found at δ ~3.55 and ~3.65.

2D ^{1}H-^{1}H correlated spectrum (COSY) for compound **34**

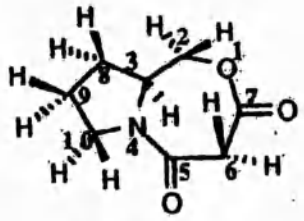

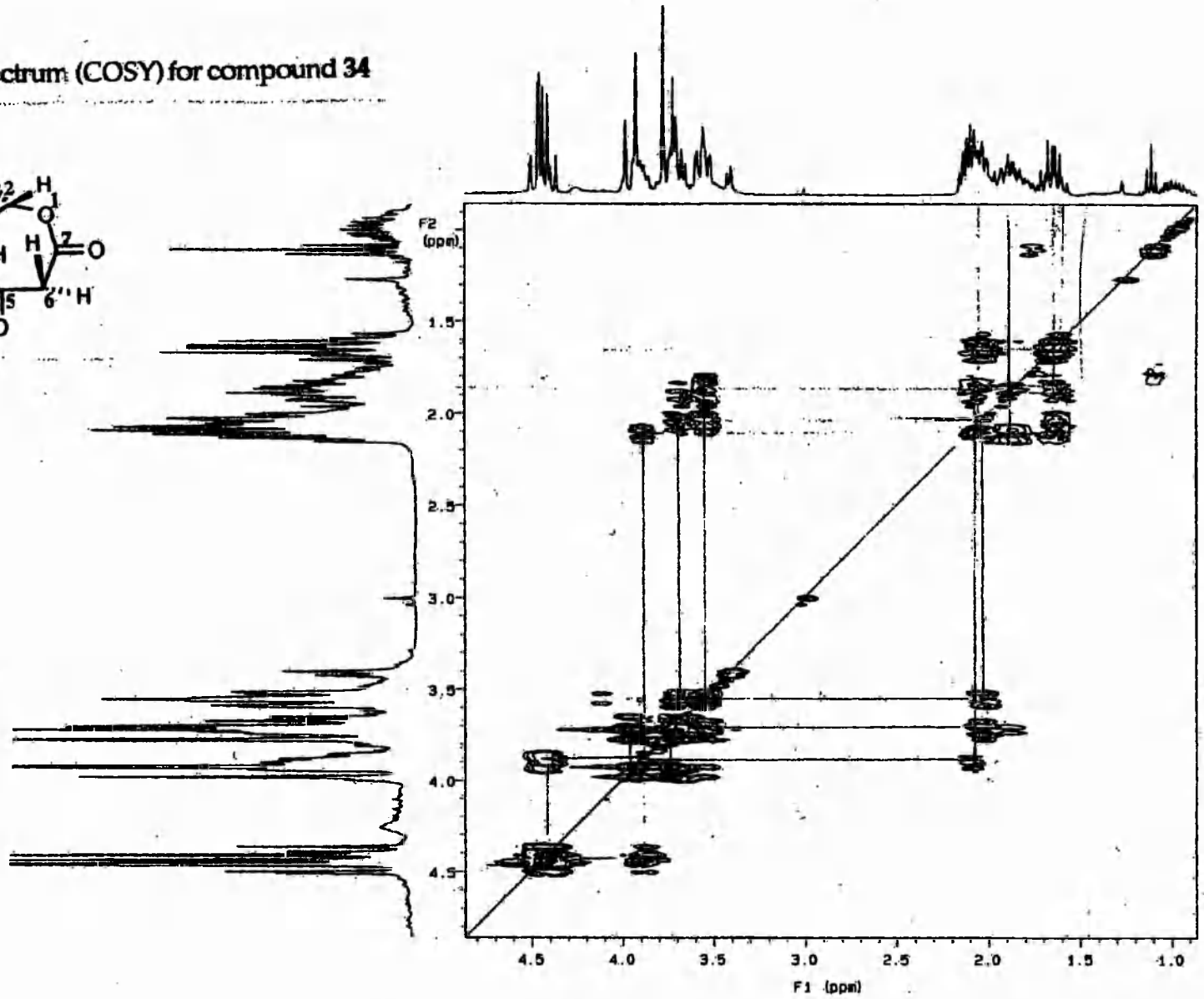

Figure 98

6.6 Conformation of the prolinol derived oxazepine ring

Figure 99 depicts the energy minimised three dimensional conformation of the ring structure.

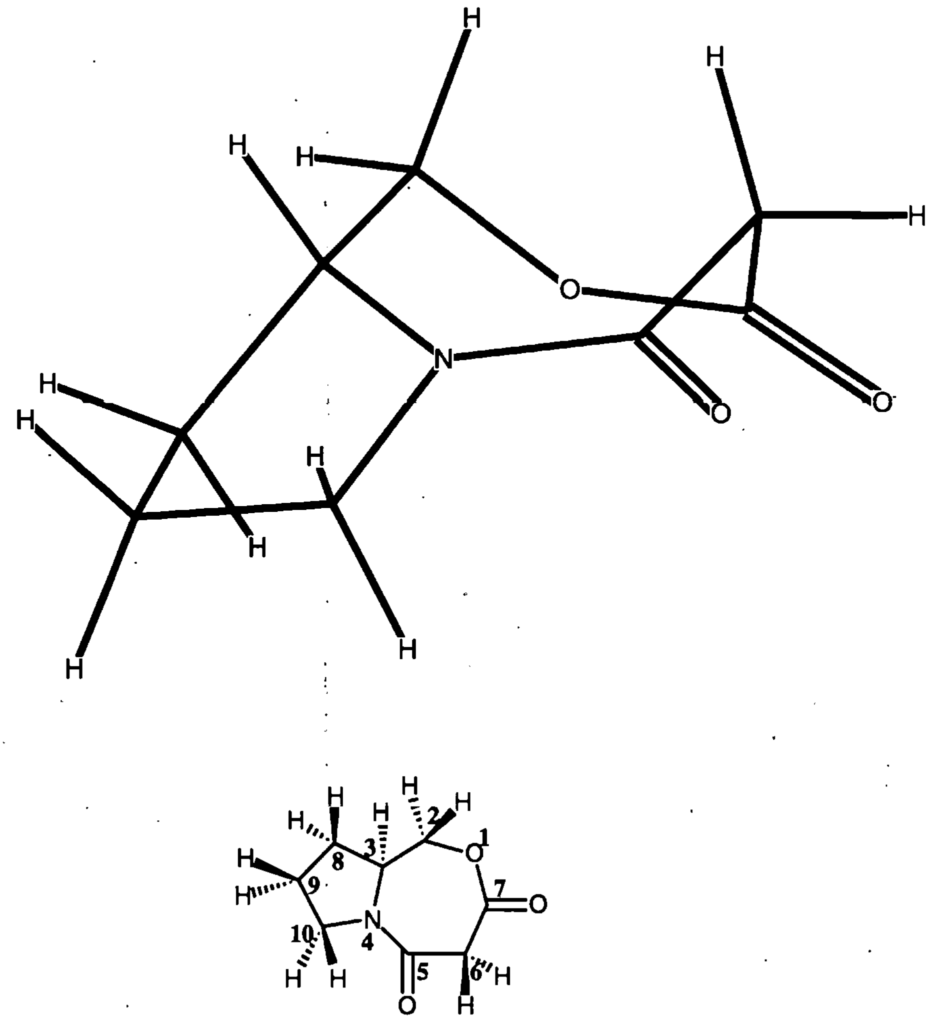

Figure 99

If the conformation of the seven-membered ring in this bicyclic oxazepine resembles the twist-boat structure of the ephedrine derived oxazepine, then there will again be a proximity between the C-2 pseudoaxial proton and the pseudoaxial proton at C-6, which was indicated in the energy minimised conformation (Figure 99). Evidence for this suggested conformation came from nOe studies on the

compound. There was enhancement between the C-2 pseudoaxial proton and the pseudoaxial proton at C-6 of 4.7%. An enhancement between the C-2 pseudoequatorial proton and the C-3 methine proton was calculated at 6.5%. Support for the conformation of the five-membered ring as shown in Figure 100, was given by the C-3 proton showing an enhancement effect with the C-10 (below the ring) proton of 2.2%. There is no observable enhancement effect by the C-10 protons on the C-8 proton positioned above the ring. Also, no enhancement was observed between the C-6 pseudoequatorial proton and either of the C-2 protons.

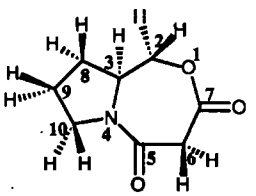

Group irradiated	Group observed	% nOe	Group irradiated	Group observed	%nOe
H_{pax}-6	H_{pax}-2	+4.7	H_{peq}-2	H**-8	+0.7
H_{pax}-6	H_{peq}-6	+5.1	H-3	H*-8	+2.3
H_{peq}-6	H_{pax}-6	+3.8	H-3	H**-8	+3.6
H_{pax}-2	H_{pax}-6	+2.5	H-3	H_{peq}-2	+3.5
H_{peq}-2	H-3	+6.5	H-3	H**-9	+1.2
H_{pax}-2	H*-8	+3.1	H-3	H*-10	+2.2

peq pseudoequatorial pax pseudoaxial * above the ring as drawn

** below the ring as drawn

Figure 100

6.7. Monosubstitution of the prolinol derived oxazepine

Although time and resources were now limited, it was decided to attempt monosubstitution of compound **34.** It was hoped to show that this compound was capable of inducing asymmetric substitution, as had been illustrated by the selective asymmetric monosubstitution reactions of the ephedrine derived oxazepine (**14-17**). The substitution method used for compounds **14-17** (p.89-92) was used for preparing compound **35** (Figure 101). The reaction progressed successfully to give 54% yield of the crude product.

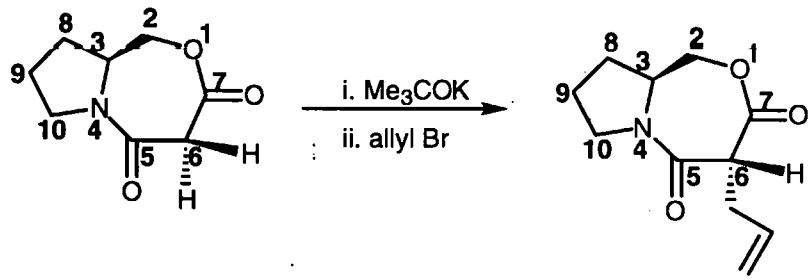

Figure 101 **34** **35**

The mass spectrum (CI) of the product **35** gave a molecular ion $(M + H)^+$ at *m/z* 210, and the ^1H NMR spectra for this compound (**35**) showed evidence that allyl substitution had taken place. The signals for the C-6 methylene protons at δ 3.62-3.67 and 3.90-4.00 with their geminal coupling of J=9.5 Hz were absent. New signals were present: a multiplet at δ 4.16-4.26 (C-6 single proton), a multiplet at δ 5.86-5.97 (methylene of allyl side-chain) and a distinctive allyl geminal signal at δ 5.24-5.38. The probable stereochemistry at C-6 is as indicated for compound **35**, but there was not sufficient time or material to carry out any nOe studies that would have confirmed this stereochemistry.

6.8 Alternative heterocyclic precursors

Alternative heterocycles that also appeared to be possible as precursors, were the homologues of the oxazepine system, formed from the condensation of ephedrine with maleic, succinic and glutaric anhydrides (Figure 102). One advantage of using these anhydrides was the elimination of the ester hydrolysis step, with its problem of possible decarboxylation.

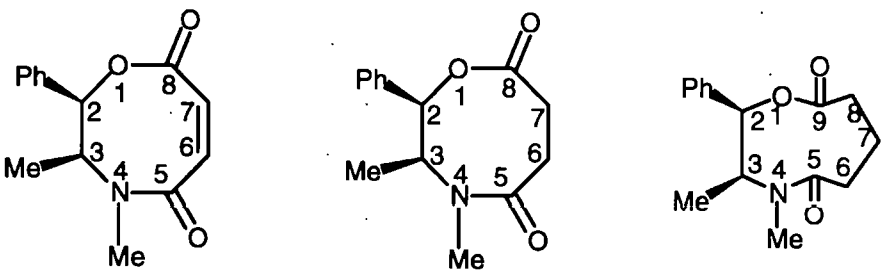

Figure 102 **X** **Y** **Z**

A further project was planned with these compounds. Thus it was envisaged that oxazecine **X** could be used as a chiral dienophile in Diels-Alder reactions (Figure 103). The advantage of oxazecine **Y**, the eight membered ring, is that this ring system should allow regio and stereoselective alkylation to produce dibasic acids (Figure 103). As in the formation of the oxazepine, the ephedrine used as the chiral precursor should direct the alkyl substitution. The final configuration would of course depend on which enantiomer of ephedrine had been used originally.

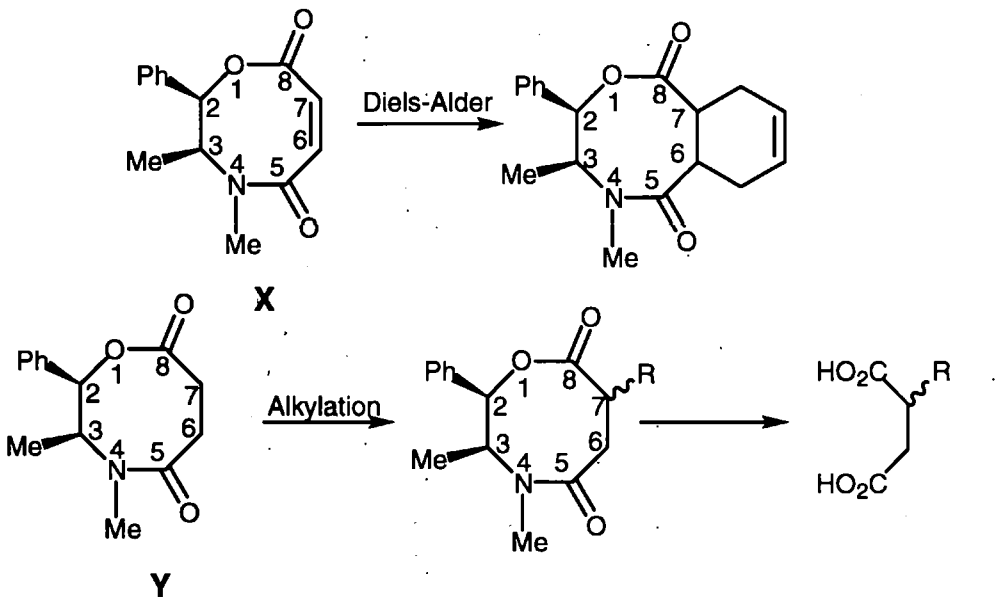

Figure 103

Reactions of β-amino alcohols with dimethylacetylenedicarboxylate (DMAD), should give a series of six-membered heterocyclic systems, containing an active centre at an enamine group (Figure 104).

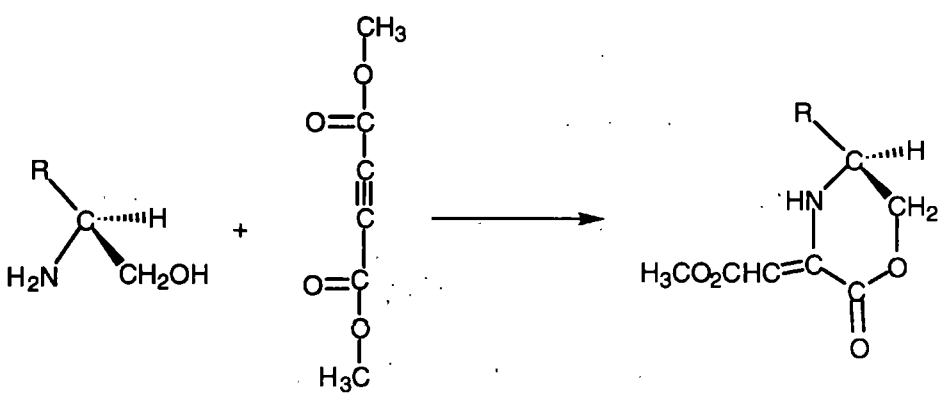

Figure 104

These six-membered rings have been prepared from (-)-ephedrine and DMAD in high yields and characterised by Bellan *et al* .[78,79] who used them to form oxazolidines.

Preparation of the homologues of the oxazepine

The first series of heterocycles we attempted to synthesise were homologues of the oxazepine. Succinic and glutaric anhydrides reacted with ephedrine to form the respective open-chain hydroxy acids. As already mentioned, the advantage of using the anhydrides (rather than diethyl malonate) was the elimimation of the ester hydrolysis step, with its attendant problem of possible decarboxylation. These reactions gave direct formation of the acid functional group, and were consistently successful with >95 % yield. Unfortunately lactonisation proved very disappointing, with little evidence of the expected product (Figure 105).

36

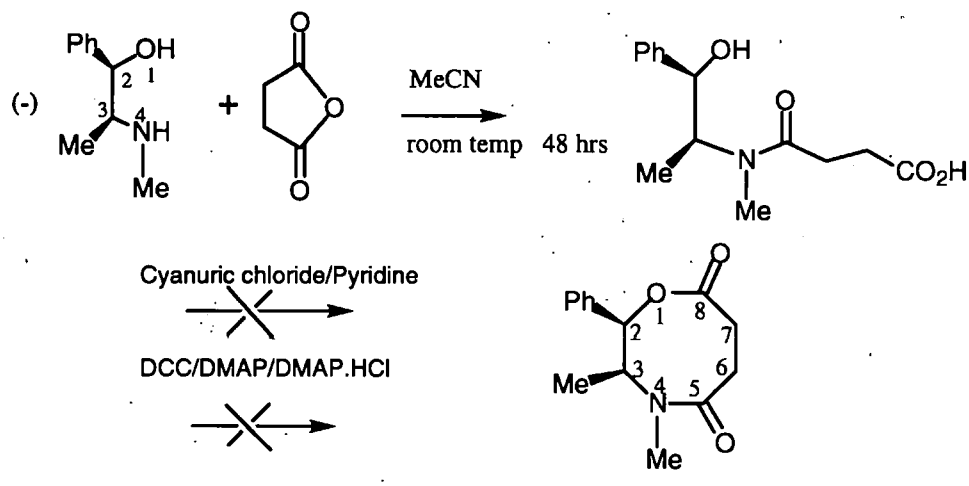

Figure 105 **Y**

In the earlier studies on malonate formation, two important pieces of evidence, which indicated lactonisation, were obtained from the ^{1}H NMR and IR spectra of the oxazepine. For this compound the IR spectrum had shown the disappearance of the carboxylic acid group, (which had been present in the *N*-malonylephedrine), and the appearance of a carbonyl group at 1747cm^{-1} (lactone). On the ^{1}H NMR there had been a down-field shift of the benzylic proton on C-2, moving from δ ~4.7 for the *N*-malonylephedrine to δ ~6.0 for the oxazepine.

None of these features was present in the products from the attempt to form the oxazecine (**Y**), in fact only the original starting material (succinyl ephedrine **36**) was positively identified. It seemed that all attempts to lactonise the *N*-succinyl ephedrine were unsuccessful.

However after the first stage of the synthesis, (the reaction of ephedrine with succinic anhydride), the ^{1}H NMR for the product showed *two* peaks for the benzylic proton at C-2, one at δ 4.85 and one at δ 5.85. If lactonisation *had* occurred at this stage to form the oxazecine (Figure 106), the benzylic proton at C-2 *would* have shown a downfield shift, possibly to about δ 6, but there was still a carboxylic acid group indicated on the IR spectrum, and no carbonyl peak in the lactone region, (even allowing for the expected effect of the enlarged ring).

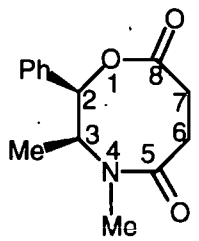

Figure 106 **Y**

No separation of the compounds giving rise to these two different peaks for the proton at C-2 could be obtained by TLC, although a number of different solvent systems was tried. HPLC was investigated and separation now proved possible, using a silica column and acetonitrile/water/acetic acid (75/25/0.5) as the eluant.

The IR spectrum for the recovered *N*-succinylephedrine (**36** Figure 105) was quite similar to the *N*-malonyl ephedrine obtained earlier. It showed a broad O-H stretching band from 3400 - 2400 $cm^{-1}$and two carbonyl peaks, one at 1721 cm^{-1} (carboxylic acid) and one at 1616 cm^{-1} (amide). Again, this lower than expected frequency for the amide carbonyl, may be due to inter- or intramolecular hydrogen bonding, as discussed on page 74 in connection with the methyl *N*-malonylephedrine. The ^1H NMR spectrum had a peak at δ 4.77 for the benzylic proton, one at δ 4.48-4.64 for the C-3 proton and the protons for the N-methyl were at δ 2.78. The corresponding ^1H NMR peaks for ephedrine are δ 4.80, δ 3.15 and CH_3-N δ 2.30 respectively.

In contrast, the IR spectrum for the new compound showed a carbonyl peak at 1737 cm^{-1} (ester), the amide carbonyl peak was absent, but there were two signals at 1610 cm^{-1} and 1410 cm^{-1} corresponding to a carboxylate anion stretching band. There was also a broad absorption from 2800 to 2200 cm^{-1}, which can be assigned to NH_2^+ stretching vibrations. The ^1H NMR gave resonances at δ 5.85 for the benzylic proton; at δ 4.79-4.97 for the C-3 proton and at δ 2.71 for the N-methyl protons. The new product isolated, had a structure consistent with that shown in Figure 107.

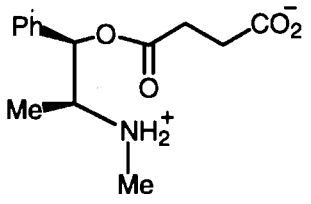

Figure 107 **37**

The chemical ionisation (CI NH_3) of this new compound (**37**) showed a molecular ion $[M+H]^+$ at *m/z* 266 with fragments at 248, 220 and 166. Loss of H_2O from the protonated molecular ion (M+H)+ gives rise to the ion at *m/z* 248, with subsequent loss of -CO to give the ion at *m/z* 220 (Figure 108). The signal at *m/z* 166 is probably due to α-cleavage at the ester group to give the protonated ephedrine portion.

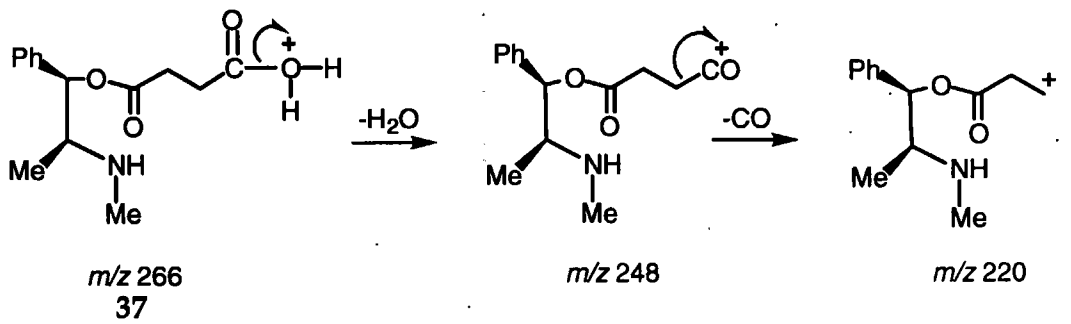

Figure 108

The CI mass spectrum of the recovered succinyl ephedrine **36** had a molecular ion $[M+H]^+$ at *m/z* 266, fragments at *m/z* 248 and 166 but with no signal at *m/z* 220 (Figure 109). The lack of a signal at *m/z* 220 may possibly indicate that α-cleavage had occurred at the amide group prior to loss of -CO.

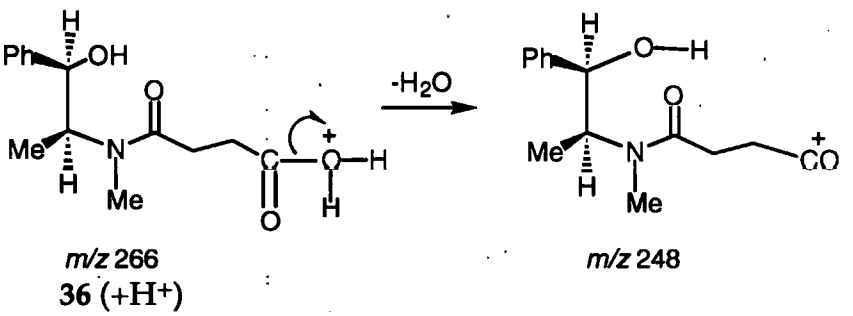

Figure 109

The new compound **37** may have been formed from a 1,4-acyl migration from nitrogen to oxygen, possibly *via* a five membered ring as shown in Fig. 110.

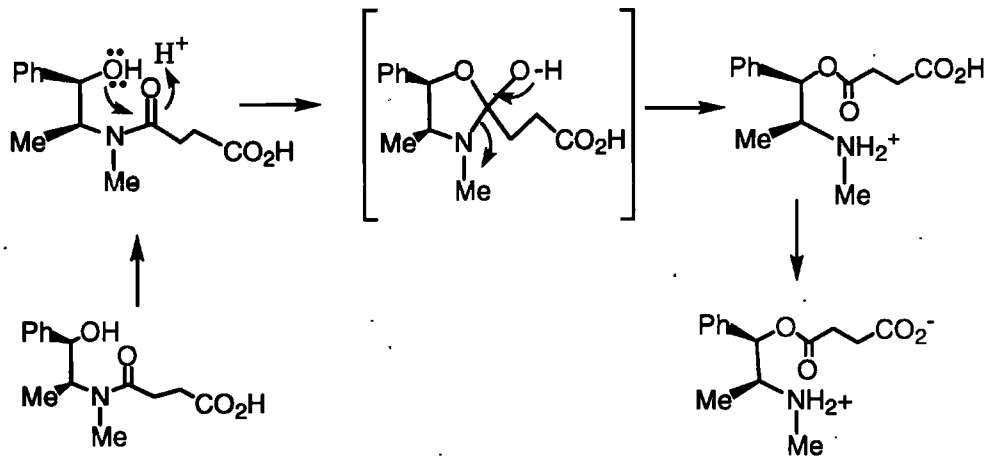

Figure 110 **36** **37**

If the events at attempted cyclisation do follow the sequence outlined above, this would suggest a reason for our failure to isolate any cyclic compound. This possible 1,4-acyl migration indicates that the larger eight membered ring is difficult to form, which may be due to the acid carbonyl carbon being a further carbon atom removed from the attacking hydroxyl group. It would appear that in this case the five membered cyclic intermediate would be more readily formed and once formed is easily cleaved in the opposite sense.

The reaction of ephedrine and glutaric anhydride followed the same pattern, with both the hydroxyl acid **38** and the amino acid **39** compounds as products, indicated by the presence of the two peaks for the benzylic proton at C-1. It was again possible to separate these by HPLC using the same conditions as for the succinyl ephedrine, to give the two compounds shown in Figure 111.

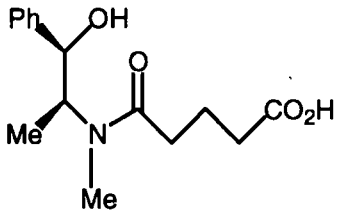

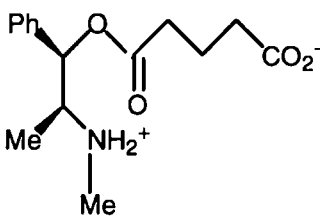

Figure 111 **38** **39**

Comparison of the physical data for the two succinylephedrine (**36** and **37**) compounds and the two glutarylephedrine (**38** and **39**) compounds are shown in Table 31.

	Succinylephedrine		Glutarylephedrine	
	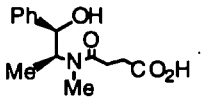 **36**	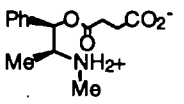 **37**	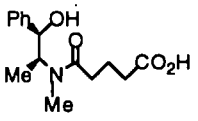 **38**	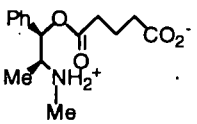 **39**
	Amide	Amine	Amide	Amine
IR	3400-2400cm^{-1}	2800-2200cm^{-1}	3600-2400cm^{-1}	2800-2300cm^{-1}
	1721cm^{-1}	1737cm^{-1}(ester)	1712cm^{-1}(acid)	1735cm^{-1}(ester)
	1616cm^{-1}(amide)	1610cm^{-1}(anion)	1612cm^{-1}(amide)	1607cm^{-1}(anion)
	-	1410cm^{-1}(anion)	-	1411cm^{-1}(anion)
^{1}H NMR	4.77 (C-1)	5.85 (C-1)	4.80 (C-1)	5.81 (C-1)
(δ value)	4.48-4.64 (C-2)	4.79-4.97 (C-2)	4.50-4.62 (C-2)	4.82-5.00 (C-2)

Table 33

The similarity of the physical data for these two pairs of compounds strongly suggests that they have the same general structures and are therefore reasonably identified as open-chain homologues of the ephedrine oxazepine **1**.

Although cyclisation has not been possible by the methods tried, there is, perhaps, the possibility of preparing the methyl ester of the amino acid of the succinyl and glutaryl ephedrines, with a view to forming the oxazacine and oxazanine by reflux in dry methanol, in the same way that the original methyl-*N*-malonyl ephedrine had been prepared for the oxazepine. Dilute solution would be needed to prevent *inter* molecular rather than *intra* molecular reactions. Succinyl ephedrine forms easily, apart from the apparent 1,4-acyl migration, so part of the reason for the difficulty encountered in cyclisation could be the conformational flexibility of the intermediate. By replacing succinic anhydride by maleic anhydride, it was thought that a molecule with a more favourable conformation for cyclisation would be generated. The incorporation of the *Z* double bond into the structure should bring the carboxylic acid and the hydroxyl groups closer together, thus facilitating lactone formation. Maleic anhydride was therefore condensed with ephedrine, and readily gave the open chain hydroxyl acid **40** (Figure 112).

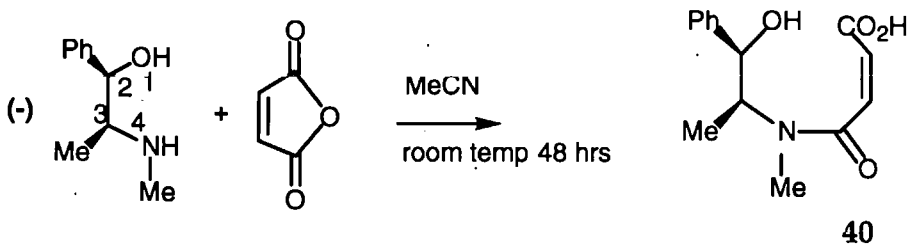

40

Figure 112

As anticipated from the earlier experiments, the physical data for this compound corresponded closely with those from the succinyl and glutaryl ephedrines. The ^1H NMR spectrum for this compound showed a signal for the benzylic proton at δ 4.90 and the proton α to the nitrogen atom at δ 4.60. On the IR spectrum there were peaks at 1716 cm^{-1} (carboxylic acid carbonyl) and at 1604cm^{-1} (conjugated amide carbonyl). Unfortunately the hope that the *Z* configuration would facilitate cyclisation, resulted in frustration again. Our attempts at cyclisation turned out to be very disappointing, with no evidence for the anticipated product. If synthesis of this oxazecine had been accomplished it would have yielded a chiral dienophile for the investigation of stereoselective Diels-Alder reactions. Presumably the conformational freedom around the single bonds to nitrogen and the general difficulty of ring-formation in medium sized rings, overides any directional advantage gained by using the *Z* configuration of the double bond. Furthermore, more forcing conditions might in addition lose even this advantage by allowing *Z* to *E* interconversion.

Preparation of heterocycles using beta-amino alcohols

The second series of heterocyclic syntheses that was investigated, was the reaction between various amino alcohols and dimethyl acetylenedicarboxylate (DMAD). The chiral amino alcohols (the chiral precursors) are readily available from naturally occurring α-amino acids and on cyclocondensation with DMAD, gave the respective six membered rings (**46, 47** and **48**) shown in Figure 113.

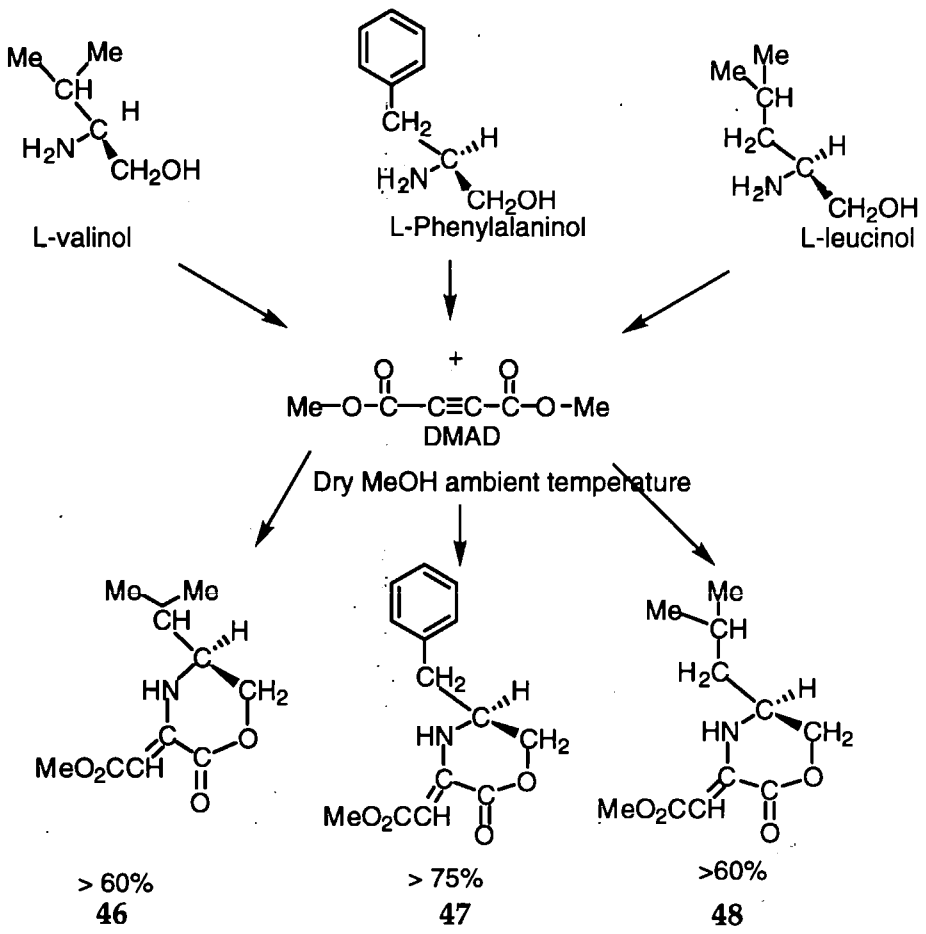

Figure 113

As well as the stereogenic centre from the amino alcohol precursor, these heterocycles have two prochiral centres; one at the ring junction α to the nitrogen atom and one at the alkene centre β to the nitrogen atom. The enamine function they contain should undergo stereoselective alkylation with alkyl halides at the carbon atom β to the nitrogen atom. However the nitrogen would also be susceptible to alkylation. To prevent this substitution at the nitrogen and to decrease the nucleophilic influence of that atom, attempts were made to tosylate or mesylate the amino alcohols on the nitrogen atom before reaction with DMAD. It was hoped that this would also increase the stereoselectivity,

particularly in the case of the phenylalaninol-DMAD compound. However, alkylation would also be possible at the ring junction, if the electron delocalisation of the enamine were suppressed. Tosylation or mesylation of the nitrogen atom would also enhance its electron withdrawing function.

In the event tosylation of L-valinol and mesylation of L- leucinol gave the ditosylated and dimesylated products respectively (Figure 114).

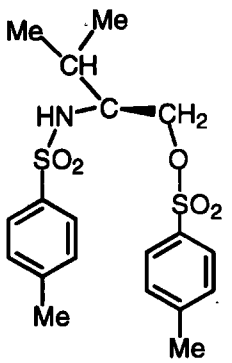

Ditosylated L-valinol

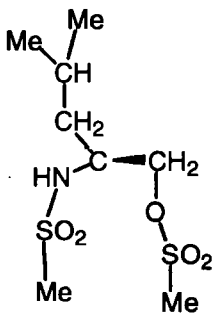

Dimesylated L-leucinol

Figure 114

As these reactions had not given the required product, an attempt was made to tosylate or mesylate the already formed heterocycles. This also proved unsatisfactory with recovery of the starting materials and so the investigation was abandoned at this stage. The hope had been that if ring closure could have been carried out as ahown in Figure 113, then a series of diastereoselective substitutions at the enamine could have been attempted.

Following these results, ephedrine, which has a secondary amine function, was reacted with DMAD. Bellan *et al* [79,80] have carried out a series of reactions between DMAD and ephedrine and these are shown in Figure 115 below.

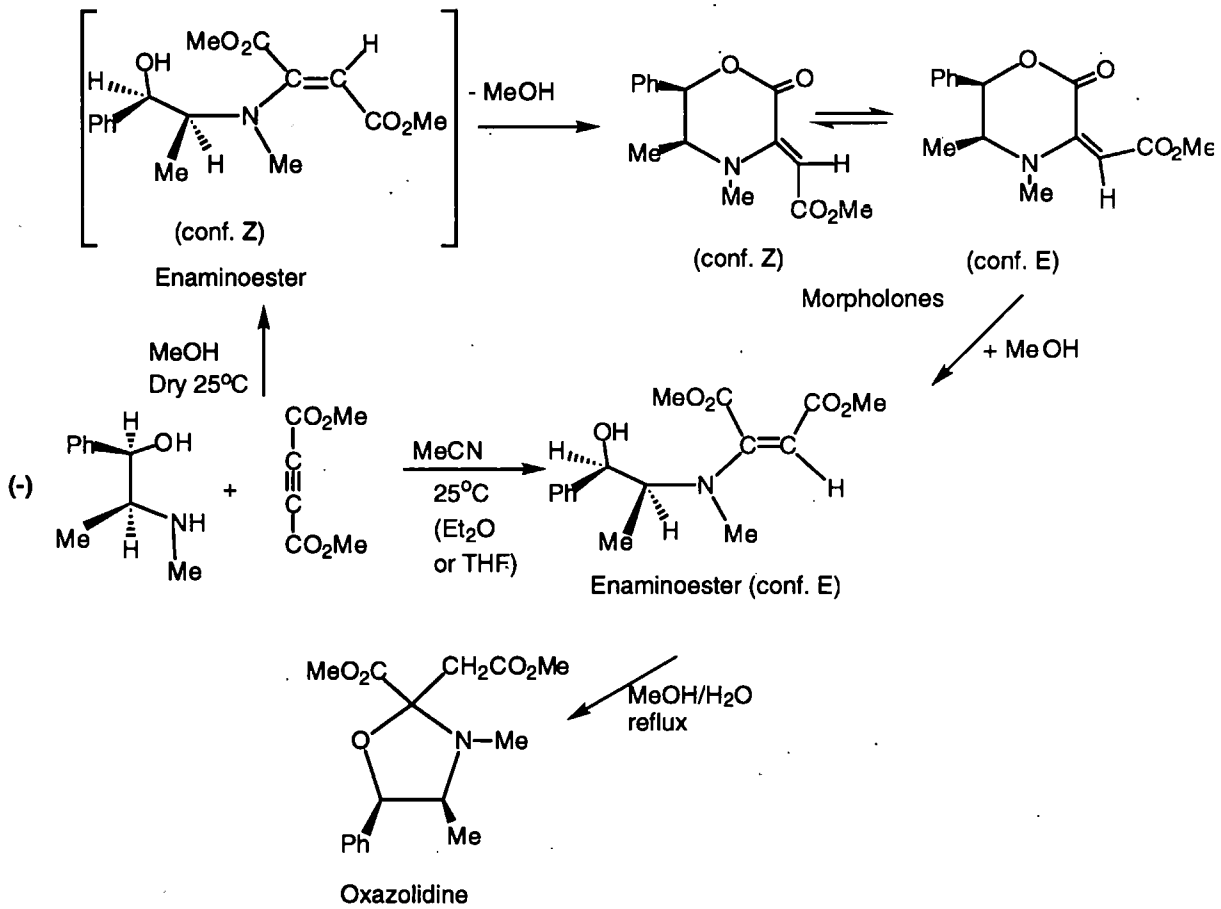

Figure 115

The results summarised in Figure 115 show, that dependent upon the reaction conditions used the products formed can be the open chain enaminoester with the *E* configuration or the 1,4,-tetrahydrooxazinones (morpholones) or both *E* and *Z* 1,3-oxazolidines. In the aprotic solvent, an intermediate enaminoester was isolated, and identified as having the *E*- configuration, but in a protic solvent no intermediate was isolated. The morpholone with the *Z*- configuration appeared to be formed directly. They postulated that in an aprotic solvent a zwitterion type intermediate was formed (Figure 116), which would lead to the correct configuration for the *E* enaminoester.

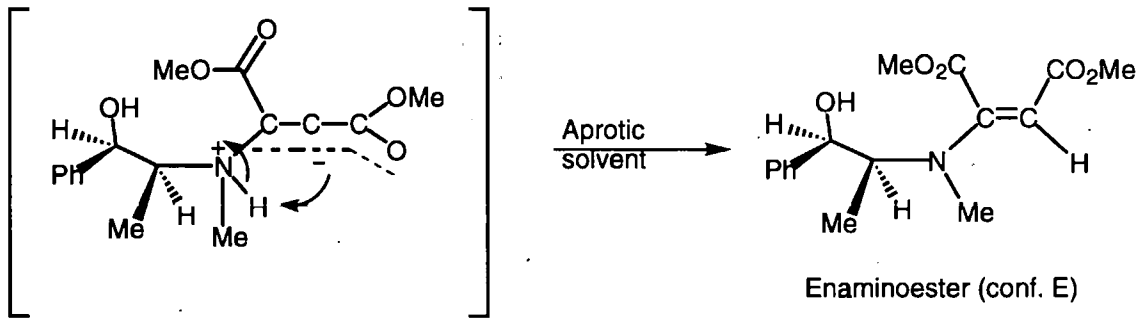

Figure 116

The *E*- and *Z*- morpholones have a similar potential for alkylation at the enamine, and with the use of butyllithium and an alkyl halide it was thought that alkylation would occur at the alkene carbon atom β to the nitrogen. Although the morpholones were successfully synthesised, time unfortunately did not allow any further investigations.

Preparation of other analogues of the oxazepine

The final pair of heterocycles whose synthesis was attempted, were the two thiazepine analogues of the oxazepine system, using L-cysteine ethyl ester with succinic and glutaric anhydrides. The open chain precursor with succinic anhydride (Figure 117) was readily formed in good yield (> of 70% crude product).

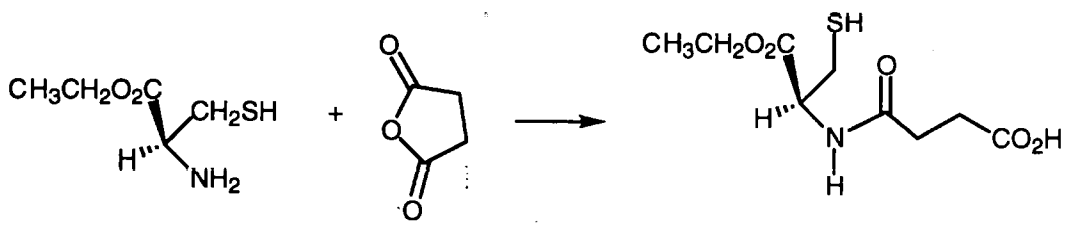

Figure 117

The IR spectrum for this compound gave an N-H stretching band at 3350 cm^{-1} and an S-H stretching peak at ~ 2550 cm^{-1}, a signal at 1734^{-1} (acid/ester carbonyl) and one at 1650 cm^{-1} (amide carbonyl). In comparison with the ephedrine succinic anhydride compound, the carbonyl stretching values are consistent with the literature values, whereas the signals for the ephedrine moiety were lowered in frequency, presumably due to hydrogen bonding. The S-H group does not generally form any extensive hydrogen bonding and the frequency of the S-H absorption shows little change on passing from the liquid state to the dilute solution.[74] The ^1H NMR spectrum contained a peak for a single N-H proton, which gradually diminished on shaking the sample with deuterium oxide. The signals due to the S-H and the O-H groups were immediately removed. The mass spectrum (CI NH_3) gave a molecular ion $(M+H)^+$ of *m/z* 250. The next stage was to attempt cyclisation.

The same method was employed as for the oxazepine, using cyanuric chloride/pyridine. Unfortunately instead of the desired product, a disulfide with an imide group was formed. The same product resulted when cyclisation was attempted using phenylphosphorodichloroidate (Figure 118).

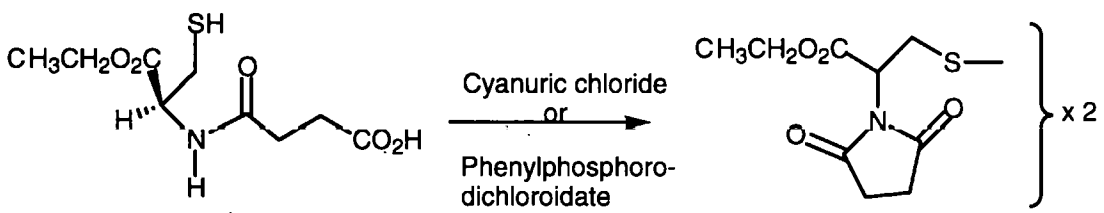

Figure 118

The evidence for formation of the disulfide came from the mass spectrum, together with the IR and the ^{1}H NMR spectra. The mass spectrum (CI NH_3) gave a molecular ion $(M+H)^+$ at *m/z* 461 and $(M+NH_4)^+$ at *m/z* 478. IR spectroscopy showed peaks at 1743 cm^{-1} (ester carbonyl) and at 1711 cm^{-1} (imide carbonyl). There was also no evidence for a thiol ester carbonyl group (1695 cm^{-1}) on the IR spectrum or for any amine group on either the IR or ^{1}H NMR spectra.

To prevent the imide from forming it was decided that the nitrogen of the cysteine ethyl ester should be protected before reacting it with the succinic anhydride. Di-*tert* -butyl dicarbonate was used initially, but this gave the *bis* substituted product **41** (Figure 119a).

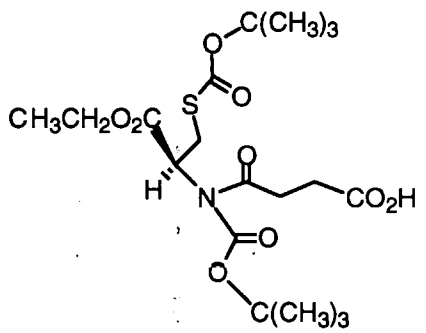

S, *N*-Di-(*tert*-butoxy carbonyl) substituted Cysteine ethyl ester

Figure 119a

Successful protection was achieved using *N*-phthalimido- or *N*-dinitrobenzoylamide protecting groups (**42** and **43** Figure 119b).

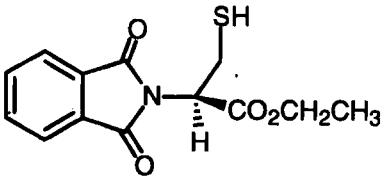

Phthalimido protected

42

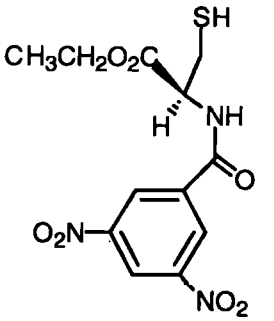

3,5-Dinitrobenzoyl protected

43

Figure 119 b

Using *N*-phthalimido protection it was possible to form the thioester **44**, with the monoethyl ester of glutaric acid (Figure 120).

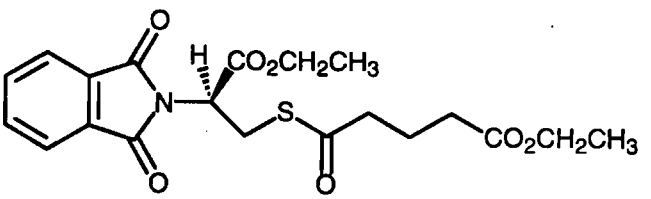

44

Figure 120

The thioester carbonyl stretching frequency on the IR spectrum was at ~1700 cm^{-1} with a broad band at 1721-1760 cm^{-1} covering the esters and imide carbonyls. The ^1H NMR spectrum showed a distinct change in the coupling pattern of the S-CH_2 protons in the compound **44**. Previously in the ^1H NMR spectrum of the cysteine ester, these protons gave a multiplet signal. Now for the thioester there was a doublet of doublets for each proton with a coupling constant of 10.0 and 5.0 Hz. Again, time did not allow any further investigation of these compounds.

6.7. Formation of racemic α-methyl phenylalanine: Discussion of an interesting by-product

Racemic α-methyl phenylalanine was prepared for use as a comparison to the physical data obtained for the isomeric α-substituted amino alcohols, which had been synthesised from the oxazepine (Table 28 p.128). The most appropriate compound to start with was dimethyl malonate. This was alkylated first with a methyl group, then with a benzyl group, this was followed by monohydrolysis (Figure 121).

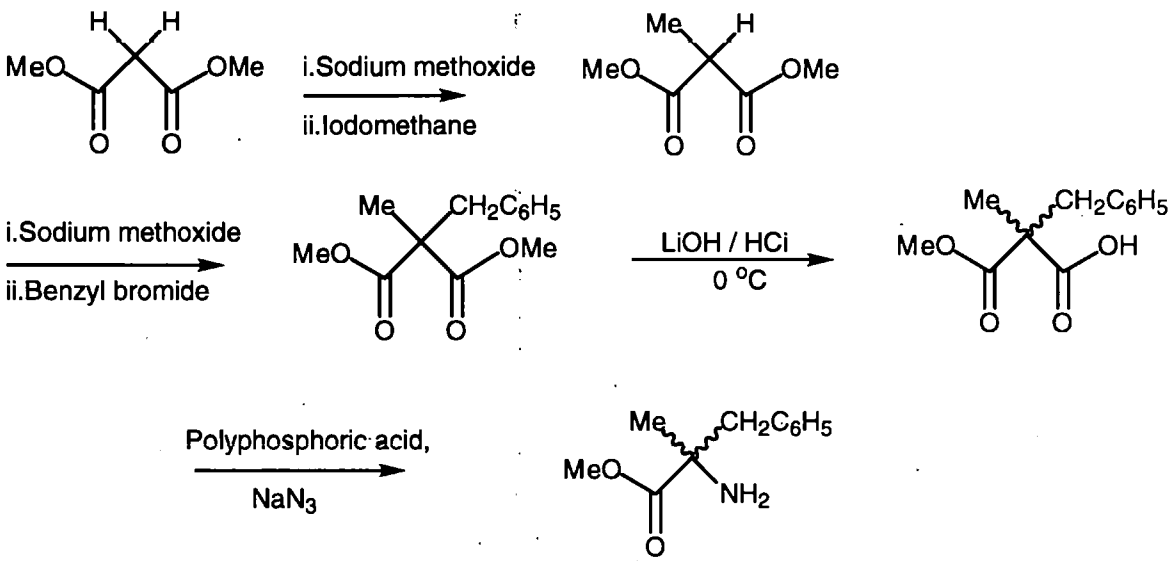

Figure 121

The next step in the synthesis was the Schmidt reaction, which allowed the conversion of a carboxylic acid to an amine, *via* an isocyanate, with migration from carbon to nitrogen and with retention of configuration, as dicussed earlier. The reaction mixture in this step was generally left to stand for not more than 8 h, but on one occasion it was left standing for about 24 h. On working-up this latter reaction mixture, two other products were isolated in addition to the expected

substituted amino ester, one was now the major product. Both new compounds showed two carbonyl peaks and one (the minor product) had a ^1H NMR spectrum similar to the expected product, except for an NH signal not an NH_2 signal. The mass spectrum for this compound $(M+H)^+$ was *m/z* 413. It was in fact a *bis*-substituted urea, which had formed by attack of the amine nitrogen on the carbonyl carbon of the intermediate isocyanate (Figure 122).

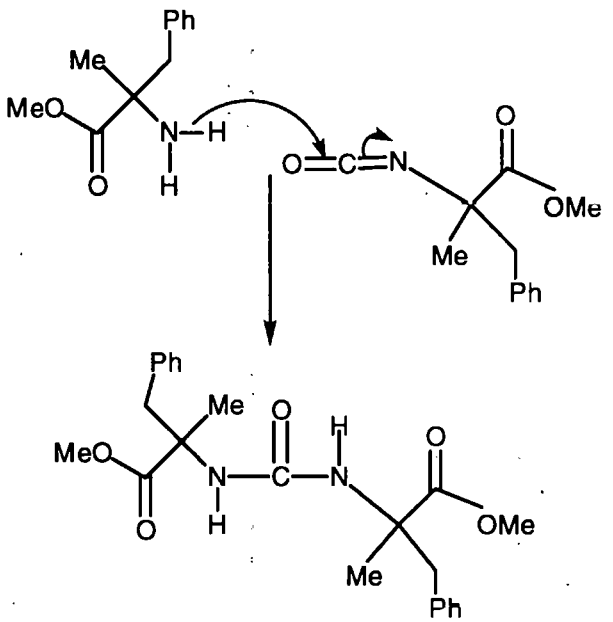

Figure 122 ***bis* - substituted Urea** (minor product)

Table 34 shows the comparison of the IR absorptions for the amino ester and the *bis*-substtuted urea.

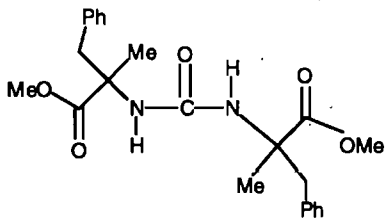

bis- urea

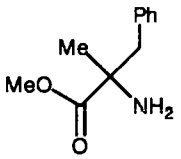

Amino ester

NH	3383 cm^{-1}	3360 and 3240 cm^{-1}
Ester carbonyl	1736 cm^{-1}	1738 cm^{-1}
Urea carbonyl	1665 cm^{-1}	—

Table 34

Accurate mass measurement for the *bis*- urea gave 413.2072 (calculated 413.2076 for $C_{23}H_{29}N_2O_5$).

The major product isolated, also gave only a single NH proton in the ^1H NMR spectrum. The two carbonyl stretching frequencies were similar to those of the urea (1739 and 1666 cm^{-1}), but the aromatic protons on the ^1H NMR spectrum showed a very different pattern to those of the ester and the dimer, and its CI mass spectrum had a molecular ion $(M+H)^+$ of *m/z* 220. It appeared that the intermediate isocyanate had undergone an *intra* molecular Friedel-Crafts reaction to give a dihydroisoquinolone (Figure 123).

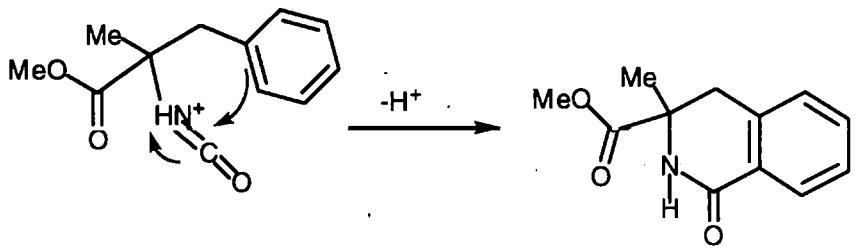

Figure 123 **dihydroisoquinolone**

Comparison of the two ^{1}H NMR spectra is shown in Figure 124 and the distinctive patterns of the aromatic protons can be clearly seen. The urea shows two sets of signals, whereas the dihydroisoquinolone shows an additional doublet that can be assigned to the protons on the ring adjacent to the stereogenic centre.

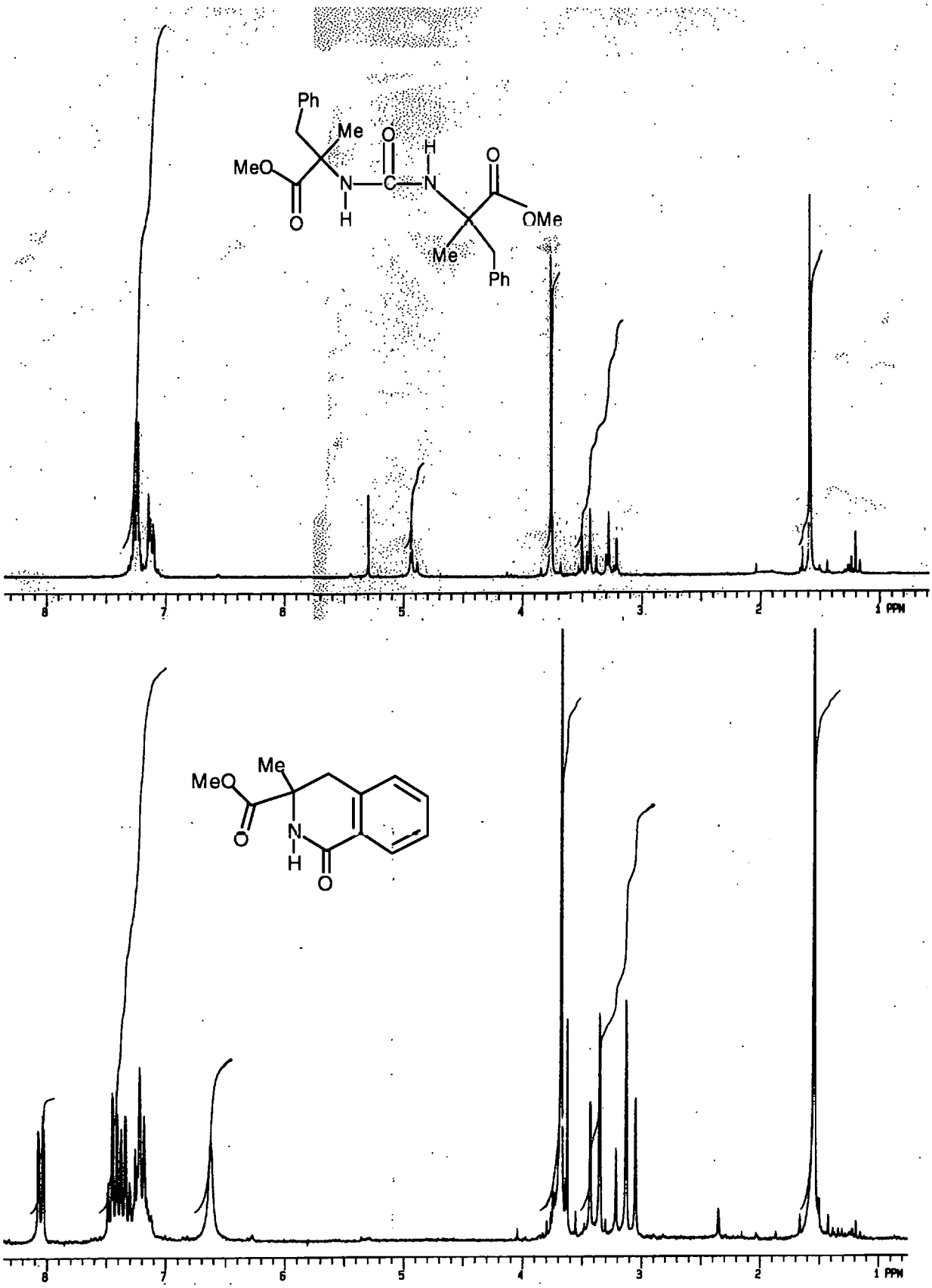
Ph
Me
MeO
O
H
N
C
N
O
OMe
Me
Ph
8
7
6
5
4
3
2
1 PPM
Me
MeO
O
N
H
O
8
7
6
5
4
3
2
1 PPM

Figure 124.

7. CONCLUSIONS AND FUTURE WORK

In this project we have attempted to show that certain heterocyclic precursors are suitable models for promoting asymmetric induction. Using the heterocycle oxazepine **1a**, derived from (+) ephedrine as the chiral auxiliary (Figure 58 p.67), it has been possible to replace the two hydrogen atoms at the prochiral C-6 atom with a high diastereoisomeric excess (>90%) and isolated yields of 80% in the alkylation cases studied.

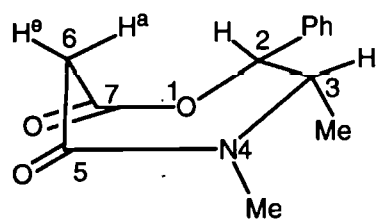

1 a

These alkylation reactions allowed the production of intermediates **18-22** (below p.100 and Appendix p.234).

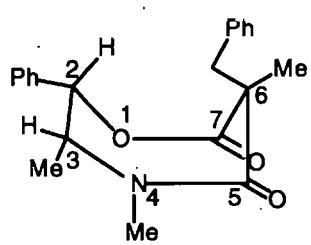

18

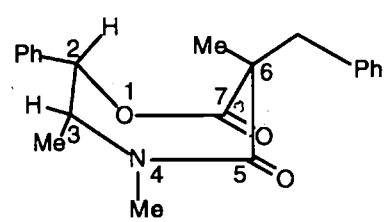

19

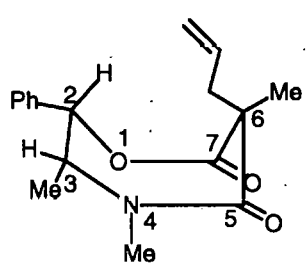

20

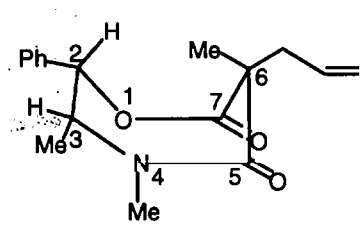

21

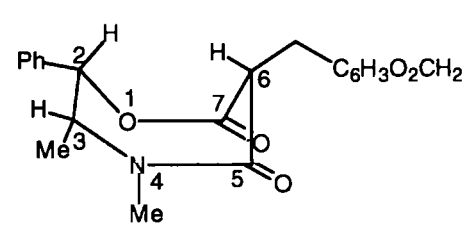

22

Replacement of the first hydrogen of the oxazepine **1a** appeared to be conformationally, and thus thermodynamically controlled whilst the second alkylation proceeded with kinetic control. Reversing the order of substitution of specific alkyl groups allowed control of the stereochemistry at C-6 in the oxazepine to give **18** or **19** and **20** or **21**. Although introduction of the bulkier group as the second substituent (**18**) did produce a lower de (4:1).

Having achieved the asymmetric induction, we then turned to production of synthetically useful products, and possible recovery of the ephedrine moiety.

Cleavage of the disubstituted oxazepine ring proved more difficult than had been anticipated, but was achieved with the use of sodium and liquid ammonia in 84% yield (Figure 87 p.117). It would appear that hydrolysis using potassium carbonate, lithium hydroxide or sodium methoxide, or hydrogenolysis methods were not suitable for the oxazepine cleavage.

Following successful cleavage of the oxazepine ring, we chose to prepare an α-substituted amino acid, by modifying the carboxyl group of the chiral intermediate arising from the ring cleavage (shown below and Figures 90 and 91 p.122 and 123).

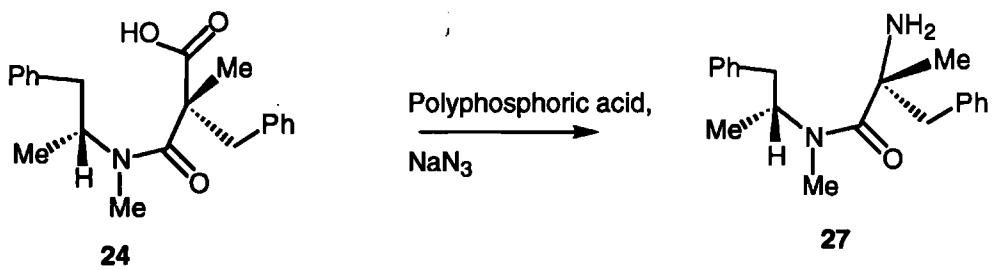

24 **27**

This conversion of the carboxyl group into an amino group was successfully achieved using sodium azide and polyphosphoric acid in a Schmidt reaction, a reaction expected to give retention of configuration at the newly

created stereogenic centre. Finally hydrolysis of the amide link to the degraded ephedrine moiety yielded the 2-methyl-3-phenylalanine as a zwitterion and *N*-methyl-1 benzyl-ethylamine (Figure 92 p.125).

The isolated yield of the alkylation steps leading to the new stereogenic centre was high in all but one of the cases studied (~80% and for compound **18** 70%), but the overall yield to the α-methylphenylalanine was disappointingly low. This arose from the relatively low yields of the ring cleavage and of the Schmidt reactions and unfortunately time did not allow optimisation of these steps to afford an efficient and practicable synthetic route to these enantiomerically pure α–substituted amino acids. The release of the chiral auxiliary (+)-ephedrine was impaired in our work, since the need to use sodium and liquid ammonia in the ring cleavage step modified the ephedrine to *N*-methyl-1 benzyl-ethylamine. Further investigation of ring opening processes is required to allow recovery of the chiral auxiliary itself.

Molecular modelling using the PCMODEL programme provided structures with minimum energy conformations predicting the observed product configuration, which was confirmed by the experimental findings of the nOe spectra and the X-ray crystallography structures. Figure 74 (p.93) illustrates this modelling for compound **14**, the lowest energy structure (monomethyl **1b**) that was predicted, is confirmed by the nOe enhancement spectrum (Figure 76 p.95).

Following the successful demonstration of the use of the oxazepine heterocyclic precursor as a model to allow a high degree of asymmetric induction, there was time to briefly investigate other chiral auxiliaries, using systems based

upon β amino alcohols other than ephedrine. The related oxazepine derived from *S*-prolinol was successfully synthesised (**34** Figure 97 p134 and reproduced here).

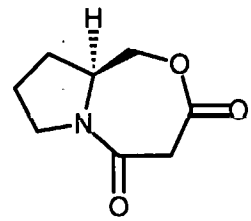

34

The conformation of this bicyclic system determined from the nOe spectrum for this compound, appeared sufficiently similar to the ephedrine derived oxazepine to assume that asymmetric induction would be possible with this novel heterocyclic compound. This successful synthesis allows the method to be used for more reactions involving the many amino alcohols that are available, perhaps resulting in more facile cleavage methods, because of the differing oxazepine compositions and conformations that would result from the different amino alcohols, with possible recovery of the starting materials.

Initial studies were begun to investigate the importance of conformational flexibility in the seven membered oxazepine ring, in our successful stereoselective synthesis method. This was by attempting to prepare eight and nine membered homologues of the oxazepine, again using ephedrine as the chiral auxiliary (**X, Y** and **Z** Figure 102 p.142). The open chain precursors to these compounds were successfully prepared from ephedrine and maleic anhydride, succinic anhydride or glutaric anhydride respectively, but initial attempts to achieve ring closure to the oxazecine and oxazenine rings did not succeed and further work would be needed to achieve this and subsequently attempt stereoselective alkylations.

There is the possibility of making the methyl ester of the succinylephedrine and glutarylephedrine (zwitterion forms **37** and **39**), with a view to forming the oxazecine and oxazenine.

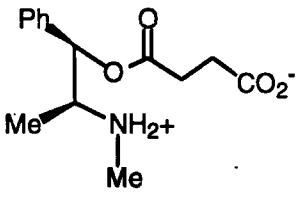

37

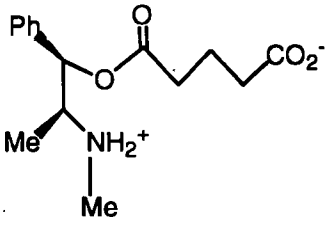

39

Refluxing in dry methanol to give the amide linkage, in the same manner as the original methyl-*N*-malonyl ephedrine had been prepared for the oxazepine (Figure 61 p.73). Dilute solution would be needed to prevent *inter* molecular rather than *intra* molecular reactions (Figure 125).

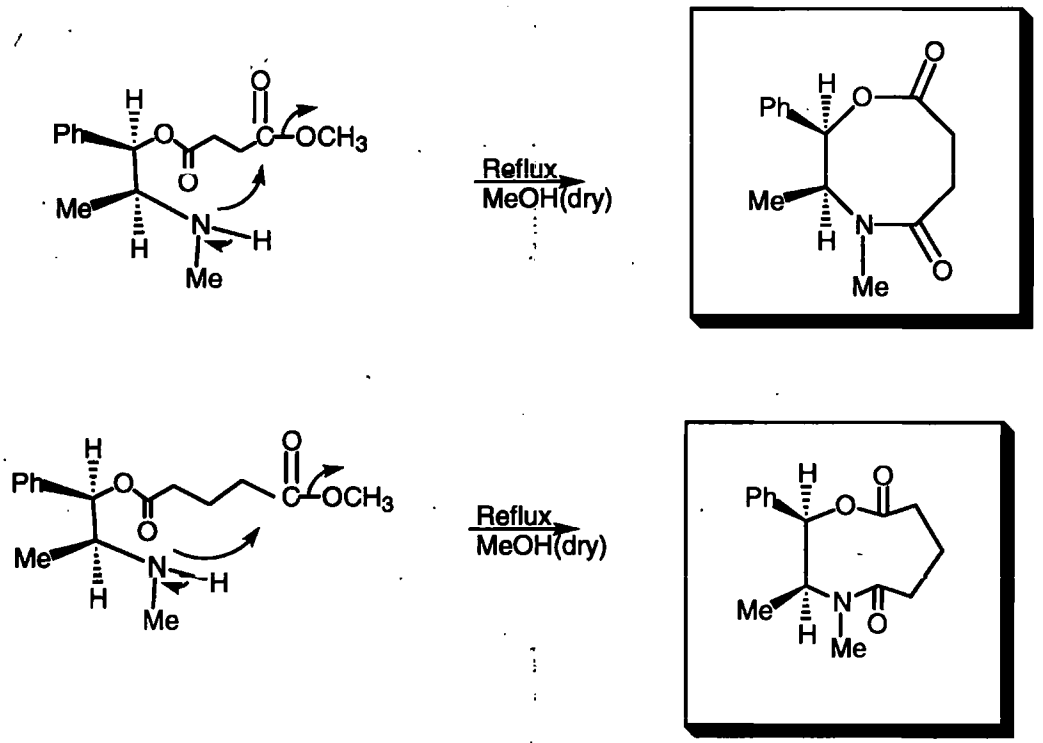

Figure 125

Preliminary experiments were carried out to attempt preparation of an 8-membered ring thiazecine analogue (**45**) of the oxazecine, but time allowed only for the preparation of the *N*-phthaloyl protected open chain precursor (**44**) (Figure 126).

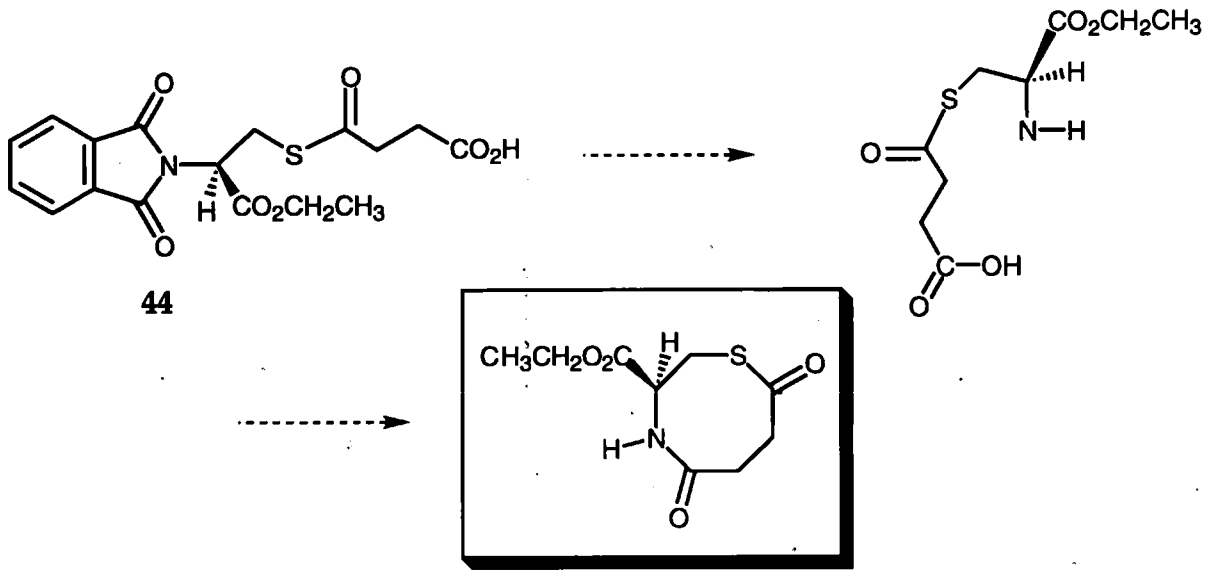

Figure 126

After cleavage of the oxazepine, which had been substituted with an allyl and a methyl group (compound **21**), there is the possibility of intramolecular cyclisation, either by acid catalysis to give a lactone (Figure 127a) or by acylation using a catalyst such as polyphosphoric acid (Figure 127b) to give a cyclopentenone, both mechanisms following Markovnikov's rule.

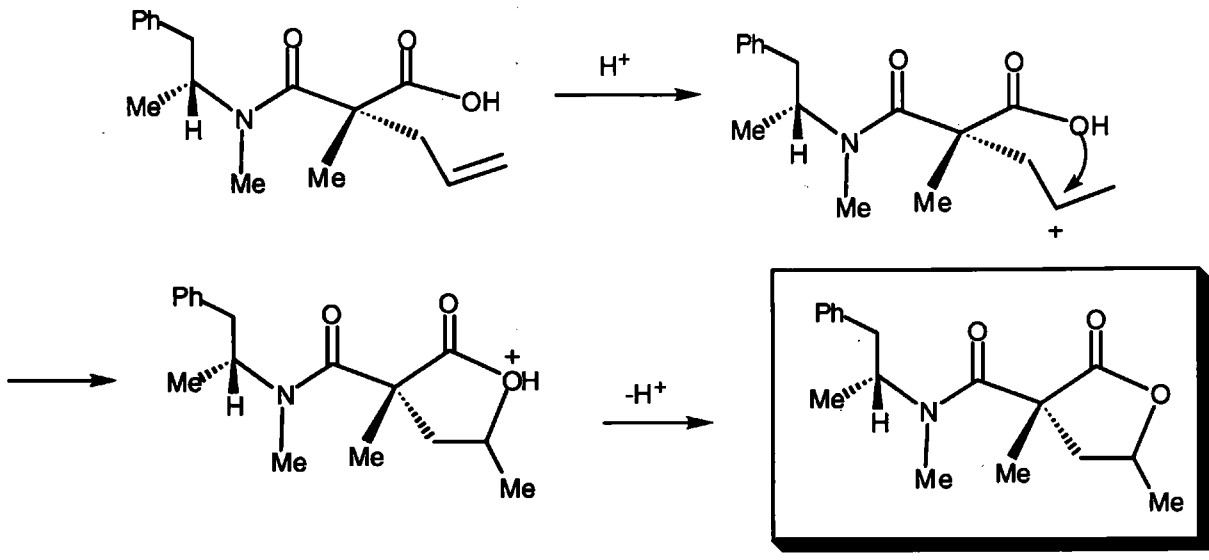

Figure 127a

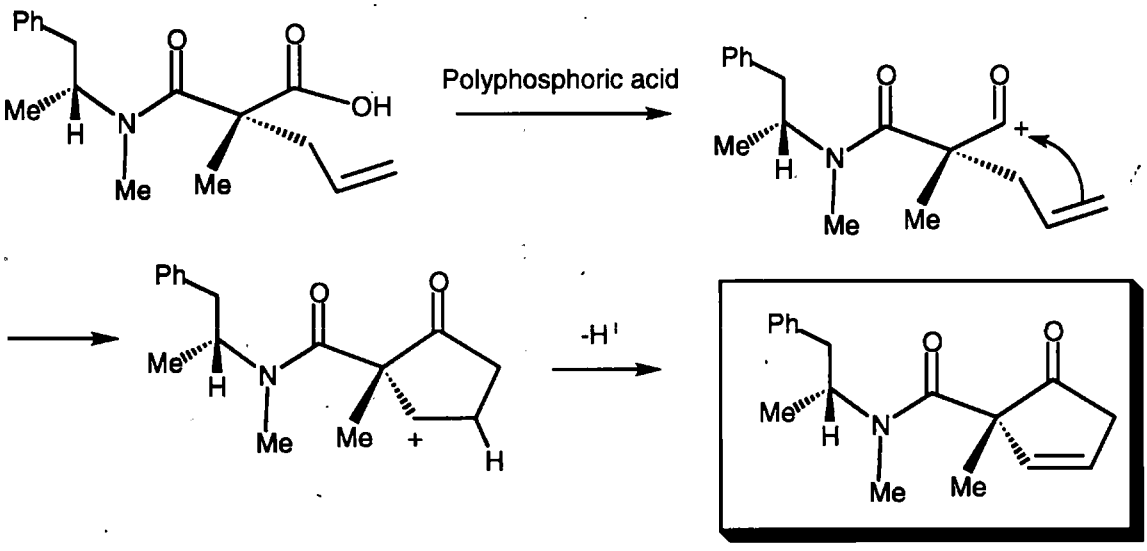

Figure 127b

Finally returning to oxazepine **1a**, central to this project, further work of interest would be the stereoselective substitution of the C-6 hydrogens by methyl and piperonyl groups leading to a synthesis of L-methyl-Dopa (compound **A1**), of current interest in the treratment of Parkinson's disease (Figure 128).

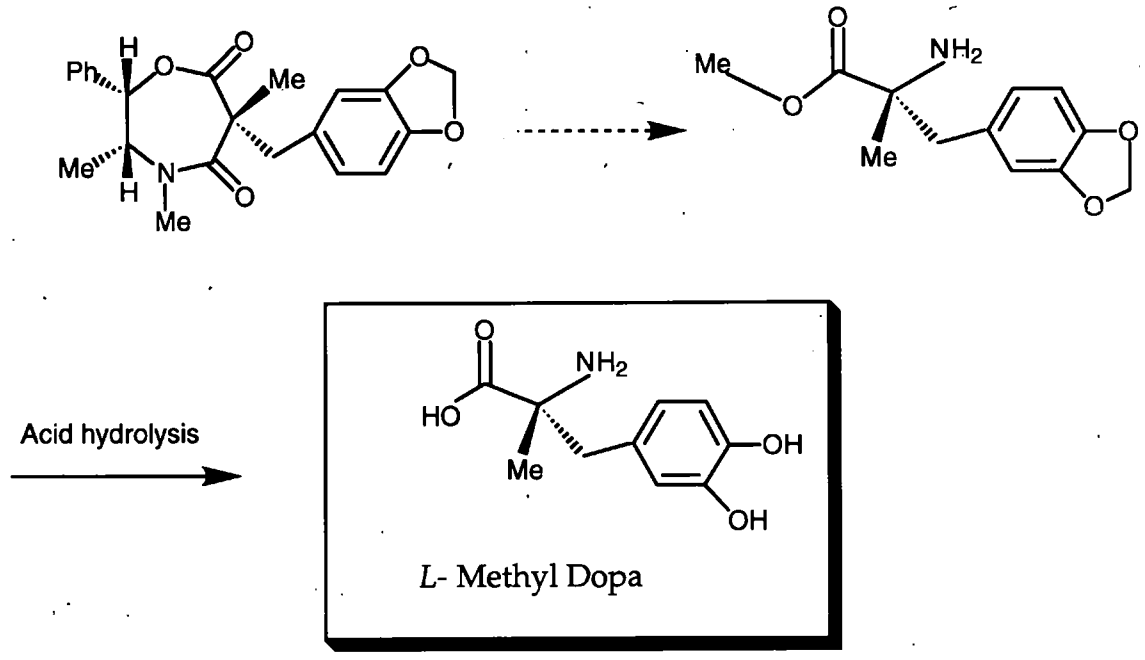

Figure 128

There are possibilities for the use of the dihydroisoquinolone (unexpectedly formed during the Schmidt reaction), as a precursor in the synthesis of some of the naturally occurring opium alkaloids (Figure 129).

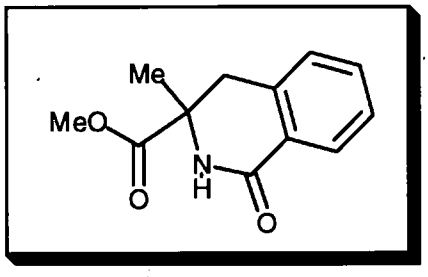

Figure 129

In conclusion, the project has successfully devised a synthesis for the preparation of a rigid heterocylic system with stereogenic centres of known absolute configuration and a built-in reactive centre. That reactive centre allowed substitution with steric control by the asymmetric elements already present, to give nine novel heterocylic systems (compounds **14-22** Appendix p.234). The new stereogenic centre was then liberated, by ring opening processes at the heteroatom sites. After ring cleavage, it was demonstrated that the preparation of α-substituted α-amino acids was possible by selective functional group interconversion to give 2-methyl-3-phenylalanine methyl ester.

8. EXPERIMENTAL

All melting points were done on a Kofler block and are uncorrected. Specific rotations ($[\alpha]_D$) were recorded at 23 °C on an Optical Activity AA-100 polarimeter, with concentrations (g/cm^3) and solvent in parentheses. Infrared spectra were recorded on a Perkin-Elmer 1710 FT spectrometer, as an evaporated film or as otherwise stated. Proton nuclear magnetic resonance spectra were recorded at 200 MHz on a Varian Gemini 200 spectrometer and at 300 MHz on a Bruker AC 300E spectrometer. The line positions or centres of multiplets are given in the δ scale, with respect to residual chloroform (δ 7.25) in the deuterated chloroform solvent. The multiplicities, integrated areas and coupling constants in Hz are indicated in parentheses. Carbon-13 nuclear magnetic resonance spectra were recorded at 300 MHz on a Bruker AC 300E spectrometer with deuterated chloroform as solvent. The atom numbering system is as shown in the "Convention" section on page viii and partly reproduced below (P.175). Mass spectra were run at high resolution (accurate mass) on a Kratos Concept IS instrument and at low resolution (EI/CI (NH_3)) on a VG TR10 2000.

High performance liquid chromatography was run on a Gilson 131 RI detector, using a silica (10 cm x 8 mm) Waters RCM module column at 2 cm^3/min and a Shimadzu CRA2X integrator.

Polygram SIL plates were used for analytical thin layer chromatography. Visualisation was with iodine vapour (I_2), or with a saturated solution of ceric sulphate in 3 M sulphuric acid (C).

Silica gel, grade 12, 80-100 mesh was used for column chromatography.

Solvents and reagents were purified, when necessary, by standard methods, as found in "Purification of Laboratory Chemicals," Perrin, Armarego and Perrin, Pergamon Press, 1966.

When the preparation of a known compound is described, the Beilstein Registry number is given.

Atom numbering system

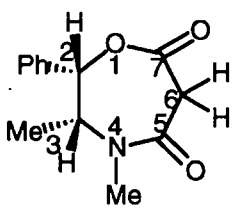

Oxazepine

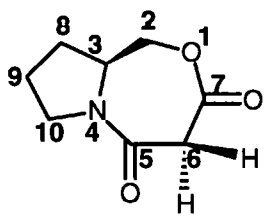

Pyrrolidinooxazepine

1. ***Preparation of Methyl N-malonylephedrine***

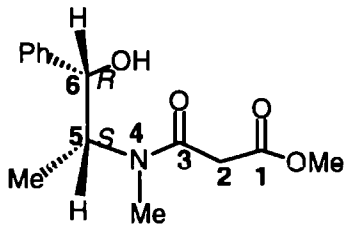

12

1*S*,2*R*-(+) Ephedrine (5.0 g, 30.3 mmol) with dimethyl malonate (5.0 g: 37.9 mmol) in dry methanol (40 cm^3) was refluxed for 2 days. Further methanol (20 cm^3) was added and reflux distillation continued for another 2 days. Reaction progress was monitored by TLC [(3:1) dichloromethane : ethyl acetate]. The methanol was evaporated and the residue taken up in chloroform (40 cm^3), washed with 2 molar HCl (2 x 20 cm^3), and brine (20 cm^3), and the organic layer dried over anhydrous sodium sulphate. The filtered organic layer was then passed through a column of silica gel with dichloromethane as the eluant. Evaporation under reduced pressure yielded methyl *N*-malonyl-1*R*, 2*S*-ephedrine **12** (Figure 61 p.73) (7.55 g, 90 %) as a colourless oil;

υ_{max} (film)/cm^{-1} 1730 (ester C=O), 1621 (amide C=O); δ_H (200 MHz; $CDCl_3$; Me_4Si) 1.02 (3 H, d, *J*10, -C-CH_3), 2.70 (3 H, s, -N-CH_3), 3.22 (2 H, s, -C-CH_2), 3.60 (3 H, s, -O-CH_3), 4.57 (1 H, dq, *J* 6.0 and 10.0, -N-C*H*), 4.71 (1 H, d, *J* 6.0, -C_6H_5-C*H*), 7.10-7.29 (5 H, br, C_6H_5).

The physical data are consistent with methyl *N*-malonylephedrine.[69]

2. *Preparation of N-Malonylephedrine*

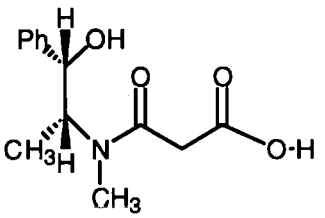

13

The crude methyl *N*-malonylephedrine (15 g) was cooled to 0 °C, and a solution of lithium hydroxide (16.8 g; 400 mmol) in water (100 cm^3) was added dropwise with stirring, maintaining the temperature below 5 °C. The solution was stirred overnight at room temperature, before the bulk of the methanol was removed under reduced pressure at <30 °C. The residue was cooled to below 5 °C, acidified with conc. hydrochloric acid (42 cm^3) and the solution was then saturated with sodium chloride and extracted with dichloromethane (1x300 cm^3, 4x150 cm^3). The extracts were dried over anhydrous sodium sulphate and evaporated under reduced pressure to give a clear colourless oil (15 g, 95 %).

υ_{max} (film)/cm^{-1} 1731 (acid C=O), 1621 (amide C=O), δ_H (200 MHz; $CDCl_3$; Me_4Si) 1.09 (3 H, d, *J* 10, -C-CH_3), 2.73 (3 H, s, -N-CH_3), 3.15 (2 H, s, -C-CH_2), 4.50 (1 H, dq, *J* 7.0 and 10.0, -N-C*H*), 4.79 (1 H, d, *J* 7.0, -C_6H_5-C*H*), 7.15-7.30 (5 H, br, -C_6H_5).

The physical data are consistent with *N*-malonylephedrine (**13** Figure 62a p.74).[69]

3. *Preparation of (2S,3R)-3,4-Dimethyl-2-phenylperhydro-1,4-oxazepine-5,7-dione*

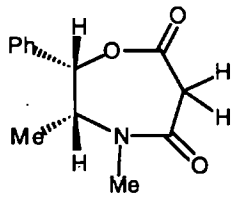

1

The crude *N*-malonylephedrine (15 g; ~60 mmol) in dry acetonitrile (350 cm^3), was transferred to a three necked flask, which was then filled with nitrogen, and the solution stirred. Solutions of cyanuric chloride (14 g; 75 mmol) in dry acetonitrile (150 cm^3) and pyridine (24.2 cm^3; 300 mmol) in dry acetonitrile (150 cm^3), were added simultaneously, dropwise over one hour. After five hours the solution was filtered, and the solid washed with dry acetonitrile (2x30 cm^3). The combined filtrates were evaporated under reduced pressure (acetonitrile recovered). Flash chromatography over silica gel (160 g) was used to separate the product, using successively dichloromethane : toluene (6:1,1x250 cm^3), dichloromethane (2x250 cm^3), dichloromethane : ether (4:1,4x250 cm^3) as eluants. Fractions 4-7 (TLC Rf 0.32 (EtOAc:cyclohexane 3:1) (I), were combined and evaporated under reduced pressure to give (+)-(2*S*, 3*R*)-3,4-dimethyl-2-phenylperhydro-1,4-oxazepine-5,7-dione **1** Scheme A p.75, as a pale yellow crystalline solid. (3.82g, 28 %); mp 125-127 °C (from acetone) (lit.[77] 125 °C), $[\alpha]_D$ -93 ° (c 0.1 in DCM) (lit.[77]-88 ° (c.0.1 in EtOH)); (Found: C, 67.35; H, 6.53; N, 6.44. $C_{13}H_{15}NO_3$ requires C, 66.94; H, 6.48; N, 6.01%);υ_{max} (film)/cm^{-1} 1745 (lactone C=O), 1638 (lactam C=O), δ_H (200 MHz; $CDCl_3$; Me_4Si) 1.19 (3 H, d, *J* 10.0, -C(3)-C*H*$_3$), 3.00 (3 H, s, -N (4)-C*H*$_3$), 3.65 (1 H, dq, *J* 8.0 and 10.0,-C(3)-*H*); 3.78 (1 H, d,J_{ab} 17.5, -C(6)-*H*), 4.16 (1 H, d, J_{ab} 17.5, -C(6)-*H*), 6.00 (1 H, s, -C(2)-*H*), 7.28-7.48 (5 H, m,-C$_6$*H*$_5$)).

The physical data are consistent with the oxazepine, (2*S*, 3*R*)-3,4-dimethyl-2-phenylperhydro-1,4-oxazepine-5,7-dione (**1** Scheme A p.75).[66, 69]

4. Reactions of "Oxazepines" with organic halides and potassium *tert*-butoxide.

4a. Preparation of (2S, 3R,6R)-3,4-Dimethyl-6-methyl-2-phenylperhydro-1,4-oxazepine-5,7-dione

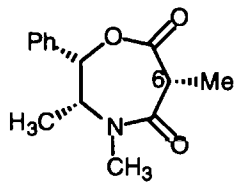

14

(2*S*, 3*R*)-3,4-Dimethyl-2-phenylperhydro-1, 4-oxazepine-5,7-dione (**1**) (0.17 g; 0.73 mmol) was dissolved in dry THF (10 cm^3), at room temperature and under nitrogen. A solution of potassium *tert*-butoxide, (0.08 g; 0.73 mmol), in dry THF (5 cm^3) was added dropwise with stirring, and the solution was stirred at room temperature for 1 hour. Iodomethane (0.52 g; 3.65 mmol), was then added dropwise, the solution was stirred at room temperature for a further 24 hours, before the solution was evaporated under reduced pressure (TLC Rf 0.47 (EtOAc: cyclohexane 3:1 I_2)). The residue was taken up into ethyl acetate (25 cm^3), washed with water (3 x 10 cm^3), dried over anhydrous Na_2SO_4, and evaporated under reduced pressure to yield a white crystalline solid (0.17 g, 95%). Recrystallisation was from acetone.

Mp 119-120 °C (from acetone); $[\alpha]_D$ +47 °(c 0.1, DCM); (Found: C, 67.70; H, 6.96; N, 5.58. $C_{14}H_{18}NO_3$ requires C, 67.99; H, 6.93; N, 5.66 %); υ_{max}(film)/cm^{-1} 1749 (lactone C=O), 1639 (lactam C=O); δ_H (200 MHz; $CDCl_3$; Me_4Si) 1.13 (3 H, d,*J* 7.5, -C(3)-CH_3), 1.50 (3 H, d,*J* 5.0, -C(6)-CH_3), 2.93 (3 H, s, -N(4)-CH_3), 3.65 (1 H , q, *J* 7.5, C(3)-*H*), 4.07 (1 H, q, *J* 5.0, -

C(6)-*H*), 6.18 (1 H, s, -C(2)-*H*), 7.25-7.45 (5 H, m, -C_6H_5); δ_C (300 MHz; $CDCl_3$; Me_4Si) 11.62 (s) (3-CH_3), 13.35 (s) (6-CH_3), 36.88 (s) (N-CH_3), 43.98 (s) (3-C), 63.73 (s) (6-C), 77.80 (s) (2-C), 125.99 (2 x s) (Ph), 128.63 (s) (Ph), 128.79 (2 x s) (Ph), 135.97 (s) (Ph), 164.15 (s) (C = O) and 170.03 (s) (C = O); *m/z* (CI (NH_3)) 248.1288 ($(M+H)^+$ $C_{14}H_{18}NO_3$ requires 248.1287).

IR, NMR, mass spectra and elemental analysis were consistent with the product (2S, 3*R*, 6*R*)-3,4-dimethyl-6-methyl-2-phenylperhydro-1,4-oxazepine-5,7-dione (**14** Table 17 p.92). nOe spectra were consistent with the 2*S*, 3*R*, 6*R* - configuration (Figure 76 p.95) .

The analogous procedure (4a) was used in the following reactions.

4b. ***Preparation of (2S,3R,6R)-3,4-Dimethyl-6-allyl-2-phenylperhydro-1,4-oxazepine-5,7-dione***

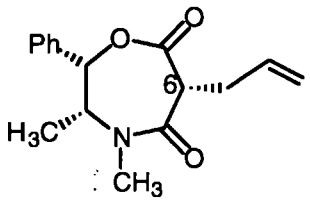

16 (Scale: 4.3 mmol of **1**)

Product **16** as a white crystalline solid 95%.

Mp 79-80 °C (from acetone); $[\alpha]_D$ +40 ° (c 0.1, DCM); (Found: C, 67.70; H, 6.96; N, 5.58. $C_{14}H_{18}NO_3$ requires C, 67.99; H, 6.93; N, 5.66 %); υ_{max}(film)/cm^{-1} 1747 (lactone C=O), 1638 (lactam C=O); δ_H (200 MHz; $CDCl_3$; Me_4Si) 1.05 (3 H, d, *J* 7.5, C(3)-CH_3), 2.765(1 H, dd, *J* 5.0 and 7.5, C(6)-$CH_{(2)}$), 2.92 (5 H, s, overlying dd, -N(4)-CH_3,

C(6)-$CH_{(2)}$), 3.65 (1 H, q, *J* 7.5 C(3)-*H*), 4.02 (1 H, dd, *J* 7.5, C6-*H*) 4.93-5.03 (2 H, dd, *J* 10.0 and 18.0, allyl CH_2), 5.75-5.86 (1 H, m, *J* 5.0 and 7.5 and 10.0, allyl C*H*), 6.23 (1 H, s, C(2)-*H*), 7.27-7.44 (5H, m, -C_6H_5); δ_C (300 MHz; $CDCl_3$; Me_4Si) 11.57 (s) (3-CH_3), 31.71 (s) (6-CH_2), 36.74 (s) (N-CH_3), 49.53 (s) (3-*C*), 63.7 (s) (6-*C*), 79.0 (s) (2-C), 112.14 (s) (alkene), 125.97 (2 x s) (Ph), 128.58 (s) (Ph), 128.74 (2 x s) (Ph), 135.89 (s) (Ph), 135.96 (s) (alkene), 163.11 (s) (C = O), 168.66 (s) (C= O); *m/z* (CI (NH_3)) 274.1446 ((M + H)$^+$ $C_{16}H_{20}NO_3$ requires 274.1443) (TLC Rf. 0.45 (EtOAc: cyclohexane 3:1 I_2).

IR, NMR and mass spectra were consistent with (2*S*, 3*R*, 6*R*)-3,4-dimethyl-6-allyl-2-phenylperhydro-1, 4-oxazepine-5,7-dione (**16** Table 17 p.89) as the product.
nOe spectra were consistent with the 2*S*, 3*R*, 6*R*-configuration (Figure 78 p.97).

4c. ***Preparation of (2S,3R,6R)-3,4-Dimethyl-6-benzyl-2-phenylperhydro-1,4-oxazepine-5,7-dione (15)***

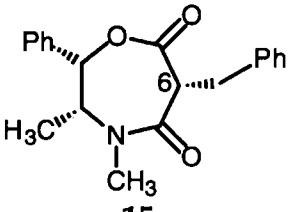

15

(Scale: 4.3 mmol of **1**)

Product **15** as a yellow crystalline solid 95%.

Mp 180-181 °C (from acetone); $[\alpha]_D$ +11 ° (c 0.1, DCM); (Found: C, 74.14; H, 6.74; N, 4.52. $C_{20}H_{22}NO_3$ requires C, 74.28; H, 6.55; N, 4.33 %); ν_{max}(film)/cm^{-1} 1750 (lactone C=O), 1641 (lactam C=O); δ_H (200 MHz; $CDCl_3$; Me_4Si) 1.14 (3 H, d, *J* 7.5, C(3)-CH_3), 3.00 (3 H, s, N(4)-CH_3), 3.25-3.35 (1 H, dd, *J* 5.0 and 10.0, C(6)-$CH_{(2)}$), 3.60-3.73 (2 H, m, dd overlying q, *J* 5.0, 7.5 and 10.0, C(3)-*H*, C(6)-C*H*), 4,22-4.29 (1 H, dd, *J* 5.0, C(6)-*H*),

6.20 (1 H, s, C(2)-*H*), 7.15-7.45 (10 H, m, 2x -C_6H_5); δ_C (300 MHz; $CDCl_3$; Me_4Si) 11.67 (s) (3-CH_3), 33.54 (s) (N-CH_3), 41.87 (s) (3-*C*), 54.39 (s) (6-CH_2-Ph), 63.04 (s) (6-*C*), 79.37 (s) (2-*C*), 124.87 (2 x s) (Ph), 125.58 (s) (Ph), 127.85 (2 x s) (Ph), 128.32 (s) (Ph), 128.67 (s) (Ph), 131.56 (2 x s) (Ph), 137.23 (s) (Ph), 137.54 (s) (Ph), 171.55 (s) (*C*= O), 172.98 (s) (*C*= O), *m/z* (CI (NH_3)) 341.1858 ((M + NH_3)$^+$ $C_{20}H_{22}NO_3$ requires 341.1865) (TLC Rf. 0.61 (EtOAc: cyclohexane 3:1 I_2).

IR, NMR and mass spectra were consistent with (2*S*, 3*R*, 6*R*)-3,4-dimethyl-6-benzyl-2-phenylperhydro-1,4-oxazepine-5,7-dione (**15** Table 17 p.92) as the product.

nOe spectra were consistent with the 2*S*, 3*R*, 6*R*-configuration (Figure 77 p.96).

4d. ***Preparation of (2S,3R,6R)-3,4-Dimethyl-6-piperonyl-2-phenylperhydro-1,4-oxazepine-5,7-dione.***

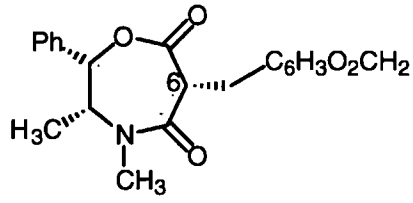

17

(Scale: 6.0 mmol of **1**)

Product **17** as a white crystalline solid 95%.

Mp 166 168 °C (from acetone); $[\alpha]_D$ +10 °(c 0.1, DCM);υ_{max}(film)/cm^{-1} 1745 (lactone C=O), 1638 (lactam C=O); δ_H (200 MHz; $CDCl_3$; Me_4Si) 1.15 (3 H, d, *J* 5.0, C(3)-CH_3), 3.00 (3 H, s, N(4)-CH_3), 3.20-3.30 (1 H, dd, *J* 15.0 and 7.5, 5.0, C(6)-$CH_{(2)}$), 3.52-3.63 (1 H, dd, *J* 15.0, 7.5 and 5.0, C(6)-$CH_{(2)}$), 3.70 (1 H, q, *J* 5.0, C3-C*H*), 4.20 (1 H, dd, *J* 7.5 and 5.0 C6-C*H*), 5.87 (2 H, s, O-CH_2-O), 6.20 (1 H, s, C(2)-*H*), 6.66-6.84 (3 H, m, C(6)-CH_2-C_6H_3),

7.30-7.44 (5 H, m, C(2)-C_6H_5); δ_C (300 MHz; $CDCl_3$; Me_4Si) 11.57 (s) (3-CH_3), 32.76 (s) (N-CH_3), 36.94 (s) (6-CH_2-C_6H_3-), 52.26 (s) (3-C), 63.99 (s) (6-C), 77.67 (s) (2-C), 100.8 (s) (O-CH_2-O); 1108.19 (s) (alkene-Pip), 109.98 (s) (alkene -Pip), 122.37 (s) (alkene-Pip), 125.83 (2 x s) (Ph), 128.64 (2 xs) (Ph), 128.69 (s) (Ph), 135.43 (s) (alkene-Pip), 135.74 (s) (Ph), 146.06 (s) (alkene-Pip), 147.48 (s) (alkene-Pip), 163.13 (s) (C= O), 168.30 (s) (C= O), *m/z* (CI (NH_3)) 368.1502 ((M + H)$^+$ $C_{21}H_{22}NO_5$ requires 368.1498) (TLC Rf. 0.61(EtOAc: cyclohexane 3:1) (I_2)).

IR, NMR and mass spectra were consistent with (2*S*, 3*R*, 6*R*)-3,4-dimethyl-6-piperonyl-2-phenylperhydro-1,4-oxazepine-5,7-dione (**17** Table 17 p.92) as the product. nOe spectra were consistent with the 2*S*, 3*R*, 6*R*-configuration (Figure 78 p. 97).

5. The procedure given in 4, was used in the following reactions, except that the reaction mixture was cooled to -78 °C, before addition of the organic halide.

5a. ***Preparation of (2S,3R,6S)-3,4, Dimethyl-6-benzyl-6-methyl-2-phenylperhydro-1,4-oxazepine-5,7-dione.***

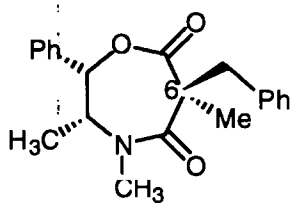

18

(Scale: 1.3 mmol of **14**)

Product **18** as a yellow crystalline solid 70%.

Mp 124-126 °C (from acetone); $[\alpha]_D$ +10 ° (c 0.1, DCM); (Found: C, 74.95; H, 6.85; N, 4.34. $C_{21}H_{24}NO_3$ requires C, 74.75; H, 6.87; N, 4.15 %); υ_{max}(film)/cm^{-1} 1727 (lactone C=O),

1638 (lactam C=O); δ_H (200 MHz; $CDCl_3$; Me_4Si) 1.25 (3 H, d, *J* 7.5, C(3)-CH_3), 1.88 (3 H, s, C(6)-CH_3), 3.02-3.17 (4 H, s overlying d, N(4)-CH_3, C(6)-$CH_{(2)}$), 3.32 (1 H, br, C(3)-*H*), 3.87 (1H, d, *J* 12.5, C(6)-$CH_{(2)}$), 4.62 (1 H, s, C(2)-*H*), 7.12-7.40 (10 H, m, -C_6H_5 x 2), *m/z* (CI (NH_3)) 338.1759 ((M + H)$^+$ $C_{21}H_{24}NO_3$ requires 338.1756), (TLC Rf. 0.63 (EtOAc: cyclohexane 3:1 I_2)). Column chromatography on silica using ethyl acetate/cyclohexane (3:1) as eluant yielded a de of 4:1. A de of 9:1was achieved after recrystallisation from acetone.

IR, NMR and mass spectra were consistent with (2*S*,3*R*, 6*S*)-3,4,-dimethyl-6-benzyl-6-methyl-2-phenylperhydro-1,4-oxazepine-5,7-dione (**18** Table 21 p. 112) as the product. X-ray crystallographic studies (Appendix) were consistent with the 2*S*, 3*R*, 6*S*-configuration.

5b. ***Preparation of (2S,3R,6S)-3,4,-Dimethyl-6-allyl-6-methyl-2-phenylperhydro-1,4-oxazepine-5,7-dione.***

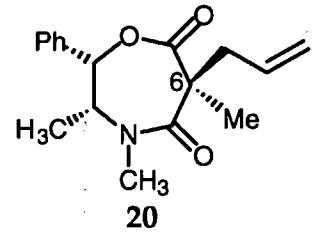

20

(Scale: 3.4 mmol of **14**)

Product **20** as a white crystalline solid 80%.

Mp 76-78 °C (from acetone); $[\alpha]_D$ +10 ° (c 0.1, DCM); (Found: C, 74.17; H, 7.56; N, 4.94. $C_{17}H_{22}NO_3$ requires C, 74.06; H, 7.37; N, 4.87 %); υ_{max}(film)/cm^{-1} 1732 (lactone C=O), 1634(lactam C=O); δ_H (200 MHz; $CDCl_3$; Me_4Si) 1.19 (3 H, d, *J* 7.5, C(3)-CH_3), 1.65 (3 H, s, C(6)-CH_3), 2.75 (1 H, dd, *J* 5.0 and 7.5, C(6)-CH_2), 3.05 (3 H, s, N(4)-CH_3), 3.44-3.59 (1 H,

br, C(3)-*H*), 4.95-5.16 (2 H, dd, *J* 7.5 and 18.0, allyl CH_2), 5.65-5.79 (1 H, m, *J* 5.0 and 7.5, allyl C*H*), 5.87 (1 H, s, C2-*H*), 7.33-7.47 (5 H, m, C_6H_5), δ_C (300 MHz; $CDCl_3$; Me_4Si) 12.23 (s) (3-CH_3), 26.14(s) (6-CH_3), 36.85 (s) (6-CH_2), 45.52 (s) (N-CH_3), 52.33 (s) (3-C), 63.71 (s) (6-C), 79.89 (s) (2-C), 118.96 (s) (alkene), 120.31 (s) (alkene), 125.99 (2 x s) (Ph), 128.77 (2 x s) (Ph), 131.73 (s) (Ph), 133.55 (s) (Ph), 171.54 (s) (C=0), 172.33 (s) (C=0), *m/z* (CI (NH_3)) 288.1598 ((M + H)$^+$ $C_{17}H_{22}NO_3$ requires 288.1600), (de 9:1), (TLC Rf. 0.55 (EtOAc:cyclohexane 3:1 I_2)).

IR, NMR and mass spectra were consistent with (2*S*, 3*R*, 6*S*)-3,4,-dimethyl-6-allyl-6-methyl-2-phenylperhydro-1,4-oxazepine-5,7-dione (**20** Table 21 p. 112) as the product nOe spectra were consistent with the 2*S*, 3*R*, 6*S*-configuration (Figure 83 p.109)

5c. ***Preparation of (2S,3R,6R)-3,4,-Dimethyl-6-benzyl-6-methyl-2-phenylperhydro-1,4-oxazepine-5,7-dione.***

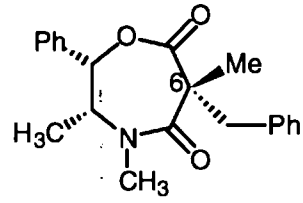

19

(Scale: 0.9 mmol of **15**)

Product **19** as a pale yellow crystalline solid 80%.

Mp 99-101 °C (from acetone); $[\alpha]_D$ +4 ° (c 0.1, DCM); (Found: C, 74.93; H, 6.92; N, 4.16. $C_{21}H_{24}NO_3$ requires C, 74.75; H, 6.87; N, 4.15 %); υ_{max}(film)/cm^{-1} 1733 (lactone C=O), 1631 (lactam C=O); δ_H (200 MHz; $CDCl_3$; Me_4Si) 0.44 (3 H, d, *J* 7.5, C(3)-CH_3), 1.77 (3 H, s, C(6)-CH_3), 2.84 (3 H, s, N(4)-CH_3), 2.99 (1 H, br, C(3)-*H*), 3.20 (1 H, d, *J* 10.0, C(6)-C$H_{(2)}$), 3.14-3.243 (1 H, br, C(3)-*H*), 3.66 (1 H, d, *J* 10.0, C(6)-C$H_{(2)}$), 5.60 (1 H, s,

C(2)-*H*), 7.09-7.35 (10 H, m, -C_6H_5 x 2); δ_C (300 MHz; $CDCl_3$; Me_4Si) 10.77 (s) (3-CH_3), 27.08 (s)(6-CH_3), 36.77 (s) (N-CH_3), 46.72 (s) (3-*C*); 59.59 (s) (6-CH_2), 63.17 (s) (6-*C*), 80.54 (s) (2-*C*), 125,73 (2 x s) (Ph), 126.88 (s) (Ph), 127.83 (2 x s) (Ph), 128.63 (s) (Ph), 128.73 (2 x s) (Ph), 130.66 (2 x s) (Ph), 137.17 (s) (Ph), 137.40 (s) (Ph), 170.65 (s) (C= O), 170.69 (s) (C= O),*m/z* (CI (NH_3)) 338.1754 ($(M + H)^+$ $C_{21}H_{25}NO_3$ requires 338.1756), (de 9:1), (TLC Rf. 0.61 (EtOAc: cyclohexane 3:1) (I_2)).

IR, NMR and mass spectra were consistent with (2*S*, 3*R*, 6*R*)-3,4,-dimethyl-6-benzyl-6-methyl-2-phenylperhydro-1,4-oxazepine-5,7-dione (**19** Table 21 p. 112) as the product. nOe spectra were consistent with the 2*S*, 3*R*, 6*R* -configuration (Figure 80 p.106).

5d. ***Preparation of (2S,3R,6R)-3,4,-Dimethyl-6-allyl-6 methyl-2-phenylperhydro 1,4 oxazepine-5,7-dione.***

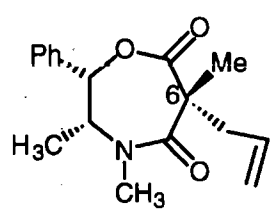

21

(Scale: 0.9 mmol of **16**)

Product **21** as a white crystalline solid 80%.

(Found: C, 70.77; H, 7.56; N, 4.94. $C_{17}H_{21}NO_3$ requires C, 71.06; H, 7.37; N, 4.87 %); υ_{max}(film)/cm^{-1} 1736 (lactone C=O), 1631 (lactam C=O); δ_H (200 MHz; $CDCl_3$; Me_4Si) 1.18 (3 H, d, *J* 7.5, C(3)-CH_3), 1.66 (3 H, s, C(6)-CH_3), 2.70 (2 H, dd, *J* 7.5, C(6)-CH_2), 2.98 (3 H, s, N(4)-CH_3), 3.45 (1 H, d, *J* 7.5, C(3)-*H*), 4.95-5.20 (2 H, dd, *J* 10.0 and 15.0, allyl -CH_2), 5.73 (2 H, s overlying dd, *J* 7.5, C(2)-*H*, allyl-*CH*), 7.33-7.46 (5 H, m, -C_6H_5), δ_C (300 MHz; $CDCl_3$; Me_4Si) 12.20 (s) (3-CH_3), 25.91(s) (6-CH_3), 36.74 (s) (6-CH_2), 45.50 (s) (N-

CH_3), 52.33 (s) (3-C), 63.73 (s) (6-C), 79.90 (s) (2-C), 118.93 (s) (alkene), 125.86 (s) (Ph), 128.70 (2 x s) (Ph),128.76 (2 x s) (Ph), 137.02 (s) (Ph), 148.54 (s) (alkene),170.98 (s) (C=0), 172.60 (s) (C=0), *m/z* (CI (NH_3)) 288.1605 ((M + H)$^+$ $C_{17}H_{22}NO_3$ requires 288.1600) (TLC Rf. 0.61 (EtOAc: cyclohexane 3:1) (I_2)).

IR, NMR and mass spectra were consistent with (2*S*, 3*R*, 6*R*)-3,4,-dimethyl-6-allyl-6-methyl-2-phenylperhydro-1,4-oxazepine-5,7-dione (**21** Table 21 p. 112) as the product, nOe spectra were consistent with the 2*S*, 3*R*, 6*R*-configuration (Figure 83 p.109). X-ray crystallographic studies (Appendix) were also consistent with this configuration.

5e. ***Preparation of (2S,3R,6R)-3,4,-Dimethyl-6-methyl-6-piperonyl-2-phenylperhydro-1,4-oxazepine-5,7-dione.***

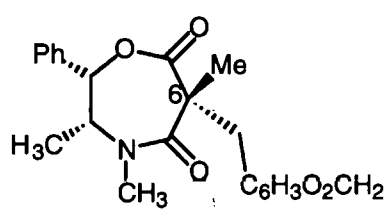

22

(Scale: 0.2 mmol of **16**)

Product **22** as a colourless oil 80%.

υ_{max}(film)/cm^{-1} 1730 (lactone C=O), 1628 (lactam C=O); δ_H (200 MHz; $CDCl_3$; Me_4Si) 0.60 (3 H, d, *J* 7.5, C(3)-C*H*$_3$), 1.80 (3 H, s, C(6)-C*H*$_3$), 2.90 (3 H, s, N(4)-C*H*$_3$), 3.17 (1 H, d, *J* 12.5, C(6)-C*H*$_{(2)}$), 3.25-3.38 (1 H, q, *J* 7.5, C(3)-*H*), 3.62 (1 H, d, *J* 12.5, C(6)-C*H*$_{(2)}$), 5.63 (1 H, s, C(2)-*H*), 5.89 (2 H, s, -O-C*H*$_2$-O-), 6.65 (1 H, d, *J* 7.5, -O-C-C*H*-CH-), 6.80 (1 H, d, *J* 7.5, -O-C-CH-C*H*-), 6.84 (1 H, s, -O-C-C*H*-C-), 7.40 (5 H, m, -C$_6$*H*$_5$).

(TLC Rf. 0.56 (EtOAc:cyclohexane 3:1 I_2)).

The physical data are consistent with (2*S*, 3*R*, 6*R*)-3,4,-dimethyl-6-methyl-6-piperonyl-2-phenylperhydro-1,4-oxazepine-5,7-dione (**22** Table 21 p. 112) as the product.

6a. ***Cleavage of (2S,3R,6R)-3,4,-Dimethyl-6-benzyl-6-methyl-2-phenylperhydro-1,4-oxazepine-5,7-dione (19) using sodium and liquid ammonia to give N-Methyl-N-[(2R)-1-phenylpropyl]-(2R)-2-carboxy-2-methyl-3-phenylpropanamide (24)***

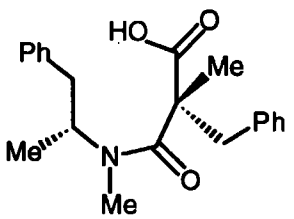

24

(Scale: 0.45 mmol of **19**)

(2*S*, 3*R*, 6*R*) -3,4,-Dimethyl-6-benzyl-6-methyl-2-phenylperhydro-1,4-oxazepine-5,7-dione (**19**) (0.15 g, 0.45 mmol.) was dissolved in dry tetrahydrofuran (10 cm^3), and added to a sodium (0.1 g) in liquid ammonia (20 cm^3) solution at -30 °C with stirring. The reaction mixture was left for half an hour, then ammonium chloride (20ml of 1% w/v) was added and the mixture allowed to warm to room temperature overnight. The residue was acidified with hydrochloric acid (6 M) and extracted with dichloromethane (3x20 cm^3), dried over anhydrous sodium sulphate, and then evaporated under reduced pressure, to give **24** as a white crystalline solid 84%. The product was recrystallised from dichloromethane.

$[\alpha]_D$ 0.94), 2 0.1, DCM);υ_{max}(film)/cm^{-1} 3200-2400 (acid O-H), 1724 (lactone C=O), 1611 (lactam C=O); δ_H (200 MHz; $CDCl_3$; Me_4Si) 0.90 (3 H, d, *J* 7.5, C(3)-CH_3), 1.13 (3 H, s, C(6)-CH_3), 2.53-3.01 (7 H, s overlying m, N(4)-CH_3, C(2)-CH_2, C(6)-CH_2), 3.17 (1 H, m, C(3)-*H*), 7.18 (10 H, m, -C_6H_5 x2), *m/z* (CI (NH_3)) 340.1913 ($(M+H)^+$ $C_{21}H_{26}NO_3$ requires 340.1913), (CI NH_4^+) 296.2018 ($(M-CO_2)^-$ $C_{20}H_{26}NO$ requires 296.2014). (TLC Rf. 0.55 (DCM:MeOH 19:1) (I_2)).

The physical data are consistent with the cleaved product, *N*-methyl-*N*-[(2*R*)-1-phenylpropyl]-(2*R*)-2-carboxy-2-methyl-3-phenylpropanamide (**24** Fig. 88).

The above procedure (6a) was used in the following reactions.

6b. ***Cleavage of (2S,3R,6S)-3,4,-Dimethyl-6-benzyl-6-methyl-2-phenylperhydro-1,4-oxazepine-5,7-dione (18) using sodium and liquid ammonia, to give N-Methyl-N-[(2R)-1-phenylpropyl]-(2S)-2-carboxy-2-methyl-3-phenylpropanamide (25)***

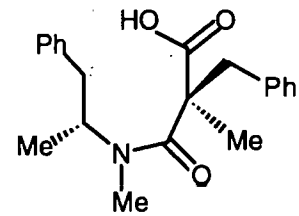

25

(Scale: 0.45 mmol of **18**)

Product **25** as a white crystalline solid 75%.

$[\alpha]_D$ -13.6 ° (c 0.1, DCM);υ_{max}(film)/cm^{-1} 3600-2400 (acid O-H), 1728 (lactone C=O), 1615 (lactam C=O); δ_H (200 MHz; $CDCl_3$; Me_4Si) 1.12 (3 H, d, *J* 7.5, C(3)-CH_3), 1.30 (3 H, s, C(6)-CH_3), 2.70-2.94 (7 H, s overlying m, N(4)-CH_3, C(2)-CH_2, C(6)-CH_2), 3.19 (1 H, m, C(3)-*H*), 7.12 (10 H, m, -C_6H_5 x2), *m/z* (CI (NH_3)) 340.1909 ($(M+H)^+$ $C_{21}H_{26}NO_3$ requires 340.1913),

The physical data are consistent with the cleaved product, *N*-methyl-*N*-[(2*R*)-1-phenylpropyl]-(2*S*)-2-carboxy-2-methyl-3-phenylpropanamide (**25** Fig. 88)).

6c. Cleavage of (2S,3R,6R)-3,4,-Dimethyl-6-allyl-6-methyl-2-phenylperhydro-1,4-oxazepine-5,7-dione (21) using sodium and liquid ammonia to give N-Methyl-N-[(2R)-1-phenylpropyl]-(2R)-2-carboxy-2-methylpent-4-enamide (26)

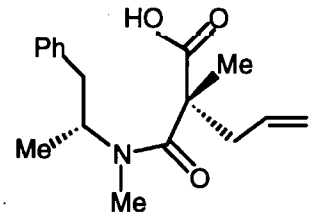

26

(Scale: 0.37 mmol of **21**)

Product **26** as a white crystalline solid 70%.

υ_{max}(film)/cm^{-1} 3400-2400 (acid O-H), 1725 (lactone C=O), 1620 (lactam C=O); δ_H (200 MHz; $CDCl_3$; Me_4Si) 0.90 (3 H, d, *J* 7.5, C(3)-CH_3), 1.27 (3 H, s, C(6)-CH_3), 2.58-2.88 (7 H, s overlying m, N(4)-CH_3, C(2)-CH_2, C(6)-CH_2), 3.71 (1 H, m, C(3)-*H*), 5.01-5.18 (2 H, m, CH=CH_2), 5.59-5.76 (1 H, m, C*H*=CH_2), 7.17-7.43 (5 H, m, -C_6H_5),

m/z (CI (NH_3)) 290.1761 ($(M+H)^+$ $C_{17}H_{23}NO_3$ requires 290.1756),

The physical data are consistent with the expected product, *N*-methyl-*N*-[(2*R*)-1-phenylpropyl]-(2*R*)-2-carboxy-2-methylpent-4-enamide (**26** Fig. 88))

7. Schmidt reaction on N-Methyl-N-[(2R)-1-phenylpropyl]-(2R)-2-carboxy-2-methyl-3-phenylpropanamide (24) and N-Methyl-N-[(2R)-1-phenylpropyl]-(2S)-2-carboxy-2-methyl-3-phenylpropanamide (25) to give N-Methyl-N-[(2R)-1-phenylpropyl]-(2R)-2-amino-2-methyl-3-phenylpropanamide (27) and N-Methyl-N-[(2R)-1-phenylpropyl]-(2S)-2-amino-2-methyl-3-phenylpropanamide (28)

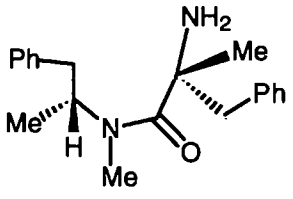

27

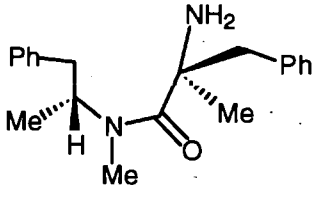

28

Polyphosphoric acid (0.59 g, 3.54 mmol) was mixed with each of the cleaved oxazepines (**24** or **25**) (0.06 g, 0.177 mmol) at 0 °C, then sodium azide (0.035 g, 0.53 mmol) was added in small portions to each whilst stirring the reaction mixtures. The reaction mixtures were allowed to warm to room temperature with

occasional stirring and left for eight hours. Crushed ice (10 g) was then added to each and the mixtures allowed to warm to room temperature. Ice cold sodium hydroxide (~4 cm^3, 50 % w/v) was added until the solutions were alkaline, before extraction of the solutions with dichloromethane (4x5 cm^3). The combined extracts of each were dried (Na_2SO_4 anhydrous) then evaporated under reduced pressure to give the products as white solids 85% and 68% respectively, *N*-methyl-*N*-[(2*R*)-1-phenylpropyl]-(2*R*)-2-amino-2-methyl-3-phenylpropanamide (**27** Fig. 91 p.125) and *N*-methyl-*N*-[(2*R*)-1-phenylpropyl]-(2*S*)-2-amino-2-methyl-3-phenylpropanamide (**28** Fig. 91 p.125)).

compound **27**; $[\alpha]_D$ -16 ° (c 0.1, DCM);

27; υ_{max}(film)/cm^{-1} 3400 (medium), 3300 (medium),1619 (amide C=O); δ_H (200 MHz; $CDCl_3$; Me_4Si) 1.15 (3 H, d, *J* 2.5, $N(CH_3)CH\text{-}CH_3$), 1.28 (3H, s, $NH_2\text{-}CH\text{-}CH_3$), 2.70-2.93 (6H, s overlying m, 6H, $N\text{-}CH_3$, $Ph\text{-}CH_2$, $N\text{-}CH\text{-}CH_3$), 3.20-3.52 (2 H, dd, *J* 2.5 and 12.5, $NH_2\text{-}C(CH_3)\text{-}CH_2$), 7.12-7.34 (5 H, m, $-C_6H_5$), 8.47 (2 H, br, $-NH_2$), (removed when shaken with D_2O); *m/z* (CI (NH_3)) 311.2112 ($(M+H)^+$ $C_{20}H_{26}N_2O$ requires 311.2123), (TLC Rf. 0.66 (DCM:MeOH 19:1) (I_2)).

28 υ_{max}(film)/cm^{-1} 3400 (medium), 3300 (medium),1634 (amide C=O); δ_H (200 MHz; $CDCl_3$; Me_4Si) 0.85 (3 H, d, *J* 2.5, $N(CH_3)CH\text{-}CH_3$), 1.10 (3H, s, $NH_2\text{-}CH\text{-}CH_3$), 2.58-2.98 (6H, s overlying m, 6H, $N\text{-}CH_3$, $Ph\text{-}CH_2$, $N\text{-}CH\text{-}CH_3$), 2.74-3.01 (2 H, dd, *J* 2.5 and 12.5, $NH_2\text{-}C(CH_3)\text{-}CH_2$), 7.11-7.35 (5 H, m, $-C_6H_5$); *m/z* (CI (NH_3)) 311.2131 ($(M+H)^+$ $C_{20}H_{26}N_2O$ requires 311.2123), *m/z* (CI (NH_3)) 337.1916 ($(M+H)^+$ $C_{21}H_{24}N_2O2$ requires 337.1916).

The physical data are consistent with *N*-methyl-*N*-[(2*R*)-1-phenylpropyl]-(2*R*)-2-amino-2-methyl-3-phenylpropanamide (**27**) and *N*-methyl-*N*-[(2*R*)-1-phenylpropyl]-(2*S*)-2-amino-2-methyl-3-phenylpropanamide (**28**) as the products.

8. Hydrolysis of N-Methyl-N-[(2R)-1-phenylpropyl]-(2R)-2-amino-2-methyl-3-phenylpropanamide (27) and N-Methyl-N-[(2R)-1-phenylpropyl]-(2S)-2-amino-2-methyl-3-phenylpropanamide (28) to give the α-Amino acids (30 and 31) and 1-Phenyl-2-(methylamino)propane (29)

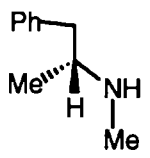

29

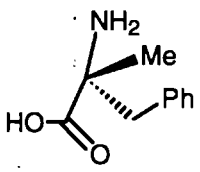

30

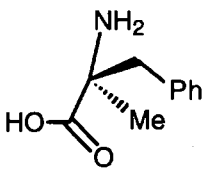

31

Products **27** and **28** from reaction **7** (20 mg, 0.07 mmol), were each refluxed in hydrochloric acid (10 cm^3, 50 %), for two days. The reaction mixture in each case was then evaporated under reduced pressure, and left in a desiccator (with potassium hydroxide pellets) for two hours. Each residue was taken up in water and made alkaline (sodium hydroxide solution 1 % w/v), then extracted with dichloromethane (3x10 cm^3). The combined extracts in each case were evaporated under reduced pressure to yield the amine, *N*-methyl,1-benzylethylamine (**29** Fig. 92 p. 125), in both cases, as a viscous oil.

29 (organic layer)υ_{max}(film)/cm^{-1} 3500-3300; δ_H (200 MHz; $CDCl_3$; Me_4Si) 0.94 (3 H, d, *J* 7.5, CH-C*H*$_3$), 2.60 (3 H, s, N-C*H*$_3$), 2.73-3.06 (3 H, m, *J* 9, 7 and 5.5, NH-C*H*, Ph-C*H*$_2$), 3.81 (1 H, br, N*H*, removed with D_2O shake), 7.15-7.39 (5 H, m, -C$_6$*H*$_5$); *m/z* (CI (NH_3)) 150.1283 ($(M+H)^+$ $C_{10}H_{15}N$ requires 150.1283).

The physical data are consistent with *N*-methyl,1-benzylethylamine(**29** Fig. 92 p. 125)[82]

Beilstein Registry Number 3081879

30 and 31 (aqueous layer)

In each case the aqueous layer was evaporated to yield the sodium salt of the substituted amino acid, 2-methyl-3-phenylalanine.

υ_{max}(film)/cm^{-1} 3500 (sharp), 3400 (sharp), 1639 (antisymmetric),1403 (symmetric); δ_H (200 MHz; D_2O; Me_4Si) 1.45 (3 H, s, NH_2-C-C*H*$_3$), 2.95 (1 H, d, *J* 17.5, Ph-C*H*-H), 3.18 (1 H, d, *J* 17.5, Ph-C*H*-H), 7.19-7.42 (5 H, m, -C$_6$*H*$_5$).

The physical data are consistent with the 2-methyl-3-phenylalanine sodium salts (**30** and **31** Fig. 92 p. 125).[83]

Beilstein Registry Number	466990	(*S*)-(+)-2-Methyl-3-phenylalanine
Beilstein Registry Number	5254151	(*R*)-(+)-2-Methyl-3-phenylalanine

9. *Preparation of 2-Methyl-3-phenylalanine methyl ester*

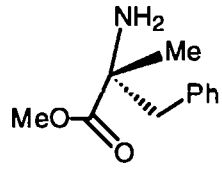

Compound **30** from reaction **8** (20 mg, 0.11 mmol), was dissolved in dry methanol (10 cm^3) and thionyl chloride (1 cm^3), was added dropwise. The solution was stirred overnight at room temperature. The reaction mixture was made alkaline, using ice-cold sodium hydroxide solution (10 % w/v), and extracted with dichloromethane (3x20 cm^3). The organic extracts were washed with water (3x10 cm^3), dried over anhydrous sodium sulphate and evaporated under reduced pressure to yield the methyl ester of 2-methyl-3-phenylalanine. $[\alpha]_D$ +5 ° (c 0.1, DCM)ν_{max}(film)/cm^{-1} 3100-3500 (broad), 1738, δ_H (200 MHz; $CDCl_3$; Me_4Si) 1.45 (3 H, s, NH_2-C-CH_3), 1.52-1.75 (2 H, br, NH_2, removed with D_2O shake), 3.19 (1 H, d, *J* 12.5, Ph-C*H*-H), 3.53 (1 H, d, *J* 12.5, Ph-C*H*-H), 3.74 (3 H, s, CH_3-O), 7.10-7.30 (5 H, m, -C_6H_5); *m/z* (CI (NH_3)) 194.1186 ($(M+H)^+$ $C_{11}H_{15}N O_2$ requires 194.1181).

The physical data are consistent with 2-methyl-3-phenylalanine methyl ester. See discussion of comparative results with the racemate on p. 128 and Table 28.

10. ***Preparation of (S)-Methyl N-malonylprolinol***

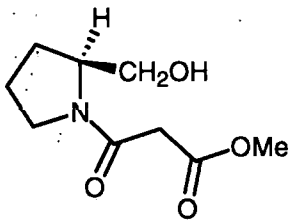

32

(*S*)-(+)-Prolinol (0.75 g, 7.43 mmol) with dimethyl malonate (1.45 g: 10.89 mmol) in dry methanol (25 cm^3) was refluxed for 2 days. Further methanol (15 cm^3) was added and reflux continued for another 1 day. Reaction progress was monitored by TLC [(3:1) dichloromethane: ethyl acetate (I_2)]. The methanol was evaporated and the residues taken up in chloroform (40 cm^3), washed with 2 molar HCl (2x20 cm^3), and brine (20 cm^3), and the organic layer dried over anhydrous sodium sulphate. Column chromatography through silica gel and dichloromethane as eluant yielded (*S*)-methyl *N*-malonylprolinol as a colourless oil 93% (730 mg, 6.93 mmol).

υ_{max}(film)/cm^{-1} 1736 (ester C=O), 1628 (amide C=O), δ_H (200 MHz; $CDCl_3$; Me_4Si) 1.82-2.10 (4 H, m, C(3)-H_2, C(4)H_2), 3.50 (2 H, s, C2'H_2), 3.55-3.82 (4 H, m, C(5)H_2, CH_2OH), 3.82 (3 H, s, O-CH_3), 4.20-4.32 (1 H, br, -C(2)*H*).

The physical data are consistent with Methyl *N*-malonylprolinol (**32** Fig. 96 p. 133).

11. ***Preparation of (S)-N-Malonylprolinol***

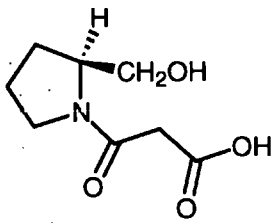

33

The crude methyl (*S*)-*N*-malonylprolinol **32** (0.5 g; 2.49mmol) was cooled to 0 °C, and a solution of lithium hydroxide (2.74 g; 65.3 mmol) in water (20 cm^3) was added dropwise with stirring, maintaining the temperature below 5 °C. After stirring overnight at room temperature, the bulk of the methanol was removed under reduced pressure at <30 °C. The residue was cooled to below 5 °C, and acidified with conc. hydrochloric acid (16 cm^3), the solution was then saturated with sodium chloride and extracted with dichloromethane (1x75 cm^3, 3 x 50 cm^3), and the extracts dried over anhydrous sodium sulphate and evaporated under reduced pressure to give a clear colourless viscous oil 80% (0.41g; 1.99 mmol). υ_{max}(film)/cm^{-1} 1727 (acid C=O), 1614 (amide C=O), δ_H (200 MHz; $CDCl_3$; Me_4Si) 1.81-2.13 (4 H, m, 4H, C(3)-H_2, C(4)H_2), 3.40 (2 H, s, C2'H_2), 3.44-3.80 (4 H, m, C(5)H_2, CH_2OH), 4.14-4.29 (1 H, br, -C(2)*H*).

The physical data are consistent with *N*-malonylprolinol (**33** Fig. 96 p.133).

12. *Preparation of the Pyrrolidinooxazepine 34*

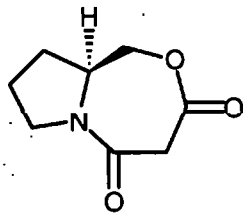

34

The crude *N*-malonylprolinol (**33**) (6.10 g; 24.3 mmol) was dissolved in dry acetonitrile (150 cm^3), transferred to a three necked flask, which was then filled with nitrogen, and the solution stirred. Solutions of cyanuric chloride (5.7 g; 30.4 mmol) in dry acetonitrile (75 cm^3) and pyridine (9.8 cm^3; 121.5 mmol) in dry acetonitrile (75 cm^3), were added simultaneously, dropwise over one hour. After five hours the solution was filtered, and the solid washed with dry acetonitrile (2x25 cm^3). The filtrates were combined and evaporated under reduced pressure (acetonitrile recovered). Flash chromatography over silica gel (70 g) was used to separate the product, using successively dichloromethane:toluene (6:1, 1x100 cm^3), dichloromethane (2x100 cm^3), dichloromethane:ether (4:1, 4x100 cm^3) as solvent. Fractions 4-7 were combined and evaporated under reduced pressure to give pyrrolidinooxazepine as a white crystalline solid (**34** Fig. 97 p. 134) (1.53g; 25%). υ_{max}(film)/cm^{-1}1742 (lactone C=O), 1630 (lactam C=O), δ_H (200 MHz; $CDCl_3$; Me_4Si) 1.49-2.08 (4 H, m, -C(8)-CH_2, -C(9)-CH_2), 3.40-3.67 (2 H, m, -C(10)-CH_2), 3.42-3.67 (1 H, d, *J* 9.5, -C(6)-*H*), 3.78-3.90 (1 H, m, -C(3)-*H*), 3.90-4.00 (1 H, d, *J* 9.5, -C(6)-*H*), 4.37-4.46 (2 H, m, -C(2)-CH_2); δ_C (300 MHz; $CDCl_3$; Me_4Si) 21..31(s) (*C*8), 29.49 (s)

(C9), 43.67 (s) (C10), 46.95(s) (C3), 59.46 (s) (C6), 68.06 (s) (C2), 160.47 (s) (C=O), 167.12 (s) (C=O); *m/z* (CI (NH_3)) 169.0738 ($(M+H)^+$ $C_8H_{11}NO_3$ requires 169.0739).

IR, NMR and mass spectra analysis were consistent with the product pyrrolidinooxazepine. COSY and nOe analysis were consistent with the assigned conformation and configuration of (3*S*)-pyrrolidinooxazepine (Figure 98 p.138).

13. ***Preparation of the 6-allyl substituted Pyrrolidinooxazepine***

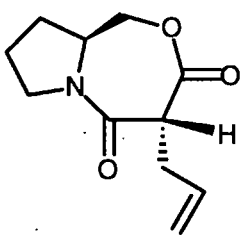

35

(3*S*)-Pyrrolidinooxazepine **34** (20 mg; 0.13 mmol) was dissolved in dry THF (20 cm^3), at room temperature and under nitrogen. A solution of potassium *tert*-butoxide, (0.016 g; 0.14 mmol), in dry THF (5 cm^3) was added dropwise with stirring, and the solution was stirred at room temperature for 1 hour. Allyl bromide (0.08 g; 0.65 mmol), was then added dropwise, the solution was stirred at room temperature for a further 24 hours, before the solution was evaporated under reduced pressure. The residue was taken up into ethyl acetate (25 cm^3), washed with water (3 x 10 cm^3), dried over anhydrous sodium sulphate, and evaporated under reduced pressure, to give the product as a white solid (**35** Fig. 101 p. 141) (15 mg; 54%).

υ_{max}(film)/cm^{-1} 1734 (lactone C=O), 1629cm (lactam C=O), δ_H (200 MHz; $CDCl_3$; Me_4Si) 1.50-2.09 (4 H, m, -C(8)-C*H*$_2$, -C(9)-C*H*$_2$), 2.88-3.02 (2 H, m, C(6)-C*H*$_2$), 3.44-3.63 (2 H, m, -C(10)-C*H*$_2$), 3.64-3.73 (1 H, m, -C(3)-*H*), 4.16-4.26 (1 H, dd, -C(6)-*H*), 4.63-4.70 (2 H, m, -C(2)-C*H*$_2$), 5.24-5.38 (2 H, dd, alkenic C*H*$_2$), 5.86-5.97 (1 H, m, alkenic C*H*) *m/z* (CI (NH_3)) 210.1126 ((M+H)$^+$ $C_{11}H_{15}N\,O_3$ requires 210.1130).

IR, NMR, and mass spectra were consistent with the compound **35**

14. ***Preparation of N-* and *O-Succinyl-1R, 2S-ephedrine***

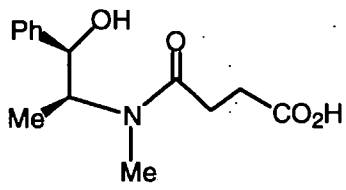

36

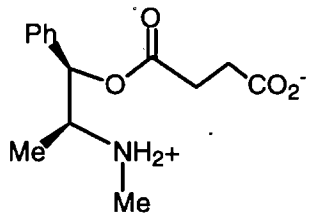

37

1*R*, 2*S*- Ephedrine (4.07 g; 24.7 mmol) in dry acetonitrile (40 cm^3), was stirred whilst a solution of freshly recrystallised succinic anhydride (2.5 g; 25 mmol): in dry acetonitrile (20 cm^3) was added dropwise. After 48h TLC (1:1 $CHCl_3$: CH_3CN) showed product formation. The solution was evaporated under reduced pressure to give a clear colourless oil, (5.33 g; >80 %). HPLC of the crude *N*-succinyl-1*R*, 2*S*-ephedrine using a silica column and acetonitrile/water/acetic acid (75/25/0,5) as the eluant, showed that there were two components present (2:1). This product is a mixture of the *N*- and *O*-succinyl-*1R*-*2S*-ephedrine compounds and HPLC gave single product fractions.

37 (Fraction 1. (30%))

υ_{max}(film)/cm^{-1} 2800 - 2200, 1737, 1610 and 1410; δ_H (200 MHz; $CDCl_3$; Me_4Si) 1.07 (3 H, d,*J* 7.5, -C-C*H*$_3$), 2.47 (2 H, d,*J* 5, -C-C*H*$_2$), 2.55 (2 H, d, *J* 5, -C-C*H*$_2$), 2.71 (3 H, s, -N-C*H*$_3$), 4.79-4.97 (1 H, dq, *J* 7.5 and 5, -N-C*H*), 5.85 (1 H, d, *J* 5, -C_6H_5-C*H*), 7.00-7.34 (5 H, br, -C$_6$*H*$_5$); *m/z* (CI NH_4^+) 266.1386 ((M+H)$^+$ $C_{14}H_{20}NO_3$ requires 266.1392), *m/z* (CI (NH_3)) 248.1281 ((M-H_2O+H)$^+$ $C_{14}H_{18}NO_3$ requires 248.1287).

The physical data are consistent with *O*-succinyl-1*R*, 2*S*-ephedrine (**37** Fig. 107 p. 147).

36 (Fraction 2. 60%)

υ_{max}(film)/cm^{-1} 3400-2400, 1721, 1616 and 1410; δ_H (200 MHz; $CDCl_3$; Me_4Si) 1.17 (3 H, d, *J* 7.5, -C-C*H*$_3$), 2.45 (2 H, d, *J* 5, -C-C*H*$_2$), 2.53 (2 H, d, *J* 5, -C-C*H*$_2$), 2.78 (3 H, s, -N-C*H*$_3$), 4.48-4.64 (1 H, dq, *J* 7.5 and 5, -N-C*H*), 4.77 (1 H, d, *J* 5, -C_6H_5-C*H*), 7.15-7.33 (5 H, br, -C$_6$*H*$_5$); *m/z* (CI (NH_3)) 266.1388 ((M+H)$^+$ $C_{14}H_{20}NO_3$ requires 266.1392), *m/z* (CI NH_4^+) 248.1281 ((M-H_2O+H)$^+$ $C_{14}H_{18}NO_3$ requires 248.1287).

The physical data are consistent with *N*-succinyl-1*R*, 2*S*-ephedrine (**36** Fig. 109 p. 151).

15. ***Preparation of N- and O-Glutaryl-1R,2S-ephedrine (38 and 39)***

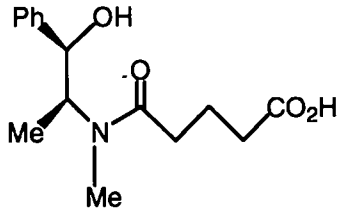

38

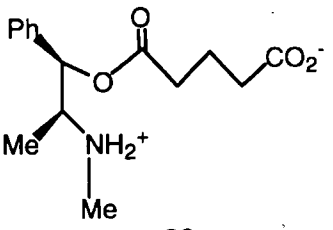

39

To a stirred solution of 1*R*, 2*S*-ephedrine (3.0 g; 18.2 mmol) in dry acetonitrile (10 cm^3), at room temperature, was added dropwise a solution of glutaric anhydride (2,07 g; 18.2 mmol) in dry acetonitrile (10 cm^3). After 48 h, TLC (DCM:acetonitrile, 1:1) showed essentially a single product.The solution was evaporated under reduced pressure, to give a clear colourless viscous oil (5.0 g; 17.9 mmol) of crude product. Column chromatography was used to separate a purer product. SiO_2 (50 g), DCM:acetonitrile (1:2). Single product fractions were combined and evaporated under reduced pressure to give a viscous product (1.126 g; 4.04 mmol). HPLC of the crude *N*-glutaryl-1*R*, 2*S*-ephedrine using a silica column and acetonitrile/water/acetic acid (75/25/0,5) as the eluant, showed that there were again two components present (2:1).

39 (Fraction 1. 30%)υ_{max}(film)/cm^{-1} 2800 - 2300, 1735, 1607 and 1411; δ_H (200 MHz; $CDCl_3$; Me_4Si) 1.20 (3 H, d,*J* 7.5, -C-C*H*$_3$), 2.17 (2 H, m, -C-C*H*$_2$), 2.45-2.59 (4 H, m, -C-C*H*$_{2(x2)}$), 2.82 (3 H, s, -N-C*H*$_3$), 4.82-5.00 (1 H, dq, *J* 7.5 and 5.0, -N-C*H*), 5.81 (1 H, d, *J* 7.5, -C_6H_5-C*H*), 7.20-7.37 (5 H, br, -C_6H_5); *m/z* (CI (NH_3)) 280 $(M+H)^+$major peak), *m/z* (CI NH_4^+) 262 $(M-H_2O+H)^+$major peak).

The physical data are consistent with the *O*-glutaryl-1*R* , 2*S*-ephedrine (**39** Fig. 111 p.150)

38 (Fraction 2. 60%)υ_{max}(film)/cm^{-1} 3600-2400, 1712 and 1612; δ_H (200 MHz; $CDCl_3$; Me_4Si) 1.18 (3 H, d, *J* 7.5, -C-C*H*$_3$), 1.84 (2 H, m, -C-C*H*$_2$), 2.22-2.35 (4 H, m, -C-C*H*$_{2(x2)}$), 2.71 (3 H, s, -N-C*H*$_3$), 4.50-4.62 (1 H, dq, *J* 7.5 and 5.0, -N-C*H*), 4.80 (1 H, d,*J* 5,0, -C_6H_5-C*H*), 7.21-7.36 (5 H, br, -C_6H_5); *m/z* (CI (NH_3)) 280 $(M+H)^+$ major peak); (TLC Rf 0.36 (CH_2Cl_2:MeCN,1:2) (I_2)).

The physical data are consistent with *N*-glutaryl-1*R*, 2*S*-ephedrine (**38** Fig. 111 p. 150).

16. ***Preparation of N-Maleyl-1R,2S-ephedrine***

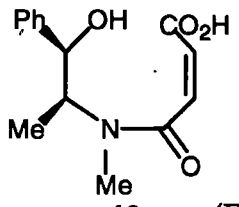

40 (Fig. 112 p. 151)

To a stirred solution of 1*R*, 2*S*-ephedrine (0.97 g; 5.88 mmol) in dry acetonitrile (15 cm^3), at room temperature, was added dropwise a solution of maleic anhydride (0.6 g; 6.12 mmol, mp 53 °C (ex chloroform) in dry acetonitrile (15 cm^3). After 72 h, TLC (DCM:acetonitrile, 1:1 (I_2)) showed essentially a single product. The solution was evaporated under reduced pressure, giving a yellow viscous oil, (1.3 g).

υ_{max}(film)/cm^{-1} 1716, 1604 and 703; δ_H (200 MHz; $CDCl_3$; Me_4Si) 1.06 (3 H, d, *J* 7.5, -C-C*H*$_3$), 2.88 (3 H, s, -N-C*H*$_3$), 4.55 (1 H, dq, *J* 12.5, 7.5 and 5.0, -N-C*H*), 4.86 (1 H, d, *J* 5.0, -C_6H_5-C*H*), 5.97-6.06 (1 H, d, *J* 12.5, alkenic C*H*), 6.43-6.50 (1 H, d, *J* 12.5, alkenic C*H*), 7.07-7.26 (H, br, -C_6H_5).

The physical data are consistent with the formation of *N*-Maleyl-1*R*, 2*S*-ephedrine.

17. ***Reaction of Amino alcohols with Dimethyl acetylenedicarboxylate (DMAD)***

17a. ***L-Valinol + DMAD***

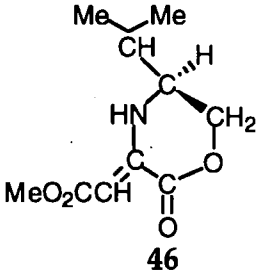

46

(Fig. 113 p. 153)

L-Valinol (0.11 g; 1.07 mmol) was dissolved in dry methanol (10 cm^3), at room temperature, and DMAD (0.13 cm^3; 1.07 mmol) was added dropwise, with stirring. After 2.5h, TLC (DCM (ceric sulphate) showed a single product, and the methanol was evaporated under reduced pressure. The product was passed though a column, (SiO_2, 5 g) with DCM as the eluant, to give the product as a colourless oil.

υ_{max}(film)/cm^{-1} 3308, 1749, 1666 and 1620; δ_H (200 MHz; $CDCl_3$; Me_4Si) 0.78 (6 H, dd, *J* 7.5 and 5.0, -CH-(CH_3)$_2$), 1.79-1.92 (1 H, dq, *J* 7.5 and 5.0, -C*H*-(CH_3)$_2$), 3.19-3.30 (1 H, m, -NH-C*H*), 3.67 (3 H, s, -O-CH_3), 4.23-4.49 (2 H, m, -O-CH_2), 5.54 (1 H, s, alkenic C*H*), 8.52 (1 H, s, -N*H*).

The physical data are consistent with the formation of compound **46** which was isolated as a colourless oil.

Procedure 17 was used with L-Leucinol with Phenylalaninol and with Ephedrine

17b. ***L- Leucinol + DMAD***

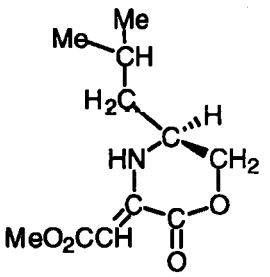

48 (Fig. 113 p. 153)

υ_{max}(film)/cm^{-1} 3308, 1749, 1666 and 1620; δ_H (200 MHz; $CDCl_3$; Me_4 Si) 0.99 (6 H, dd, *J* 7.5 and 5.0, -CH-(CH_3)$_2$) , 1.50-1.75 (2 H, m, CH_2 -CH-(CH_3)$_2$), 3.30-3.42 (1 H, m, -NH-C*H*), 3.69 (3 H, s, -O-CH_3), 4.28-4.50 (2 H, m, -O-CH_2), 5.60 (1 H, s, = C*H*), 8.52 (1 H, br -N*H*).

The physical data are consistent with the formation of compound **48** which was isolated as a colourless oil.

17c. ***L-Phenylalaninol + DMAD***

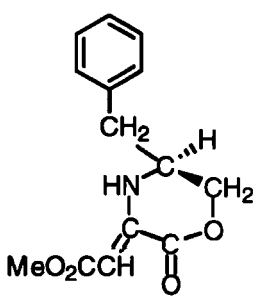

47 (Fig. 113 p. 153)

υ_{max}(film)/cm^{-1} 3308, 1745, 1666 and 1619; δ_H (200 MHz; $CDCl_3$; Me_4Si) 2.84 (2 H, d,*J* 7.5, -CH_2-C_6H_5), 3.65 (3 H, s, -O-CH_3), 3.72-3.98 (1 H, m, -NH-C*H*),

4.20-4.48 (2 H, m, -O-CH_2), 5.62 (1 H, s, = C*H*), 7.19-7.42 (5 H, m, CH_2-C_6H_5), 8.38 (1 H, br -N*H*).

The physical data are consistent with the formation of compound **47** which was isolated as a white solid.

17d. ***Ephedrine + DMAD (Morpholone)***

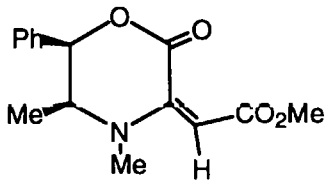

Morpholone (Fig.115 p. 155)

Mp. 117-119 °C (from acetone)υ_{max}(film)/cm^{-1} 1741, 1694 and 1603; δ_H (200 MHz; $CDCl_3$; Me_4Si) 1.04 (3 H, d,*J* 7.5, -CH-CH_3), 3.10 (3 H, s, -N-CH_3), 3.59 (1 H, dq, *J* 7.5 and 2.5, -N-C*H*), 3.64 (3 H, s, -O-CH_3), 5.63 (1 H, d, *J* 2.5, -C_6H_5-C*H*), 5.81 (1 H, s, = C*H*), 7.30-7.47 (5 H, m, -C_6H_5); *m/z* (CI (NH_3)) 276 $(M+H)^+$ major peak).

The physical data are consistent with the formation of the morpholone isolated as a white crystalline solid and recrystallised from acetone. [79,80]

18. ***Formation of N-protected L-Valinol by tosylation***

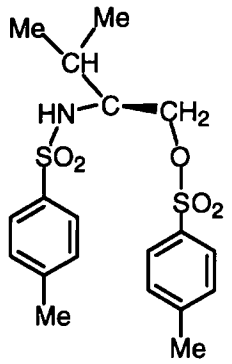

Ditosylated L-Valinol (Fig. 114 p. 154)

L-Valinol (0.1 g; 0.97 mmol) was dissolved in dry DCM (15 cm^3), pyridine (0.16 cm^3; 2 mmol) was added and the solution stirred at 0 °C. A solution of *p*-toluenesulphonyl chloride (0.123 g; 0.97 mmol) in dry DCM (5 cm^3), was added dropwise. After the addition was completed, the solution was allowed to warm to room temperature, and then evaporated under reduced pressure. After passage though a silica column using DCM:MeOH (4:1) as eluant, the major product (as shown by TLC) fractions were combined. ^1H NMR was consistent with product formation, but the product appeared to be both N and O tosylated. The peak for O-CH_2 was not split as it was in the L-valinol alone, but there was a peak at δ 3.58 which was probably the O-tosylated signal. There was no broad hydroxyl stretching frequency band on the IR spectrum for this compound.

δ_H (200 MHz; $CDCl_3$; Me_4Si) 0.78 (6H, d, -CH(CH_3)$_2$), 1.65-1.84 (1H, dq, -C*H*(CH_3)$_2$), 2.40 (6H, s, -Ph(CH_3)$_2$), 2.93-3.08 (1H, m, -C*H*-NH), 3.58 (2H, d, -CH_2-O-), 5.50 (1H, d, -NH), 7.28 (2H,*p*-substituted Ph), 7.81 (2H,*p*-substituted Ph).

19. *Formation of N-protected L-Leucinol by mesylation*

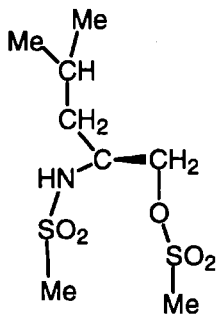

Dimesylated L-Leucinol (Fig. 114 p. 154)

To L-Leucinol (0.1 g; 0.86 mmol) dissolved in dry DCM (10 cm^3), pyridine (0.16 cm^3; 2 mmol) was added, and the solution stirred at 0 °C. Methane sulphonyl chloride (0.1 g; 0.86 mmol) was added dropwise. After the addition the solution was allowed to warm to room temperature, and was then evaporated under reduced pressure, passed though a silica column using DCM:MeOH (4:1) as eluant. The major product fractions were combined and evaporated to dryness. The residue was dissolved in HCl_{aq} (2 M) and this aqueous acid solution extracted with fresh DCM, the extract was then evaporated to dryness.^{1}H NMR was consistent with product formation, but again the peak for O-CH_2- was not split as in the original, and the compound was probably dimesylated.

δ_H (200 MHz; $CDCl_3$; Me_4Si) 1.00 (6H, d, -CH(CH_3)$_2$), 1.03-1.18 (1H, dq, -C*H*(CH_3)$_2$) 1.49-1.68 (2H, m, -CH_2-CH(CH_3)$_2$, 3.10 (6H,s, CH_3-SO_2-)$_2$), 3.43-3.55 (1H, m, -NH-C*H*-), 4.16-4.30 (2H, m, -CH_2-O-), 5.21 (1H, d, -NH-).

20. ***Preparation of N-Succinyl-L-cysteine ethyl ester***

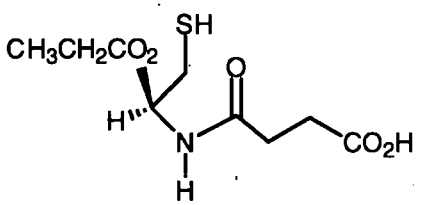

(Fig. 117 p. 156)

The same procedure was used as for the reaction between ephedrine and succinic anhydride (p.200). The product was passed through a silica gel column with DCM:MeOH (19:1) as eluant and isolated as a white crystalline solid. TLC on the column fractions indicated a single product.

υ_{max}(film)/cm^{-1} 1734 and 1650; δ_H (200 MHz; $CDCl_3$; Me_4Si) 1.28 (3 H, t, *J* 7.5, -CH_2-CH_3), 2.54-2.77 (4 H, m, (-C-CH_2) x2), 3.02 (2 H, m, SH-CH_2-), 4.18-4.29 (2 H, m, -O-CH_2-), 4.77-4.89 (1 H, m, -NH-C*H*-), 6.81 (1 H, d, *J* 7.5, -N*H*); *m/z* (CI (NH_3)) 250 $(M+H)^+$(major peak).

IR, ^{1}H NMR and mass spectra, were all consistent with *N*-succinyl-L-cysteine ethyl ester as the product.

21. ***Formation N-protected L-Cysteine ethyl ester using phthalic anhydride (42)***

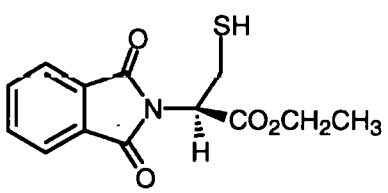

42

(Fig. 119 p. 159)

L-Cysteine ethyl ester (1.5 g; 10.07 mmol.) and phthalic anhydride (1.49 g; 10.07 mmol.) were dissolved in toluene (50 cm^3), triethylamine (0.1 cm^3) was added, the solution was refluxed for 2 h using a Dean and Stark apparatus, The solution was evaporated under reduced pressure and then triturated with 10 cm^3 of dilute hydrochloric acid (1%) to give the product as a white crysalline solid. υ_{max} (film)/cm^{-1} 1742 and 1717; δ_H (200 MHz; $CDCl_3$; Me_4Si) 1.09 (3 H, t, *J* 7.5, -CH_2-CH_3), 3.32 (2 H, m, -SH-CH_2), 4.12 (2 H, q, *J* 7.5, -O-CH_2), 4.85 (1 H, dd, -N-C*H*), 7.70 (2 H, m, ring), 7.81 (2 H, m, ring).

IR and ^1H NMR were consistent with the *N*-phthaloyl-L-cysteine ethyl ester as product.

22. ***Formation of N-(3.5-Dinitro benzoyl)-L-cysteine ethyl ester (43)***

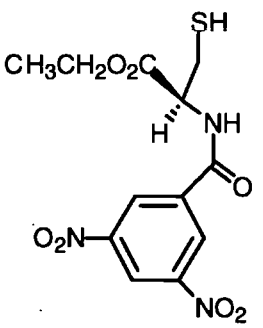

43

(Fig. 119 p. 159)

L-Cysteine ethyl ester (0.5 g; 4.13 mmol.) was dissolved in dry THF (15 cm^3) under nitrogen, and a solution of 3,5-dinitro benzoyl chloride (0.95 g; 4.13 mmol in dry THF 10 cm^3) was added dropwise, with stirring. The solution was stirred at room temperature for 4 h before being evaporated under reduced pressure to give the crude product as a yellow solid (>95%).

υ_{max}(film)/cm^{-1} 1739 (ester C=O), 1629 (2 ° amide C=O); δ_H (200 MHz; $CDCl_3$; Me_4Si) 1.30 (3 H, t, *J* 7.5, -CH_2-CH_3), 3.10-3.20 (2 H, m, -SH-CH_2), 4.25 (2 H, q, *J* 7.5 , -O-CH_2), 5.05 (1 H, m, -N-C*H*), 9.00-9.15 (3 H, m, ring); *m/z* (CI (NH_3)) 344 $(M+H)^+$.

IR and ^{1}H NMR are consistent with *N*-(3.5-dinitro benzoyl)-L-cysteine ethyl ester.

23. ***Preparation of N-Phthaloyl-S-(thioglutaryl mono ethyl ester)-L cysteine ethyl ester***

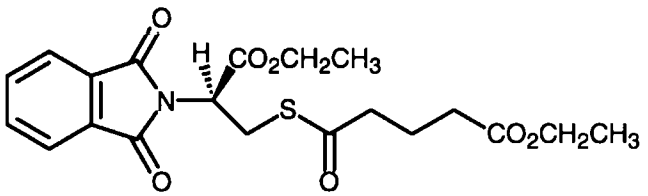

44 (Fig. 120 p. 159)

N-Phthaloyl-L-cysteine ethyl ester (0.78 g; 2.8 mmol), the mono ethyl ester of glutaric acid (0.9 g; 5.6 mmol), pyridine (1.0 cm^3; 12 mmol) and phenyl phosphorodichloroidate were dissolved in 1,2-dimethoxyethane (10 cm^3) in a nitrogen atmosphere at 0 °C. The solution was stirred and allowed to warm to room temperature with stirring for 16 h. After this time the reaction mixture was poured into aqueous sodium hydroxide (40 cm^3; 1M) at 0 °C and the product extracted from the aqueous solution using dichloromethane (3x20 cm^3). The combined extracts were dried (Na_2SO_4 anhyd) and evaporated under reduced pressure to give the product **44** as a yellow crystalline solid (85%).

υ_{max}(film)/cm^{-1} 1778, 1750 and 1721; δ_H (200 MHz; $CDCl_3$; Me_4Si) 1.25 (6 H, m, (-CH_2-CH_3)$_2$), 1.95 (2 H, m, -C-CH_2), 2.35 (2 H, m, -C-CH_2), 2.55 (2 H, m, -C-CH_2), 3.55 (1 H, dd, *J* 10.0 and 5.0, -SH-CH_2), 3.85 (2 H, dd, *J* 10.0 and 5.0, SH-CH_2), 4.10 (2 H, m, O-CH_2), 4.25 (2 H, m, O-CH_2), 5.05 (1 H, dd, *J* 5, N-C*H*), 7.70 (2 H, m, ring), 7.80 (2H, m, ring).

IR and ^{1}H NMR are consistent with N-phthaloyl-S-(thioglutaryl mono ethyl ester)-L-cysteine ethyl ester.

24. ***Attempted cyclisation of N-Maleyl-1R,2S-ephedrine***

N-Maleyl-1*R*,2*S*-ephedrine (1.3 g; 4.94 mmol) in dry acetonitrile (30 cm^3) was stirred, in an atmosphere of nitrogen. Solutions of cyanuric chloride (0.92 g; 5.0 mmol) in dry acetonitrile (20 cm^3) and pyridine (2.0 g; 25.2 mmol) in dry acetonitrile (20 cm^3),were added simultaneously and dropwise to the stirred maleic-ephedrine,. After 5h, the solution was filtered and evaporated under reduced pressure, to give a dark brown residue. TLC in various solvent systems showed as many as five components present, in the residue. The previously prepared oxazapine was run on the same plates, but there was no similarity between it and the residue. No further investigation was undertaken with this compound.

25. ***Preparation of the racemate of α–Methylphenylalalanine methyl ester***

a) ***Preparation of Dimethyl 2-methyl malonate***

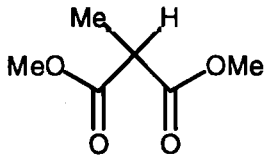

Beistein Registry Number 1763727 (Fig. 121 p. 160)

Sodium metal (0.5 g; 21.7 mmol) was added in small portions (CAUTION), to dry methanol (20 cm^3; 32.3 mmol) and cooled to room temperature. Dimethyl malonate (2.9 g; 22 mmol) was added dropwise and the mixture stirred at room temperature for 30 min. Methyl iodide (3.4 g; 24 mmol) was then added dropwise and left stirring over night. The reaction mixture was evaporated under reduced pressure and the residue taken up in DCM, dried over anhydrous sodium sulphate, and evaporated under reduced pressure to give a colourless viscous oil (84%).

δ_H (200 MHz; $CDCl_3$; Me_4Si) 1.28 (3 H, d, *J* 5, -CH-CH_3), 3.31-3.42 (1 H, q, *J* 5, -C*H*-CH_3), 3.65, (6 H, s, (-O-CH_3)$_2$).

The ^{1}H NMR is consistent with the formation of Dimethyl 2-methyl malonate. [84]

b) Benzylation of Dimethyl2-methyl malonate

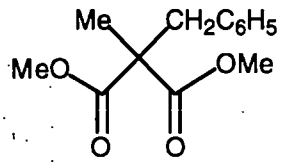

Beistein Registry Number 2118469 (Fig. 121 p. 160)

Dimethyl 2-methyl malonate (1.4 g; 9.6 mmol) was dissolved in dry methanol (50 cm^3), and potassium *tert* -butoxide (1.3 g; 11.52 mmol) dissolved in dry methanol (25 cm^3) was added dropwise with stirring. Benzyl bromide (1.4 cm^3; 11.5 mmol) was then added dropwise. The reaction mixture was allowed to stir at room temperature for 24h. The reaction mixture was then evaporated under reduced pressure and the residue taken up in DCM, dried over anhydrous sodium sulphate and re-evaporated, to give a colourless viscous oil (61%).

υ_{max}(film)/cm^{-1} 1737; δ_H (200 MHz; $CDCl_3$; Me_4Si) 1.40 (3 H, s, -C-CH_3), 3.35 (2 H, s, -CH_2-C_6H_5), 3.69 (6 H, s, (-O-CH_3)$_2$), 7.10-7.42 (5 H, m, -CH_2-C_6H_5); (TLC Rf 0.55 (DCM) (I_2)).

The IR and ^1H NMR are consistent with the formation of Dimethyl-2-benzyl-2-methyl malonate. [85]

c) Monohydrolysis of the Dimethyl 2-benzyl-2-methyl malonate

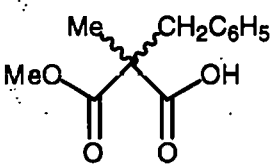

Beistein Registry Number 4746252 (Fig. 121 p. 160)

Dimethyl 2-benzyl-2-methyl malonate (0.9 g; 3.82 mmol) was dissolved in methanol (20 cm^3) and a solution of sodium hydroxide (0.22 g; 3.82 mmol/15 cm^3 of water) was added slowly. The reaction mixture was allowed to stir at room temperature for 12h, then acidified with HCl_{aq} (2x10 cm^3, 6M) and evaporated under reduced pressure. The residue was dissolved in DCM (20 cm^3) to give 2-benzyl-2-methyl-malonic acid monomethyl ester as a colourless viscous oil (86%).

υ_{max}(film)/cm^{-1} 1700 and 1578 (Na salt C=O); δ_H (200 MHz; $CDCl_3$; Me_4Si) 1.12 (3 H, s, -C-CH_3), 2.90-3.18 (2 H, dd, *J* 7.5, -CH_2-C_6H_5), 3.65 (3 H, s, -O-CH_3), 7.11-7.42 (5H, m, -CH_2-C_6H_5).

The IR and ^1H NMR are consistent with the formation of the 2-benzyl-2-methyl malonic acid monomethyl ester.[85]

d) Schmidt reaction on the 2-Benzyl-2-methyl malonic acid monomethyl ester to give racemic α-methylphenylalanine methyl ester

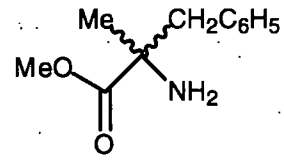

(Fig. 121 p. 160)

The method described in 7 (p.191) was followed for this reaction. Methyl-2-benzyl-2-methyl malonate (0.45 g; 1.59 mmol), Polyphosphoric acid (5.3 g; 31.7 mmol) were mixed together at 0 °C, then sodium azide (0.21 g; 3.2 mmol) was added in small portions whilst stirring the reaction mixture. The reaction mixture was allowed to warm to room temperature with occasional stirring and left for eight hours. Crushed ice (10 g) was then added and the mixture allowed to warm to room temperature. Ice cold sodium hydroxide (~4 cm^3, 50 % w/v) was added until the solution was alkaline, before extraction of the solution with dichloromethane (4x5 cm^3). The combined extracts were dried (Na_2SO_4 anhyd.) then evaporated under reduced pressure to give the product as a colourless viscous oil (89%).

υ_{max}(film)/cm^{-1} 3360 (2 ° amine) and 1736; δ_H (200 MHz; $CDCl_3$; Me_4Si) 1.60 (3 H, s, -C-CH_3), 3.20-3.48 (2 H, dd, *J* 7.5, -CH_2-C_6H_5), 3.80 (3 H, s, -O-CH_3), 4.88 (2 H, s, -NH_2), 7.10-7.30 (5 H, m, -CH_2-C_6H_5); *m/z* (CI (NH_3)) 194.1181 ($(M+H)^+$ $C_{11}H_{15}NO_2$ requires 194.1181)

The IR, ^1H NMR and mass spec analysis are consistent with the formation of racemic α-methylphenylalanine methyl ester.

26. *Preparation of 6-Chloro-2,4-dimethoxy-1,3,5-triazine* [81]

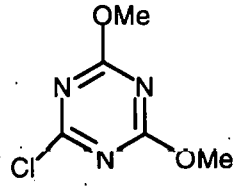

(Appendix Fig. 130 p. 237)

Sodium hydrogen carbonate (13.4 g; 0.16 mol.) was dissolved in a mixture of methanol and water ((40 cm^3: 4 cm^3). Cyanuric chloride (14.8 g; 0.08 mol) was added to the stirred solution in small portions, whilst keeping the temperature at 30 °C. After stirring for 7h. The reaction mixture was extracted with DCM (1x60 cm^3, 2x20 cm^3). These extracts were combined and washed with water until neutral (3x20 cm^3 H_2O), dried over anhydrous magnesium sulphate and evaporated under reduced pressure to give white solid (62.5%). The product was recrystallised from *n*-hexane. The reaction temperature is critical to achieve the required substitution:-

- <20 °C for monosubstitution.
- 30 °C for disubstitution.
- >30 °C for trisubstitution.

Separation of a mixture of substituted products was achieved using HPLC.

Monosubstituted

δ_H (200 MHz; $CDCl_3$; Me_4Si) 4.10 (3 H, s, -OCH_3);

(TLC Rf 0.44 (DCM:40:60 light petroleum) 1:1) (U.V.)).

Disubstituted

Mp 75-76 °C (from *n*-hexane); δ_H (200 MHz; $CDCl_3$; Me_4Si) 4.05 (6 H, s, -OCH_3);

(TLC Rf 0.22 (DCM: 40:60 light petroleum)1:1) (U.V.).

Trisubstituted

δ_H (200 MHz; $CDCl_3$; Me_4Si) 3.80 (9 H, s, -OCH_3);

(TLC Rf 0.11 (DCM:40:60 light petroleum) 1:1) (U.V.)).

HPLC conditions

Mobile phase	MeCN (70):H_2O (30) (TFA 0.11)	
Δ_{max}	254 nm	
Flow rate	1cm^3/min	
Retention time	2.7 mins	Trisubstituted
	3.9 mins	Disubstituted
	4.4 mins	Monosubstituted

27. ***Attempted reaction of (2S, 3R)-3,4-Dimethyl-2-phenylperhydro-1,4-oxazepine-5,7-dione (1A) with triethylamine and benzyl chloride.***

(2*S*, 3*R*)-3,4-Dimethyl-2-phenylperhydro-1,4-oxazepine-5,7-dione (0.1 g, 0.4 mmol) and triethylamine (0.2 cm^3, 1.8 mmol) were dissolved in dry dichloromethane (20 cm^3) at room temperature. Benzyl chloride (0.026 g, 0.2 mmol) was then added dropwise with stirring. The reaction mixture was refluxed for 1 h and monitored by TLC (chloroform:diethyl ether 2:1). After this time there was no spot for the oxazepine or the benzyl chloride. There was no identifiable product.

28. ***Attempted reaction of (2S, 3R)-3,4-Dimethyl-2-phenylperhydro-1,4-oxazepine-5,7-dione (1A) with potassium carbonate and benzyl chloride.***

(2*S*, 3*R*)-3,4-Dimethyl-2-phenylperhydro-1, 4-oxazepine-5,7-dione (O.111 g, 0.44 mmol) and anhydrous potassium carbonate (0.27 g, 1.98 mmol) were dissolved in dry dichloromethane (25 cm^3) at room temperature. Benzyl chloride (0.026 g, 0.2 mmol) was then added dropwise with stirring, and the mixture allowed to stir for 5 days. The reaction was monitored by TLC (chloroform:diethyl ether 2:1), after five days there were still only two spots, one due to the benzyl chloride and one to the unreacted oxazepine **1A**.

29 ***Attempted reaction of (2S, 3R)-3,4-Dimethyl-2-phenylperhydro-1,4-oxazepine-5,7-dione (1A) with lithium diisopropylamide (LDA) and ethyl iodide.***

Dry diisopropylamine (DIPA) (0.76 cm^3, 5.39 mmol) was dissolved in dry tetrahydrofuran (THF) (50 cm^3),and cooled to <10 °C. Butyllithium (3.06 cm^3, 4.9

mmol) was added dropwise with stirring, and the reaction mixture allowed to warm to room temperature, then cooled to -78° C. (2*S*, 3*R*)-3,4-Dimethyl-2-phenylperhydro-1,4-oxazepine-5,7-dione (1.135 g, 4.9 mmol) dissolved in dry THF (5 cm^3) was added slowly dropwise, and allowed to stir at -78°C for one hour. Ethyl iodide (freshly distilled) (0.84 g, 5.4 mmol) was added slowly dropwise. The reaction mixture was left stirring for half an hour at -78°C, and monitored by TLC (chloroform:diethyl ether 2:1), and then allowed to warm to room temperature when distilled water (5 cm^3) was added. The THF fraction was dried over anhydrous sodium sulphate, and then evaporated. The residue was then passed though a column to separate the components, (silica gel with chloroform:diethyl ether (2: 1) as the eluant). There was a residue of unreacted oxazepine **1A** (0.07 g), but no identification of the remaining residue was possible.

30. ***Attempted reaction of (2S, 3R)-3,4-Dimethyl-2-phenylperhydro-1,4-oxazepine-5,7-dione (1A) with 1,8-diazabicyclo [5, 4, 0] undec-7-ene (DBU) and ethyl iodide.***

Diazabicyclo [5, 4, 0] undec-7-ene (0.36 g, 2.37 mmol) was dissolved in dry THF (100 cm^3) and cooled to -78° C. (2*S*, 3*R*)-3,4-Dimethyl-2-phenylperhydro-1,4-oxazepine-5,7-dione (0.5 g, 2.15 mmol) dissolved in dry THF (10 cm^3) was added slowly with stirring to the DBU solution, this was left stirring for 10 min. Ethyl iodide (0.37g, 2.37 mmol) was added and the reaction mixture was left stirring at -78°C for a further 30 min. The reaction was monitored by TLC (cyclohexane:ethyl acetate 1:1). The bulk of the THF was evaporated under reduced pressure, distilled water (5 cm^3) was added, and the solution was extracted with dichloromethane (2x

20 cm^3). The extracts were washed with a solution of sodium bisulphite (5% w/v) to remove iodine contamination, dried over anhydrous sodium sulphate and evaporated. After column chomatography (silica gel with cyclohexane:ethyl acetate 1:1 as the eluant), ^1H NMR indicated that the major component was probably a mixture of unreacted oxazepine and *N*-malonyl ephedrine **(13)**.

31. ***Attempted reaction of (2S, 3R)-3,4-Dimethyl-2-phenylperhydro-1,4-oxazepine-5,7-dione (1A) with sodium hydride and ethyl iodide.***

Sodium hydride (0.012 g, 0.48 mmol) was dissolved in dry THF (50 cm^3) and cooled to -30 °C. (2*S*, 3*R*)-3,4-Dimethyl-2-phenylperhydro-1,4-oxazepine-5,7-dione (0.1 g, 0.43 mmol) dissolved in dry THF (5 cm^3) was added slowly with stirring to the solution, and allowd to stir for 10 mins. Ethyl iodide (0.075 g, 0.48 mmol) was added and the reaction mixture was left stirring at -30 °C for a further 30 min. The reaction was monitored by TLC (cyclohexane:ethyl acetate 1:1). The bulk of the THF was evaporated under reduced pressure, distilled water (5 cm^3) was added, and the solution extracted with dichloromethane (2x 20 cm^3), dried over anhydrous sodium sulphate and evaporated. Unreacted oxazepine was recovered, with no indication of any other product.

32. ***Attempted cleavage reactions of the disubstituted oxazepines***

32a Compound **19** (~0.1 g; ~0.4 mmol) was added to a solution of potassium carbonate (15 cm^3, 1% w/v aqueous MeOH) with stirring. The reaction mixture was allowed to stir for 3 days at room temperature. After this time the solution

was acidified (HCl_{aq} 1:1), extracted with dichloromethane (2x10 cm^3), and the extracts were washed with water, dried over anhydrous sodium sulphate, and evaporated under reduced pressure. ^1H NMR and IR spectra showed starting material present with no evidence of cleavage of the ring.

32b Compound **19** (~0.1 g; ~0.4 mmol) was added to a solution of potassium carbonate (15 cm^3, 1% w/v aqueous MeOH) with stirring. The reaction mixture was then heated under reflux for 2 h. The solution was then cooled to room temperature, acidified (HCl_{aq} 1:1), and extracted with dichloromethane (2x10 cm^3). The extracts were washed with water (2x10 cm^3), dried over anhydrous sodium sulphate, then evaporated under reduced pressure. Again ^1H NMR and IR spectra showed starting material present with no evidence of cleavage of the ring.

32c Compound **19** (30 mg; 0.12 mmol) was dissolved in aqueous methanol (25 cm^3), lithium hydroxide (3 mg; 1.2 mmol) was added to the stirred solution. The reaction mixture was allowed to stir at room temperature for 2 days. The solution was then acidified (HCl_{aq} 1:1), extracted with dichloromethane (2x10 cm^3) and the extracts washed with water (2x10 cm^3), dried over anhydrous sodium sulphate, then evaporated under reduced pressure. Again ^1H NMR and IR spectra showed starting material present with no evidence of cleavage of the ring.

32d Compound **19** (~10 mg; ~0.003mmol) was dissolved in methanol (2 cm^3), lithium hydroxide (0.84 mg; 0.02 mmol) dissolved in H_2O (2 cm^3) was added

dropwise to the stirred solution. The reaction mixture was then heated to ~ 90 °C on a water bath and left stirring at this temperature for 4 h. The solution was cooled to room temperature, then acidified (HCl_{aq} 1:1), extracted with dichloromethane (2x10 cm^3) and the extracts washed with water (2x10 cm^3), dried over anhydrous sodium sulphate, then evaporated under reduced pressure. Again ^1H NMR and IR spectra showed starting material present with no evidence of cleavage of the ring.

32e Compound **19** (0.87 g; 2.26 mmol) was dissolved in dry methanol (6 cm^3), sodium methoxide (2 cm^3; 2.4 mmol) was added dropwise to the stirred solution and the reaction mixture was left stirring for 24 h. The reaction mixture was then evaporated under reduced pressure, the residue was taken up into dichloromethane (20 cm^3) and washed with water (2x10 cm^3), dried over anhydrous sodium sulphate, then evaporated under reduced pressure. Again ^1H NMR and IR spectra showed starting material present with no evidence of cleavage of the ring.

32f Compound **19** (0.2 g) was dissolved in a 50/50 ethanol/ethyl acetate solution, Adam's catalyst (10 mg; PtO_2) was put into the reaction vessel and hydrogen passed through the solution (under atmospheric pressure) for 6 days. After this time the solution was filtered and then evaporated under reduced pressure. ^1H NMR and IR spectra showed starting material present with no evidence of cleavage of the ring.

9. REFERENCES

1. E. Fischer, *Ber. Dtsch. Chem. Ges.*, 1894, **27**, 2895.

2. J. N. Langley, *Proc. Roy. Soc., B*, 1906, **78**, 170.

3. P. Ehrlich, *Brit.ish Med.cal Journal*, 1913, **11**, 353.

4 R. A. Sheldon, *Chirotechnology*, Marcel Dekker, New York, 1993, 58.

5 M. R. De Camp, *Chirality*, 1989, **1**, 2. B. Testa *et al*, *Chirality*, 1993, **5**, 105.

6 R. A. Aitken and S. N. Kilenyi, *Asymmetric Synthesis*, Blackie A & P, Glasgow, 1992.

7 D. J. Cram and F. A. A. Elhafez, *J. Am. Chem. Soc.*, 1952, **74**, 5828.

8 D. J. Cram and K. R. Kopecky, *J. Am. Chem. Soc.*, 1959, **81**, 2748.

9 T. J. Leitereg and D. J. Cram, *J. Am. Chem. Soc.*, 1968, **90**, 4019.

10 M. Cherest and H. Felkin, *Tetrahedron Lett.*, 1968, 2205.

11 N. T. Anh and O. Eisenstein, *Nouv. J. Chim.*, 1977, **1**, 61.

12 E. L. Eliel, *Asymmetric Synthesis*, 1983, **1**, Academic, New York, 125.

13 G. Wess, K. Kesseler, E. Baader, W. Bartmann, G. Beck, A. Bergmann, H. Jendralla, K. Bock, G. Holzstein, H. Kleine and M. Schierer, *Tetrahedron Lett.*, 1990, **31**, 2545.

14 M. Cherest, H. Felkin and N. Prudent, *Tetrahedron Lett.*, 1968, 2199, Y. -D. Wu and K. N. Houk, *J. Am. Chem. Soc.*, 1987, **109**, 908.

15 D. Seebach, M. Boes, R. Naef and W. B. Schweizer, *J. Am. Chem.Soc.*, 1983, **105**, 5390.

16 R. Naef, D.Seebach, *Helv. Chim. Acta.*, 1985, **68**, 135.

17 D. Seebach, J. D.Aebi, R. Naef and T. Weber, *Helv. Chim. Acta.*, 1985, **68**, 144.

18 For a review see: D. Seebach, A. R. Sting and M. Hoffman, *Angew. Chem. Int. Ed. Engl.*, 1996, **35**, 2708.

19 M. J. O'Donnell, Z. Fang, X. Ma and J. C. Huffman, *Heterocycles* , 1997, **46**, 617.

20 M. J. O'Donnell, L. K. Lawley, P. B. Pushpavanam, A. Burger, F. G. Bordwell and X. M. Zhang,*Tetrahedron Lett.*, 1994, **35**, 642.

21 D. Seebach, R. Naef and G. Calderari,*Tetrahedron*, 1984, **40**, 1313.

22 R. M. Williams and M-N Im, *J. Am. Chem. Soc.*, 1991, **113**, 9276.

23 H. O. House, B. A. Tefertiller and H. D. Olmstead, *J. Org. Chem.*, 1968, **33**, 935.

24 R. M. Williams, P. J. Colson and W Zhai, *Tetrahedron Lett.*, 1994, **35**, 9371.

25 C. Agami, F. Couty, B. Prince and C. Puchot, *Tetrahedron* 1991, **47**, 4343.

26 C. Agami, F. Couty, L. Hamon, B. Prince, and C. Puchot, *Tetrahedron*, 1990, **46**, 7003.

27 C. Agami, F. Couty and C. Puchot-Kadouri, *Synlett.*, 1997, **5**, 449.

28 C. Agami, D. Bihan and C. Puchot-Kadouri, *Tetrahedron*, 1996, **52**, 79.

29 H. C. Brown and P. V. Ramachandran, *Acc. Chem. Res.*, 1992, **25**, 16.

30 E. J. Corey and Raman K. Bakshi, *Tetrahedron Lett.*, 1990, **31**, 611.

31 E. J. Corey, R. K. Bakshi and S. Shibata, *J. Am. Chem. Soc.*, 1987, **109**, 5551.

32 H. C. Brown and B. Singaram, *Acc. Chem. Res.*, 1988, **21**, 287.

33 M. Srebnik and P. V. Ramachandran, *Aldrichimica Acta*, 1987, **20**, 9.

34 D. H. Hua, N. Lagneau, H. Wang and J. Chen,*Tetrahedron Asymmetry*, 1995, **6**, 349.

35 A .S. Demir, *Pure Appl. Chem.*, 1997, **69**, 105.

36 F. A. Davis, P. Zhou, and B-C. Chen, *Chem. Soc. Rev.*, 1998, **27**, 13.

37 F. A. Davis, R. E. Reddy and P. S. Portonovo,*Tetrahedron Lett.*, 1994, **35**, 9351.

38 E. J. Corey and J. O. Link, *J. Am. Chem. Soc.*, 1992, **114**, 1906.

39 W. S. Knowles, M. J. Sabacky, B. D. Vineyard and D. J. Weinkauf, *J. Am. Chem., Soc.* 1975, **97**, 2567.

40 B. D. Vineyard, W. S. Knowles, M. J. Sabacky, G. L. Bachman and D. J. Weinkauf, *J. Am. Chem. Soc.*, 1977, **99**, 5946.

41 B. D. Vineyard, W. S. Knowles and M. J. Sabacky, *J. Mol. Catal.*, 1983, **19**, 159.

42 B. M. Trost and X. Ariza, *Angew. Chem. Int. Ed*, 1997, **36**, 2635.

43 B. M. Trost, *Acc. Chem. Res.*, 1996, **29**, 355.

44 U. Schollkopf, U. Groth and C. Deng, *Angew. Chem. Int. Edn*, 1981, **20**, 798.

45 U. Schollkopf and H-J. Neubauer, *Synthesis*, 1982, 861.

46 U. Groth, U. Schollkopf and Y-C. Chiang, *Synthesis*, 1982, 864.

47 U. Schollkopf, *Tetrahedron*, 1983, **39**, 2085.

48 U. Schollkopf, S. Gruttner, R. Anderskewitz, E. Egert and M. Dyrbusch, *Angew. Chem. Int. Edn*, 1987, **26**, 683.

49 U. Schollkopf, T. Tiller and J. Bardenhagen,*Tetrahedron* , 1988, **44**, 5293.

50 U. Groth, U. Schollkopf and T. Tiller, *Tetrahedron*, 1991, **47**, 2835.

51 R. Chinchilla, L. R. Falvello, N. Galindo and C. Najera, *Angew. Chem. Int. Ed. Engl.*, 1997, **36**, 995.

52 A. Lopez, M. Moreno-Manas, R. Pleixats, A. Roglans, J. Ezquerra, C. Pedregal, *Tetrahedron*, 1996, **52**, 8365.

53 S. D. Bull, S. G. Davies, S .W. Epstein and J. V. A. Ouzman, *Chem. Commun.*, 1998, 659.

54 A. G. Myers, J. L. Gleason and T. Yoon, *J. Am. Chem. Soc.*, 1995, **117**, 8488.

55 G. Porzi and S. Sandra, *Tetrahedron Asymmetry*, 1996, **7**, 189.

56 T. K. Chakraborty, K. Azhar Hussain and G. Venkat Reddy, *Tetrahedron*, **51**, 9179.

57 T-L. Yeh, C-C. Liao and B-J. Uang,*Tetrahedron*, 1997, **53**, 11141.

58 J. M. McIntosh, R. K. Leavitt, P. Mishra, K. C. Cassidy, J. E. Drake and R. Chadha, *J. Org. Chem.*, 1988, **53**, 1947.

59 G. Guillena and C. Najera,*Tetrahedron Asymmetry*, 1998, **9**, 1125.

60 H. Takahashi, I. Morimoto and K. Higashiyama, *Heterocycles*, 1990, **30**, 287.

61 A. I. Meyers, M. Harre and R. Garland, *J. Am. Chem. Soc.*, 1984, **106**, 1146.

62 A. I. Meyers, R. H. Wallace, M. Harre and R. Garland, *J. Org. Chem,*. 1990, **55**, 3137.

63 D. Romo and A. I. Meyers, *Tetrahedron*, 1991, **47**, 9504.

64 A. I. Meyers and D. Berney, *J. Org. Chem.*, 1989, **54**, 4673.

65 A. I. Meyers and G. P. Brengel, *Chem. Commun.*, 1997, 1.

66 T. Mukaiyama, Y. Hirako and T. Takedo, *Chem. Lett.*, 1978, 461.

67 T. Mukaiyama, T. Takeda and K. Fujimoto, *Bull. Chem. Soc. Jpn.*, 1978, **51**, 3368.

68 R. T. Brown and M. J. Ford, *Synth. Commun.*, 1988, **18**, 1801.

69 M. J. Ford, *PhD Thesis.* Manchester University, 1988.

70 W. P. Blackstock, R. T. Brown and M. Wingfield, *Tetrahedron Lett.*, 1984, 1831.

71 R. T. Brown and M. J. Ford, *Tetrahedron Lett.*, 1990, **31**, 2029.

72 R. T. Brown and M. J. Ford, *Tetrahedron Lett.*, 1990, **31**, 2033.

73 R. M. Williams, *Synthesis of Optically Active α-Amino Acids;* Pergamon Press, Oxford, 1989.

74 L. J. Bellamy, *The Infrared Spectra of Complex Molecules*, Vol.1, 211 (3rd Edition 1975).

75 L. J. Bellamy and R. L. Williams, *J. Chem. Soc.*, 1957, 861.

76 Nemesis for PC software, *Oxford Molecular Limited, Oxford, U.K.*

77 J. G. Vinter, A. Davis and M. R. Saunders, *J. of Computer-Aided Molecular Design*, 1987, **1**, 31.

78 Cambridge Scientific Comp., Inc. *Chem. 3D Plus 2.01.* (1986-1989)

79 J. Bellan, J. C. Rossi and M. Sanchez.*Tetrahedron Lett.*, 1976, **50**, 4621.

80 J. Bellan, A. Klaebe and M. Sanchez, *Nouv. J. Chim.*, 1980, **4**, 329.

80 Y. Hirako, T. Mukaiyama and T. Takeda, *Chem. Lett.*, 1978, 461.

81 A. J. M.Weber, W. G. B. Huysmans and W. J. Mijs, *J. Royal Netherlands Chem. Soc.*, 1978, **97/4**, 107.

82 Marco, Royer and Husson, *Synth. Commun.*, 1987, EN, **6**, 669.

83 Subramnian, Pullachipatti and Woodward, *J. Org. Chem.*, 1987, **52,** 1, 15.

84 Dieckmann and Wittmann, *Chem. Ber.*, 1922, **55**, 3346.

85 Ahmar, Bloch and Bortolussi, *Synth. Commun.* 1991, EN, **21**, 8,9, 1071.

10.0.

APPENDIX.

10.1 Characterised novel compounds indicative of asymmetric induction which were synthesised during the course of this research project are given below:

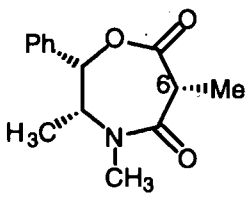

14

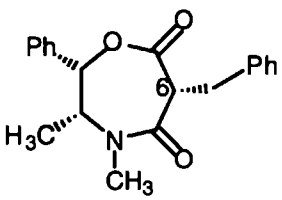

15

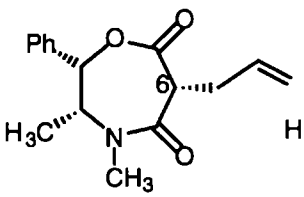

16

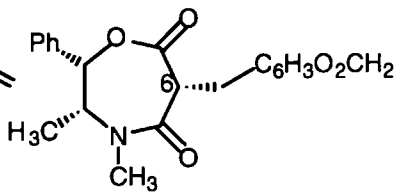

17

(pps. 89-98)

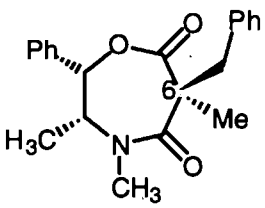

18

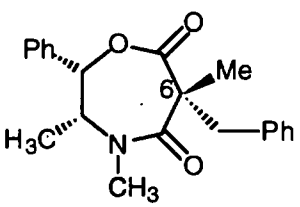

19

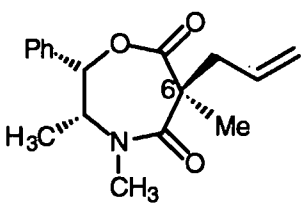

20

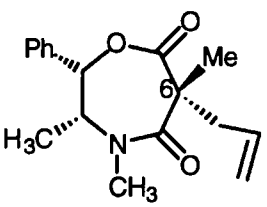

21

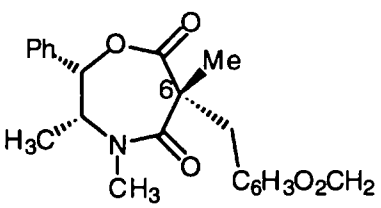

22

(pps. 98-112)

Other new compounds, lacking Beilstein Registry numbers prepared during this work are listed below:

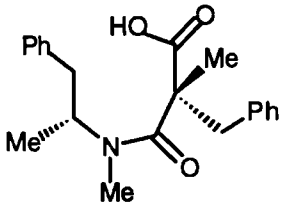

24

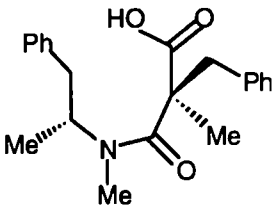

25

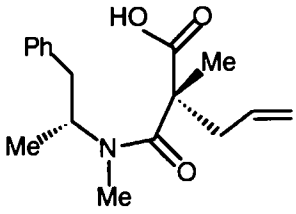

26

(pps. 113-121)

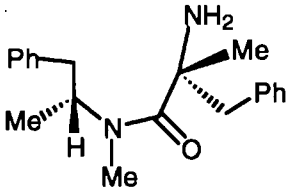

27

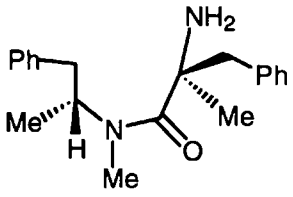

28

(pps. 121-125)

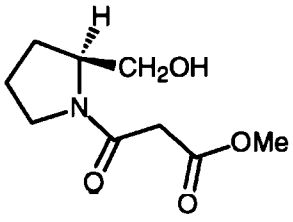

32

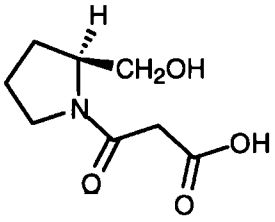

33

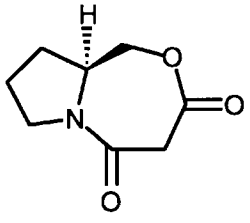

34

(pps. 132-137)

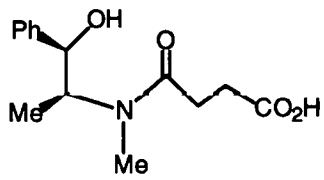

36

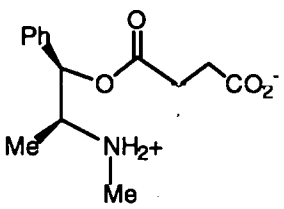

37

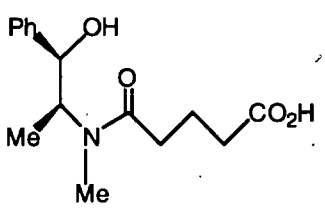

38

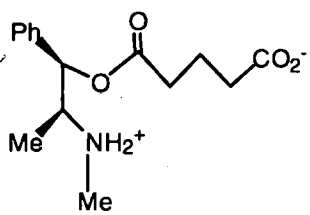

39

(pps. 144-151)

10.2. An alternative reagent for the oxazepine synthesis.

One of the problems associated with the oxazepine synthesis was the relatively low yield at the lactonisation stage. It was thought that the pyridine was activating the cyanuric chloride perhaps as the reactive species[66] **RS** (shown below). If this was the case then there might also be the possibility of disubstitution by the pyridine in the cyanuric chloride molecule, which would present a much bulkier reagent and cause steric hindrance for the reaction.

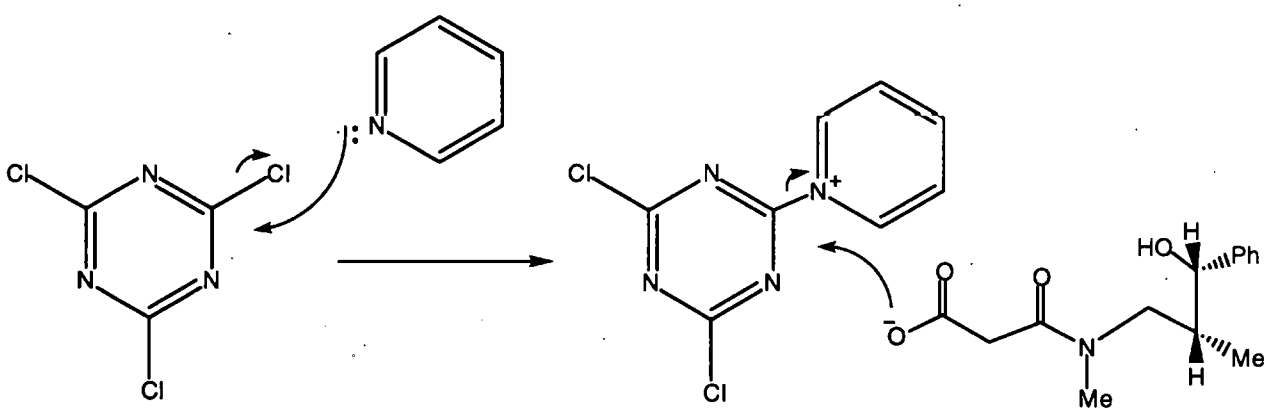

RS

A reagent prepared directly from cyanuric chloride (see below) was suggested. It was hoped that the reagent would be as reactive as the cyanuric chloride but less likely to produce the yellow precipitate that forms when cyanuric chloride and pyridine are mixed together in tetrahydrofuran, dichloromethane or acetonitrile. This yellow precipitate was thought to be related to the reactive species (**RS**) shown above[66].

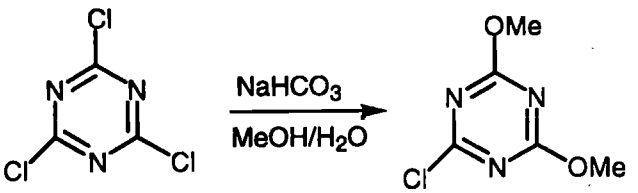

cyanuric chloride 6-chloro-2,4-dimethoxy-1,3,5-triazine

Unfortunately neither 6-chloro-2,4-dimethoxy-1,3,5-triazine nor 4,6-dichloro-2-methoxy-1,3,5-triazine were successful in producing the oxazepine.

10.3 X-Ray crystallographic structures.

S311

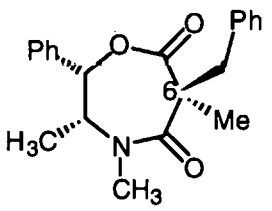

(2*S*,3*R*,6*S*)-3,4-dimethyl-6-benzyl-6-methyl-2-phenyl-1,4-oxazepine-5,7-dione

S308

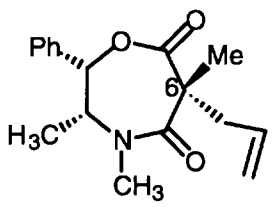

(2*S*,3*R*,6*S*)-3,4-dimethyl-6-allyl-6-methyl-2-phenyl-1,4-oxazpine-5,7-dione

These X-ray crystallographic structures have been deposited with

The Cambridge Crystallographic Data Centre.

Reference	CCDC 143345	**S311**
Reference	CCDC 143344	**S308**

The author would like to thank R. L. Beddoes of the Crystallographic Research Service Department at Manchester University, for obtaining the X-ray structures.

Status of project

28-SEP-93 10:50:50

PROJECT DIRECTORY : [TEXSAN.STRUCTURES.S311]

TITLE : S311/1 27-SEP-93

CELL : a= 11.831 b= 17.672 c= 8.852 alpha= 90.00 beta= 90.00 gamma= 90.00

SPACEG : P212121 S.G.# 19 DENSITY : Dc= 1.211 Absorption coef.= 6.110

STORED formula		CURRENT formula		STATUS
C	21.00	C	21.00	O.K.
H	23.00	H	23.00	O.K.
N	1.00	N	1.00	O.K.
O	3.00	O	3.00	O.K.

parameters : # of reflections= 1510 # of variables= 226 shift/error= 0.000

R-factors : R= 0.043 Rw= 0.056 Goodness of fit= 3.489 LS cycles= 6

corrections : absorption=on -type=DIF decay=on redundant=on average=off

INTRODUCTION

The structure which is related to that reported recently (see S308 16th. September 1993) has been confirmed.

The spacegroup is non-centrosymmetric with the origin of the unit cell equidistant from the three orthogonal two-fold screw axes. There is one molecule in the asymmetric unit.

Intermolecular contacts are H to H only.

The enantiomeric structure was again refined although the anomalous scattering terms are small. The resultant R and Rw agreement factors of 0.0433 and 0.0564 are only marginally inferior to those (0.0427 and 0.0563) of the predicted absolute configuration reported below.

EXPERIMENTAL

DATA COLLECTION

A colourless prism crystal of $C_{21}H_{23}NO_3$ having approximate dimensions of 0.30 X 0.45 X 0.45 mm was mounted on a glass fibre. All measurements were made on a Rigaku AFC5R X-ray diffractometer with graphite-monochromated Cu Kα radiation and a 12KW rotating anode generator.

Cell constants and an orientation matrix for data collection, obtained from a least-squares refinement using the setting angles of 16 carefully-centred reflections in the range $78.92 < 2\theta < 80.07°$ corresponded to an orthorhombic cell with dimensions:

$a = 11.831\ (4)\text{Å}$
$b = 17.672\ (3)\text{Å}$
$c = 8.852\ (2)\text{Å}$
$V = 1850.8\ (8)\text{Å}^3$

For $Z = 4$ and F.W. = 337.42, the calculated density is 1.211 g/cm^3. Based on the systematic absences of:

h00: $h \neq 2n$
0k0: $k \neq 2n$
00l: $l \neq 2n$

and the successful solution and refinement of the structure, the space group was determined to be:

$P2_12_12_1$ (#19)

The data were collected at a temperature of 22 ± 1°C using the ω/2θ scanning technique to a maximum 2θ value of 120.3°. Omega scans of several intense reflections, made prior to data collection, had an average width at half-height of 0.27° with a take-off angle of 6.0°. Scans of $(1.31 + 0.30 \tan\theta)°$ were made at a speed of 8.0°/min (in omega). The weak reflections ($I < 10.0\sigma(I)$) were rescanned (maximum of 2 rescans) and the counts were accumulated to assure good counting statistics. Stationary background counts were recorded on each side of the reflection. The ratio of peak counting time to background counting time was 2:1. The diameter of the incident beam collimator was 0.5 mm and the crystal to detector distance was 400.0 mm.

DATA REDUCTION

A total of 1606 reflections was collected. The intensities of three representative reflections which were measured after every 150 reflections declined by -2.80%. A linear correction factor was applied to the data to account for this phenomenon.

The linear absorption coefficient for Copper Kα is 6.1 cm^{-1}. An empirical absorption correction, using the program DIFABS[3], was applied which resulted in transmission factors ranging from 0.92 to 1.04. The data were corrected for Lorentz and polarization effects.

STRUCTURE SOLUTION AND REFINEMENT

The structure was solved by direct methods[4]. The non-hydrogen atoms were refined anisotropically. Hydrogen atoms were included in the structure factor calculation in idealized positions (C-H = 0.95Å) , and were assigned isotropic thermal parameters which were 20% greater than the equivalent B value of the atom to which they were bonded. The final cycle of full-matrix least-squares refinement[5] was based on 1510 observed reflections ($I > 3.00\sigma(I)$) and 226 variable parameters and converged (largest parameter shift was <0.01 times its esd) with unweighted and weighted agreement factors of:

$$R = \Sigma \, ||Fo| - |Fc|| \, / \, \Sigma \, |Fo| = 0.043$$

$$R_w = [(\Sigma \, w \, (|Fo| - |Fc|)^2 \, / \, \Sigma \, w \, Fo^2)]^{1/2} = 0.056$$

The standard deviation of an observation of unit weight[6] was 3.49. The weighting scheme was based on counting statistics and included a factor (p = 0.02) to downweight the intense reflections. Plots of $\Sigma \, w \, (|Fo| - |Fc|)^2$ versus |Fo|, reflection order in data collection, $\sin \theta/\lambda$, and various classes of indices showed no unusual trends. The maximum and minimum peaks on the final difference Fourier map corresponded to 0.21 and -0.14 $e^-/Å^3$, respectively.

Neutral atom scattering factors were taken from Cromer and Waber[7]. Anomalous dispersion effects were included in Fcalc[8]; the values for Δf′ and Δf″ were those of Cromer[9]. All calculations were performed using the TEXSAN[10] crystallographic software package of Molecular Structure Corporation.

References

(1) PLUTO:
Motherwell,S. & Clegg,W.; PLUTO. Program for plotting molecular and crystal structures. Univ. of Cambridge, England (1978).

(2) ORTEP:
Johnson,C.K.; ORTEPII. Report ORNL-5138. Oak Ridge National Laboratory, Oak Ridge, Tennessee (1976).

(3) DIFABS:
Walker & Stuart, Acta Cryst. A39, 158-166, (1983).

(4) Structure Solution Method:
SHELXS-86
Sheldrick,G.M.; (1985). SHELXS-86 In "Crystallographic Computing 3" , edited by G.M.Sheldrick, C.Krueger and R.Goddard p175-189. Oxford University Press.

(5) Least-Squares:
Function minimized: $\Sigma\ w\ (|Fo| - |Fc|)^2$
where: $w = 4Fo^2/\sigma^2(Fo^2)$
$\sigma^2(Fo^2) = [S^2(C+R^2B) + (pFo^2)^2]/Lp^2$
S = Scan rate
C = Total Integrated Peak Count
R = Ratio of Scan Time to background counting time.
B = Total Background Count
Lp = Lorentz-polarization factor
p = p-factor

(6) Standard deviation of an observation of unit weight:

$$[\Sigma\ w(|Fo| - |Fc|)^2/(No - Nv)]^{1/2}$$

where: No = number of observations
Nv = number of variables

(7) Cromer,D.T. & Waber,J.T.; "International Tables for X-ray Crystallography", Vol. IV, The Kynoch Press, Birmingham, England, Table 2.2 A (1974).

(8) Ibers,J.A. & Hamilton,W.C.; Acta Crystallogr., 17, 781 (1964).

(9) D.T. Cromer, "International Tables for X-ray Crystallography", Vol/ IV, The Kynoch Press, Birmingham, England, Table 2.3.1 (1974).

(10) TEXSAN - TEXRAY Structure Analysis Package, Molecular Structure Corporation (1985).

EXPERIMENTAL DETAILS

1. Crystal Data

Empirical Formula	$C_{21}H_{23}NO_3$
Formula Weight	337.42
Crystal Colour, Habit	colourless, prism
Crystal Dimensions (mm)	0.30 X 0.45 X 0.45
Crystal System	orthorhombic
No. Reflections Used for Unit Cell Determination (2θ range)	16 (78.9 - 80.1°)
Omega Scan Peak Width at Half-height	0.27
Lattice Parameters:	
	a = 11.831 (4)Å
	b = 17.672 (3)Å
	c = 8.852 (2)Å
	V = 1850.8 (8)Å^3
Space Group	$P2_12_12_1$ (#19)
Z value	4
D_{calc}	1.211 g/cm^3
F_{000}	720
$\mu_{(CuK\alpha)}$	6.11 cm^{-1}

2. Intensity Measurements

Diffractometer	Rigaku AFC5R
Radiation	CuKα (λ = 1.54178 Å)
Temperature	22°C
Attenuators	Zr foil (factors: 3.6, 12.2, 44.0)
Take-off Angle	6.0°

Detector Aperture	6.0 mm horizontal 6.0 mm vertical
Crystal to Detector Distance	40 cm
Scan Type	$\omega/2\theta$
Scan Rate	8.0°/min (in omega) (2 rescans)
Scan Width	$(1.31 + 0.30 \tan\theta)°$
$2\theta_{max}$	120.3°
No. of Reflections Measured	Total: 1606
Ranges of h,k,l	-12 to 13, -13 to 19, -9 to 9
Corrections	Lorentz-polarization Absorption (trans. factors: 0.92 - 1.04) Decay (-2.80% decline)

3. Structure Solution and Refinement

Structure Solution	Direct Methods
Hydrogen Atom Treatment	Included in calculated positions (d_{C-H} = 0.95Å)
Refinement	Full-matrix least-squares
Function Minimized	Σ w $(\|Fo\| - \|Fc\|)^2$
Least-squares Weights	$4Fo^2/\sigma^2(Fo^2)$
p-factor	0.02
Anomalous Dispersion	All non-hydrogen atoms
No. Observations (I>3.00σ(I))	1510
No. Variables	226
Reflection/Parameter Ratio	6.68
Residuals: R; R_w	0.043; 0.056
Goodness of Fit Indicator	3.49
Max Shift/Error in Final Cycle	<0.01
Maximum Peak in Final Diff. Map	0.21 $e^-/Å^3$
Minimum Peak in Final Diff. Map	-0.14 $e^-/Å^3$

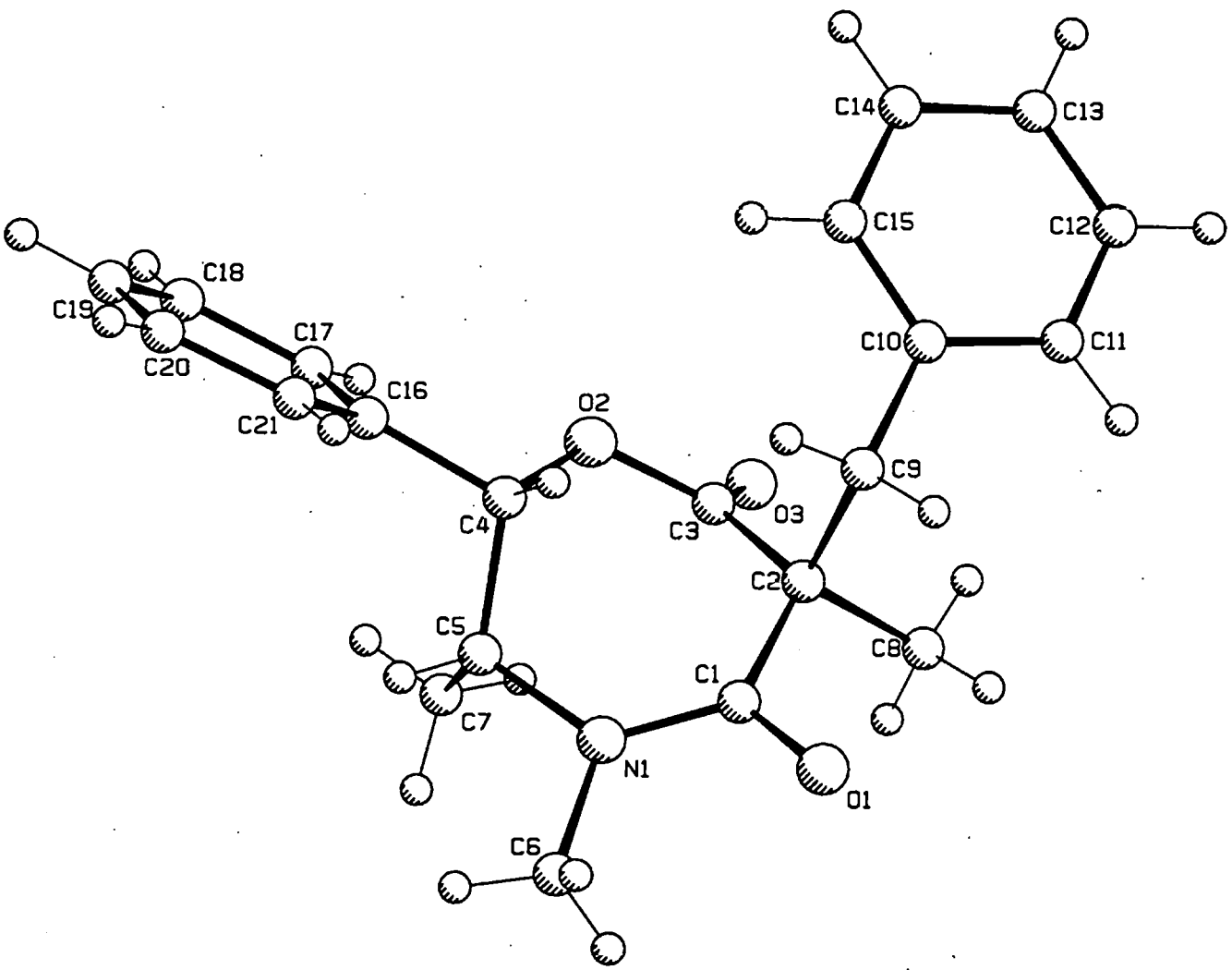
C14
C13
C15
C12
C10
C11
C9
O3
C3
O2
C4
C16
C17
C18
C19
C20
C21
C2
C8
C5
C1
C7
N1
O1
C6

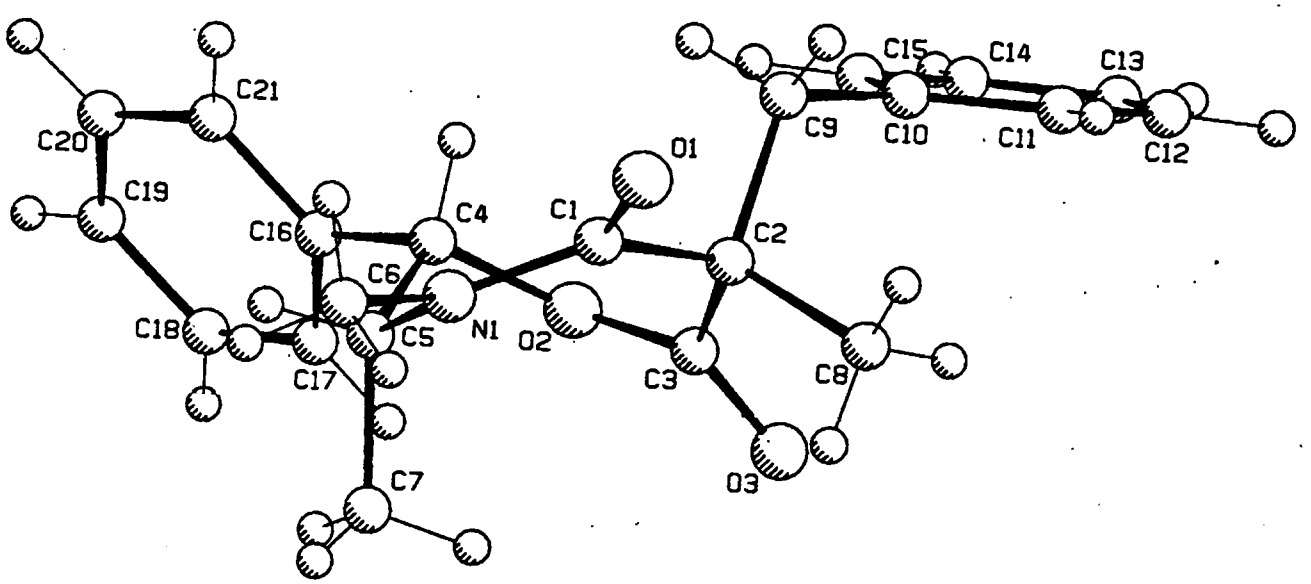
C21
C20
C19
C16
C4
C1
O1
C2
C15
C14
C13
C9
C10
C11
C12
C6
C18
C5
N1
O2
C3
C8
C17
O3
C7

Status of project

16-SEP-93 07:55:27

PROJECT DIRECTORY : [TEXSAN.STRUCTURES.S308]

TITLE : S308/1 15-SEP-93

CELL : a= 9.176 b= 14.668 c= 11.608 alpha= 90.00 beta= 93.78 gamma= 90.00

SPACEG : P21 S.G.# 4 DENSITY : Dc= 1.224 Absorption coef.= 6.387

STORED formula		CURRENT formula		STATUS
C	17.00	C	17.00	O.K.
H	21.00	H	21.00	O.K.
N	1.00	N	1.00	O.K.
O	3.00	O	3.00	O.K.

parameters : # of reflections= 2035 # of variables= 378 shift/error= 0.015

R-factors : R= 0.042 Rw= 0.050 Goodness of fit= 1.829 LS cycles= 3

corrections : absorption=on -type=DIF decay=on redundant=on average=off

INTRODUCTION

The structure proposed has been confirmed.

The spacegroup is non-centrosymmetric and the origin of the unit cell is fixed by constraining the y value of O1. There are four molecules in the unit cell and two independent molecules of the same hand in the asymmetric unit. These two are found to be closely similar in molecular geometry and so affords a guide to accuracy additional to the e.s.d. values derived from the least-squares process.

There does not appear to be evidence of hydrogen bonding, close intermolecular approaches being H to H only.

The enantiomeric structure was also refined making use of small anomalous scattering terms. The resultant R and Rw were 0.0425 and 0.0503 : the predicted absolute configuration which is reported below gives slightly lower (better) values of both 0.0422 and 0.0499.

EXPERIMENTAL

DATA COLLECTION

A colourless prism crystal of $C_{17}H_{21}NO_3$ having approximate dimensions of 0.12 X 0.20 X 0.30 mm was mounted on a glass fibre. All measurements were made on a Rigaku AFC5R diffractometer with graphite-monochromated Copper Kα radiation and a 12KW rotating anode generator.

Cell constants and an orientation matrix for data collection, obtained from a least-squares refinement using the setting angles of 8 carefully-centred reflections in the range $77.90 < 2\theta < 79.94°$ corresponded to a monoclinic cell with dimensions:

a =	9.176 (3)Å		
b =	14.668 (4)Å	β =	93.78 (2)°
c =	11.608 (1)Å		
V =	1558.9 (7)Å^3		

For $Z = 4$ and F.W. = 287.36, the calculated density is 1.224 g/cm^3. Based on the systematic absences of:

$0k0: k \neq 2n$

packing considerations, a statistical analysis of intensity distribution, and the successful solution and refinement of the structure, the space group was determined to be:

$P2_1$ (#4)

The data were collected at a temperature of 25 ± 1°C using the $\omega/2\theta$ scanning technique to a maximum 2θ value of 120.4°. Omega scans of several intense reflections, made prior to data collection, had an average width at half-height of 0.29° with a take-off angle of 6.0°. Scans of $(1.37 + 0.30 \tan\theta)°$ were made at a speed of 16.0°/min (in omega). The weak reflections ($I < 10.0\sigma(I)$) were rescanned (maximum of 2 rescans) and the counts were accumulated to assure good counting statistics. Stationary background counts were recorded on each side of the reflection. The ratio of peak counting time to background counting time was 2:1. The diameter of the incident beam collimator was 0.5 mm and the crystal to detector distance was 400.0 mm.

DATA REDUCTION

Of the 2605 reflections which were collected, 2438 were unique (R_{int} = .044). The intensities of three representative reflections which were measured after every 150 reflections declined by 0.13%. A linear correction factor was applied to the data to account for this phenomenon.

The linear absorption coefficient for Copper Kα is 6.4 cm^{-1}. An empirical absorption correction, using the program DIFABS[3], was applied which resulted in transmission factors ranging from 0.76 to 1.20. The data were corrected for Lorentz and polarization effects.

STRUCTURE SOLUTION AND REFINEMENT

The structure was solved by direct methods[4]. The non-hydrogen atoms were refined anisotropically. Hydrogen atoms were included in the structure factor calculation in idealized positions (C-H = 0.95Å) , and were assigned isotropic thermal parameters which were 20% greater than the equivalent B value of the atom to which they were bonded. The final cycle of full-matrix least-squares refinement[5] was based on 2035 observed reflections ($I > 3.00\sigma(I)$) and 378 variable parameters and converged (largest parameter shift was <0.02 times its esd) with unweighted and weighted agreement factors of:

$$R = \Sigma \; ||Fo| - |Fc|| \; / \; \Sigma \; |Fo| = 0.042$$

$$R_w = [(\Sigma \; w \; (|Fo| - |Fc|)^2 \; / \; \Sigma \; w \; Fo^2)]^{1/2} = 0.050$$

The standard deviation of an observation of unit weight[6] was 1.83. The weighting scheme was based on counting statistics and included a factor (p = 0.03) to downweight the intense reflections. Plots of $\Sigma \; w \; (|Fo| - |Fc|)^2$ versus |Fo|, reflection order in data collection, $\sin\theta/\lambda$, and various classes of indices showed no unusual trends. The maximum and minimum peaks on the final difference Fourier map corresponded to 0.18 and -0.14 $e^-/Å^3$, respectively.

Neutral atom scattering factors were taken from Cromer and Waber[7]. Anomalous dispersion effects were included in Fcalc[8]; the values for Δf' and Δf" were those of Cromer[9]. All calculations were performed using the TEXSAN[10] crystallographic software package of Molecular Structure Corporation.

References

(1) PLUTO:
Motherwell,S. & Clegg,W.; PLUTO. Program for plotting molecular and crystal structures. Univ. of Cambridge, England (1978).

(2) ORTEP:
Johnson,C.K.; ORTEPII. Report ORNL-5138. Oak Ridge National Laboratory, Oak Ridge, Tennessee (1976).

(3) DIFABS:
Walker & Stuart, Acta Cryst. A39, 158-166, (1983).

(4) Structure Solution Method:
SHELXS-86
Sheldrick,G.M.; (1985). SHELXS-86 In "Crystallographic Computing 3" , edited by G.M.Sheldrick, C.Krueger and R.Goddard p175-189. Oxford University Press.

(5) Least-Squares:
Function minimized: $\Sigma\ w\ (|Fo| - |Fc|)^2$
where: $w = 4Fo^2/\sigma^2(Fo^2)$
$\sigma^2(Fo^2) = [S^2(C+R^2B) + (pFo^2)^2]/Lp^2$
S = Scan rate
C = Total Integrated Peak Count
R = Ratio of Scan Time to background counting time.
B = Total Background Count
Lp = Lorentz-polarization factor
p = p-factor

(6) Standard deviation of an observation of unit weight:

$$[\Sigma\ w(|Fo| - |Fc|)^2/(No - Nv)]^{1/2}$$

where: No = number of observations
Nv = number of variables

(7) Cromer,D.T. & Waber,J.T.; "International Tables for X-ray Crystallography", Vol. IV, The Kynoch Press, Birmingham, England, Table 2.2 A (1974).

(8) Ibers,J.A. & Hamilton,W.C.; Acta Crystallogr., 17, 781 (1964).

(9) D.T. Cromer, "International Tables for X-ray Crystallography", Vol/ IV, The Kynoch Press, Birmingham, England, Table 2.3.1 (1974).

(10) TEXSAN - TEXRAY Structure Analysis Package, Molecular Structure Corporation (1985).

EXPERIMENTAL DETAILS

1. Crystal Data

Empirical Formula	$C_{17}H_{21}NO_3$
Formula Weight	287.36
Crystal Colour, Habit	colourless, prism
Crystal Dimensions (mm)	0.12 X 0.20 X 0.30
Crystal System	monoclinic
No. Reflections Used for Unit Cell Determination (2θ range)	8 (77.9 - 79.9°)
Omega Scan Peak Width at Half-height	0.29
Lattice Parameters:	a = 9.176 (3)Å b = 14.668 (4)Å c = 11.608 (1)Å β = 93.78 (2)° V = 1558.9 (7)Å^3
Space Group	$P2_1$ (#4)
Z value	4
D_{calc}	1.224 g/cm^3
F_{000}	616
$\mu_{(CuK\alpha)}$	6.39 cm^{-1}

2. Intensity Measurements

Diffractometer	Rigaku AFC5R
Radiation	CuKα (λ = 1.54178 Å)
Temperature	25°C
Attenuators	Zr foil (factors: 3.6, 12.2, 44.0)
Take-off Angle	6.0°

Detector Aperture	6.0 mm horizontal 6.0 mm vertical
Crystal to Detector Distance	40 cm
Scan Type	$\omega/2\theta$
Scan Rate	16.0°/min (in omega) (2 rescans)
Scan Width	$(1.37 + 0.30 \tan\theta)°$
$2\theta_{max}$	120.4°
No. of Reflections Measured	Total: 2605 Unique: 2438 (R_{int} = .044)
Ranges of h,k,l	0 to 10, 0 to 16, -13 to 12
Corrections	Lorentz-polarization Absorption (trans. factors: 0.76 - 1.20) Decay (0.13% decline)

3. Structure Solution and Refinement

Structure Solution	Direct Methods
Hydrogen Atom Treatment	Included in calculated positions (d_{C-H} = 0.95Å)
Refinement	Full-matrix least-squares
Function Minimized	Σ w $(\|Fo\| - \|Fc\|)^2$
Least-squares Weights	$4Fo^2/\sigma^2(Fo^2)$
p-factor	0.03
Anomalous Dispersion	All non-hydrogen atoms
No. Observations ($I>3.00\sigma(I)$)	2035
No. Variables	378
Reflection/Parameter Ratio	5.38
Residuals: R; R_w	0.042; 0.050
Goodness of Fit Indicator	1.83
Max Shift/Error in Final Cycle	0.02
Maximum Peak in Final Diff. Map	0.18 $e^-/Å^3$
Minimum Peak in Final Diff. Map	-0.14 $e^-/Å^3$